Substituted Pyridines for the Development of Novel Therapeutics - Antifungals and Antidiabetics

Substituierte Pyridine für die Entwicklung neuer antifungischer und antidiabetischer Wirkstoffe

DISSERTATION

der Fakultät für Chemie und Pharmazie
der Eberhard Karls Universität Tübingen

zur Erlangung des Grades eines Doktors
der Naturwissenschaften

2010

vorgelegt von
Katarzyna Kaczanowska

Tag der mündlichen Prüfung:	24. August 2010
Dekan:	Prof. Dr. Lars Wesemann
1. Berichterstatter:	Prof. Dr. Karl-Heinz Wiesmüller
2. Berichterstatter:	Prof. Dr. Klaus Albert

This Dissertation was carried out from August 2007 to August 2010 at EMC microcollections GmbH, Tübingen and at the Institute of Organic Chemistry, Eberhard Karls Universität Tübingen under the supervision of:

Prof. Dr. Karl-Heinz Wiesmüller

and

Prof. Dr. Klaus Albert

Acknowledgment

I wish to thank my supervisors Prof. Dr. Karl-Heinz Wiesmüller and Prof. Dr. Klaus Albert.
I appreciate the constructive discussions with and advises from Dr. Arnaud-Pierre Schaffner, Dr. Holger Eickhoff, Prof. Dr. Günther Jung and Prof. Dr. Eberhard Breitmaier.
I thank Dr. Dorothee Wistuba for the FT-ICR-MS measurements and Dr. Klaus Eichele for the support in the NMR analysis.
I wish to thank Dr. Hartmut Röhm for 'guiding' me through the University and for all his help.
I acknowledge Dr. Steffen Rupp (Fraunhofer Institute, Germany), Prof. Dr. Karl Kuchler (University and Biocenter of Vienna, Austria) and Prof. Dr. Gerald Kleymann (Eberhard Karls Universität Tübingen) for performing antifungal screening.
I am grateful for financial support of the EC Marie Curie RTN "CanTrain" (CT-2004-512481).

Contents

Abbreviations

Ac	Acetyl
abs.	Absolute
anhyd.	Anhydrous
aq	Aqueous
Ar	Aryl
atm.	Atmosphere(s)
BMDMs	Bone marrow-derived macrophages
Boc	*tert*-Butoxycarbonyl
bs	Broad singled (spectral)
t-Bu	*tert*-Butyl
°C	Degrees Celsius
CC_{50}	50 % Cytotoxic concentration
CD	Cluster of differentiation
CFU	Colony forming units
CHO	Chinese hamster ovary
Compd	Compound
COSY	Correlation Spectroscopy
d	day(s); doublet (spectral);
DASH	DPP-4 activity and/or structure homologue family
DCM	Dichloromethan
DDQ	2,3-Dichloro-5,6-dicyano-1,4-benzoquinone
DEPT	Distortionless enhancement by polarization transfer
DIC	Diisopropylcarbodiimid
DIPEA	Diisopropylethylamin
DMAP	4-(*N,N*-dimethylamino)pyridine
DMF	Dimethylformamide
DMSO	Dimethyl sulfoxide
DNA	Deoxyribonucleic acid
DPP-4	Dipeptidyl peptidase IV
DPP-8	Dipeptidyl peptidase 8
EA	Ethyl acetate
eq	Equivalent
ESI	Electrospray Iionization
Et	Ethyl
eV	Electronvolt
FAB	Fast Atom Bombardment
FDA	Food and Drug Administration
FID	Flame ionization detector
GIP	Glucose dependent insulinotropic peptide
GK	Glucokinase
GLP-1	Glucagon-like peptide 1
h	Hour(s)
ha	Hectare
HbA_{1c}	Glycosylated hemoglobin
$_{11b}$HSD1	11b hydroxysteroid dehydrogenase type 1
HMBC	Heteronuclear multiple bond correlation
HPLC	High-performance liquid chromatography
HRMS	High-resolution mass spectrometry
HTS	High-throughput screening

Hz	Hertz
i	Inhibitor concentration
IC_{50}	Half maximal inhibitory concentration
IGT	Impaired glucose tolerance
IFG	Impaired fasting plasma glucose
IPI	Isoleucine-Proline-Isoleucine
IR	Infrared
J	Coupling constant (in NMR spectrometry)
K_i	Absolute inhibition constant
K_m	Concentration of the substrate that leads to V_m
K_p	Effective Michaelis constant
LAH	Lithium aluminum hydride
LC	Liquid chromatography
m	Multiplet (spectral), mass
M	Molar (moles per liter)
$[M + H]^+$	Parent molecular ion
MALDI	Matrix-Assisted Laser Desorption
mL	Milliliter(s)
Me	Methyl
MetAP	Methionine aminopeptidase
MHz	Megahertz
MIC	Minimum inhibitory concentration
min	Minute(s)
mol	Mole(s)
m.p.	Melting point
MS	Mass Spectrometry
MW	Molecular Weight
m/*z*	Mass-to-charge ratio
NADP	Nicotinamide adenine dinucleotide phosphate
nm	Nanometer(s)
NMR	Nuclear Magnetic Resonance
OD_{600}	Optical density at 600 nm
ODS	Octadecyl silica
PBS	Phosphate-buffered saline
PDA	Photodiode Array Detector
Pd/C	Palladium on carbon
PE	Petroleum ether
Ph	Phenyl
pNA	*p*-nitroaniline
PP	Polypropylene
PPAR	peroxisome proliferator-activated receptor
ppm	Part(s) per million
PyBOP	Benzotriazol-1-yl-oxytripyrrolidinophosphonium hexafluorophosphate
q	Quartet (spectral)
QSAR	Quantitative Structure–Activity Relationship
RFU	Relative Fluorescence Units
rt	Room temperature
s	Singlet (spectral); second(s)
S	Substrate concentration
SAR	Structure–activity relationship
SGLT2	Sodium-glucose transporter-2

SPOS	Solid phase organic synthesis
SQD	Single Quadrupol
t	Triplet (spectral)
TFA	Trifluoroacetic acid
THF	Tetrahydrofuran
TLC	Thin-layer chromatography
TMS	Tetramethylsilane
Tris	Tris(hydroxymethyl)methylamine
UV	Ultraviolet
V	Initial velocity of the negative control
V_i	Iinitial velocity in presence of the inhibitor at concentration *i*
V_M	Half-maximal velocity
YPD	Yeast peptone dextrose agar

1. Introduction.

Dynamic development and automation of medicinal chemistry approaches lead to an increased demand of compounds for biological evaluation.

The search for novel therapeutics is based on four major strategies:

a) Screening of natural and synthetic compound libraries - mixture of compounds
b) Screening of random compound collections, combinatorial chemistry
c) Focused compound collections - literature based drug design
d) Computational drug design

As an early approach to produce numerous compounds and complex libraries in microgram quantities, split-and-mix synthesis in combination with solid phase organic chemistry was used.[1-2] Limited success from biological screening with regard to false-positives and problems with identification of active ingredients in the screened mixtures, due to insufficient purification and quality control methods, was the major drawback of the strategy.[3] The high expectations placed upon early combinatorial libraries remained therefore unfulfilled.

The mentioned problems were avoided by high throughput screening of random compound collections. The approach is based on the investigation of a series of single, characterized compounds with defined purity criteria. When no specific structure or substructure is obligatory as a starting point the approach initially requires a large number of diverse compounds in order to increase the chance to identify a compound of the novel biological target or an alternative lead structure for a known target.[2] In addition to the collection sizes the probability to find a hit molecule might be further increased by using structural motifs that are appearing frequently in potent drugs and drug candidates or by selecting scaffolds which are straightforward to prepare and allow the synthesis of highly diverse compounds.[2,4]

Further improvement in drug development was reached by generation of focused collections. The main task of this approach is not necessarily to provide large numbers of compounds but rather to improve hit rates by exploring molecular space. The term focused is not clearly defined. One category are target-family oriented collections that consist of compounds specifically designed to target certain protein families. Such sets of compounds require up to 50000 molecules. More specific collections address a certain target protein and therefore the number of compounds may decrease to 2000, designed around a specific scaffold class. In a hit-to-lead or lead-optimization the compound number is smaller, around 20-500.[3]

Careful and smart design of libraries is crucial for the success in respect of physicochemical properties of molecules. The design principles can vary depending on the purpose of a collection. For a hit finding or target-oriented collection a basic tool is Lipinski's rule of five.[4] Advances in molecular biology, protein engineering, and biophysical techniques are providing structural information about therapeutic targets, which are of great importance for creation of active candidates. Incorporation of key structures and recognition elements for receptor binding that are relevant to the particular biological target is often essential. However, the prediction of the influence of the specific lead modification is highly limited, due to the changes of ligand binding affinity or certain biological effects caused by nonspecific inhibition phenomena. Therefore often structure-based discovery strategies still require the preparation of many 'designed' compounds.[3,5]

To increase the efficiency of the drug discovery process efforts are focused on computer-based techniques that assist drug development. Software programs are used for the creation of the corresponding virtual compound library, and the selection of the compounds to be synthesized and screened based on drug-likeness. There are enzyme pocket-homology models available for enzymes, which are used to assess proposals for new scaffolds taking into consideration their fit into binding pockets. Additionally more sophisticated tools, such as docking, pharmacophore- or QSAR (Quantitative Structure-Activity Relationship)-based models might be used in combination with or instead of other mentioned approaches in more advanced stages of lead optimization.[2-8]

Experimental methods which promise to shorten the drug discovery and development time or its cost are eagerly taken up. One of the useful technique is combinatorial chemistry, that allows the preparation of a large number of structurally related compounds either as mixtures in the same reaction vessel or individually by parallel synthesis. Combinatorial collections have been prepared using both solution chemistry and solid phase synthesis or by the combination of both. The great power of the high-throughput chemistry techniques is clearly seen when they are integrated with other tools used in drug discovery.[2-8]

An extensive advance and success enhancement in medicinal chemistry and drug discovery is nowadays achieved by combining the speed power of combinatorial chemistry with the precision of structure-based design and potential of computational methods.

2. Objectives.

The aim of this study is the discovery of novel lead structures in a search for antifungal and antidiabetic therapeutics by applying two drug discovery concepts, a screening of random compound collections and a focused drug design, both supported by solid phase and solution phase combinatorial chemistry.

In the first part of the dissertation the search for antifungals based on a random high throughput screening is discussed. The compounds should be generated by the diversity-oriented combinatorial synthesis.

The focus of this work is placed on pyridines **1** and the fused pyridine system of pyrazolopyridines **2** as promising scaffolds due to the high probability to identify biologically active lead structures (Scheme 1).

Scheme 1. General structures of the investigated scaffolds.

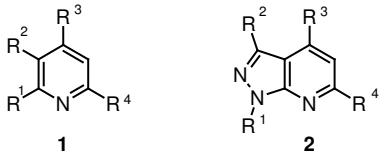

The objective of this study is to establish straightforward synthetic protocols for the generation of the desired molecules **1** and **2** and to prepare subsets of compounds varying only on the certain substituents in the pyridine ring **1**.

The synthesized compounds should be evaluated for their antifungal properties and toxicity in an in vitro cellular assay and result in the identification of the lead structure.

The second part of the dissertation is dedicated to the rational design, synthesis and preliminary biological screening of novel DPP-4 inhibitors as antidiabetics. Literature search and structural data available for this target support the design of potential protein ligands that are based on pyridine rings and involve important structural motifs for the high binding affinity. In this context the intention is to synthesize novel pyridines as DPP-4 inhibitors and to establish their synthesis, starting with the scaffold **1**, described in the first part of this study.

The synthesized, isolated and analytically characterized collections should be then evaluated for DPP-4 inhibition and selectivity over related DPP-8, allowing a structure activity relationship discussion.

3. Pyridines as scaffolds for antifungals and antidiabetics.

In respect to the main goals of the dissertation, this part of the work is focused on the active compounds based on the pyridine ring in the field of antifungal research and in the development of antidiabetics. The review presents active agents already on the market, but also examples from the recent literature of compounds with promising *in vitro* activity.

The significance of pyridines was recognized in the 1930s when niacin **3** was used for the prevention of dermatitis and dementia. Since the middle of the last century, pyridine derivatives supported progress in understanding chemistry of biological systems, because they participate in biochemical processes. In many enzymes the prosthetic pyridine nucleotide (NADP) is involved in various reduction-oxidation reactions. Other important activity of pyridine in biological systems is its presence in the vitamins niacin **3** and pyridoxin **4** (vitamin B6) but also in highly toxic alkaloids such as nicotine **5** (Scheme 2).[9] Pyridines find ubiquitous applications in medicaments[10] and in agrochemicals.[11] In the pharmaceutical industry, pyridine forms the nucleus of over 7000 existing drugs.[9] Search in DrugBank (containing nearly 4800 drug entries and 1350 FDA-approved small molecule drugs) for the pyridine ring in approved medicaments gave 104 hits (similarity threshold = 0.7).[10] They are addressed to a number of the various targets. The leading group are antimicrobials (isoniazid **6**) and histamine h1 antagonists such as pheniramine **7**, but also anticancer, analgesic, and antidepressant agents (Scheme 2).

Scheme 2. Structures of some biologically active pyridines.

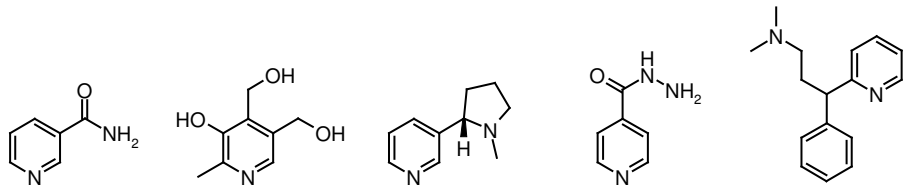

3 **4** **5** **6** **7**

3. 1 Pyridines as antifungal agents.

Pyridines are extensively investigated for its antifungal activity as therapeutics or for agricultural use.

Up to date there is only one approved antifungal drug on the market based on the 2-pyridone skeleton (Scheme 3).[10] Ciclopiroxolamine **8**, a drug with a long history, is marketed worldwide, as a topical antifungal agent. It shows in vitro activity against a number of fungi such as *T. rubrum, T. mentagrophytes, M. canis, E. floccosum, H. capsulatum, S. schenckii, T. glabrata, B. dermatitidis*, *Candida* species and *Aspergillus* species. It is mainly used against skin mycoses and vaginal candidosis. It is also effective in the treatment of dermatophytoses. The drug exhibits no significant toxicity and is well tolerated after topical administration.[12] An important feature of **8** is that it does not cause *Candida albicans* to develop resistance even with long-term treatment and, in addition, it is an excellent anti-inflammatory agent. In contrast to the other topical antifungals, the mode of action of ciclopiroxolamine is poorly understood. It has no effect on sterol synthesis, but was shown to inhibit several metal-dependent enzymes. S. H. Leem *et al.* screened the drug against several *Saccharomyces cerevisiae* mutants. Results suggested that ciclopiroxolamine may exert its effect by disrupting DNA repair, cell division signals and structures as well as some elements of intracellular transport.[13]

Scheme 3. Structure of the antifungal ciclopiroxolamine.

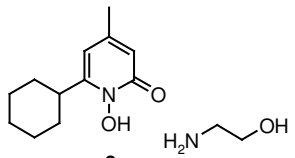

8

A number of pyridine-based compounds are used in the crop protection as fungicides (Scheme 4). They mainly affect sterol biosynthesis in membranes, but also mitosis and cell division or respiration process.[11,14]

Pyrifenox **9** is a systematic fungicide with protective and curative action absorbed by the leaves and roots and translocated acropetally. The compound **9** as well as buthiobate **15** was proved to be an inhibitor of ergosterol biosynthesis.[15-16] It is used for the control of powdery mildew, scab and other pathogenic Ascomycetes, Basidiomycetes, Deuteromycetes in vines, fruits and vegetables.[11]

Pyroxychlor **13** possess its antifungal activity due to DNA synthesis inhibition. It is used for controlling phycomycetous soliborne pathogens (e.g. *Pythium aphanidermatum*).[17]

Fluazinam **20** has an uncoupling activity on mitochondrial oxidative phosphorylation. It is used to treat grey mould on vines, apple scab, *Phytophthora infestans* on potatoes.[11]

Various pyridine *N*-oxide derivatives possess antibacterial and antifungal activity. Due to their broad spectrum antimicrobial activity they were used in shampoos as antidandruff agents and in cosmetics as preservatives. Dipyrithione **16** was incorporated into shampoos as its magnesium sulfate adduct.[11,18]

Scheme 4. Pyridine-based fungicides.

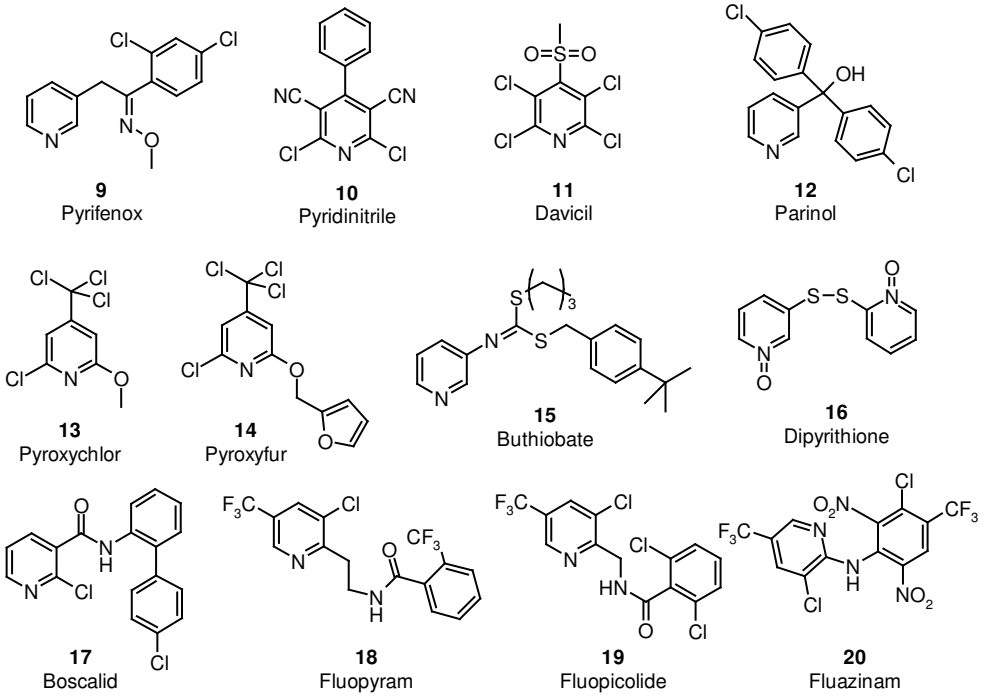

The scientific journals and patent literature show that there is ongoing search for novel potent antifungals and pyridines.

A series of publications reported SAR studies based on the hit structure **21** obtained from the screening of 12800 antifungal drug candidates, inhibitors of the methionine aminopeptidase (MetAP).[19] The pyridine-2-carboxylic acid derivatives **21-23** have shown submicromolar inhibition of the two enzyme type (Scheme 5, **23**: IC_{50} = 130 nM for EcMetAP1 and IC_{50} = 380 nM for ScMetAP1). These compounds represent the first small-molecule MetAP inhibitors with novel structures different from alkylating Fumagillin derivatives and peptidic bestatin-based MetAP inhibitors.

Scheme 5. Examples of the MetAP inhibitors.

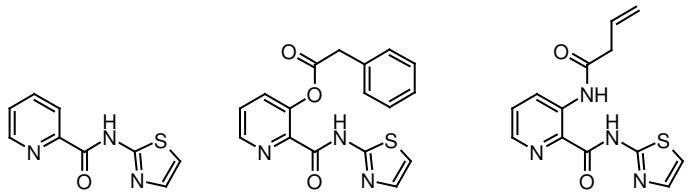

21 **22** **23**

M. S. Yar *et al.* reported a series of pyrazolyl-4-pyridylmethanones that has been tested against baceria *Staphylococcus aureus*, *Escherichia coli,* as well as for its antifungal activity against *Aspergillus fumigatus* and Candidas: *C. albicans*, *C. krusei, C. glabrata*.[20] The minimum inhibitory concentration (MIC) of the two most active derivatives **24a-b** was less than 0.5 μg/mL and they were equally active as the standard drugs Ofloxacin and Fluconazole (Scheme 6).

Scheme 6. Structure of the antifungal pyrazolyl-4-pyridylmethanones.

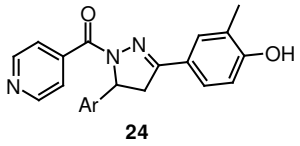

24

Compd	Ar
24a	4-Dimethylamino-phenyl
24b	2,6-Dichloro-phenyl

Pyridines substituted with the chalcone moiety **25** have been reported as potent antifungals (Scheme 7).[21]

Scheme 7. Antifungal chalcones **25**.

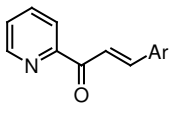

25

Ar
4-Chloro-phenyl
2,4-Dichloro-phenyl
3-Bromo-phenyl
4-Methoxy-phenyl
3,4-Dimethoxy-phenyl
3,4,5-Trimethoxy-phenyl

Their antibacterial activity against *B. pumilis*, *B. subtilis*, *E. coli* and *P. vulgaris* was comparable to that of Penicillin and comparable to Fluconazole when the antifungal properties against *A. niger* and *Penicillium chrysogenum* were tested at the concentration of 1000 μg/mL.

Scheme 8. Antifungal pyridinium salts.

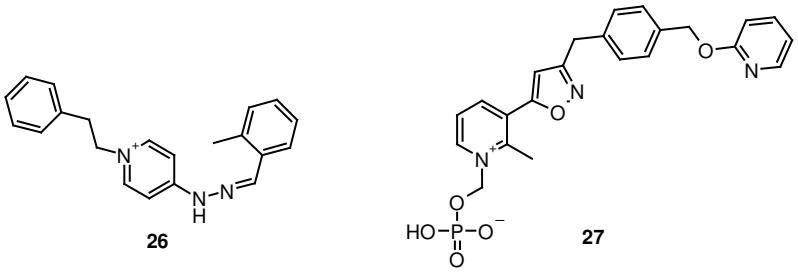

Some substituted benzylidenehydrazinylpyridinium derivatives bearing benzyl, ethylphenyl and propylphenyl groups on the pyridinium nitrogen were synthesized and screened for possible antibacterial and antifungal activities against *Staphylococcus aureus*, *Escherichia coli*, *Pseudomonas aeruginosa* and *Candida albicans.* The compound **26** was the most active in the series against many strains of bacteria and fungi (Scheme 8).[22a]

Recently another series of pyridinium salts substituted with phosphonoxymethyl group was patented for its antifungal activity against a number of fungi (Scheme 8, **27**).[22b]

As a result of the search for antifungals based on the similarity to the phospholipids, a series of bis(alkylpyridinium)alkanes **28** with a twelve carbon spacer between the positive charges was found to be potent antifungal agents with MICs in the range of 1.4-2.7 μM against reference strains *Cryptococcus neoformans* and *Candida albicans*.[23] Two most active compounds **28a** and **28b** (Scheme 9) were assayed against a wider range of yeasts and moulds and were found to have broad spectrum fungicidal activity, including the emerging pathogen *S. prolificans*.[23a] In order to understand the mode of action the antifungals were screened for the inhibition of the secreted enzyme, fungal phospholipase B (PLB), that is a proven virulence determinant of the pathogenic fungi, *Candida albicans* and *Cryptococcus neoformans*, and which is also secreted by other pathogenic fungi including *Aspergillus* spp. Previous studies on a series of bis(amino)pyridiniumalkanes, based on the known disinfectants dequalinium and octenidine, indicated that while these compounds are strongly antifungal, they do not inhibit cryptococcal PLB1.[23b] Interestingly in the most recent study there was no clear correlation with antifungal activity. Preliminary experiments however indicated that bis(alkylpyridinium)alkanes **28** may play a role in disrupting fungal mitochondrial function.[23a]

Scheme 9. Representative antifungal bis(alkylpyridinium)alkanes **28**.

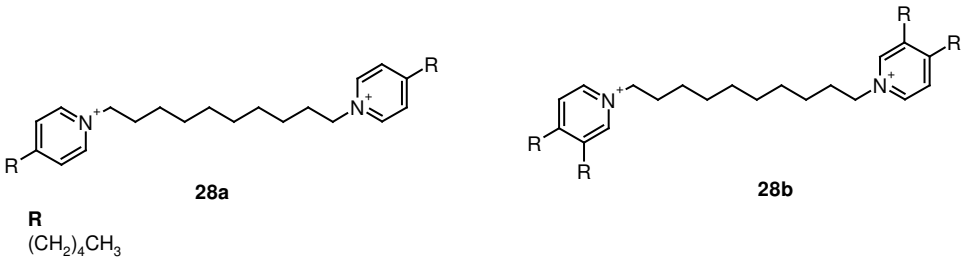

A novel group of antifungals is represented by dicationic 2,5-bis(4-guanidinophenyl)furans.[24] The fungicidals were screened against *Candida albicans* and exhibit MICs of 2 μg/mL. The compound **29** (Scheme 10) showed in addition good activity against *Cryptococcus neoformans* and *Rhizopus arrhizus*.

Scheme 10. Representative potent antifungal dicationic 2,5-bis(4-guanidinophenyl)furan **29**.

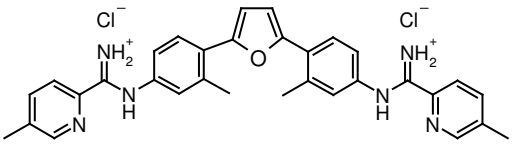

A. El-Galil *et al.*[25a] Based on the peptidocalixarene derivatives studied as analogues of vancomycin-type antibiotics designed macrocyclic peptidocalixarenes **30** and investigated them for antimicrobial activity.[25]

Scheme 11. Antifungal macrocycles **30**.

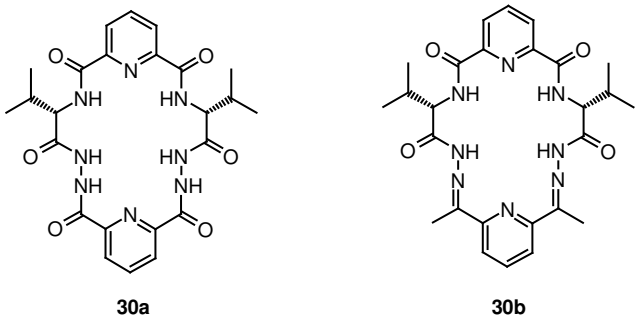

Among the series several macrocycles showed high antimicrobial activity comparable to Ampicillin and Chloramphenicol against *Bacillus subtilis*, *Bacillus aureus*, *Staphylococcus aureus*, *Escherichia coli*, and against fungi: *Candida albicans* and *Aspergillus niger*. The structure of the most potent antifungal macrocycles **30a** and **30b** is presented on the scheme 11.

The attempts to use quantitative structure-activity relationships (QSAR) models in order to give an insight in the design of potent antifungal agents based on pyridines have been reported recently.[26] A. Buciński and coworkers performed QSAR studies of antifungal activity against *Candida albicans* of 44 pyridines belonging to a class of quaternary ammonium salts.[26a]

Scheme 12. Examples of the pyridines **31** used for QSAR studies.[26b]

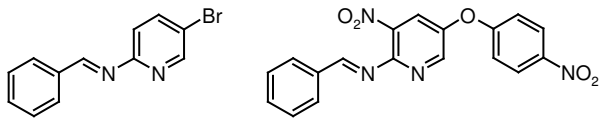

31a **31b**

Similarly QSAR studies were performed for 5-substituted (arylmethylene) pyridin-2-amine derivatives **31** (Scheme 12) to correlate the selected electronic, steric and liphophillic parameters with antifungal activity against *A. niger*, *A. flavus*, *P. crysogenum* and *F. oxysporium*.[26b] Both studies gave a good correlation of the predicted activity by the artificial neural networks and from the biological experiments.

Scheme 13. Potential fungicides.

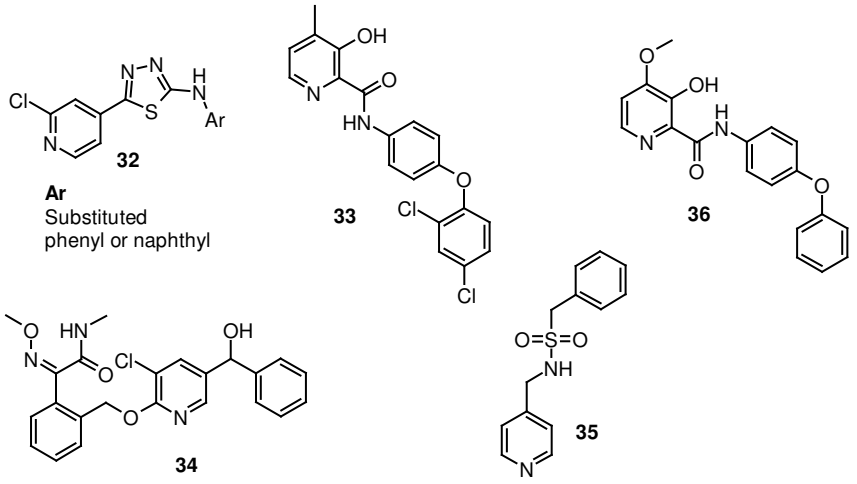

32 **33** **36**

34 **35**

A series of 2-[(2-chloropyrid)-4-yl]-5-arylamino-1,3,4- thiadiazoles **32** are potent inhibitors of *R. solani* (Palo) at 500 μg/mL. The amide **33** was reported to be more than 91% effective against Botrytis on beans at 500 g/ha. Fungicidal 2-methoxyimino-2-[(pyridinyloxymethyl)phenyl] acetamides **34** showed 75-100% control of plant diseases like mildew of wheat, brown rust, glume blotch of wheat and late blight of tomatoes.[12] **35** was reported as a potent fungicide for agricultural purposes.[27] Picolinic acid derivatives were tested for activity against fungal strains such as *Alternaria brassicae* or *Septoria nodorum,*

and hydroxypicolin amide derivative **36** was proposed for pharmaceutical usage as fungicide[12] (Scheme 13).

Fungicides presently available on the market differ widely in chemical structure and functional groups. Nevertheless the compounds with the optimum antifungal properties have not been found yet and this fact stimulates continuing research for the synthesis of new molecules. The pyridine-based active compounds constitute a promising group in the search of potent antifungals exerting selective toxicity against fungi without interacting with other eukaryotic cells.

3. 2 Pyridines as DPP-4 inhibitors for treatment of diabetes mellitus.

3. 2. 1 Approaches for diabetes treatment.

Diabetes is a growing health problem, with an estimated 220 million people worldwide suffering from this disease, and type 2 diabetes comprises 90% of them.[28-29]

M. L. Mohler *et al.* have recently reported a progress in diabetes treatment. The number of exciting approaches to treat the disease was estimated for more than 20. The treatment involving incretin actions together with PPAR (peroxisome proliferator-activated receptor)-activators make up the main classes of medicaments under investigation for controlling blood glucose in type 2 diabetes, but the number of cellular processes affected by the disease is so high that these approaches are far from exhausting all possibilities. Some other strategies, such as affecting glucose production (inhibition of gluconeogenesis, formation of glucose in the liver, or glycogenolysis, breakdown of stored glycogen in the liver) or glucokinase activators are in earlier stages of clinical research. Other interesting approaches are based on sodium-glucose transporter-2 (SGLT2) inhibition or amylin analogues and, as they do not intervene with glucose metabolism, might be complementary to the previously mentioned.[30]

The field of antidiabetics is vast from both, biological and synthetic point of view. Pyridines represent a group of the widely investigated compounds in every emerging target and therefore a comprehensive discussion is beyond the scope of this work. Here mainly the DPP-4 inhibition will be discussed. Nevertheless, it is worth mentioning, that pyridine-based agents are extensively investigated for other targets in diabetes field.

Scheme 14. Pyridine-based PPARs inhibitors.

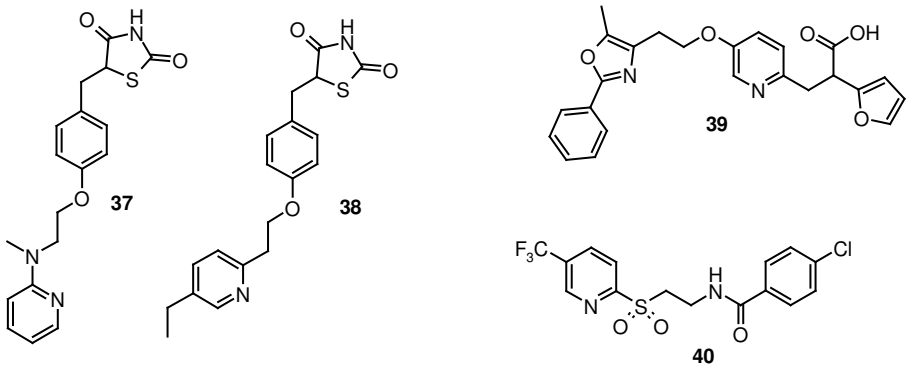

Rosiglitazone **37** and pioglitazone **38** are potent PPARγ agonists currently marketed for the treatment of type 2 diabetes (Scheme 14). PPARs regulate the expression of genes that affect blood lipid metabolism, the generation of adipocytes, and blood glucose control. The

pyridine-2-propanoic acid **39** represents a class of potent dual PPAR agonists. *S*-enantiomer of compound **39** displayed a higher oral efficacy than the rosiglitazone **37** in a mouse model of diabetes.[31a] 2-Sulfonyl-pyridine **40** (GSK3787) was identified as a potent and selective ligand for PPARδ with good pharmacokinetic properties.[31b]

Scheme 15. Pyridine-based 11b-hydroxysteroid dehydrogenase type 1 inhibitor **41** (PF-915275).

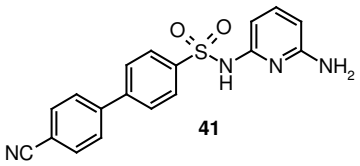

41

N-(Pyridin-2-yl)arylsulfonamides were disclosed by Pfizer as inhibitors of 11b hydroxysteroid dehydrogenase type 1 (11bHSD1), that represent a novel approach to treat patients with diabetes and metabolic syndrome by blocking adipogenesis. The studies led to the clinical candidate **41** (PF-915275) for the treatment of diabetes and metabolic disorders (Scheme 15).[32]

Scheme 16. Pyridine-based glucokinase activators.

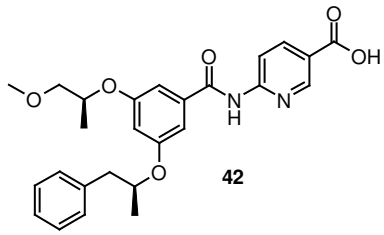

42

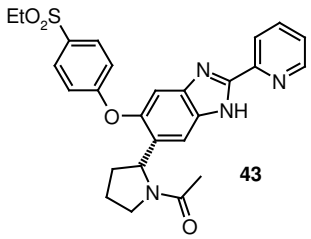

43

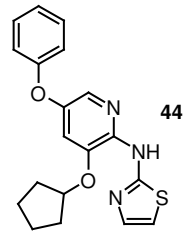

44

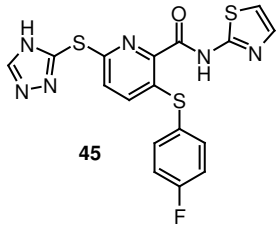

45

To date, several amide classes of glucokinase activators, including nicotinic acid derivative **42** (GKA50, AstraZeneca),[33] have been discovered, and some of these compounds have entered human clinical trials. Glucokinase catalyses the phosphorylation of glucose to glucose 6-phosphate in glucosensitive cells (Scheme 16). In pancreatic β-cells, this reaction is the rate-limiting step of insulin release. Small-molecule activators of GK that stimulate β-cell

physiology and subsequently enhance the glucose-dependent release of insulin are expected to be useful for the diabetes treatment.[34]

Besides of **42**, numerous further pyridine-based glucokinase activators recently appeared in the patent literature. A series of of 2-pyridine-benzimidazoles, represented by compound **43**, were intensively evaluated for the enzyme activation.[35] In 2008 Merck invented a series of pyridines delineated by **44** and most recently 2-pyridinecarboxamide derivatives represented by disulfanyl-pyridines **45**, as glucokinase-activating agents for the therapy of diabetes mellitus (Scheme 16).[36-37]

3. 2. 2 Inhibition of DPP-4 - a novel target for antidiabetics development.

In 1996 the first *in vivo* experiments indicated that dipeptidyl peptidase IV (DPP-4) inhibition resulted in improved glucose tolerance and could be used as an approach for the development of new treatment for type 2 diabetes.[38]

DPP-4 is a highly specific atypical serine protease, which specifically cleaves dipeptides from proteins and oligopeptides after a penultimate *N*-terminal proline or alanine. This enzyme was described in 1966 for the first time.[39] DPP-4 as a complex enzyme is released in almost all tissues and organs. It is expressed on the surface of most cell types and can also be found in plasma and urine. By its important modulatory activity on a number of chemokines, neuropeptides, and peptide hormones it is associated, among other processes, with immune regulation, signal transduction, and apoptosis.[29,40] Plasma DPP-4 rapidly deactivates incretins.

Incretin hormones, glucose dependent insulinotropic peptide (GIP) and glucagon-like peptide 1 (GLP-1), are defined as intestinal hormones released in response to nutrient ingestion, which potentiate the glucose-induced insulin response (the incretin effect).[41] A higher activity of the incretin hormones should result in an increase of the insulin secretion and counterbalance the problems in non-insulin dependent diabetes. But because of the short *in vivo* half-life of about 1.5 min[42] it is not useful to administrate the GLP-1 as it is. Therefore the synthesis of DPP-4 resistant incretin mimetics, like exenatide was a promising approach. But these therapeutic agents as well as synthetic GLP-1 have to be administered parenterally, cause some side effects and are only approved in combination with other oral antidiabetic agents.[43]

Another therapeutic approach regarding the incretin-effect, the inhibition of DPP-4, has been shown to be able to prolong the beneficial effects of primarily GLP-1 and GIP by stabilizing the intact (active) form of the hormones.[44] The longer activity of the incretins like GLP-1 permits an increased secretion of insulin and inhibits the glucagon release, which in turn decreases the chronically high blood glucose to near-normal levels, shown by HbA_{1c} values. It could also be proven that a higher GLP-1 level protects the remaining pancreatic β-cells, increases their activity and promotes their growth resulting in an increasing number and mass of ß cells. By slowing the rate of gastric emptying and promoting the satiety, GLP-1 is also useful for reduction of the caloric intake and in this turn for weight reduction. Since the activity of incretin hormones depends on the blood glucose level, there is a lower risk of hypoglycemia, compared to conventional anti-diabetic agents.[41]

Owing the impressive antidiabetic actions of GLP-1, targeting both fasting and prandial glucose concentrations, an effective inhibition of DPP-4 became a pathway for treatment of diabetes, particularly non-insulin dependent diabetes and related diseases. Since GLP-1 inhibits the glucagon release also, inhibitors of DPP-4 should also be usable for the treatment of type I diabetes.

When in 1996 the first *in vivo* experiments indicated that DPP-4 inhibition results in improved glucose tolerance, an elevated interest in the inhibition of DPP-4 enzyme for treatment of diabetes was observed.[45]

Extensive research efforts from both the academia and the pharmaceutical industry have led to launch of Sitagliptin **46** (2006, Merck & Co. Inc.),[45c,46a] Vildagliptin **47** (2007, Novartis AG)[46b] and Saxagliptin **48** (2009, Brystol-Myers Squibb Co.) (Scheme 17).[46c]

Scheme 17. Launched DPP-4 inhibitors.

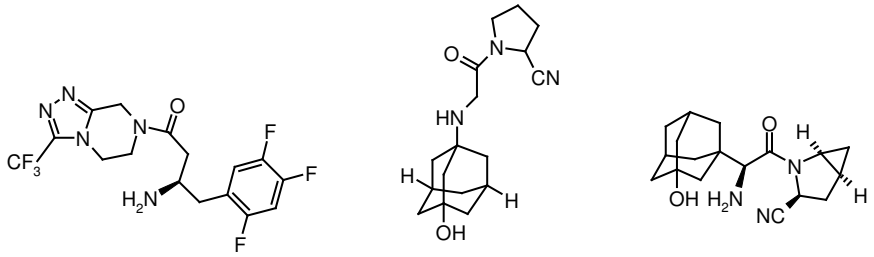

46 **47** **48**

Nevertheless, continuing search for small molecules as potent and selective orally available inhibitors remains a major challenge and is indicated by an explosion of patents and publications regarding a big variety of scaffolds, in particular from pharmaceutical industry. A

lot of efforts were made to prolong the stability and the long-acting potential of conventional DPP-4 inhibitors.[47] Also some approaches were made on the base of crystal structure analysis by target-oriented design.[48] A comprehensive review about the recent approaches in medicinal chemistry to the inhibition of DPP-4 for treatment of type II diabetes is given by Havale and Pal.[43] Many DPP-4 inhibitors were developed before the discussion on potential toxicity due to the inhibition of other members of DPP family resulting in unforeseen side effects and low tolerance.[49] In this context especially two closely related proteases, DPP-8 and DPP-9, were recently investigated intensively. The high degree of sequence homology between DPP-8, DPP-9 and DPP-4 makes selective inhibitor design a challenging task.[50] It has become necessary to design not only potent, but also more selective inhibitors targeting DPP-4.

First DPP-4 inhibitors based on the pyridine backbone appeared just after evaluating the DPP-4 as a target for diabetes treatment.

In 1999, Novartis reported modification of the previously described DPP-4 inhibitors, *L*-amino acids with *N*-terminal primary amine in the P-2 site. Validation of pyridine collections led to the selection of the slow binding inhibitor **49** (NVP-DPP728) as a clinical development candidate for type 2 diabetes (Scheme 18).[51]

Scheme 18. Structure of NVP-DPP728 **49**.

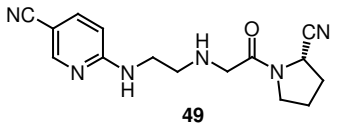

49

In 2006, Abbott Laboratories introduced **50** based on **49**. SAR of substitutions at the C5 position of the 2-cyanopyrrolidide led to an extremely potent (K_{iDPP-4} = 1.0 nM) and selective (K_{iDPP-8} > 30 μM) clinical candidate, ABT-279 **50**, that is orally available, efficacious, and remarkably safe in preclinical safety studies (Scheme 19).[51c,52]

Scheme 19. Clinical candidate **50** for type 2 diabetes treatment.

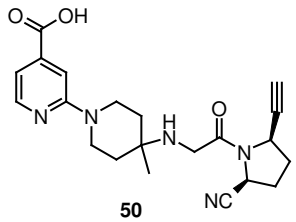

50

In 2003, F. Hoffmann-La Roche AG reported compounds of formula **51**.[53a] The most active compound, a substituted pyrimidine **51a** had IC_{50} value in picomolar range (Scheme 20).

Scheme 20. Series of pyridines and pyrimidines **51** and **52** developed by F. Hoffmann-La Roche AG.

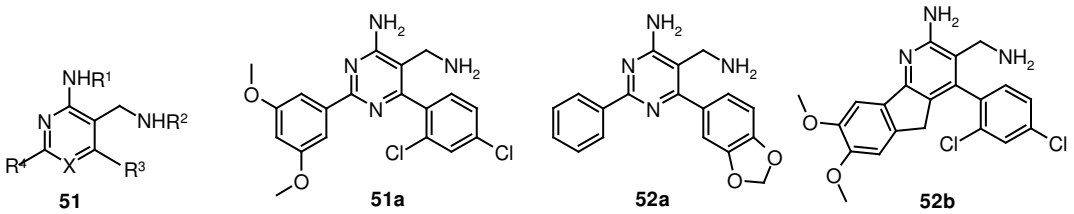

Further studies made at F. Hoffmann-La Roche AG, starting from another weakly active pyrimidine screening hit **52a**, were focused on the optimization of the aromatic ring itself, its substitution and conformational restrictions. The structure optimization resulted in the discovery of the potent DPP-4 inhibitor, pyridine **52b** (Scheme 20).[53b]

A 2005 patent by Takeda (Japan) disclosed a series of pyridine-based DPP-4 inhibitors **53**[54a-b] and in 2006 a second series of pyridyl acetic acid derivatives **54**.[54c] Substituted 3-aminomethyl pyridines give high flexibility regarding the position 5 on the ring without significant influence on the DPP-4 inhibitory activity (**53a-c**, **54**, Scheme 21).

Scheme 21. Pyridine-based DPP-4 inhibitors **53** and **54** investigated by Takeda.

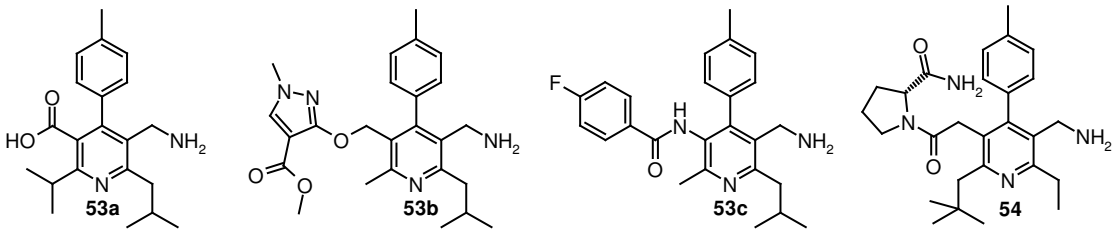

In 2006, another series of pyridines **55** was patented by Eli Lilly & Co as DPP-4 inhibitors.[55] One of the most active analogues is shown on the scheme 22.

Scheme 22. Structure of the representative potent DPP-4 inhibitor-pyridine **55**.

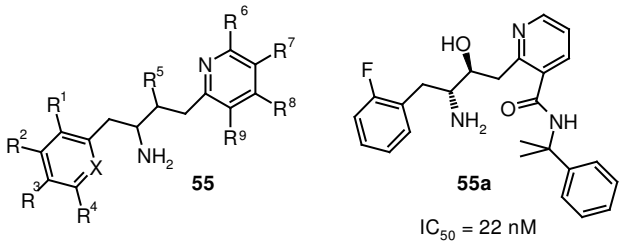

The same year, Bristol-Myers Squibb Company reported pyrrolopyridine-based inhibitors of DPP-4 **56**, and methods to synthesize them (Scheme 23).[56a]

Scheme 23. Bicyclic pyridines - DPP-4 inhibitors.

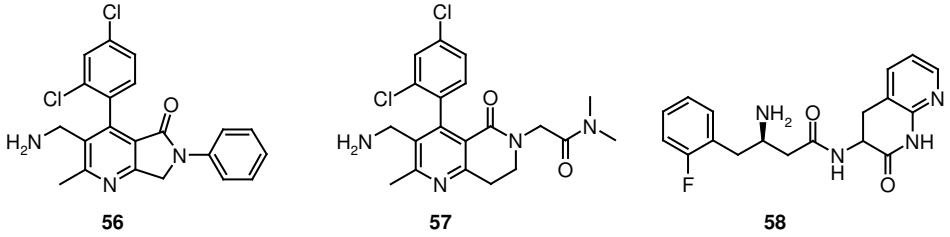

56 **57** **58**

Most recently, Bristol-Myers Squibb Company extended the previous invention to 6-membered rings. The patented series exhibit high inhibitory activity, and **57** was one of most active analogs (IC_{50} = 2 nM).[56b] Simultaneously AstraZeneca reported **58**, based on dihydro-1*H*-[1,5]naphthyridin-2-one ring as an active DPP-4 inhibitor (Scheme 23).[57]

In recent years a remarkable progress has been made towards understanding the biology of DPP family and incretins action. The improvement has been reflected in the number of creative publications and reviews. First group of early DPP-4 inhibitors were dipeptidomimetic compounds bearing structural resemblance to the *N*-terminal dipeptide of the enzyme substrates. The use of high throughput screening in combination with rational drug design has resulted in discovery of diverse classes of inhibitors. Among them pyridines incessantly attract attention of the pharmaceutical industry by serving as a promising scaffold for the development of novel therapeutics.

4. Results and disscusion.

4. 1 Random collection of pyridines and pyrazolopyridines.

4. 1. 1 Solid phase synthesis of pyridines and pyrazolopyridines.

As a key intermediate in the synthetic pathway, commercially available or easily accessible (*E*)-2-oxo-4-aryl-but-3-enoic acids **59**[58] and (*E*)-4-oxo-4-aryl-but-2-enoic acids **60** were chosen (Scheme 24).[59]

Scheme 24. General structures of the intermediates.

Although the addition of various amines to the related chalcones is well documented,[60] the synthesis of dicarbonyl systems of **59** and **60** has been poorly studied. From the synthetic point of view it would therefore be interesting to evaluate the possibilities to access various heterocyclic compounds such as pyridines, pyrazolopyridines, or pyrimidines using unsaturated ketoacids **59** and **60**.

Scheme 25. The synthetic pathways.

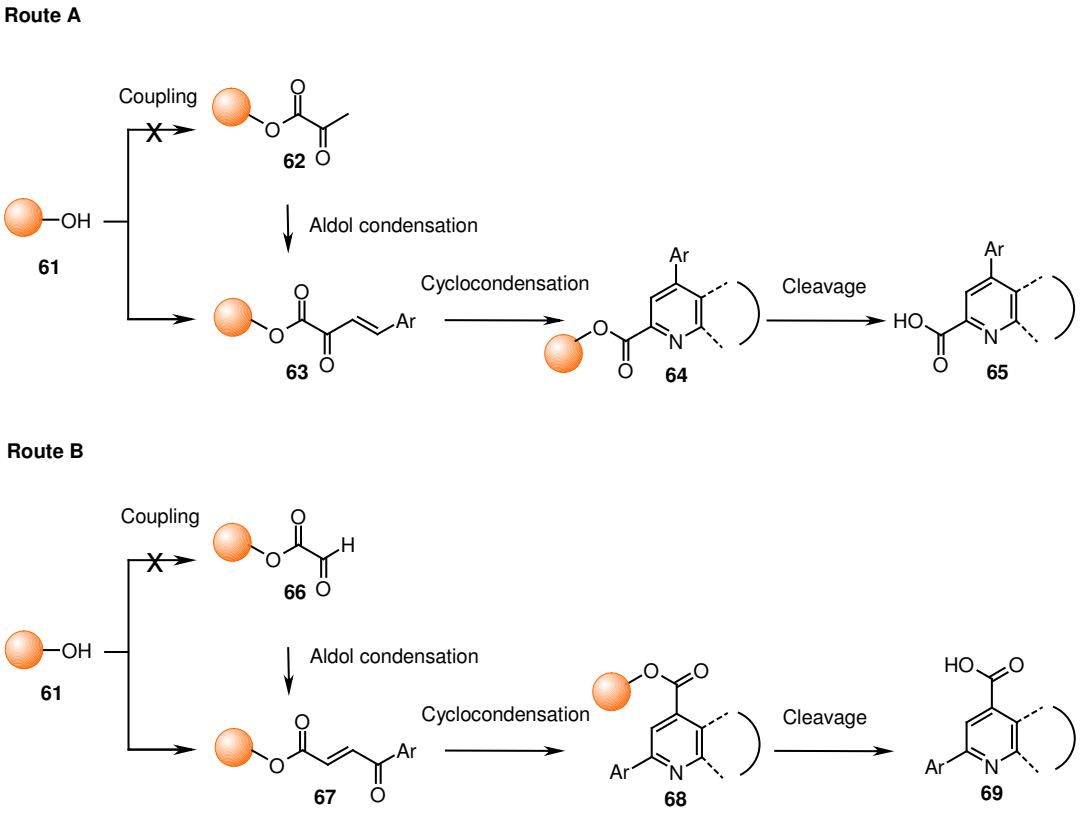

Cyclization reactions leading to the final ring constructions often require harsh conditions, such as high temperatures or low pH, therefore Wang resin was chosen to be the most appropriate solid support as it is characterized by high physical stability and its compatibility with a range of reaction conditions.[62]

The approach was initiated by the synthesis of the intermediates **59** and **60** on a solid support. However, the attempted coupling of the pyruvic acid or glyoxylic acid to the resin **61** using various coupling reagents and bases failed, although attachment of the carboxylic acids to the resin is well known and often used.[62] Therefore the pathways were modified by direct attachment of the intermediates **59** and **60** prepared in solution[58-59] to the Wang resin **61**. The resin was loaded with 50-90% efficacy to give **63** and **67** and no significant loss of the starting material purities (purity > 85% as proved by LC-MS analysis of the intermediate after cleavage). The next step of the synthesis was the cyclocondensation reaction of **63** and **67** with the appropriate amines to construct immobilized heterocycles **64** and **68** that, after cleavage, gave the desired products **65** and **69**.

Scheme 26. Synthesis of the pyridines **74** and pyrazolopyridines **78**.

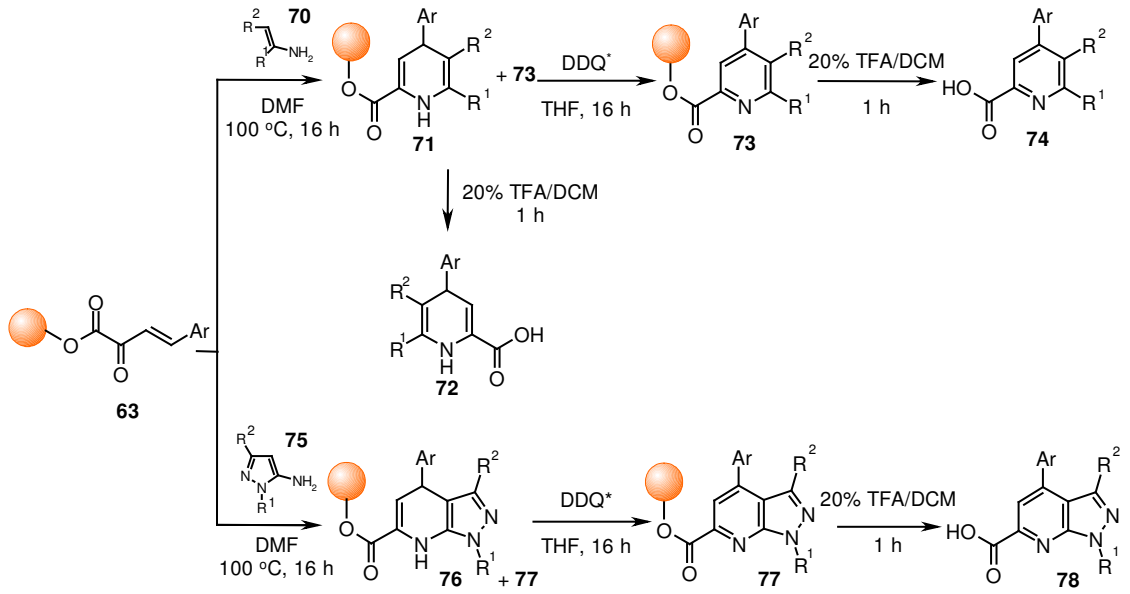

*Oxidation step used if required.

The pyridines **74** were synthesized by the cyclization of starting materials **63** with enamines **70** (Scheme 26). In the reaction with enamine **70** substituted with a keto group in position 2, the intermediates, dihydropyridines **71**, were stable enough to give **72** after cleavage from resin **71** (Table 1, **72a-b**). The compounds **71** were oxidized with DDQ at room temperature to give the desired pyridines **74** in good yields and purities after cleavage (Table 1, **74a-d**).

Compound **70** with a cyano group in position 2 reacted to give directly cyclocondensed products **73** and **74** after cleavage, thus the oxidation step could be avoided (Table 1, **74e-n**).

Table 1. Results of the synthesis of pyridines **72**, **74** and pyrazolopyridines **78**.

Compd	Ar	R^1	R^2	Yield (%)[a]	Purity (%)[b]
72a	4-Chloro-phenyl	Me	COMe	68	93
72b	4-Bromo-phenyl	Me	COMe	68	89
74a	4-Chloro-phenyl	Me	COMe	72	86
74b	2,4-Dichloro-phenyl	Me	COMe	85	87
74c	4-Bromo-phenyl	Me	COMe	93	80
74d	5-Chloro-thiophen-2-yl	Me	COMe	99	94
74e	3-Chloro-phenyl	Me	CN	74	80
74f	2,4-Dichloro-phenyl	Me	CN	80	99
74g	3,5-Dichloro-phenyl	Me	CN	99	76
74h	4-Bromo-phenyl	Me	CN	67	71
74i	4-Methoxy-phenyl	Me	CN	73	86
74j	2,4-Dimethoxy-3-methyl-phenyl	Me	CN	38	84
74k	4-Dimethylamino-phenyl	Me	CN	56	78
74l	4,5-Dimethyl-furan-2-yl	Me	CN	60	84
74m	Thiophen-2-yl	Me	CN	40	93
74n	5-Chloro-thiophen-2-yl	Me	CN	38	73
78a	4-Fluoro-phenyl	Ph	Me	85	82
78b	3-Chloro-phenyl	Ph	Me	99	79
78c	2,4-Dichloro-phenyl	Me	Me	98	82
78d	2,4-Dichloro-phenyl	Ph	Me	79	99
78e	3,5-Dichloro-phenyl	Ph	Me	99	80
78f	4-Bromo-phenyl	Me	Me	99	88
78g	4-Bromo-phenyl	Ph	Me	84	91
78h	4-Methoxy-phenyl	Me	Me	84	75
78i	4-Methoxy-phenyl	Ph	Me	78	88
78j	2,4-Dimethoxy-3-methyl-phenyl	Me	Me	72	89
78k	4-Dimethylamino-phenyl	Ph	Me	80	77
78l	4,5-Dimethyl-furan-2-yl	Me	Me	72	85
78m	4,5-Dimethyl-furan-2-yl	Ph	Me	99	88
78n	Thiophen-2-yl	Me	Me	91	78
78o	5-Methyl-thiophen-2-yl	Ph	Me	73	76
78p	5-Chloro-thiophen-2-yl	Me	Me	28	80

[a]Yields refer to isolated products after cleavage from the resin.
[b]Purities were determined by HPLC-MS (210 - 400 nm) after cleavage from the resin.

The pyrazolopyridines **78** were prepared analogously by the cyclization step with pyrazoloamines **75** (Scheme 26). As it was previously reported,[63] the reaction proceeds *via* formation of dihydropyrazolopyridines **76**. The amount of non-aromatized **77** in the reaction

mixture after cleavage did not exceed 10%. Only synthesis of **78p** required oxidation with DDQ as the cyclization step gave a mixture of **76** and **77** in the ratio 1:1.

The products **72**, **74** and **78** were obtained in high yields and purities after the cleavage from the resin with 20% TFA in DCM (Table 1) and, if required, washing the products with acetonitrile (for **72**, **78**) or with diethyl ether (for **74**).

In an analogous manner solid supported intermediates **67** were used to approach **81** and **85** (Scheme 27).

Scheme 27. Synthetic pathway for the synthesis of **81** and **85**.

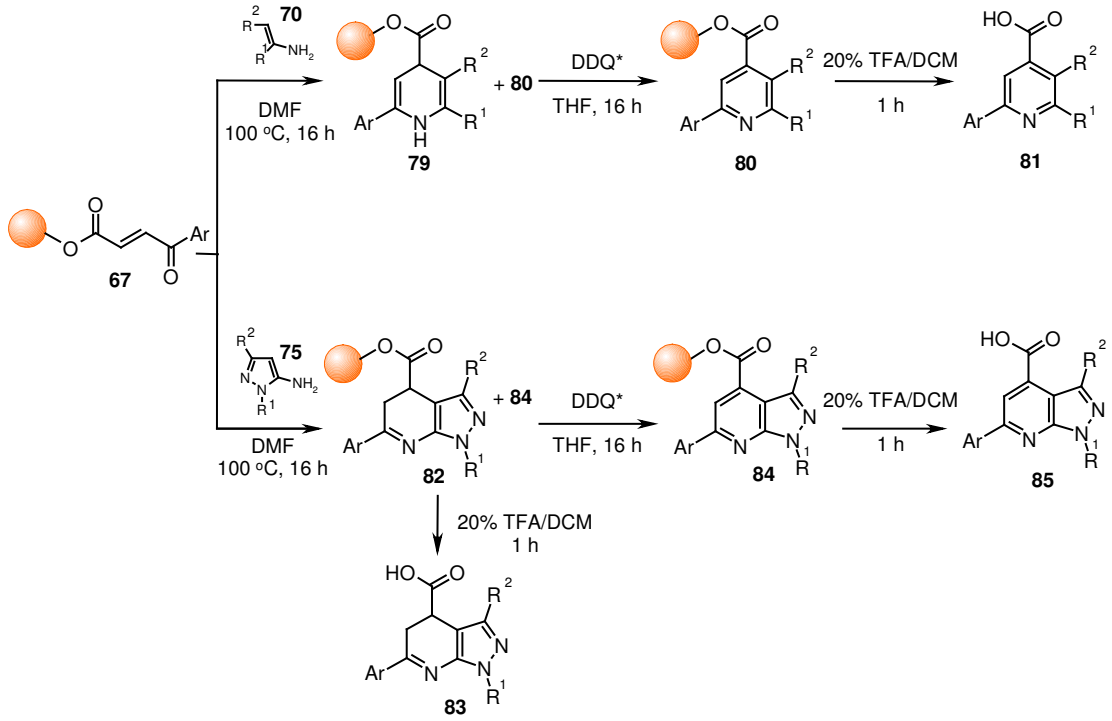

*Oxidation step used if required.

Synthesis of pyridines **81** required the oxidation step only after reaction with enamine **70** bearing keto group in position 2. To increase purities of pyrazolopyridines **85** oxidation was necessary as the amount of non-aromatized **82** in the reaction mixture usually exceeded 40%. In case of **67** substituted with a furan or thiophene ring, the intermediates **82** were first formed exclusively, which allowed isolation and characterization of **83a** and **83b**.

The products **81**, **83** and **85** were obtained in high yields and in most cases excellent purities (Table 2). To increase the purity washing with acetonitrile or diethyl ether was sufficient.

Table 2. Results of the synthesis of pyridines **81** and pyrazolopyridines **83** and **85**.

Compd	Ar	R^1	R^2	Yield (%)[a]	Purity (%)[b]
81a	2,4-Dichloro-phenyl	Me	COMe	88	73
81b	4-Bromo-phenyl	Me	COMe	36	84
81c	2,4-Dichloro-phenyl	Me	CN	80	72
83a	Furan-2-yl	Ph	Me	56	90
83b	Thiophen-2-yl	Ph	Me	88	99
85a	4-Fluoro-phenyl	Me	Me	89	88
85b	4-Fluoro-phenyl	Ph	Me	58	79
85c	3-Chloro-phenyl	Me	Me	73	87
85d	2,4-Dichloro-phenyl	H	Me	75	79
85e	2,4-Dichloro-phenyl	Me	Me	72	89
85f	2,4-Dichloro-phenyl	Ph	Me	55	99
85g	3,4-Dichloro-phenyl	Me	Me	80	83
85h	3,4-Dichloro-phenyl	Ph	Me	56	71
85i	4-Bromo-phenyl	Me	Me	49	82
85j	4-Bromo-phenyl	Ph	Me	24	95
85k	Furan-2-yl	Me	Me	65	79
85l	Furan-2-yl	Ph	Me	57	63
85m	Thiophen-2-yl	Me	Me	99	96
85n	Thiophen-2-yl	Ph	Me	54	86

[a]Yields refer to isolated products after cleavage from the resin.
[b]Purities were determined by HPLC-MS (210 - 400 nm) after cleavage from the resin.

The conditions identical to those previously described for pyridines **74**, **81** and pyrazolopyridines **78**, **85** were used to generate pyrimidine and fused pyrimidine ring systems. The intermediates **63** were reacted with amines, and series of pyrimidines **86**, pyrazolopyrimidine **88**, benzo-imidazopyrimidine **90** and triazolopyrimidine **92** were obtained in excellent yields and purities (Scheme 28). The cyclization with isonicotinamidine after heating in DMF for 16 hours afforded **86**. In case of the reaction with pyrazol-3-ylamine**,** benzoimidazol-2-ylamine and triazol-3-ylamine only non-aromatized compounds were formed and the dihydro-derivatives **87**, **89** and **91** were isolated and characterized. In contrary, the attempts to prepare a collection of the regioisomers using the intermediate **67** failed. In most of the cases the reaction mixtures contained less than 40% of the expected products.

Scheme 28. Synthesis of pyrimidines.

	Ar	R	Yield (%)[a]	Purity (%)[b]
86a	2-Fluoro-phenyl	Pyridin-4-yl	67	83
86b	4-Chloro-phenyl	Pyridin-4-yl	92	86
87a	4-Chloro-phenyl	-C(O)OEt	90	79
87b	4-Bromo-phenyl	-C(O)OEt	79	96
87c	5-Chloro-thiophen-2-yl	-C(O)OEt	68	81
88a	4-Chloro-phenyl	-C(O)OEt	86	91
88b	4-Bromo-phenyl	-C(O)OEt	79	82
89a	4-Chloro-phenyl		83	82
89b	4-Bromo-phenyl		82	95
89c	5-Chloro-thiophen-2-yl		92	88
90a	4-Chloro-phenyl		65	91
90b	4-Bromo-phenyl		96	91
90c	5-Chloro-thiophen-2-yl		86	90
91a	4-Chloro-phenyl		87	86
91b	4-Bromo-phenyl		81	93
91c	5-Chloro-thiophen-2-yl		70	80
92a	4-Chloro-phenyl		82	89
92b	4-Bromo-phenyl		63	82
92c	5-Chloro-thiophen-2-yl		74	98

1) DMF, 100 ˚C, 16 h. 2) DDQ, THF, rt, 16 h. [a]Yields refer to isolated products after cleavage from the resin. [b]Purities were determined by HPLC-MS (210 - 400 nm) after cleavage from the resin.

4. 1. 2 Synthesis of pyridine derivatives in solution.

The substitution pattern of the pyridines **74** and **81** offer a number of possibilities of further modifications. The most interesting derivatives concerning their potential antifungal[64-65] activity and their novelty as building blocks were chosen using literature database search. Initially identical modifications of **74** and **81** were planned to achieve a set of regioisomers differing on position 2 and 4 in the pyridine ring. The reactivity of **74** and **81** restricted the number of compounds (Scheme 29).

Scheme 29. Modifications of the pyridines **74** and **81**.

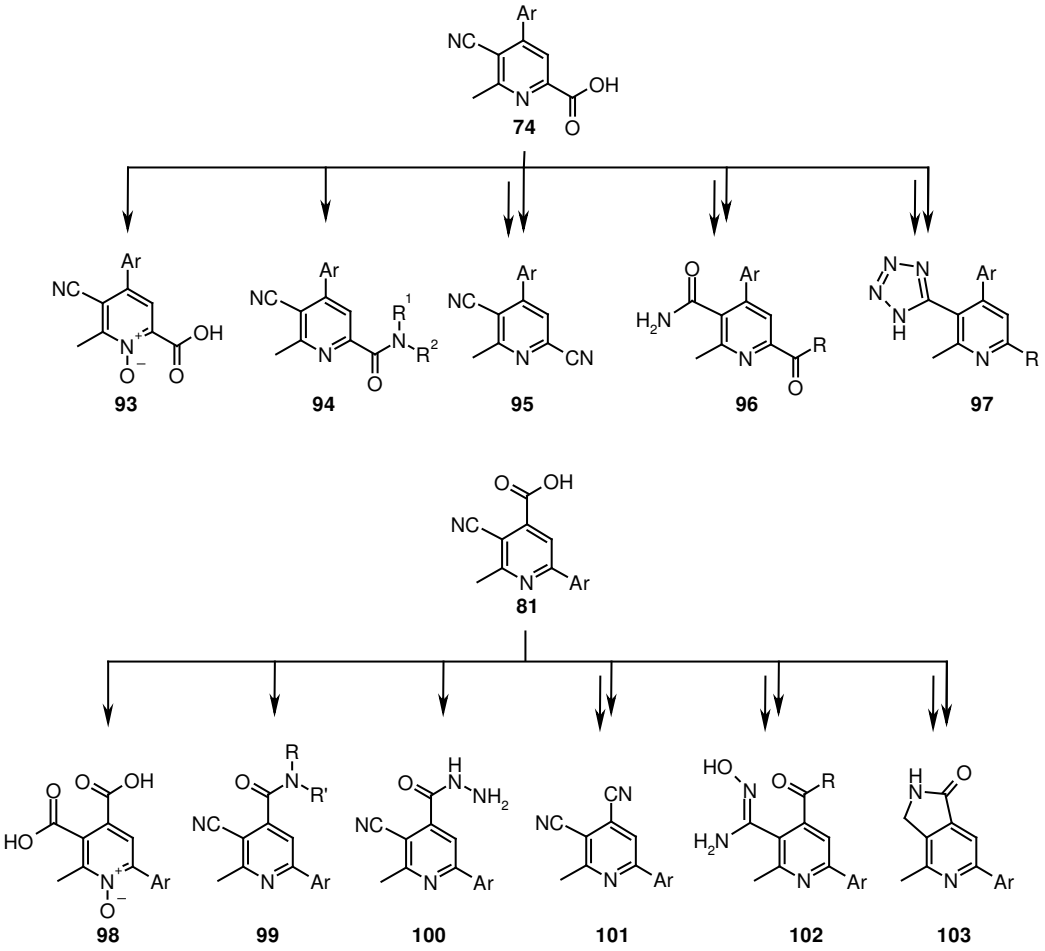

One of the chosen modifications was the synthesis of pyridine *N*-oxides **93** and **98**. The chemistry and applications of heterocyclic *N*-oxides receive much attention due to their application as synthetic intermediates or as protecting groups, oxidants, ligands in metal complexes and catalysts but also due to their biological importance.[64c] The pyridine amides **94**, **96** and **99** are related with vitamins (niacin), as well as other active pyridine-based molecules such as phenoxynicotinamide **104**, a herbicide, and were used in this dissertation as

intermediates (Scheme 30). The structures of dicyanopyridines **95** and **101**, are close to those of fungicides such as pyridinitrile **10**. Tetrazolyl-pyridines, carboxyhydrazides, as well as pyridine derivatives with hydroxyamidine motif are known as well for their pharmacological activity,[65] thus **97**, **100** and **102** were prepared. The presence of the cyano next to the carboxy group in **81** gave the opportunity for the generation of the fused ring system as in the pyrrolopyridines **103**, that is related to the adenosine receptor agonist **105** (Scheme 30).

Scheme 30. Example of the active pyridines.

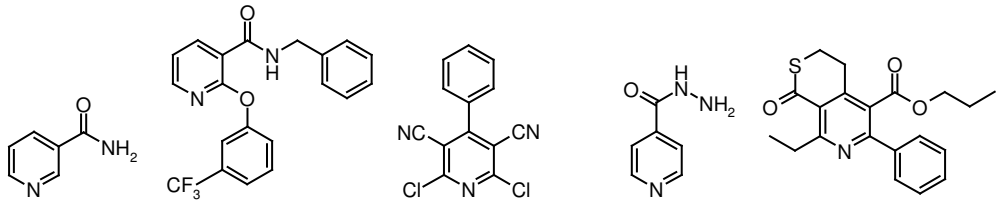

Although solid phase protocols have a number of advantages, one of the main disadvantages of the method is the limitation in scaling up the synthesis. As the amount of the starting materials **74** and **81** needed for evaluation and then synthesis of the derivative collections was in the gram range, the protocols in solution had to be established.

4. 1. 2. 1 Synthesis of pyridine carboxylic acids.

Treatment of (*E*)-2-oxo-4-aryl-but-3-enoic acids **59** with potassium *t*-butoxide in acetonitrile at ambient temperature afforded pyridines **74** in good yields (Scheme 31).

The formation of the product proceeds by condensation of **59** with β-aminocrotonitrile **70a** generated *in situ*. When the reaction was performed in dichloromethane or in tetrahydrofuran with commercially available β-aminocrotonitrile, no improvement of the yield or the reaction time was observed. Depending on the substitution pattern of the aromatic ring, full conversion required 3-16 hours. The increase of the amount of *t*-butoxide did not significantly influence the reaction time. The ketoacids **59** with phenyl ring substituted with bromine in *para* position did not react at the described conditions.

Usage of (*E*)-4-oxo-4-aryl-but-2-enoic acids **60** under the same reaction conditions allows substituent flexibility at the position 2- and 4- of the target molecule **1**. Compounds **60** reacted with β-aminocrotonitrile **70a** to give the regioisomers **81** in good to excellent yields.

Scheme 31. Solution phase synthesis of pyridines **74**.

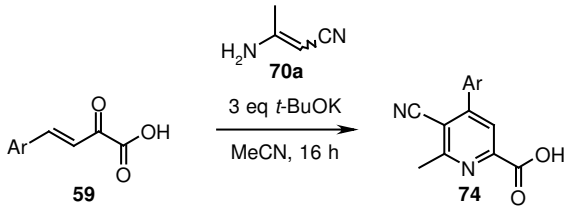

Compd	Ar	Yield (%)
74m	2-Fluoro-phenyl	61/51*
74n	4-Fluoro-phenyl	66
74o	2,4-Difluoro-phenyl	30*
74e	3-Chloro-phenyl	60
74p	4-Chloro-phenyl	73
74f	2,4-Dichloro-phenyl	40*
74r	3,4-Dichloro-phenyl	42
74s	2,6-Dichloro-phenyl	81
74i	4-Methoxy-phenyl	71/50*
74t	Benzo[1,3]dioxol-5-yl	62
74k	4-Dimethylamino-phenyl	87
74u	Furan-2-yl	29*
74m	Thiophen-2-yl	62
74w	Thiophen-3-yl	60*

*Yields refer to 20 mmol scale; 1.5 eq of *t*-BuOK was used in case of **74n** and **74f**; compounds isolated by crystallization.

Scheme 32. Solution phase synthesis of pyridines **81**.

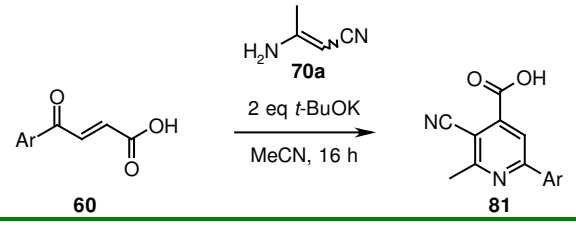

Compd	Ar	Yield (%)
81d	4-Fluoro-phenyl	74
81e	2,4-Difluoro-phenyl	30*
81f	2-Fluoro-4-chloro-phenyl	40
81g	3-Chloro-phenyl	67
81h	4-Chloro-phenyl	86
81c	2,4-Dichloro-phenyl	81/65*
81i	3,4-Dichloro-phenyl	54
81j	4-Bromo-phenyl	72/35*
81k	4-Methoxy-phenyl	81/55*
81l	Furan-2-yl	63
81m	Thiophen-2-yl	61

*Yields refer to 20 mmol scale, 1.5 eq of *t*-BuOK was used; compounds isolated by crystallization.

Similarly, for **59** differences in the reactivity depending on the substitution of the aromatic ring were observed. Nevertheless, 16 hours were sufficient for the full conversion. Two equivalents of potassium *t*-butoxide were used, because an increase of the amount of base lead to the formation of byproducts. As for the synthesis of the regioisomers **74**, reactions in dichloromethane or tetrahydrofuran with commercially available *β*-aminocrotonitrile did not improve reaction times and yields of the pyridines **81**. It was observed that the cyano group of the regioisomers **81** is particularly sensitive and its hydrolysis appeared during acidic workup. Therefore water free 4M HCl/dioxane was used.

The procedure was easily scaled up to 20 mmol and the products were isolated in good yields by crystallization from acetonitrile (Scheme 31: **74m**, **74o**, **74f**, **74i**, **74u**, **74w**; Scheme 32: **81d**, **81c**, **81k**).

Scheme 33. Synthesis of 2-aryl pyridines **81** - the mechanism.

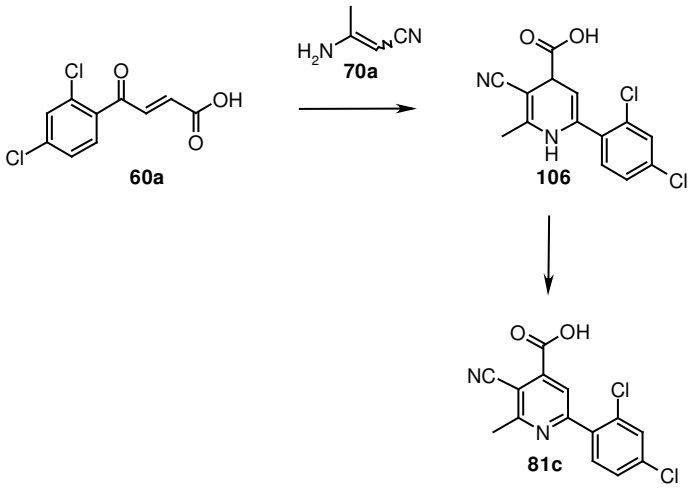

The formation of products **74** and **81** can be described as cyclocondensation reactions of the corresponding substrates **59** and **60** with *β*-aminocrotonitrile **70a**. The enamine **70a** is formed *in situ* by dimerization of acetonitrile catalyzed by potassium *t*-butoxide. Within the first hour **60a** gave the intermediate/dihydropyridine **106**, which slowly aromatised to the pyridine **81c** (Scheme 33). The aromatization proceeded even under argon atmosphere.

4. 1. 2. 2 Synthesis of pyridine carboxylic acid *N*-oxides.

The pyridines were readily converted to the corresponding *N*-oxides **93** and **98** as outlined in Scheme 34.[64c] 2-Aryl pyridines **74** reacted only at higher temperature. At 100 °C *N*-oxide

formation of **81** was observed as well as hydrolysis of the cyano group to the corresponding pyridine dicarboxylic acid **98**. The derivatives were isolated in very good yields.

Scheme 34. Results of the *N*-oxides synthesis.

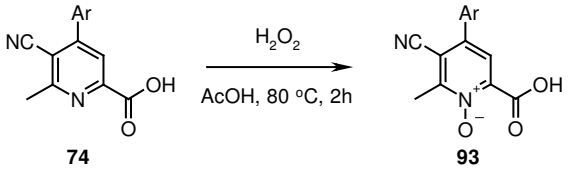

Compd	Ar	Yield (%)
93a	2-Fluoro-phenyl	62
93b	4-Fluoro-phenyl	60
93c	4-Chloro-phenyl	50
93d	2,4-Dichloro-phenyl	56
93e	4-Methoxy-phenyl	88

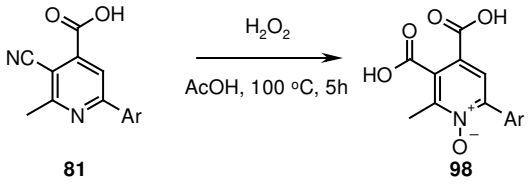

Compd	Ar	Yield (%)
98a	4-Fluoro-phenyl	90
98b	4-Chloro-phenyl	75
98c	2,4-Dichloro-phenyl	88
98d	3,4-Dichloro-phenyl	65
98e	4-Methoxy-phenyl	82

4. 1. 2. 3 Synthesis of pyridine carboxylic acid amides.

Pyridine carboxylic acides **74** and **81** were amidated with amines using benzotriazol-1-yl-oxytripyrrolidinophosphonium hexafluorophosphate (PyBOP) as coupling reagent (Scheme 35-36) to give **94** and **99** respectively. Both regioisomers were isolated in excellent yields.

Scheme 35. Results of the amidation of pyridine-2-carboxylic acids to amides **94**.

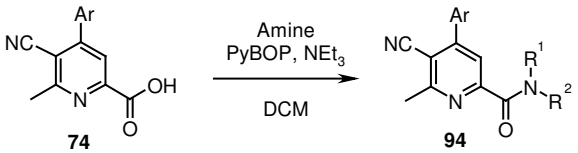

Compd	Ar	R^1	R^2	Yield (%)
94a-1	2-Fluoro-phenyl	H	H	90
94a-2	2-Fluoro-phenyl	Me	H	89
94a-3	2-Fluoro-phenyl	Cyclopropyl	H	99
94a-4	2-Fluoro-phenyl	Pyrrolidin-1-yl		95
94a-5	2-Fluoro-phenyl	Morpholin-4-yl		89
94a-6	2-Fluoro-phenyl	1-Piperidine-4-carboxylic acid ethyl ester		90
94b-1	4-Fluoro-phenyl	Cyclopropyl	H	94
94b-2	4-Fluoro-phenyl	Pyrrolidin-1-yl		99
94c-1	2,4-Difluoro-phenyl	H	H	86
94c-2	2,4-Difluoro-phenyl	Me	H	75
94c-3	2,4-Difluoro-phenyl	Acetic acid methyl ester	H	82
94c-4	2,4-Difluoro-phenyl	Cyclopropyl	H	81
94c-5	2,4-Difluoro-phenyl	Me	Me	94
94c-6	2,4-Difluoro-phenyl	Pyrrolidin-1-yl		76

94c-7	2,4-Difluoro-phenyl	Morpholin-4-yl		87
94c-8	2,4-Difluoro-phenyl	1-Piperidine-4-carboxylic acid ethyl ester	H	76
94c-9	2,4-Difluoro-phenyl	5-Methyl-isoxazol-3-yl	H	71
94d-1	4-Chloro-phenyl	H	H	73
94d-2	4-Chloro-phenyl	Me	H	79
94e-1	2,4-Dichloro-phenyl	H	H	80
94e-2	2,4-Dichloro-phenyl	Me	H	83
94e-3	2,4-Dichloro-phenyl	Acetic acid methyl ester	H	99
94e-4	2,4-Dichloro-phenyl	Acetamide	H	99
94e-5	2,4-Dichloro-phenyl	Cyclopropyl	H	88
94e-6	2,4-Dichloro-phenyl	Me	Me	99
94e-7	2,4-Dichloro-phenyl	Pyrrolidin-1-yl		78
94e-8	2,4-Dichloro-phenyl	Morpholin-4-yl		81
94e-9	2,4-Dichloro-phenyl	1-Piperidine-4-carboxylic acid ethyl ester		87
94e-10	2,4-Dichloro-phenyl	5-Methyl-isoxazol-3-yl	H	85
94f	4-Bromo-phenyl	H	H	63
94g-1	4-Methoxy-phenyl	H	H	67
94g-2	4-Methoxy-phenyl	Me	H	60
94g-3	4-Methoxy-phenyl	Acetic acid methyl ester	H	93
94g-4	4-Methoxy-phenyl	Cyclopropyl	H	79
94g-5	4-Methoxy-phenyl	Me	Me	99
94g-6	4-Methoxy-phenyl	Pyrrolidin-1-yl		99
94g-7	4-Methoxy-phenyl	Morpholin-4-yl		99
94g-8	4-Methoxy-phenyl	1-Pyrrolidine-2-carboxylic acid methyl ester		80
94g-9	4-Methoxy-phenyl	1-Piperidine-4-carboxylic acid ethyl ester		99
94g-10	4-Methoxy-phenyl	3-Chloro-benzyl	H	99
94g-11	4-Methoxy-phenyl	3,4-Dichloro-benzyl	H	99
94g-12	4-Methoxy-phenyl	Thiophen-2-ylmethyl	H	81
94g-13	4-Methoxy-phenyl	Thiazol-2-yl	H	79
94g-14	4-Methoxy-phenyl	2-Thiazol-4-yl-acetic acid ethyl ester	H	69
94g-15	4-Methoxy-phenyl	2,5-Dimethyl-2H-pyrazol-3-yl	H	99
94g-16	4-Methoxy-phenyl	5-Methyl-isoxazol-3-yl	H	26
94h	Benzo[1,3]dioxol-5-yl	H	H	99
94i-1	4-Trimethylamine-phenyl	Cyclopropyl	H	86
94i-2	4-Trimethylamine-phenyl	Pyrrolidin-1-yl		66
94j-1	Furan-2-yl	H	H	99
94j-2	Furan-2-yl	Me	H	99
94j-3	Furan-2-yl	Cyclopropyl	H	87
94j-4	Furan-2-yl	Me	Me	99
94j-5	Furan-2-yl	Pyrrolidin-1-yl		93
94j-6	Furan-2-yl	Morpholin-4-yl		99

94j-7	Furan-2-yl	Thiazol-2-yl	H	99
94k	Thiophen-2-yl	Pyrrolidin-1-yl		81
94l-1	Thiophen-3-yl	Cyclopropyl	H	86
94l-2	Thiophen-3-yl	Pyrrolidin-1-yl		80
94l-3	Thiophen-3-yl	Morpholin-4-yl		99

Scheme 36. Results of the amidation of pyridine-4-carboxylic acids **81** to amides **99**.

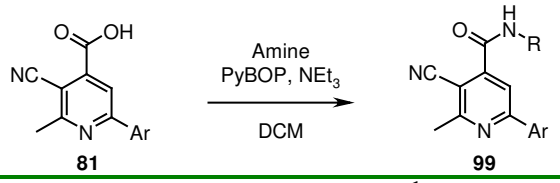

81 **99**

Compd	Ar	R^1	R^2	Yield (%)
99a-1	4-Fluoro-phenyl	Pyrrolidin-1-yl		68
99a-2	4-Fluoro-phenyl	5-Methyl-isoxazol-3-yl	H	99
99b-1	4-Chloro-phenyl	H	H	99
99b-2	4-Chloro-phenyl	Acetic acid methyl ester	H	80
99b-3	4-Chloro-phenyl	Cyclopropyl		95
99b-4	4-Chloro-phenyl	Me	Me	80
99b-5	4-Chloro-phenyl	Pyrrolidin-1-yl		99
99b-6	4-Chloro-phenyl	Morpholin-4-yl		92
99b-7	4-Chloro-phenyl	1-Piperidine-4-carboxylic acid ethyl ester	H	99
99c	2-Fluoro-4-Chloro-phenyl	Me	H	85
99d-1	2,4-Dichloro-phenyl	H	H	89
99d-2	2,4-Dichloro-phenyl	Pyrrolidin-1-yl		90
99d-3	2,4-Dichloro-phenyl	Morpholin-4-yl		83
99e	3,4-Dichloro-phenyl	H	H	99
99f-1	4-Methoxy-phenyl	H	H	99
99f-2	4-Methoxy-phenyl	Pyrrolidin-1-yl		89
99f-3	4-Methoxy-phenyl	3,4-Dichloro-benzyl	H	99
99g	Thiophen-2-yl	H	H	86

4. 1. 2. 4 Synthesis of pyridine hydrazides.

The attempts to form the hydrazide directly from acids **74** failed. Compounds **74** were not reactive in aqueous solution of hydrazine at 100 °C and occurred to be unstable at higher temperatures. The carboxylic acids **81**, however, were successfully reacted with hydrazine to give the hydrazides **100** in excellent yield (Scheme 37).[66]

Scheme 37. Synthesis of pyridine hydrazides **100**.

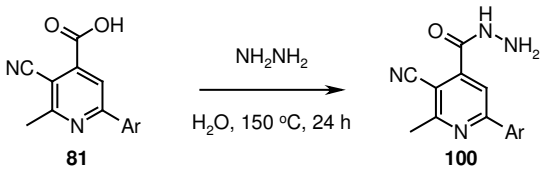

Compd	Ar	Yield (%)
100a	4-Chloro-phenyl	94
100b	3,4-Dichloro-phenyl	75

4. 1. 2. 5 Synthesis of dicyanopyridines.

The dicyanopyridines **95** and **101** were synthesized in high yields by dehydration of the primary amides **94** and **99** respectively with phosphorous oxychloride (Scheme 38).[67] All products were isolated by a fast filtration on silica gel in very good yields.

Scheme 38. Dehydration of pyridine primary amides.

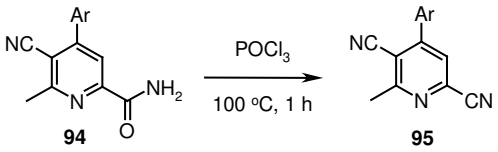

Compd	Ar	Yield (%)
95a	2-Fluoro-phenyl	79
95b	2,4-Difluoro-phenyl	70
95c	4-Chloro-phenyl	86
95d	2,4-Dichloro-phenyl	99
95e	4-Bromo-phenyl	94
95f	Benzo[1,3]dioxol-5-yl	99

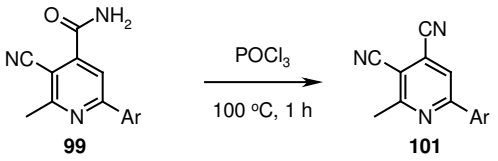

Compd	Ar	Yield (%)
101a	4-Chloro-phenyl	84
101b	2,4-Dichloro-phenyl	80
101c	3,4-Dichloro-phenyl	75
101d	4-Methoxy-phenyl	99

4. 1. 2. 6 Synthesis of nicotinic amides.

The cyano group of **74** hydrolyzed to the amides **96** when heated in water at 100 ^{o}C for 3 hours. The amide **94g-11** could be converted to the diamide **96e** using the same conditions. The nicotinic amides **96** were isolated by a simple extraction and directly characterized (Scheme 39). Surprisingly, neither the carboxylic acids **81** nor their amides **99** hydrolyzed to the expected amides and started to decompose when the temperature was raised to 120 ^{o}C.

Scheme 39. Nicotinic amides **96** from cyanopyridines.

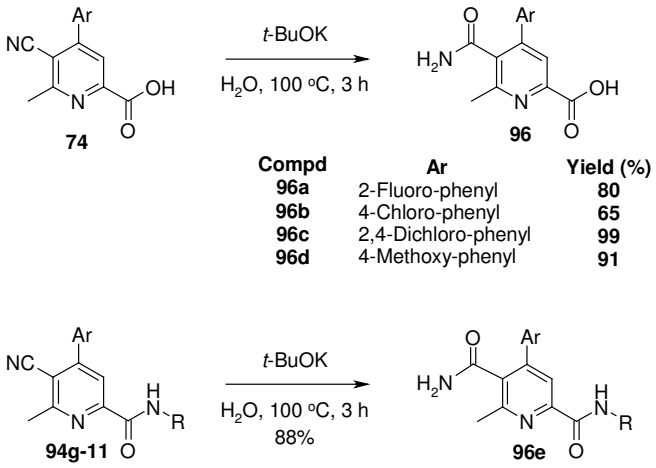

4. 1. 2. 7 Synthesis of pyridine *N*-hydroxyamidines.

In order to form *N*-hydroxyamidines, cyanopyridines **94** and **99** were treated with hydroxylamine and potassium *t*-butoxide in dimethyl sulfoxide at 100 °C (Scheme 40, 43).[68]

Scheme 40. Synthesis of *N*-hydroxyamidines.

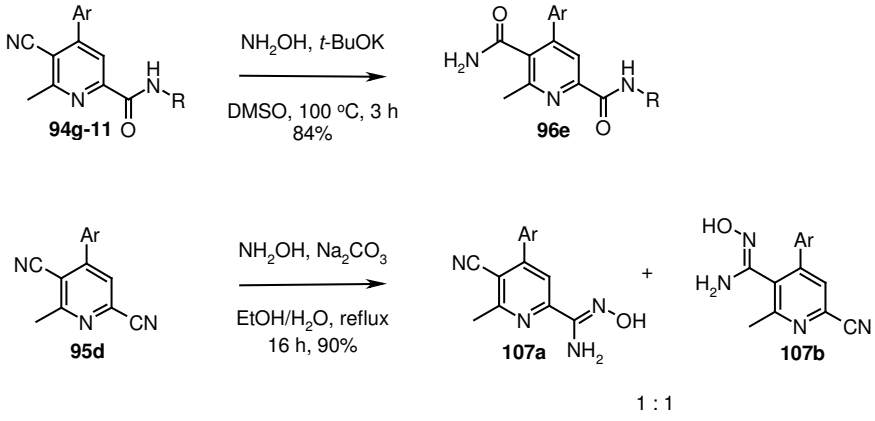

The regioisomers **94** appeared to be sensitive to the conditions and hydrolysed to give the diamide **96e** although water free conditions were used. Any other combination of bases and solvents did not lead to the formation of the hydoxyamidines from **94**. Additionally it was observed, that 4-aryl pyridines **74** with free carboxy groups stayed unaffected under the described conditions, but their regioisomers, 2-aryl pyridines **81** with carboxy group in position 4 decomposed.

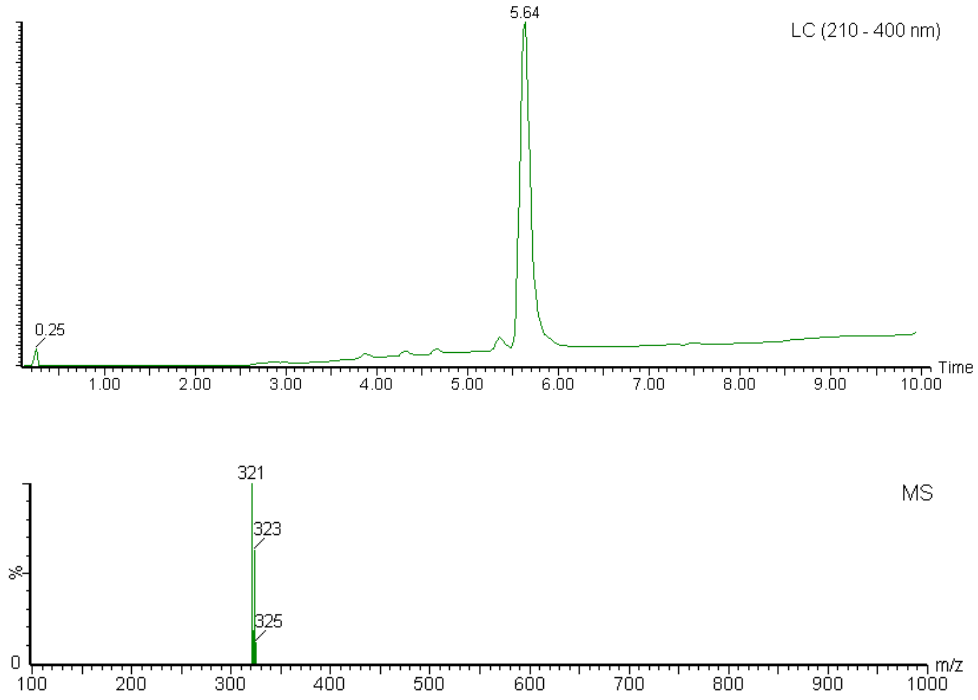

Figure 1. LC-MS data for pyridine derivative **107** (MW 321.17).

Contrary to the amides **94**, dicyanopyridine **95d** reacted when refluxed with hydroxylamine and sodium carbonate to give a mixture of **107a** and **107b**. The chromatogram (210-400 nm) showed one main peak of **107** (Figure 1). ^{1}H and ^{13}C NMR analysis however indicated the mixture of **107a** and **107b** in ratio 1:1 (Figure 2, doubled signals).

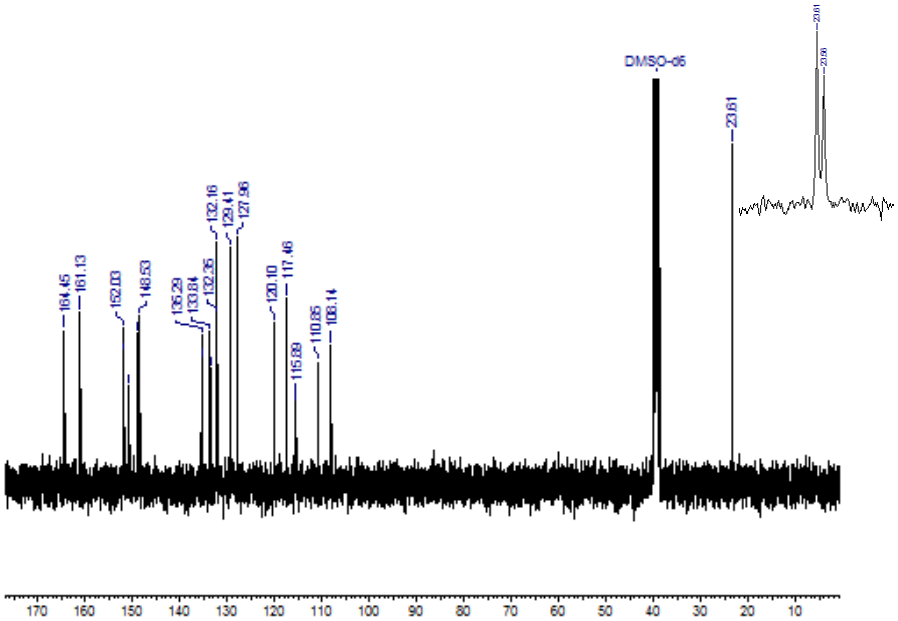

Figure 2. ^{13}C NMR experiment for pyridine derivative **107**.

In contrast, 2-aryl pyridine **99f-2** formed the expected product **102** within 2 hours (Scheme 41).

Scheme 41. Synthesis of the *N*-hydroxyamidine **102**.

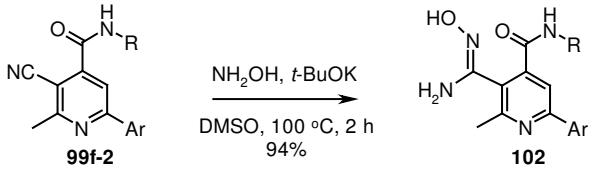

4. 1. 2. 8 Synthesis of pyridine tetrazoles.

Differences in reactivity of both regioisomers were observed during tetrazole synthesis. The amides **94** required high temperature and long reaction times for the formation of the tetrazoles **97** (Scheme 42).[69]

Scheme 42. Synthesis of the tetrazoles **97.**

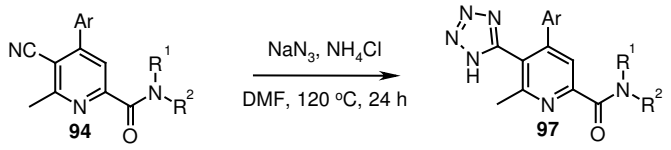

Compd	Ar	R^1	R^2	Yield (%)
97a	2,4-Dichloro-phenyl	H	H	80
97b	4-Methoxy-phenyl	H	3,4-Dichlorobenzyl	89
97c	4-Methoxy-phenyl	H	Methyl-thiophen-2-yl	99

Interestingly, the dicyano derivative **95d** gave tetrazole **108** regioselectively within 3 hours when treated with sodium azide at 70 °C (Scheme 43). Reaction time elongation, increase of temperature and excess of reagent equivalents did not lead to the di-tetrazole. The basic hydrolysis of **108** yielded the tetrazole **109**. All derivatives were isolated in excellent yields.

Scheme 43. Click reaction of the dicyano derivative **95b**.

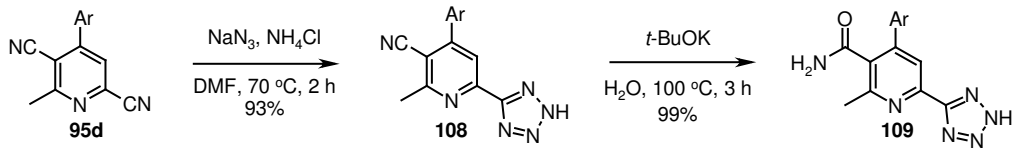

Scheme 44. Click reaction of **99** and **101.**

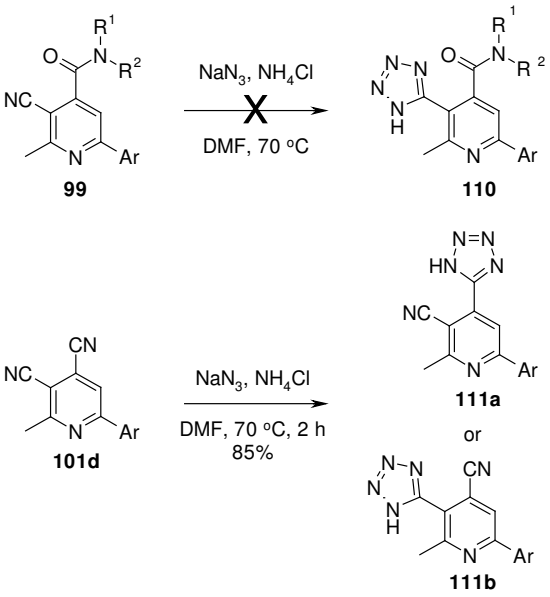

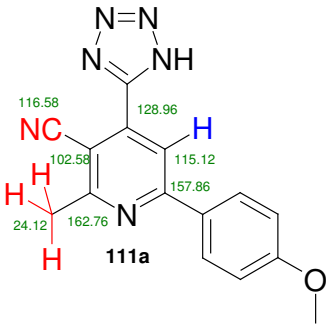

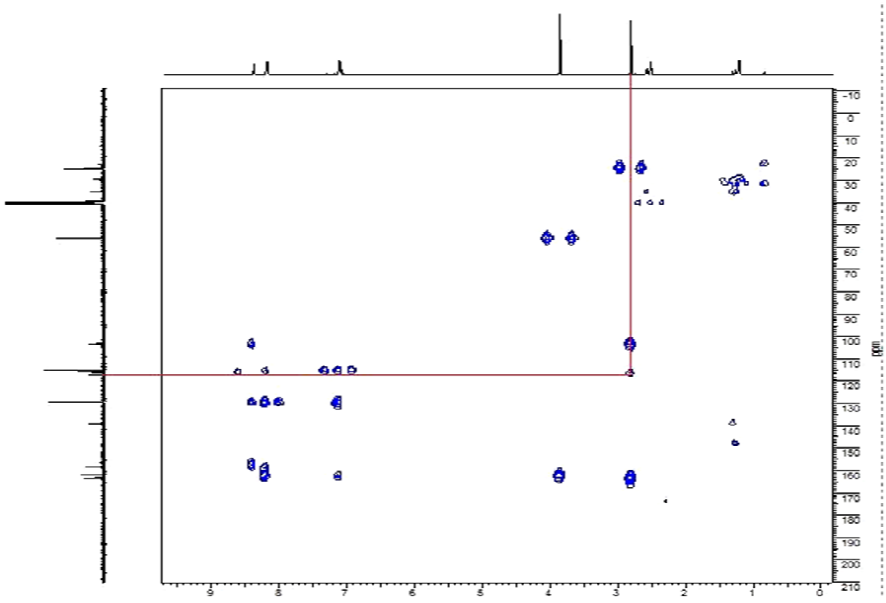

Figure 3. HMBC analysis of the product **111a**.

In contrast, the regioisomers **99** did not react at 50 ^{o}C and started to decompose when the temperature was increased (Scheme 44). The dicyanopyridine **101d** however reacted efficiently to form tetrazole **111** after 2 hours at 70 ^{o}C.

HMBC (Heteronuclear Multiple Bond Coherence) method is a two-dimensional nuclear magnetic resonance spectroscopy, that allows the determination of carbon to hydrogen connectivity. By performing the HMBC NMR of the tetrazole it was possible to prove the structure of the formed product. The main evidence is the correlation signal between protons of the methyl group and carbon from the cyano substituent (Figure 3, corresponding groups marked in red, the correlation signals marked with red line), that should not be observed if **111b** would have been formed. And vice versa, the protons in the pyridine ring (Figure 3, marked in blue) do not correlate with the carbon of the cyano group, thus they are in a distance over more than three bonds as in **111a**.

4. 1. 2. 9 Synthesis of pyrrolopyridines.

Tertiary amides **99** cyclized spontaneously in the presence of Raney Nickel and hydrazine hydrate, giving an easy access to the pyrrolopyridines **103** (Scheme 45).[70]

Scheme 45. Synthesis of the pyrrolopyridin-1-one **103**.

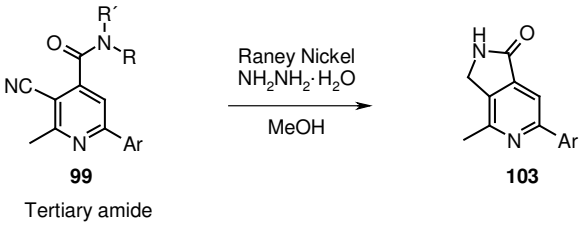

99
Tertiary amide

103

Compd	Ar	Yield (%)
103a	4-Chloro-phenyl	80
103b	2,4-Dichloro-phenyl	66
103c	4-Methoxy-phenyl	69

The scope of the reaction was investigated on the benzyl amide **113** prepared from the acid **112**. The hydrogenation product **114** was formed slowly together with cyclization product **115** that was isolated in 90% yield after 5 days reaction (Scheme 46).

Scheme 46. Results of the 2,3-dihydro-isoindol-1-one **115** synthesis.

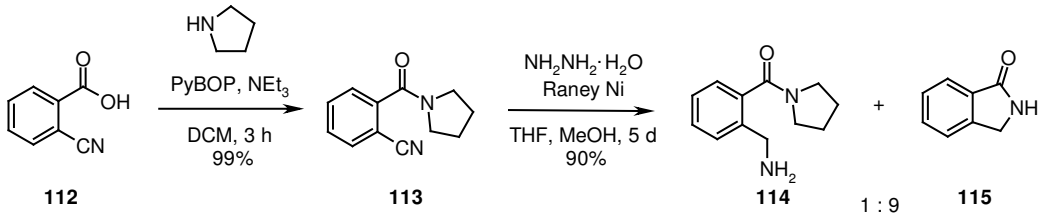

112 **113** **114** **115**

Boc-protection[71] of the amine **116** prepared from **81**[70] resulted in the formation of **117**. When dioxane was used as solvent, up to 20% of cyclized **117** was observed. When 4M aqueous NaOH was added to the reaction mixture, the pyrrolopyridin-1-one **117** was obtained exclusively. **117** was deprotected quantitatively to give **103** using TFA (Scheme 47).

Scheme 47. Alternative synthesis of the 2,3-dihydro-pyrrolo[3,4-*c*]pyridin-1-ones **103**.

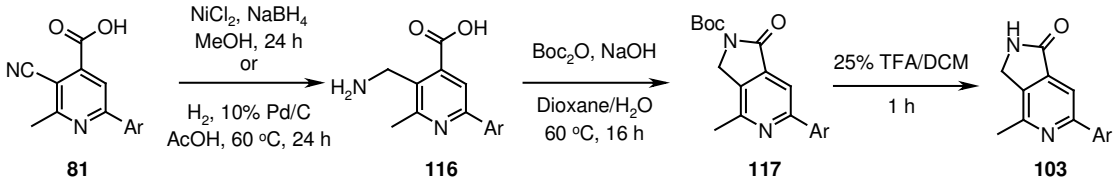

81 **116** **117** **103**

Ar	Compd	Yield (%)	Compd	Yield (%)
2,4-Dichloro-phenyl	**117a**	85	**103b**	99
4-Methoxy-phenyl	**117b**	74	**103c**	95

The compound **103b** was then further modified by oxidation to give pyrrolo[3,4-*c*]pyridine-1,3-dione **118** in good yield (Scheme 48).[72] It is worth to note, that the applied conditions gave selective oxidation in the pyrrol ring, while the methyl group in α position to the pyridine nitrogen stayed unaffected.

Scheme 48. Synthesis of the pyrrolo[3,4-*c*]pyridine-1,3-dione **118.**

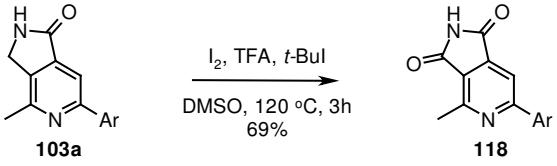

103a **118**

4. 1. 3 Antifungal screening.

The synthesized compounds were tested for antimycotic activity by the Project Partners. The fluorimetric HTS assay used at the University of Tübingen as well as at the Fraunhofer Institute was based on published procedures.[73] The only difference in case of the antimycotic screening at the Fraunhofer Institute was usage of HeLa cells instead of CHO cells as HeLa cells characterize robust growth behaviour and reproducible sensitivity to the *Candida albicans* strains used. In all cases the compounds were investigated simultaneously for activity against pathogens and tolerability by human cells. It is critical to ensure rapid and complete destruction of the host cells in the presence of the fungal pathogen (pathogen control), but protection from it in the presence of an antifungal compound during the entire incubation period of 5 days (drug control). For comparison the well established potent antifungal amphotericin B was used (drug control).

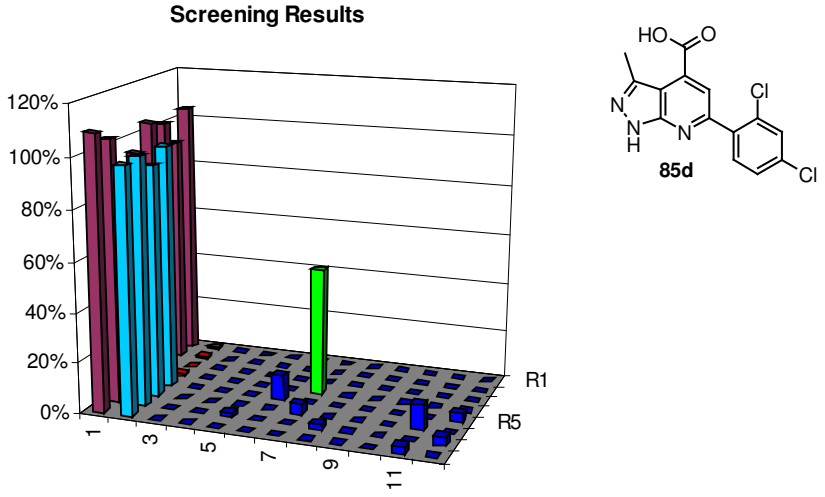

Figure 4. Fluorescence read-out of a high throughput screening plate to identify tolerable and active molecules in compound collections.

The compounds were screened at a concentration of 10 µM. No antibacterial or antiviral compounds have been identified. At the Fraunhofer Institute one compound **85d** exhibited a weak antifungal activity with 51% inhibition of the yeast growth (Figure 4). All primary hits had to be then retested and evaluated in a dose-response assay in order to determine the IC_{50} in the setting of the screening assay (determining the concentration of the compound required to ensure vitality of 50% of the host cells due to growth inhibition of the pathogen) and CC_{50} of the compound (concentration of the compound resulting in a 50% reduction of the vitality of HeLa cells due to the toxicity of the compound). Hits with a high selectivity, defined as the

ratio between CC_{50} and IC_{50} are then selected for further studies. The pyrazolopyridine **85d** however appeared to be toxic to the HeLa cells. Due to the weak antimycotic activity and toxicity of the hit **85d** it was not further investigated.

The collection of 60 compounds was screened for activity against *Candida glabrata*. The compounds were titrated at 8 different concentrations and coincubated with the yeast cells as well as with the immune BMDMs cells (Figure 5 and 6).

	1	2	3	4	5	6	7	8	9	10	11	12
A	128										2,5% DMSO ctrl	Contam ctrl
B	32											
C	8											
D	2											
E	0,5										Growth ctrl YPD	Fluconaz ctrl
F	0,125											
G	0,03											
H	0,0075											
	Compound 1	Compound 2	Compound 3	Compound 4	Compound 5	Compound 6	Compound 7	Compound 8	Compound 9	Compound 10	controls	controls

Figure 5. Preparation of the 96 well plate: A1-H1 to A10-H10 wells with tested compounds (0.0075-128 µM); E11-H11 cell control; A12-D12 contamination control; E12-H12 drug control.

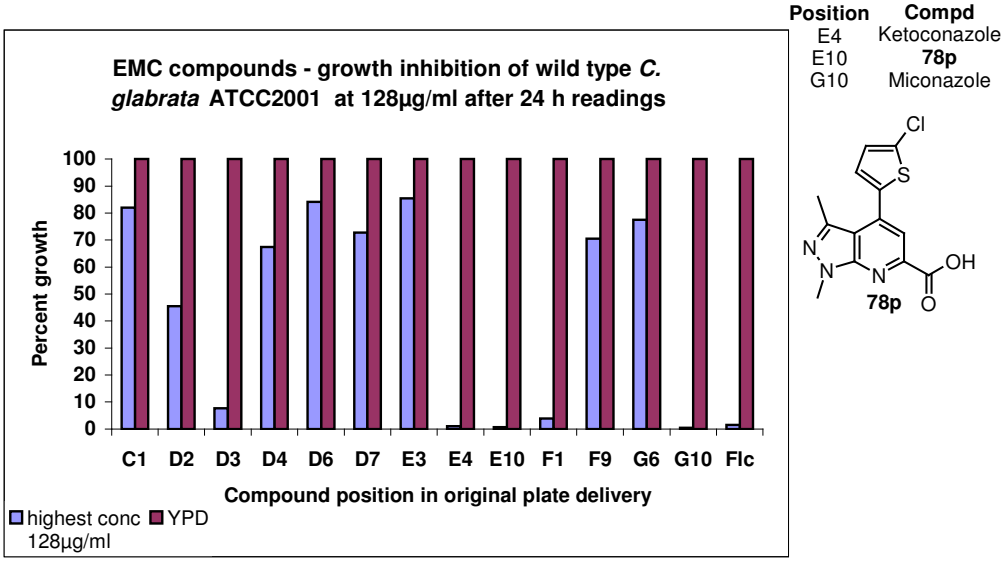

Figure 6. Absorbance read-out of a screening plate: inhibition of *Candida glabrata* growth by the tested compounds.

Compound **78p** (Figure 6, row E10) significantly inhibited growth of the wild type *Candida glabrata* after 24 h incubation. However, after 48 h incubation time the fungicidal effect was not observed, while the miconazole was still active (Figure 7). The IC_{50} of the active compounds was estimated for over 200 µM.

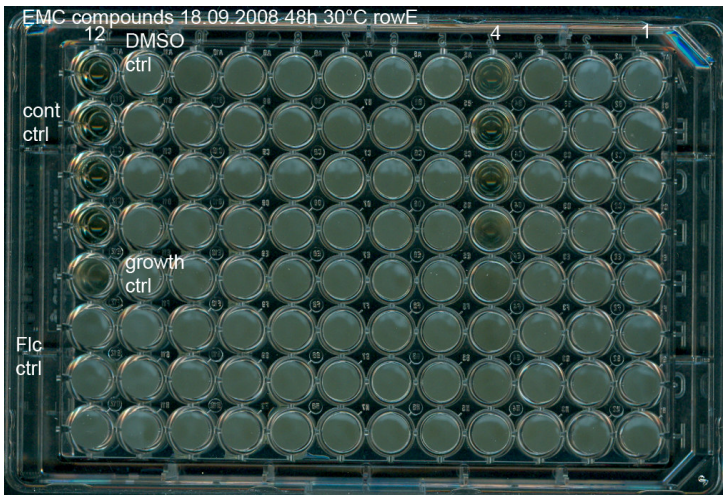

Compound **78p** (row 10) Miconazole (row 4)

Figure 7. Microtiter plate after 48 h incubation.

The antifungal screening performed at the two independent institutions lead to two pyrazolopyridines **85d** and **78p** exhibiting antimycotic activity. The compound **85d** is active against *Candida albicans* at 10 µM, but is toxic to HeLa cells. The pyrazolopyridine **78p** is not toxic and inhibits *Candida glabrata* cell growth. The inhibitory effect is weak (over 200 µM) and short lasting.

4. 2 Novel DPP-4 inhibitors - focused compound collection.

4. 2. 1 Design of potential DPP-4 inhibitors.

Human DPP-4 is a non-classical serine protease with the catalytic triad of Ser, Asp, His, found in the *C*-terminal region, in reverse order to the ones found in classical serine proteases. DPP-4 is a membrane-associated glycoprotein of 766 amino acids consisting of a cytoplasmic tail (residues 1-6), a transmembrane region (residues 7-28), and an extracellular part (29-766). The extracellular part can be further divided into two domains: the catalytic domain (residues 508-766) containing the catalytic triad Ser630-Asp708-His740 and the domain consisting of the residues 56-497 which also contributes to the inhibitor binding site. The enzyme is widely distributed in numerous tissues, and is expressed on epithelial and endothelial cells of tissues like intestine, liver, lung, kidney or placenta. DPP-4 is expressed on circulating T-lymphocytes and has been proven to be synonymous with cell-surface antigen, CD-26. The enzyme also exists as a circulating form in plasma, that lacks the hydrophobic transmembrane domain, but has identical function as its membrane-bound form.[29,45,74]

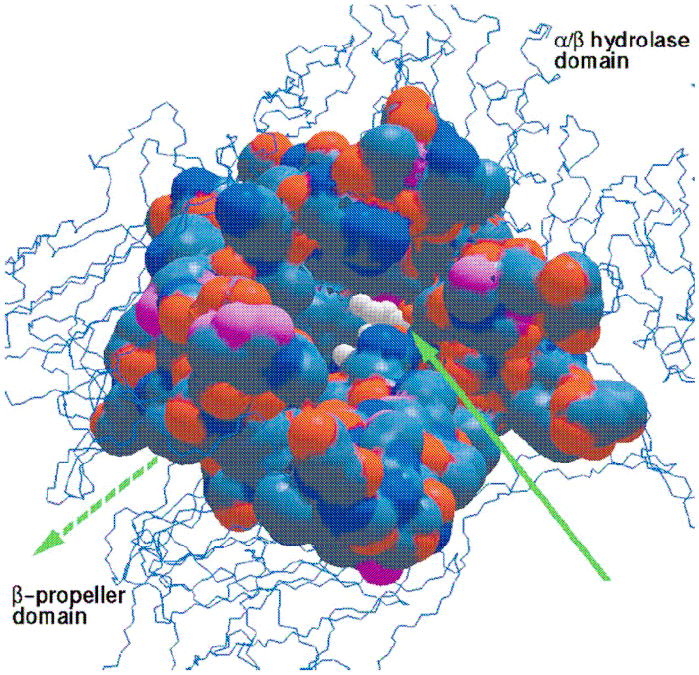

Figure 8. Schematic view on the subunit of DPP-4 with the active site surface colored according to the atom types.[50a]

DPP-4 has many physiological substrates such as chemokines, eotaxin, macrophage-derived chemokine, neuropeptides or vasoactive peptides. It is specific to peptides with an amino-

terminal proline or alanine at position 2 but might cleave substrates with non-preferred amino acids at position 2 as well. By cleaving dipeptides Xaa-Pro- or Xaa-Ala- from the *N*-terminus of biologically active peptides, DPP-4 transforms them into an inactive (as in the case of incretins) or even antagonistic form.[29,74]

DPP-4 is enzymatically active as a homodimer. Since the crystal structure of the enzyme (Figure 8), first reported in 2003, a number of X-ray informations for protein-ligand complexes were published.[50a,74d] The catalytic site lies in a large cavity between two extracellular domains and can be accessed by two active site openings. The substrate diprotin A (IPI) (Figure 8, marked in white) indicates the binding site. The substrate may enter the active site at the well accessible and open active site cleft, the dipeptidic product of the catalytic reaction may leave the active site cavity via the narrower tunnel that is formed by the β-propeller (Figure 8, green arrows).[74d]

The molecular recognition of the ligands involves a serine nucleophile within the catalytic triad Ser-Asp-His. In several early inhibitors, X-ray structures confirmed that the nitrile carbon is in covalent bond distance from the oxygen atom of catalytic serine side chain. Several studies confirmed that presence of the nitrile group increases inhibitor activity, even up to 1000-fold (Figure 9, marked in green).[45a]

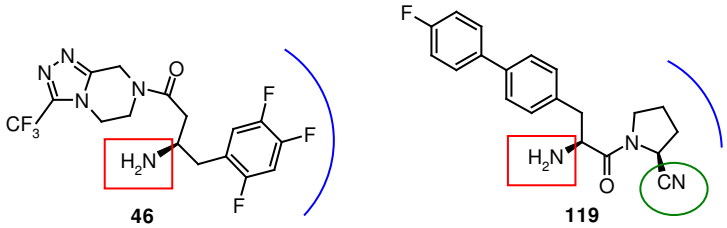

Figure 9. Examples of known DPP-4 inhibitors and their main interaction elements: the location of the S1 pocket marked by a curved blue line, the elements interacting with the Glu 205-206 indicated by a red rectangle, the motif forming a covalent bond to Ser 630 underlined in green.

Filling of the S1 pocket is one of the most important interactions. The specificity pocket S1 is composed of the side chains of Tyr 631, Val 656, Trp 659, Tyr 666, Val 711. The rigidity of this pocket appears to be highly specific to the proline residues, but the asymmetry in the pocket allows a possibility of mimicking this part by introducing small substituents such as fluorine atoms on the aromatic ring of the inhibitors (Figure 9, marked in blue).

Polar side chains of Arg 125 and Asn 710 interact via formation of hydrogen bonds with the amido-groups of the inhibitors. The favorable electrostatic interaction of the carbonyl dipole with the protein environment was additionally confirmed by SAR studies.

Besides of the S1 pocket, the second most important point for the high ligand affinity is hydrogen bonding ineractions with the side chains of the 205 and 206 glutamate residues. Most of the DPP-IV inhibitors discovered so far contain primary or secondary amine group that form hydrogen bonds with Glu 205, Glu 206 and, in case of the terminal amine, additional interactions via hydrogen bonding with Tyr 662 was observed (Figure 9, marked in red).

Further affinity gains might be achieved by exploring the phenyl rings of Phe 357 and Tyr 547 are exposed to the ligand binding site. One of the energically favorable arrangements are aromatic edge-to-face interactions as indicated for **119** (Figure 9).[45,50,74c]

These information about DPP-4 molecular recognition could be graphically summarized as presented in the Figure 10.

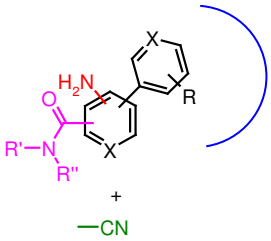

Figure 10. Important interaction elements: the location of the S1 pocket marked by a curved blue line, the elements interacting with the Glu 205-206 indicated in red, the motif forming a covalent bond to Ser 630 in green, group interacting with Arg 125 and Asn 710 marked in magenta.

According to the mentioned information, the biaryl sceleton of the pyridines **74** and **81** appeared to be a good starting point for the inhibitor design. Incorporating other important elements for high affinity binding, the three regioisomers: 5-aminomethyl-6-methyl-4-aryl-pyridine-2-carboxylic acid amide **120**, 6-aminomethyl-2-methyl-4-aryl-nicotinamide **121,** 3-aminomethyl-2-methyl-6-aryl-isonicotinamide **122**, were designed (Scheme 49).

Scheme 49. General structures of the target molecules. The colors correspond to the interaction elements presented in the Figure 10.

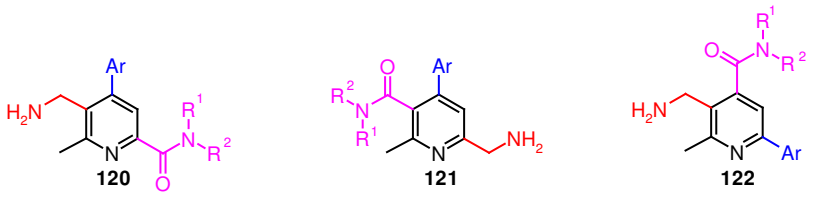

The calculated logP values for the series **120-122** were in the 2-3 range (OSIRIS Property Explorer, Software provided by Actelion Pharmaceuticals Ltd.) and, together with the structural elements and molecular weight (250-400 daltons) of the chosen analogs **120-122**, are in accordance with Lipinski's rule of five.[4]

4. 2. 2 Synthesis of potential DPP-4 inhibitors.

4. 2. 2. 1 Synthesis of 5-aminomethyl-6-methyl-4-aryl-pyridine-2-carboxylic acid amides.

Two approaches to target the aminomethyl-pyridines **120** are outlined in Scheme 50. In both the critical modification was the generation the aminomethyl group from the cyano group of **74** or **94**.[75] Although the route A requires more steps, it limits the number of hydrogenations to one for each series with different aromatic substituent.

Scheme 50. Synthetic approaches to the target molecule **120**.

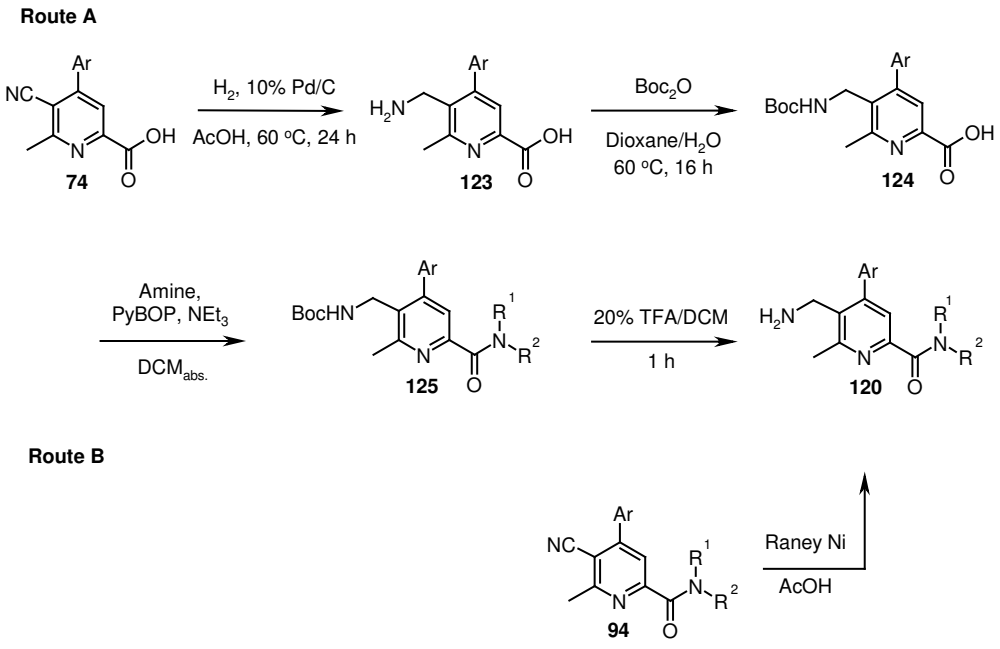

Table 3. Yields of the synthesis of pyridines **120**.

Compd	Ar	R^1	R^2	Yield (%)
Route A				
123a	4-Fluoro-phenyl			52
123b	2,4-Difluoro-phenyl			68
123c	4-Methoxy-phenyl			72
124a	4-Fluoro-phenyl			68
124b	2,4-Difluoro-phenyl			62
124c	4-Methoxy-phenyl			79
125a-1	4-Fluoro-phenyl	Cyclopropyl	H	57
125a-2	4-Fluoro-phenyl	Pyrrolidin-1-yl		92
125a-3	4-Fluoro-phenyl	Morpholin-4-yl		84
125a-4	4-Fluoro-phenyl	1-Piperidine-4-carboxylic acid ethyl ester		92
125b-1	2,4-Difluoro-phenyl	Cyclopropyl	H	46
125b-2	2,4-Difluoro-phenyl	Acetic acid methyl ester		67
125b-3	2,4-Difluoro-phenyl	Pyrrolidin-1-yl		92
125b-4	2,4-Difluoro-phenyl	Morpholin-4-yl		91
125b-5	2,4-Difluoro-phenyl	1-Piperidine-4-carboxylic acid ethyl ester		76
125b-6	2,4-Difluoro-phenyl	5-Methyl-isoxazol-3-yl	H	58
125b-7	2,4-Difluoro-phenyl	((R)-3-Boc-amino-pyrrolidin-1-yl)-methanone		92
125c-1	4-Methoxy-phenyl	Cyclopropyl		74
125c-2	4-Methoxy-phenyl	Pyrrolidin-1-yl	H	72
125c-3	4-Methoxy-phenyl	Morpholin-4-yl		92
125c-4	4-Methoxy-phenyl	3,4-Dichloro-benzyl	H	88
125c-5	4-Methoxy-phenyl	2,5-Dimethyl-2H-pyrazol-3-yl	H	62
125c-6	4-Methoxy-phenyl	5-Methyl-isoxazol-3-yl	H	57
125c-7	4-Methoxy-phenyl	((R)-3-Boc-amino-pyrrolidin-1-yl)-methanone		89
125c-8	4-Methoxy-phenyl	(4-Boc-amino-piperidin-1-yl)-methanone		53
125c-9	4-Methoxy-phenyl	2-(4-Boc-piperazin-1-yl)-ethyl	H	92
120a-1	4-Fluoro-phenyl	Cyclopropyl	H	99
120a-2	4-Fluoro-phenyl	Pyrrolidin-1-yl		95
120a-3	4-Fluoro-phenyl	Morpholin-4-yl		89
120a-4	4-Fluoro-phenyl	1-Piperidine-4-carboxylic acid ethyl ester		99
120b-1	2,4-Difluoro-phenyl	Cyclopropyl	H	86
120b-2	2,4-Difluoro-phenyl	Acetic acid methyl ester	H	99
120b-3	2,4-Difluoro-phenyl	Pyrrolidin-1-yl	H	95
120b-4	2,4-Difluoro-phenyl	Morpholin-4-yl	H	91

120b-5	2,4-Difluoro-phenyl	1-Piperidine-4-carboxylic acid ethyl ester	H	89
120b-6	2,4-Difluoro-phenyl	5-Methyl-isoxazol-3-yl		98
120b-7	2,4-Difluoro-phenyl	((R)-3-amino-pyrrolidin-1-yl)-methanone		92
120c-1	4-Methoxy-phenyl	Cyclopropyl	H	87
120c-2	4-Methoxy-phenyl	Pyrrolidin-1-yl		78
120c-3	4-Methoxy-phenyl	Morpholin-4-yl		99
120c-4	4-Methoxy-phenyl	3,4-Dichloro-benzyl	H	99
120c-5	4-Methoxy-phenyl	2,5-Dimethyl-2H-pyrazol-3-yl	H	68
120c-6	4-Methoxy-phenyl	5-Methyl-isoxazol-3-yl	H	87
120c-7	4-Methoxy-phenyl	((R)-3-Amino-pyrrolidin-1-yl)-methanone		82
120c-8	4-Methoxy-phenyl	(4-Amino-piperidin-1-yl)-methanone		79
120c-9	4-Methoxy-phenyl	2-Piperazin-1-yl-ethyl	H	88
Route B				
120d-1	2-Fluoro-phenyl	H	H	64
120d-2	2-Fluoro-phenyl	Me	H	70
120d-3	2-Fluoro-phenyl	Cyclopropyl	H	53
120d-4	2-Fluoro-phenyl	Pyrrolidin-1-yl		48
120d-5	2-Fluoro-phenyl	1-Piperidine-4-carboxylic acid ethyl ester		25
120e	4-Chloro-phenyl	Me	H	38
120f-1	2,4-Dichloro-phenyl	H	H	45
120f-2	2,4-Dichloro-phenyl	Me	H	51
120f-3	2,4-Dichloro-phenyl	Cyclopropyl	H	34
120f-4	2,4-Dichloro-phenyl	Pyrrolidin-1-yl		48
120f-5	2,4-Dichloro-phenyl	Morpholin-4-yl		44
120f-6	2,4-Dichloro-phenyl	1-Piperidine-4-carboxylic acid ethyl ester		15

Various conditions were investigated for the conversion of the cyano group to the amines. Lithium aluminium hydride caused partial -CN hydrogenation and conversion of amide carbonyl of **94** to the corresponding alcohol. When **74** was used in the reaction, only reduction of the carboxy group occurred. Sodium borohydride with nickel chloride[70b] partially reduced the carbonyl group in the amides **94**, and acids **74** gave only a minor amount of the desired products. Transfer hydrogenation using palladium on charcoal and formic acid that is known for *O*-benzyl group deprotection[76a] was also tested. Pyridines **74** without halogens in the aromatic ring gave 50% conversion after 2 hours. The reaction time elongation resulted in a reverse reaction. The hydrogenation with palladium on charcoal and gaseous hydrogen[70a] was

found to be most convenient, however in case of **74f** deactivated by chlorines the method failed.

The further modifications, Boc protection leading to **124**, amidation of the protected aminomethyl-pyridine **124** that gives **125** and removal of the protecting group to afford **120** were in most of the cases high yielding and the products relatively easy to purify (Table 3).

The catalytic hydrogenation with Raney Nickel (Scheme 50, route B)[70] was not compatible with the amides **94** with several substituents such as 5-methyl-isoxazol-3-yl or 2,5-dimethyl-2H-pyrazol-3-yl (Scheme 35, entries **94c-9**, **94e-10**, **94g-15**, **94g-16**) or with the substrates containing ester group (Scheme 35, entries **94a-6**, **94c-3**) as its hydrolysis was observed. In addition, in many cases the conversion was not complete, and/or byproducts were formed which were difficult to remove and caused often low yields (Table 3, entries **120d-5**, **120e**, **120f-3**, **120f-6**).

Synthesis of the aminomethyl-pyridine **120h** required a modified approach. The amide **94e-4** was reduced to give the amine **120g**. The primary amide of **120g** was then dehydrated to give desired product **120h** in good yield (Scheme 51).

Scheme 51. Synthesis of the pyridine **120h**.

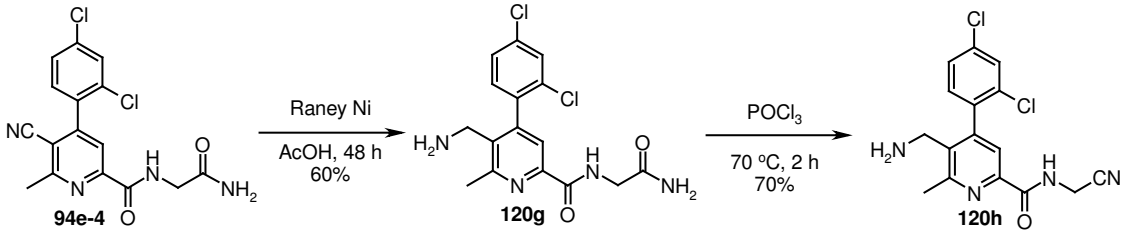

4. 2. 2. 2 Synthesis of 6-aminomethyl-2-methyl-4-aryl-nicotinamides.

The synthesis of the aminomethyl-pyridines **121** was initiated by the conversion of the carboxylic acids **96** to the alcohols **126**,[76b] which were then reacted with thionyl chloride to form the corresponding chlorides **127** (Scheme 52). Displacement of the chloride by the phthalimide led to **128**. Basic hydrolysis of **128** afforded **121** in good to very good yields (Table 4).

Scheme 52. Synthesis of the target molecule **121**.

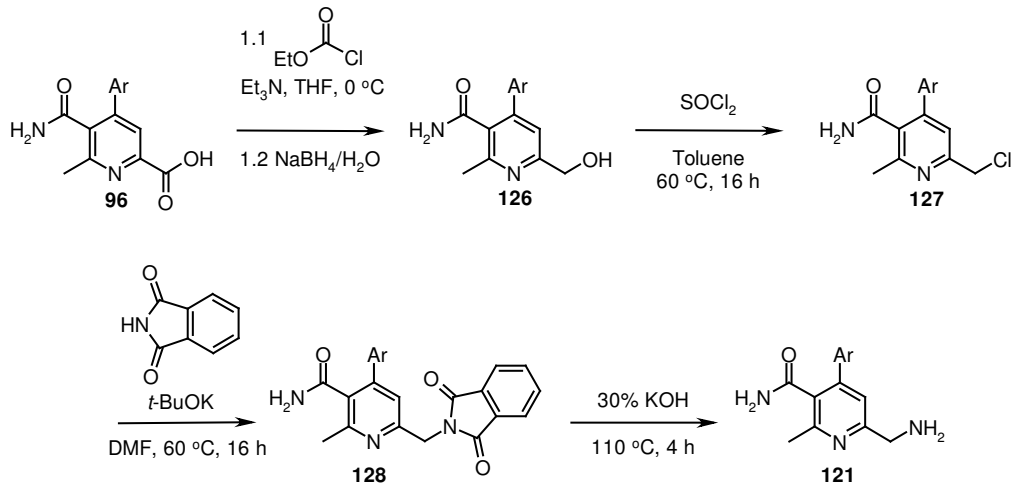

Table 4. Results of the **121** synthesis.

Compd	Ar	Yield (%)
126a	2-Fluoro-phenyl	61
126b	4-Chloro-phenyl	71
126c	2,4-Dichloro-phenyl	77
126d	4-Methoxy-phenyl	99
127a	2-Fluoro-phenyl	85
127b	4-Chloro-phenyl	76
127c	2,4-Dichloro-phenyl	75
127d	4-Methoxy-phenyl	79
128a	2-Fluoro-phenyl	65
128b	4-Chloro-phenyl	82
128c	2,4-Dichloro-phenyl	80
128d	4-Methoxy-phenyl	90
121a	2-Fluoro-phenyl	91
121b	4-Chloro-phenyl	89
121c	2,4-Dichloro-phenyl	84
121d	4-Methoxy-phenyl	79

4. 2. 2. 3 Synthesis of 3-aminomethyl-2-methyl-6-aryl-isonicotinamides.

3-Aminomethyl-2-methyl-6-aryl-isonicotinamides **122** were synthesized using two alternative approaches as for the aminomethyl-pyridine **120** (Scheme 53).

Scheme 53. Synthetic approaches to the target molecule **122**.

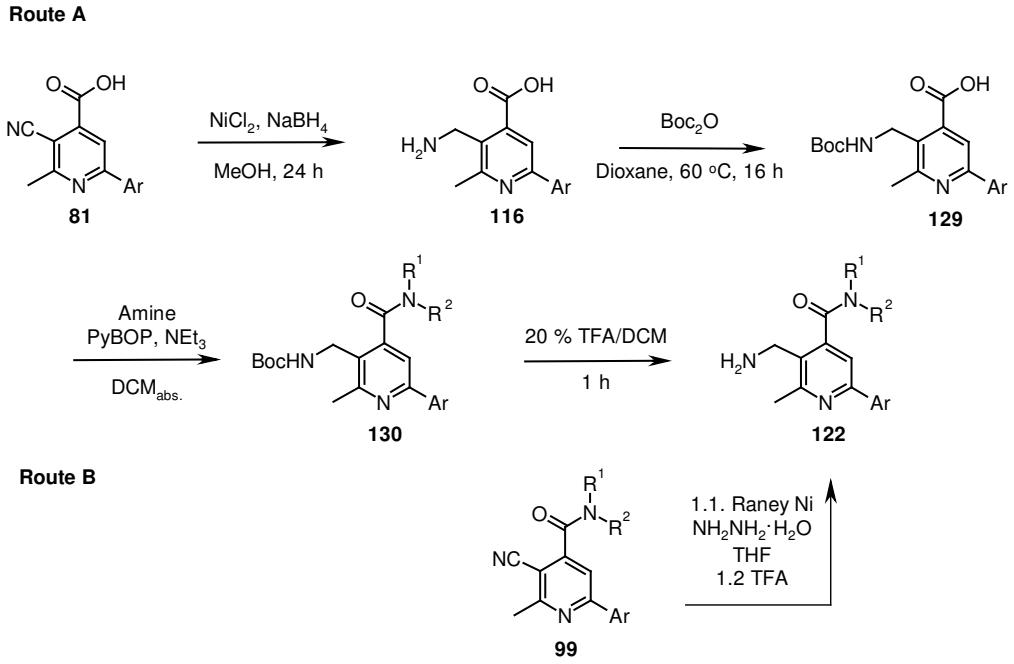

Table 5. Yields of the synthesis of pyridines **122**.

Compd	Ar	R^1	R^2	Yield (%)
Route A				
129a	2,4-Dichloro-phenyl			43
129b	4-Methoxy-phenyl			38
130a-1	2,4-Dichloro-phenyl	Cyclopropyl	H	63
130a-2	2,4-Dichloro-phenyl	Pyrrolidin-1-yl		54
130a-3	2,4-Dichloro-phenyl	Morpholin-4-yl		80
130b-1	4-Methoxy-phenyl	Cyclopropyl	H	76
130b-2	4-Methoxy-phenyl	Pyrrolidin-1-yl		86
130b-3	4-Methoxy-phenyl	Morpholin-4-yl		92
122a-1	2,4-Dichloro-phenyl	Cyclopropyl	H	65
122a-2	2,4-Dichloro-phenyl	Pyrrolidin-1-yl		57
122a-3	2,4-Dichloro-phenyl	Morpholin-4-yl		63
122b-1	4-Methoxy-phenyl	Cyclopropyl	H	75
122b-2	4-Methoxy-phenyl	Pyrrolidin-1-yl		83
122b-3	4-Methoxy-phenyl	Morpholin-4-yl		70
Route B				
122c	4-Fluoro-phenyl	Pyrrolidin-1-yl		46
122d-1	4-Chloro-phenyl	Pyrrolidin-1-yl		53
122d-2	4-Chloro-phenyl	Morpholin-4-yl		48
122d-3	4-Chloro-phenyl	1-Piperidine-4-carboxylic acid ethyl ester		52

The hydrogenation of the cyano group of **81** afforded the formation of the corresponding amines **116** that were directly Boc protected to give **129**. The reaction was performed in dioxane without addition of water to avoid the formation of cyclized products **117**. Compounds **129** were isolated in moderate yields (Table 5) and then amidated to give **130** and **122** after deprotection. For the catalytic hydrogenation (Scheme 53, route B), the use of hydrazine hydrate as a hydrogen source was more efficient than the conditions applied for the synthesis of **120**. The protocol required acidification of the reaction mixture with TFA in order to minimize the formation of the pyrrolopyridines **103**. It is important to mention that the aminomethyl-pyridines **122** had to be stored as hydrochlorides or trifluoroacetate salts to avoid their spontaneous cyclization reaction to form **103**. In addition, the method was limited only to the tertiary amides (Table 4, **122c**, **122d**).

4. 2. 3 Biological screening and structure activity relationship.

The synthesized amines **120-122** and intermediates were evaluated for inhibition of human DPP-4 in an in vitro assay. The initial SAR breakthrough was the discovery that the aminomethyl-pyridines **120** exhibit high inhibitory activity (Figure 11, position 3-6, 8) contrary to the analogs **121** (Figure 11, position 2, 9) and **122** (Figure 11, position 11-13).

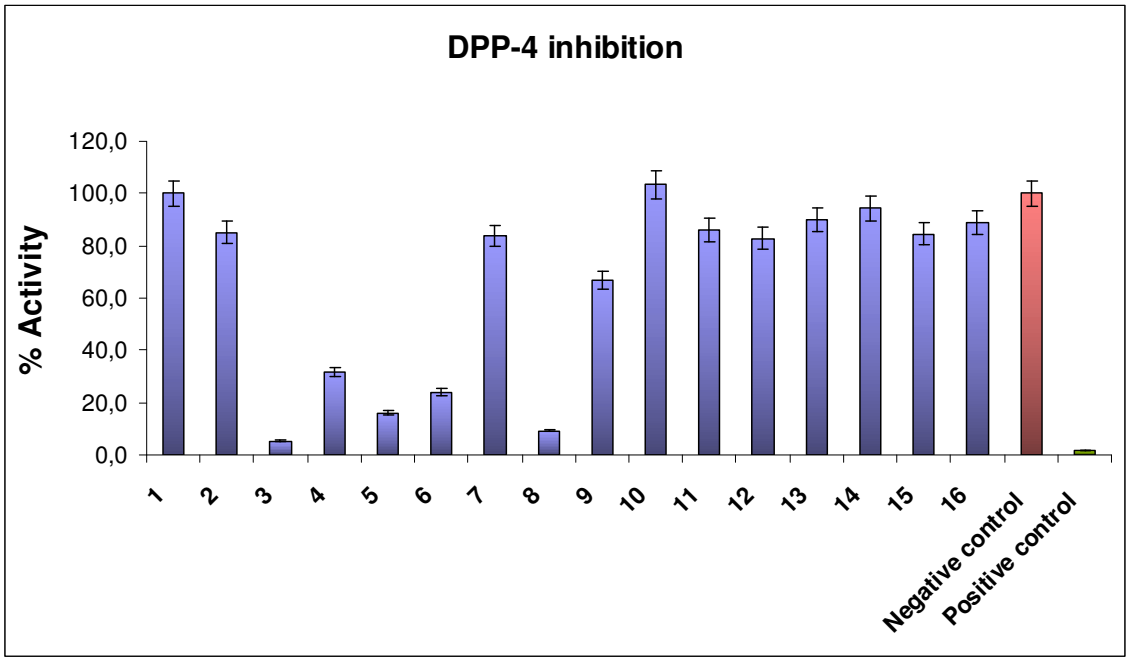

Figure 11. Screening results for the inhibition of DPP-4 by aminomethyl-pyridine regioisomers **120-122** (percent inhibition: mean ± standard deviation; N = 3).

The substituent pattern appeared to be crucial for the compound activity. The pyridine **120d-1** with an amine group in the β position to the nitrogen of the pyridine showed an activity with a IC_{50} value under 50 μM, compare to the regioisomer **121a** bearing an amine group in the α position had a IC_{50} value over 50 μM (Scheme 54).

Scheme 54. Differences in DPP-4 inhibition by the regioisomers **120** and **121**.

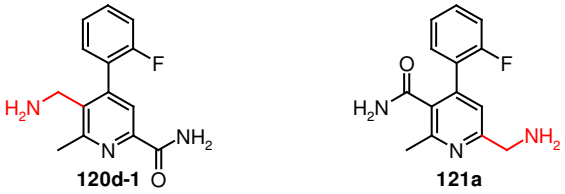

IC_{50} < 50 μM IC_{50} > 50 μM

Similarly the distance between the amine group and the amide functionality was proven to be of great importance. The change of the amide group position from α (as in aminomethyl-pyridines **120**) to β (in pyridines **122**) results in a loss of the inhibitory activity (Scheme 55).

Scheme 55. Differences in DPP-4 inhibition by **120** and **122**.

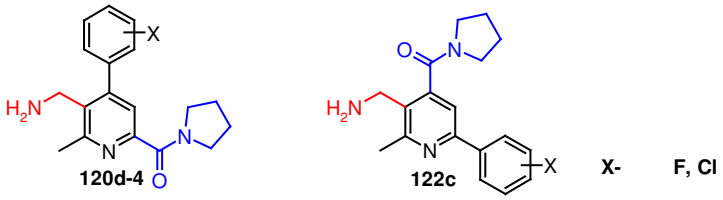

IC_{50} < 50 μM IC_{50} > 50 μM

A series of aminomethyl-pyridines **120** has been prepared in order to further optimize its structure. As expected the intermediates **94** without an amine moiety were not active. Interestingly the free carboxylic acids **123** remain inhibitory activity (IC_{50} < 50 μM).

Scheme 56. Influence of the aromatic ring substitution on the DPP-4 inhibitory activity.

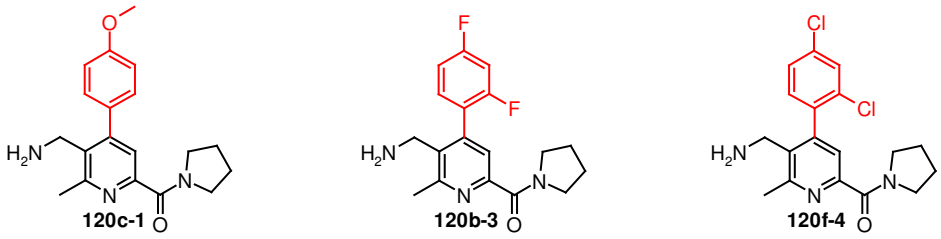

IC_{50} > 50 μM 0.050 μM < IC_{50} < 50 μM IC_{50} < 0.050 μM

The comparison of the analogs substitution in regard to the phenyl ring in the bicyclic system of **120** indicated the importance of the chlorine atom: **120f-4** was more potent (IC_{50} = 0.050 µM) compared to **120c-1** and **120b-3** (Scheme 56).

Representative analogs that possessed superior potency profiles were then investigated for the effectiveness in inhibiting DPP-4 in dose dependent experiments (Scheme 57).

Scheme 57. Influence of the aromatic ring substitution on the DPP-4 inhibitory activity.

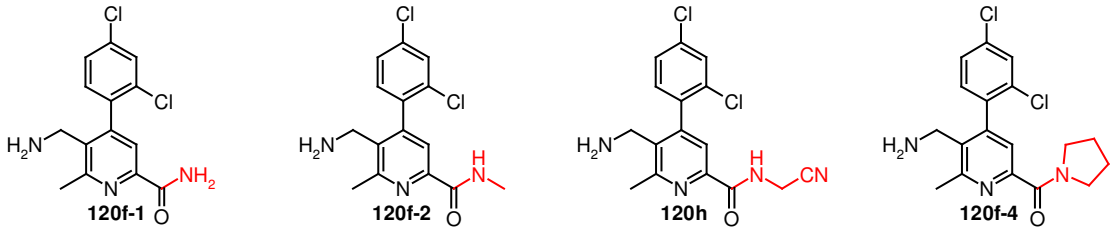

IC_{50} = 16 ± 2 nM | IC_{50} = 11 ± 0.5 nM | IC_{50} = 10 ± 0.7 nM | IC_{50} = 44 ± 5 nM

The substitution of the primary amide **120f-1** with the methyl group as in **120f-2** gratified in a significant improvement in potency. The analog **120h** possessed similar IC_{50} value compared to **120f-2**. The increase of the size of the amide group in **120f-4** suffered in its potency and the IC_{50} value dropped down to 44 nM.

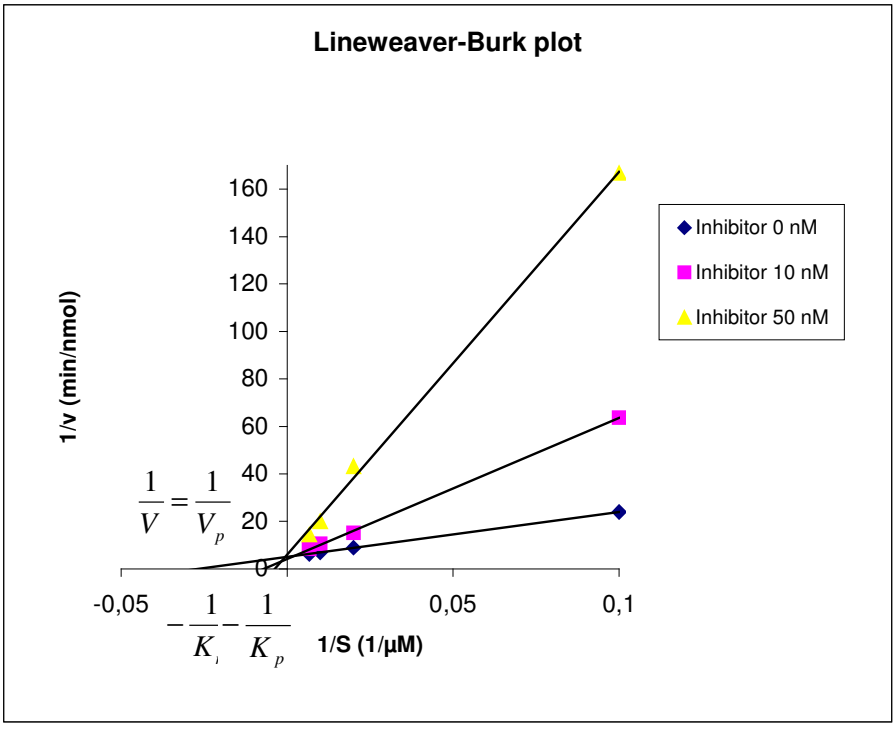

Figure 12. Lineweaver-Burk plot for **120f-2** indicating competitive inhibition.

One of the most potent analogs, **120f-2** was then chosen to investigate the type of the inhibition. Measurement of the inhibitory activity at various inhibitor and substrate concentrations allowed data plotting (Figure 12).[77] A Lineweaver-Burk plot indicated a competitive type of inhibition. This is a typical observation for compounds that bind in the same site of the enzyme as the substrate.

The inhibitory concentration dependent experiment showed clearly that the system is characterized by a define degree of inhibition, depending on the inhibitor concentration, which is reached within the first 20 minutes and thereafter is independent on time (Figure 13). This kind of inhibition is characteristic for reversible inhibitors.

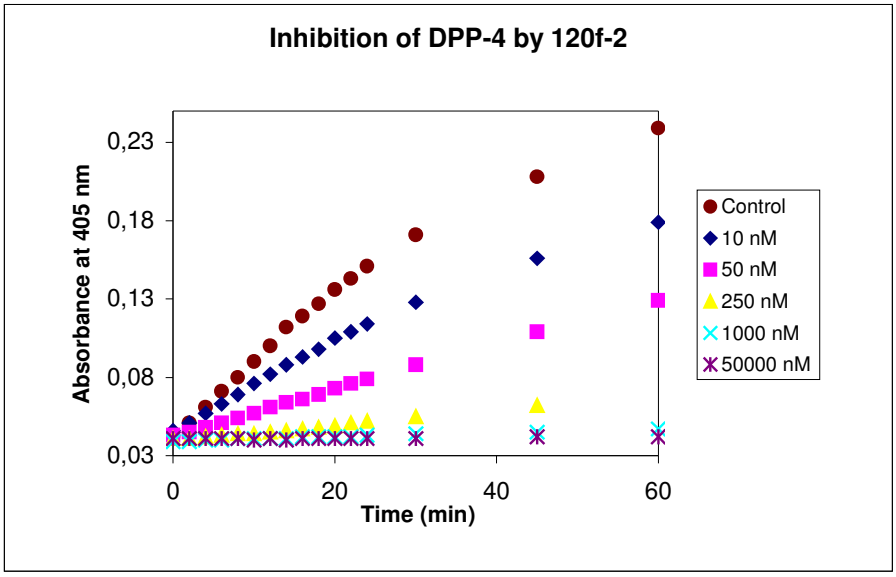

Figure 13. Inhibition of DPP-4 by **120f-2**.

The effectiveness of the reversible inhibitors is expressed by the K_i constant that describes enzyme-inhibitor affinity. For the K_i of the **120f-2** calculation the data obtained from Lineweaver-Burk plot were as follows:

$$V_m = 3.3\frac{pmol}{s}$$

$$K_m = 37.5\mu M$$

$$-\frac{1}{K_p} = \frac{1}{K_m\left(1+\frac{i}{K_i}\right)}$$

$$K_i = 5.5 \pm 2nM$$

wherein K_m is the concentration of the substrate that leads to half-maximal velocity (V_m), and K_p is the effective Michaelis constant in presence of the inhibitor at concentration i.

In addition the K_i was calculated from the previous experiments using the equation:

$$K_i = \frac{IC_{50}}{\left(1 + \frac{S}{K_m}\right)}$$

$$IC_{50} = 11.44\ nM$$

$$K_i = 4.90 \pm 0.5\ nM$$

Where: S - substrate concentration.

The obtained values remain in good coherence.

The series of active DPP-4 inhibitors was also tested against DASH family member, DPP-8. Selectivity over DPP-8 is of particular concern as inhibition of this enzyme is associated with toxicity in preclinical species and the relevance of these toxic effects to humans is not yet known.[50,74] Selectivity of the early DPP-4 inhibitors was not previously investigated at the beginning of DPP-4 research, as the related enzymes FAP, DPP-8 and DPP-9 were not yet discovered.[50]The most active inhibitors were investigated for the DPP-4 selectivity over DPP-8 in dose dependent experiments. All of the tested compounds showed high selectivity: 2500-6600 fold compared to DPP-4 (Scheme 58). The secondary amide **120f-2** was slightly more selective in comparison to the primary amide **120f-1**. The aminomethyl-pyridine **120h** was almost 2 fold less potent against DPP-8 than the **120f-2**. The derivative **120f-4** with a bulkier pyrrolidine ring is less preferable due to its lower potency and selectivity.

Scheme 58. Selectivity of the novel DPP-4 inhibitors.

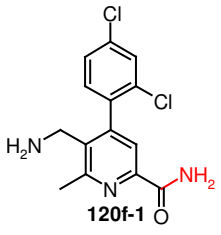

120f-1

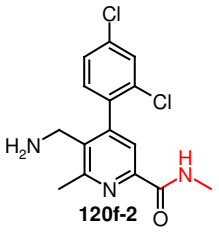

120f-2

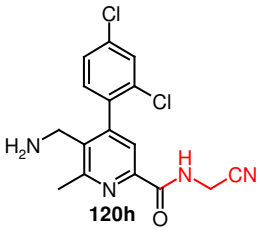

120h

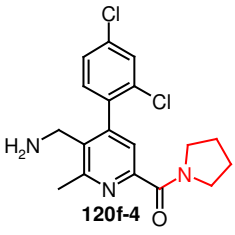

120f-4

DPP-4	IC_{50} = 16 ± 2 nM	IC_{50} = 11 ± 0.5 nM	IC_{50} = 10 ± 0.7 nM	IC_{50} = 44 ± 5 nM
DPP-8	IC_{50} = 33 ± 0.5 µM	IC_{50} = 39 ± 1 µM	IC_{50} = 66 ± 0.3 µM	IC_{50} = 25 ± 0.5 µM

The results from biological screening in comparison to the values from literature of the known inhibitors[50a] are summarized in Table 6.

The compounds **120** are highly potent DPP-4 inhibitors with IC_{50} values in nanomolar range. The IC_{50} levels of novel inhibitors are comparable to the values of drugs (Table 6, Vildagliptin, Sitagliptin). In addition the series **120** shows 6600 fold selectivity to DPP-4 over DPP-8.

Table 6. Selectivity of the novel DPP-4 inhibitors **120** over DPP-8 in comparison to Vildagliptin and Sitagliptin.

Compd	IC_{50} (K_i) [µM]	
	DPP-4	**DPP-8**
120f-1	0.016	33
120f-2	0.011 (0.006)	39
120h	0.010	66
120f-4	0.044	25
120a-1	0.080	106
120a-2	0.686	137
120b-1	0.937	182
120b-6	0.674	179
Vildagliptin[50b]	0.12	9
Sitagliptin[50b]	0.04	> 50

5. Summary.

In this work dedicated to the discovery of novel biologically active compounds, antifungals and antidiabetics, the focus was placed on the pyridine motif. The substituted pyridines and pyrazolopyridines were chosen as a promising scaffold in a search for novel therapeutics.

The overview of the pyridine-based antifungals and antidiabetics was reported in the part *Pyridines as scaffolds for antifungals and antidiabetics.*

Solution and solid phase combinatorial chemistry methods were used to approach target compounds. Efficient protocols were evaluated for the synthesis of pyridines and pyrazolopyridines applying solid supported 2-oxo-4-aryl-but-3-enoic acids and 4-oxo-4-aryl-but-2-enoic acids. In addition, the synthetic possibilities of the resin-bound intermediates were investigated and resulted in a collection of easily accessible pyrimidines and dihydropyrimidines (Chapter 4. 1. 1).

The solid phase protocol was adapted to the solution phase. A series of pyridines was synthesized in gram scale as starting materials for the generation of sub-sets of compounds varying only on the pyridine ring substitution. Differences in the reactivity of 2-aryl pyridines and 4-aryl pyridines were observed and investigated. Depending on the ring substitution pattern, deactivation or activation of certain positions resulted in reactivity limitations, but on the other hand, gave a possibility of additional structural variations (Chapter 4. 1. 2).

Based on the data available for the enzyme DPP-4 in the literature, a series of potential DPP-4 inhibitors (aminomethyl-pyridines: 5-aminomethyl-6-methyl-4-aryl-pyridine-2-carboxylic acid amides, 6-aminomethyl-2-methyl-4-aryl-nicotinamides and 3-aminomethyl-2-methyl-6-aryl-isonicotinamides) were designed and synthesized. Several synthetic pathways using 2-aryl pyridines and 4-aryl pyridines as starting materials were evaluated in order to obtain analogs.

All compounds were isolated and analyzed by HPLC-ESI-MS. Representative products were characterized using NMR and IR spectroscopy and FT-ICR-MS. For structure confirmation additional 2-D NMR experiments were used (COSY and HMBC NMR).

The synthesized compound collection was evaluated for its antifungal properties in an *in vitro* screening. As a result, two hit structures 6-(2,4-dichloro-phenyl)-3-methyl-1*H*-pyrazolo[3,4-*b*]pyridine-4-carboxylic acid (*Candida albicans*) and 4-(5-chloro-thiophen-2-yl)-1,3-dimethyl-1*H*-pyrazolo[3,4-*b*]pyridine-6-carboxylic acid (*Candida glabrata*) were identified. The compound 6-(2,4-dichloro-phenyl)-3-methyl-1*H*-pyrazolo[3,4-*b*]pyridine-4-carboxylic

acid was disqualified as a lead structure due to its toxic effect on the host cells. Inhibitory effect of 4-(5-chloro-thiophen-2-yl)-1,3-dimethyl-1*H*-pyrazolo[3,4-*b*]pyridine-6-carboxylic acid on *Candida glabrata* cells was too weak to consider the compound as a lead structure (Chapter 4.1.3).

The collection of aminomethyl-pyridines was investigated for its DPP-4 inhibitory activity in an *in vitro* assay. The lead structure of 5-aminomethyl-6-methyl-4-aryl-pyridine-2-carboxylic acid amides was found and structure activity relationship led to a potent series of the novel DPP-4 inhibitors. Furthermore, *in vitro* experiments proved excellent selectivity (up to 6600 fold for 5-aminomethyl-4-(2,4-dichloro-phenyl)-6-methyl-pyridine-2-carboxylic acid cyanomethyl-amide) of the inhibitors over closely related DPP-8 (Chapter 4. 2. 3). The results were described and patented.

This study clearly confirms the potential of the investigated scaffolds. As the biological activity of substituted pyridines highly depends on its substitution pattern. The synthesized and described herein compounds should be extensively investigated for other pharmaceutical targets.

Although preliminary biological data of the novel DPP-4 inhibitors are doubtlessly promising, the crucial point for their further development is the pharmacological profile of 5-aminomethyl-6-methyl-4-aryl-pyridine-2-carboxylic acid amides. Therefore additional biological experiments are required to further optimize the structure and to identify a clinical candidate.

Apart from the glucose metabolism, a number of different biological functions of DPP-4 have been recognized recently. The discoveries attract a great attention to the DPP-4 inhibitors, as such compounds could be useful for the treatment of other metabolic, but also autoimmune and inflammatory diseases.[74b] It is therefore important to further study of the described series in order to fully explore therapeutic potential of the DPP-4 enzyme.

6. Experimental part.

6. 1 Syntheses.

6. 1. 1 General.

Starting materials (*E*)-2-oxo-4-aryl-but-3-enoic acids **59** and (*E*)-4-oxo-4-aryl-but-2-enoic **60** acids were synthesized according to the literature procedures[58-59] or were obtained commercially and used as received. Other chemicals were used as purchased from commercial suppliers. Analytical TLC were performed with ALUGRAM silica gel 60 F254 plate. Flash chromatographies were performed on Combi Flash 5q 16x with a UV-detector. Column chromatographies were carried out using MN silica gel 60 (70-230 mesh ASTM). The mass spectra were measured on a Waters LC/MS system (Alliance 2795 HPLC, SQD mass detector, PDA 996 detector; Grom-Sil 80 ODS-7 PH 4 µm, 2.0 x 40 mm; ionizing voltage 10 eV). Ion mass (m/z) signals are reported as values in atomic mass units. For FT-ICR-MS measurements the APEX II Bruker Daltonics (4.7 Tesla) spectrometer was used. ^{1}H, ^{13}C, COSY and HMBC NMR analyses were performed on a Bruker 400 Ultra Shield instrument. NMR spectra were performed as DMSO-D_6 or $CDCl_3$ solutions (reported in ppm), using solvent peak or TMS as the reference. Other NMR solvents were used as needed. When peak multiplets are given, the following abbreviations are used: s = singlet, d = doublet, t = triplet, m = multiplet, bs = broad singlet, dd = doublet of doublets, dt = doublet of triplets. Coupling constants, when given, are reported in Hz. Melting points were measured on Büchi Melting Point B-540. IR spectra were Prepared on Bruker - Vector 22.

6. 1. 2 Synthesis protocols.

6. 1. 2. 1 Synthesis of (*E*)-2-oxo-4-aryl-but-3-enoic acids 59 - general procedure.

A solution of KOH (1.5 eq, 45 mmol, 2.52 g) in MeOH (7.5 mL) was added dropwise to a solution of pyruvic acid (1 eq, 30 mmol, 2.09 mL) and benzaldehyde (1 eq, 30 mmol) in MeOH (15 mL) at 0 °C. The reaction temperature was kept for 1 h at 25 °C and at 0 °C for 16 h. The yellow solid was filtered off and washed twice with cold MeOH and once with Et_2O. The crude residue was taken up in water, acidified with 1M HCl and extracted with DCM. The combined organic phases were dried over anhydrous Na_2SO_4 and concentrated to afford the product as a solid that was used without further purification.

6. 1. 2. 2 Synthesis of (*E*)-4-oxo-4-aryl-but-2-enoic acids 60 - general procedure.

Glyoxylic acid monohydrate (1 eq, 40 mmol, 3.68 g) was added to a solution of acetophenone (1 eq, 40 mmol) in acetic acid (50 mL) and concentrated HCl (5 mL). The mixture was refluxed for 16 h. After evaporation of the solvent, the residue was taken up in EA, filtered and air dried to afford the desired product as a yellow solid that was used in the next step without further purification.

6. 1. 2. 3 Synthesis of pyridines 74, 72, 81 and pyrazolopyridines 78, 83, 85 - general procedures.

Method A

A1. Loading of the Wang resin

Wang resin (1 eq, 0.5 mmol) in 5 mL PP syringe was first preswollen in DCM for 0.5 h, then (*E*)-2-oxo-4-aryl-but-3-enoic acids **59** or (*E*)-4-oxo-4-aryl-but-2-enoic acids **60** (2 eq, 1

mmol) and DMAP (0.3 eq, 0.15 mmol, 0.018 g) were introduced. DCM (5 mL) and DIC (3 eq, 1.5 mmol, 0.235 mL) were added and the syringe was shaken for 16 h at rt. The resin was filtered and washed with DMF (3x), MeOH (3x), THF (3x), DCM (3x) and finally with dry DMF.

A2. Capping

The capping of non-loaded hydroxyl functions was performed in dry DMF with DIPEA (10 eq, 5 mmol, 0.871 mL) and acetic anhydride (10 eq, 5 mmol, 0.472 mL) for 30 min at rt. The resin was washed with DMF (3x), MeOH (3x), THF (3x), DCM (3x) and dried. 0.050 g of the resin was cleaved to determine the loading.

A3. Cyclization

The amine (3eq) and DMF (2mL) were added to resin-bounded keto acids **63** or **67** (0.25 mmol) in a PP syringe. The suspension was stirred for 16 h at 100 ^{o}C. The resin was washed with DMF and DCM and dried in vacuo.

A4. Oxidation

DDQ (2 eq, 0.5 mmol, 0.114 g) and THF (2 mL) were added to the resin-bound non-aromatized heterocycle (1 eq, 0.25 mmol) in a 5 mL PP syringe. The suspension was shaken for 16 h at rt, then washed with DMF (3x), MeOH (3x), THF (3x), DCM (3x), Et_2O (3x) and dried in vacuo.

A5. Cleavage

To the resin-bound heterocycle (0.1 mmol) was added 20% TFA/DCM (5 mL) and the syringe was shaken one hour at rt. The resin was removed by filtration and washed with DCM (3x). The solvent was removed in vacuum. The crude product, if required, washed with MeCN or Et_2O.

Method B

Solution phase synthesis of 4-aryl pyridines 74 - general procedure: Potassium *t*-butoxide (3 eq, 3 mmol, 0.337 g) was added portionwise to a solution of (*E*)-2-oxo-4-(aryl)-but-3-enoic acid **59** (1 eq, 1 mmol) in MeCN (5 mL) at room temperature. After 16 h (the reaction monitored by LC/MS), the solvent was removed under reduced pressure. The crude product was taken up in water, acidified with 1M HCl and extracted with DCM. The combined organic phases were dried over anhydrous Na_2SO_4 and concentrated. The solid product **3** was isolated by column chromatography with silica gel using a gradient of PE/EA (from 4:1 to 1:1).

Method C

Solution phase synthesis of 2-aryl pyridines 81 - general procedure: *t*-BuOK (2 eq, 2 mmol, 0.224 g) was added portionwise to a solution of (*E*)-4-oxo-4-(aryl)-but-2-enoic acid **60** (1 eq, 1 mmol) in MeCN (5 mL) at room temperature. After 16 h (reaction monitored by LC/MS) the solvent was removed under reduced pressure. The mixture was suspended in dioxane and acidified with water free 4M HCl in dioxane. After evaporation of the solvent, the residue was taken up in water and extracted with DCM. The combined organic phases were dried over anhydrous Na_2SO_4 and concentrated. The solid product **81** was isolated by flash chromatography using DCM/MeOH gradient (from 99:1 to 95:5).

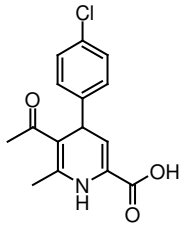

72a

72a; Prepared according to the method A (steps A1 - A3, A5) using 4-amino-pent-3-en-2-one in the step A3; brown solid; 68% yield, 93% purity (HPLC-ESI-MS, 210-400 nm), $C_{15}H_{14}ClNO_3$, M = 291.74 g/mol, HPLC-ESI-MS: $[M + H]^+$ = 292 *m/z*.

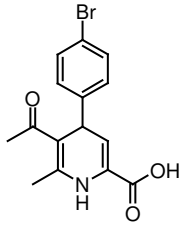

72b

72b; Prepared according to the method A (steps A1 - A3, A5) using 4-amino-pent-3-en-2-one in the step A3; brown solid; 68% yield, 89% purity (HPLC-ESI-MS, 210-400 nm), $C_{15}H_{14}BrNO_3$, M = 336.19 g/mol, HPLC-ESI-MS: $[M + H]^+$ = 336 *m/z*. ^{1}H NMR (400 MHz, DMSO-D_6) δ 1.97 (s, 3 H), 2.35 (s, 3 H), 4.67 (d, J = 6.10 Hz, 1 H), 5.93 (d, J = 6.10 Hz, 1 H), 7.13 (m, 2 H), 7.48 (m, 2 H), 8.27 (s, 1 H). ^{13}C NMR (100 MHz, DMSO-D_6) δ 19.9 (CH_3), 30.0 (CH_3), 39.75 (CH), 105.2 (C), 114.8 (CH), 119.4 (C), 126.9 (C), 129.3 (CH), 131.5 (CH), 146.5 (C), 148.6 (C), 163.5 (C), 195.8 (C).

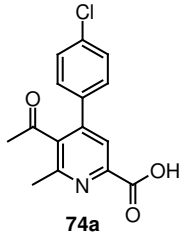

74a

74a; Prepared according to the method A (steps A1 - A3, A5) using 4-amino-pent-3-en-2-one in the step A3; brown solid; 72% yield, 86% purity (HPLC-ESI-MS, 210-400 nm), $C_{15}H_{12}ClNO_3$, M = 289.72 g/mol, HPLC-ESI-MS: $[M + H]^+$ = 290 *m/z*. ^{1}H NMR (400 MHz, DMSO-D_6) δ 2.12 (s, 3 H), 2.51 (s, 3 H), 7.42 (m, 2 H), 7.60 (m, 2 H), 7.87 (s, 1 H). ^{13}C NMR (100 MHz, DMSO-D_6) δ 22.4 (CH_3), 31.8 (CH_3), 122.6 (CH), 129.2 (CH), 130.2 (CH), 134.4 (C), 135.6 (C), 137.9 (C), 145.3 (C), 148.0 (C), 153.7 (C), 165.5 (C), 205.2 (C).

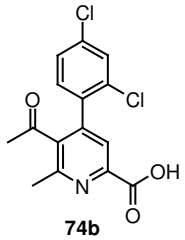

74b

74b; Prepared according to the method A (steps A1 - A3, A5) using 4-amino-pent-3-en-2-one in the step A3; brown solid; 85% yield, 87% purity (HPLC-ESI-MS, 210-400 nm), $C_{15}H_{11}Cl_2NO_3$, M = 324.17 g/mol, HPLC-ESI-MS: $[M + H]^+$ = 324 *m/z*.

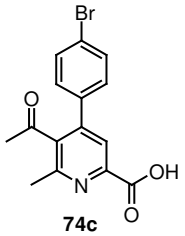

74c

74c; Prepared according to the method A (steps A1 - A3, A5) using 4-amino-pent-3-en-2-one in the step A3; yellow solid; 93% yield, 80% purity (HPLC-ESI-MS, 210-400 nm), $C_{15}H_{12}BrNO_3$, M = 334.17 g/mol, HPLC-ESI-MS: $[M + H]^+$ = 334 *m/z*.

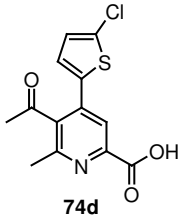

74d

74d; Prepared according to the method A (steps A1 - A3, A5) using 4-amino-pent-3-en-2-one in the step A3; brown solid; 99% yield, 94% purity (HPLC-ESI-MS, 210-400 nm), $C_{13}H_{10}ClNO_3S$, M = 295.75 g/mol, HPLC-ESI-MS: $[M + H]^+$ = 296 *m/z*.

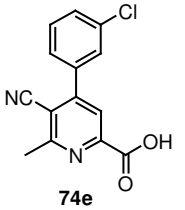

74e

74e; Prepared according to the method A (steps A1 - A3, A5; 74% yield, 80% purity, HPLC-ESI-MS, 210-400 nm) using 3-amino-but-2-enenitrile as the amine in the step A3 and method B (60% yield); colorless solid; $C_{14}H_9ClN_2O_2$, M = 272.69 g/mol, HPLC-ESI-MS: $[M + H]^+$ = 273 *m/z*; m.p. 206 °C. ^{1}H NMR (400 MHz, DMSO-D_6) δ 2.80 (s, 3 H), 7.64 (m, 3 H), 7.79 (m, 1 H), 7.98 (s, 1 H). ^{13}C NMR (100 MHz, DMSO-D_6) δ 23.8 (CH_3), 109.8 (C), 116.3 (C), 121.9 (CH), 127.4 (CH), 128.4 (CH), 130.1 (CH), 130.9 (CH), 133.7 (C), 137.4 (C), 150.3 (C), 152.1 (C), 162.2 (C), 165.1 (C). IR (neat, cm^{-1}) λ_{max}: 3078, 3048, 2886, 2775, 2672, 2605, 2222, 1705, 1565, 1543, 1447, 1381, 1329, 1270, 1233, 1144, 1108, 908, 879, 798. FT-ICR-MS: calculated for $C_{14}H_9ClN_2O_2H^+$: 273.0425, found: 273.0426.

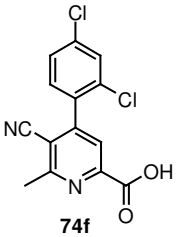

74f

74f; Prepared according to the method A (steps A1 - A3, A5; 80% yield, 99% purity, HPLC-ESI-MS, 210-400 nm) using 3-amino-but-2-enenitrile as the amine in the step A3 and method B (40% yield, 20 mmol scale, 1.5 eq *t*-BuOK, precipitation from MeCN/Et_2O); pale solid; $C_{14}H_8Cl_2N_2O_2$, M = 307.14 g/mol, HPLC-ESI-MS: $[M + H]^+$ = 307 *m/z*. ^{1}H NMR (400 MHz, DMSO-D_6) δ 2.80 (s, 3 H), 7.59 (d, J = 8.33 Hz, 1 H), 7.65 (dd, J = 8.42, 2.03 Hz, 1 H), 7.90 (d, J = 2.02 Hz, 1 H), 7.95 (s, 1 H). ^{13}C NMR (100 MHz, DMSO-D_6) δ 23.6 (CH_3), 109.4 (C),

115.9 (C), 121.8 (CH), 128.0 (CH), 129.4 (CH), 132.2 (CH), 132.4 (C), 133.9 (C), 135.3 (C), 150.1 (C), 155.4 (C), 161.2 (C), 166.0 (C).

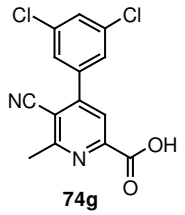

74g

74g; Prepared according to the method A (steps A1 - A3, A5) using 3-amino-but-2-enenitrile as the amine in the step A3; colorless solid; pale solid; 99% yield, 76% purity (HPLC-ESI-MS, 210-400 nm), $C_{14}H_8Cl_2N_2O_2$, M = 307.14 g/mol, HPLC-ESI-MS: $[M + H]^+$ = 307 *m/z*.

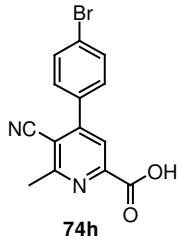

74h

74h; Prepared according to the method A (steps A1 - A3, A5) using 3-amino-but-2-enenitrile as the amine in the step A3; pale solid; 67% yield, 71% purity (HPLC-ESI-MS, 210-400 nm), $C_{14}H_9BrN_2O_2$, M = 317.14 g/mol, HPLC-ESI-MS: $[M + H]^+$ = 317 *m/z*. ^{1}H NMR (400 MHz, DMSO-D_6) δ 2.77 (s, 3 H), 7.57 (m, 3 H), 7.74 (m, 2 H), 7.86 (s, 1 H). ^{13}C NMR (100 MHz, DMSO-D_6) δ 23.6 (CH_3), 107.1 (C), 170.0 (C), 120.7 (C), 123.8 (CH), 130.7 (CH), 132.1 (CH), 135.3 (C), 151.9 (C), 157.9 (C), 161.8 (C), 167.1 (C).

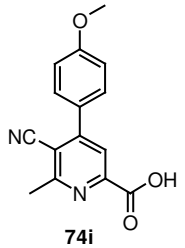

74i

74i; Prepared according to the method A (steps A1 - A3, A5; 73% yield, 86% purity, HPLC-ESI-MS, 210-400 nm) using 3-amino-but-2-enenitrile as the amine in the step A3 and method B (71% yield - column chromatography; 50% - 20 mmol scale, crystallization from MeCN); colorless solid; $C_{15}H_{12}N_2O_3$, M = 268.27 g/mol, HPLC-ESI-MS: $[M + H]^+$ = 269 *m/z*; m.p. 196 °C. ^{1}H NMR (400 MHz, DMSO-D_6) δ 2.77 (s, 3 H), 3.84 (s, 3 H), 7.13 (m, 2 H), 7.67 (m, 2 H), 7.92 (s, 1 H). ^{13}C NMR (100 MHz, DMSO-D_6) δ 23.8 (CH_3), 55.5 (CH_3), 109.2 (C), 114.6 (CH), 116.8 (C), 121.6 (CH), 127.4 (C), 130.2 (CH), 150.0 (C), 153.3 (C), 161.0 (C), 162.3 (C), 165.3 (C). IR (neat, cm^{-1}) λ_{max}: 3284, 3174, 2974, 2937, 2871, 2229, 1727, 1602, 1536, 1499, 1425, 1388, 1336, 1233, 1174, 1130, 1063, 1026, 916, 835. FT-ICR-MS: calculated for $C_{15}H_{12}N_2O_3H^+$: 269.0921, found: 269.0919.

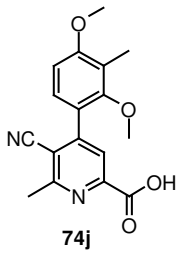

74j

74j; Prepared according to the method A (steps A1 - A3, A5) using 3-amino-but-2-enenitrile as the amine in the step A3; pale solid; 38% yield, 84% purity (HPLC-ESI-MS, 210-400 nm), $C_{17}H_{16}N_2O_4$, M = 312.33 g/mol, HPLC-ESI-MS: $[M + H]^+$ = 313 *m/z*.

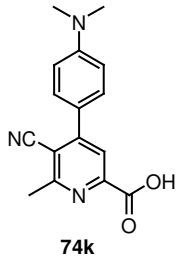

74k

74k; Prepared according to the method A (steps A1 - A3, A5) using 3-amino-but-2-enenitrile as the amine in the step A3 and method B (87% yield); pale yellow solid; 56% yield, 78% purity (HPLC-ESI-MS, 210-400 nm), $C_{16}H_{15}N_3O_2$, M = 281.32 g/mol, HPLC-ESI-MS: $[M + H]^+$ = 282 *m/z*.

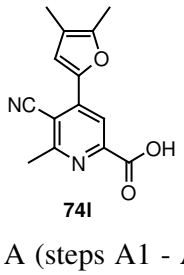

74l

74l; Prepared according to the method A (steps A1 - A3, A5) using 3-amino-but-2-enenitrile as the amine in the step A3; pale solid; 60% yield, 84% purity (HPLC-ESI-MS, 210-400 nm), $C_{14}H_{12}N_2O_3$, M = 256.26 g/mol, HPLC-ESI-MS: $[M + H]^+$ = 257 *m/z*.

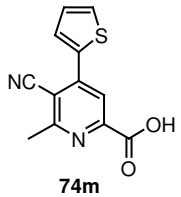

74m

74m; Prepared according to the method A (steps A1 - A3, A5; 40% yield, 93% purity, HPLC-ESI-MS, 210-400 nm) using 3-amino-but-2-enenitrile as the amine in the step A3 and method B (62% yield); yellow solid; $C_{12}H_8N_2O_2S$, M = 245.27 g/mol, HPLC-ESI-MS: $[M + H]^+$ = 245 *m/z*; m.p. 200 °C. ^{1}H NMR (400 MHz, DMSO-D_6) δ 2.77 (s, 3 H), 7.33 (m, 1 H), 7.97 (m, 2 H), 8.04 (s, 1 H). ^{13}C NMR (100 MHz, DMSO-D_6) δ 23.9 (CH_3), 106.8 (C), 116.9 (C), 120.3 (CH), 129.1 (CH), 130.5 (CH), 131.5 (CH), 136.2 (C), 145.3 (C), 150.3 (C), 163.1 (C), 165.1 (C). IR (neat, cm^{-1}) λ_{max}: 3336, 3100, 2893, 2849, 2222, 1919, 1764, 1713, 1580, 1536, 1417, 1388, 1299, 1218, 1144, 849, 798, 702. FT-ICR-MS: calculated for $C_{12}H_8N_2O_2SH^+$: 245.0379, found: 245.0378.

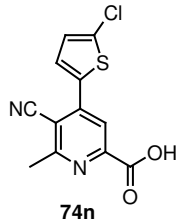

74n

74n; Prepared according to the method A (steps A1 - A3, A5) using 3-amino-but-2-enenitrile as the amine in the step A3; brown solid; 38% yield, 73% purity (HPLC-ESI-MS, 210-400 nm), $C_{12}H_7ClN_2O_2S$, M = 278.72 g/mol, HPLC-ESI-MS: $[M + H]^+$ = 279 *m/z*.

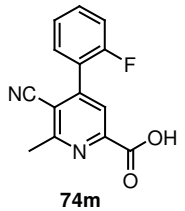

74m

74m; Prepared according to the method B; colorless solid; 61% yield - column chromatography, 51% - 20 mmol scale, crystallization from MeCN; $C_{14}H_9FN_2O_2$, M = 256.24 g/mol, HPLC-ESI-MS: $[M + H]^+$ = 257 *m/z*; m.p. 188.0 °C. ^{1}H NMR (400 MHz, DMSO-D_6) δ 2.81 (s, 3 H), 7.43 (m, 2 H), 7.63 (m, 2 H), 7.98 (s, 1 H). ^{13}C NMR (100 MHz, DMSO-D_6) δ 23.7 (CH_3), 111.0 (C), 115.8 (C), 116.2 (d, $^2J_{C\text{-}F}$ = 21.22 Hz, CH), 122.7 (CH), 123.1 (d, $^2J_{C\text{-}F}$ = 14.63 Hz, C), 125.2 (d, $^3J_{C\text{-}F}$ = 3.66 Hz, CH), 131.2 (d, $^4J_{C\text{-}F}$ = 2.19 Hz, CH), 132.7 (d, $^3J_{C\text{-}F}$ = 8.05 Hz, CH), 148.4 (C), 150.4 (C), 158.5 (d, $^1J_{C\text{-}F}$ =248.10 Hz, C), 161.9 (C), 165.1 (C). IR (neat, cm^{-1}) λ_{max}: 3085, 2882, 2792, 2230, 1945, 1705, 1614, 1581, 1546, 1493, 1452, 1386, 1255, 1220, 919, 869, 796, 756. FT-ICR-MS: calculated for $C_{14}H_9FN_2O_2H^+$: 257.0721, found: 257.0721.

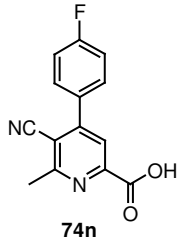

74n

74n; Prepared according to the method B; colorless solid; 66% yield; $C_{14}H_9FN_2O_2$, M = 256.24 g/mol, HPLC-ESI-MS: M = 256.24 g/mol, HPLC-ESI-MS: $[M + H]^+$ = 257 *m/z*; m.p. 201 °C. ^{1}H NMR (400 MHz, DMSO-D_6) δ 2.79 (s, 3 H), 7.43 (m, 2 H), 7.77 (m, 2 H), 7.96 (s, 1 H). ^{13}C NMR (100 MHz, DMSO-D_6) δ 23.8 (CH_3), 109.7 (C), 116.0 (C), 116.3 (d, $^2J_{C\text{-}F}$ = 21.96, CH), 121.9 (CH), 131.1 (d, $^3J_{C\text{-}F}$ = 8.78, CH), 131.8 (d, $^4J_{C\text{-}F}$ = 2.93, C), 150.1 (C), 152.6 (C), 162.2 (C), 163.3 (d, $^1J_{C\text{-}F}$ = 248.83, C), 165.2 (C). IR (neat, cm^{-1}) λ_{max}: 3292, 3115, 3078, 2229, 1757, 1602, 1550, 1506, 1417, 1388, 1344, 1314, 1226, 1159, 1108, 849, 717. FT-ICR-MS: calculated for $C_{14}H_9FN_2O_2H^+$: 257.0721, found: 257.0719.

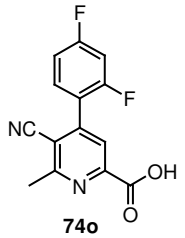

74o

74o; Prepared according to the method B; colorless solid; 30% yield, 20 mmol scale, 1.5 eq *t*-BuOK, crystallization from MeCN; $C_{14}H_8F_2N_2O_2$, M = 274.23 g/mol, HPLC-ESI-MS: $[M + H]^+$ = 275 *m/z*. ^{1}H NMR (400 MHz, $CDCl_3$) δ 2.80 (s, 3 H), 7.32 (m, 1 H), 7.53 (m, 1 H), 7.71 (m, 1 H), 7.98 (s, 1 H). ^{13}C NMR (100 MHz, $CDCl_3$) δ 23.7 (CH_3), 104.9 (t, $^2J_{C\text{-}F}$ = 25.99, CH), 111.1 (C), 112.6 (dd, $^{2,4}J_{C\text{-}F}$ = 22.06, 3.66 Hz, CH), 115.8 (C), 119.8 (dd, $^{2,4}J_{C\text{-}F}$ = 13.72, 3.66 Hz, C), 122.9 (CH), 132.8 (dd, $^3J_{C\text{-}F}$ = 10.22, 3.66 Hz, CH), 147.6 (C), 150.4 (C), 159.0 (dd, $^{1,3}J_{C\text{-}F}$ = 250.41, 12.81 Hz, C), 162.0 (C), 163.6 (dd, $^{1,3}J_{C\text{-}F}$ = 250.40, 12.08 Hz, C), 165.1 (C).

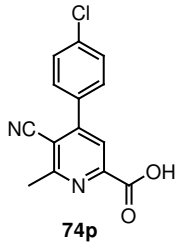

74p

74p; Prepared according to the method B; colorless solid; 73% yield; $C_{14}H_9ClN_2O_2$, M = 272.69 g/mol, HPLC-ESI-MS: $[M + H]^+$ = 273 *m/z*; m.p. 208 °C. ^{1}H NMR (400 MHz, DMSO-D_6) δ 2.79 (s, 3 H), 7.66 (m, 2 H), 7.73 (m, 2 H), 7.97 (s, 1 H). ^{13}C NMR (100 MHz, DMSO-D6) δ 23.8 (CH_3), 109.7 (C), 116.3 (C), 121.8 (CH), 129.1 (CH), 130.5 (CH), 134.2 (C), 135.3 (C), 150.2 (C), 152.4 (C), 162.2 (C), 165.1 (C). IR (neat, cm^{-1}) λ_{max}: 3085, 2982, 2937, 2864, 2229, 1742, 1713, 1602, 1580, 1543, 1506, 1417, 1226, 1181, 1144, 1085, 1049, 967, 857. FT-ICR-MS: calculated for $C_{14}H_9ClN_2O_2H^+$: 273.0425, found: 273.0425.

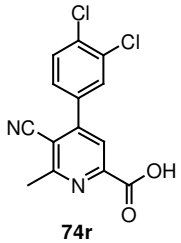

74r

74r; Prepared according to the method B; colorless solid; 42% yield; $C_{14}H_8Cl_2N_2O_2$, M = 307.14 g/mol, HPLC-ESI-MS: $[M + H]^+$ = 307 *m/z*.

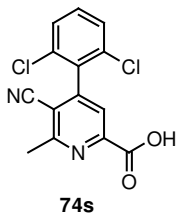

74s

74s; Prepared according to the method B; colorless solid; 81% yield; $C_{14}H_8Cl_2N_2O_2$, M = 307.14 g/mol, HPLC-ESI-MS: $[M + H]^+$ = 307 *m/z*; m.p. 226-227°C (decomp.). ^{1}H NMR (400 MHz, DMSO-D_6) δ 2.78 (s, 3 H) 7.59 (m, 1 H) 7.70 (m, 2 H) 7.81 (s, 1 H). ^{13}C NMR (100 MHz, DMSO-D_6) δ 23.5 (CH_3), 109.1 (C), 115.4 (C), 121.8 (CH), 128.7 (CH), 132.3 (C), 132.9 (CH), 133.6 (C), 149.0 (C), 156.4 (C), 161.5 (C), 166.0 (C). IR (neat, cm^{-1}) λ_{max}: 3144, 2974, 2937, 2878, 2827, 2229, 1683, 1587, 1558, 1477, 1432, 1388, 1226, 1181, 1056, 1004. FT-ICR-MS: calculated for $C_{14}H_8Cl_2N_2O_2H^+$: 307.0036, found: 307.0036

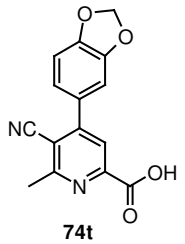

74t

74t; Prepared according to the method B; colorless solid; 62% yield, 20 mmol scale, crystallization from MeCN; $C_{15}H_{10}N_2O_4$, M = 282.26 g/mol, HPLC-ESI-MS: $[M + H]^+$ = 283 *m/z*; m.p. 211 °C. ^{1}H NMR (400 MHz, DMSO-D_6) δ 2.77 (s, 3 H), 6.14 (s, 2 H), 7.11 (m, 1 H), 7.19 (m, 1 H), 7.29 (m, 1 H), 7.91 (m, 1 H). ^{13}C NMR (100 MHz, DMSO-D_6) δ 23.8 (CH_3), 101.9 (CH_2), 108.7 (CH), 108.8 (CH), 109.4 (C), 116.6 (C), 121.7 (CH), 123.2 (CH), 129.0 (C), 147.9 (C), 149.1 (C), 150.0 (C), 153.2 (C), 162.2 (C), 165.2 (C). IR (neat, cm^{-1}) λ_{max}: 3306, 3174, 3078, 2974, 2945, 2871, 2229, 1764, 1727, 1587, 1536, 1499, 1447, 1388, 1336, 1233, 1196, 1152, 1034, 916. FT-ICR-MS: calculated for $C_{15}H_{10}N_2O_4H^+$: 283.0713, found: 283.0712.

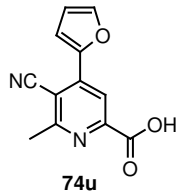

74u

74u; Prepared according to the method B; colorless solid; 29% yield (crystallization from MeCN); $C_{12}H_8N_2O_3$, M = 228.21 g/mol, HPLC-ESI-MS: $[M + H]^+$ = 229 *m/z*.

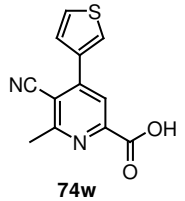

74w

74w; Prepared according to the method B; pale solid; 60% yield, 20 mmol scale, crystallization from MeCN; $C_{12}H_8N_2O_2S$, M = 244.27 g/mol, HPLC-ESI-MS: $[M + H]^+$ = 245 *m/z*.

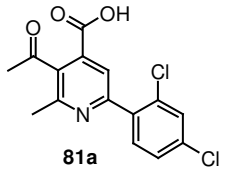

81a

81a; Prepared according to the method A (steps A1 - A3, A5) using 4-amino-pent-3-en-2-one in the step A3; brown solid; 88% yield, 73% purity (HPLC-ESI-MS, 210-400 nm), $C_{15}H_{11}Cl_2NO_3$, M = 324.17 g/mol, HPLC-ESI-MS: $[M + H]^+$ = 324 *m/z*.

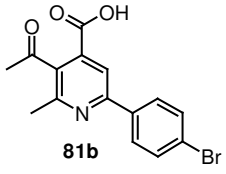

81b

81b; Prepared according to the method A (steps A1 - A3, A5) using 4-amino-pent-3-en-2-one in the step A3; brown solid; 36% yield, 84% purity (HPLC-ESI-MS, 210-400 nm), $C_{15}H_{12}BrNO_3$, M = 334.17 g/mol, HPLC-ESI-MS: $[M + H]^+$ = 334 *m/z*.

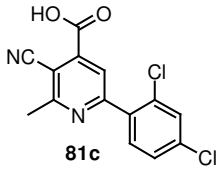

81c

81c; Prepared according to the method A (steps A1 - A3, A5; 80% yield, 72% purity, HPLC-ESI-MS, 210-400 nm) using 3-amino-but-2-enenitrile as the amine in the step A3 and method B (81% yield - column chromatography; 65% - 20 mmol scale, 1.5 eq *t*-BuOK, crystallization from MeCN); red solid; $C_{14}H_8Cl_2N_2O_2$, M = 307.14 g/mol, HPLC-ESI-MS: $[M + H]^+$ = 307 *m/z*; m.p. 180 °C (decomp.). ^{1}H NMR (400 MHz, DMSO-D_6) δ 2.80 (s, 3 H), 7.58 (dd, *J* = 8.34, 2.02 Hz, 1 H), 7.67 (d, *J* = 8.33 Hz, 1 H), 7.79 (d, *J* = 2.02 Hz, 1 H), 8.05 (s, 1 H). ^{13}C NMR (100 MHz, DMSO-D_6) δ 23.7 (CH_3), 105.9 (C), 115.8 (C), 121.8 (CH), 127.9 (CH), 129.7 (CH), 132.2 (C) , 133.1 (CH), 135.1 (C), 135.8 (C), 142.6 (C), 157.6 (C), 162.9 (C), 164.3 (C). IR (neat, cm^{-1}) λ_{max}: 3100, 3070, 2882, 2852, 2230, 1750, 1584, 1554, 1404, 1329, 1224, 1142, 1097, 1037, 872, 819, 789, 722, 609. FT-ICR-MS: calculated for $C_{14}H_8Cl_2N_2O_2H^+$: 307.0036, found: 307.0037.

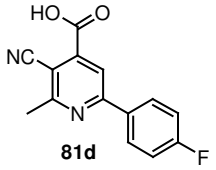

81d

81d; Prepared according to the method C; colorless solid; 74% yield; $C_{14}H_9FN_2O_2$, M = 256.24 g/mol, HPLC-ESI-MS: $[M + H]^+$ = 257 *m/z*; m.p. 286-287 °C (decomp.). ^{1}H NMR (400 MHz, DMSO-D_6) δ 2.78 (s, 3 H), 7.33 (m, 2 H), 8.22 (m, 3 H). ^{13}C NMR (100 MHz, DMSO-D_6) δ 23.9 (CH_3), 104.9 (C), 116.0 (d, $^2J_{C\text{-}F}$ = 21.23 Hz, CH), 116.0 (C), 117.1 (CH), 129.8 (d, $^3J_{C\text{-}F}$ = 9.52 Hz, CH),132.8 (d, $^4J_{C\text{-}F}$ = 2.93 Hz, C), 142.8 (C), 157.4 (C), 162.8 (C), 163.8 (d, $^1J_{C\text{-}F}$ = 248.83 Hz, C), 164.5 (C). IR (neat, cm^{-1}) λ_{max}: 3240, 3085, 2229, 1794, 1727, 1602, 1580, 1558, 1513, 1454, 1403, 1358, 1307, 1226, 1159, 1137, 842, 657. FT-ICR-MS: calculated for $C_{14}H_9FN_2O_2Na^+$: 279.0540, found: 279.0541.

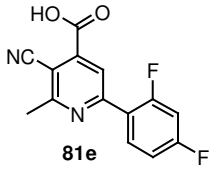

81e

81e; Prepared according to the method C; colorless solid; 30% yield, 20 mmol scale, 1.5 eq *t*-BuOK, crystallization from MeCN; $C_{14}H_8F_2N_2O_2$, M = 274.23 g/mol, HPLC-ESI-MS: $[M + H]^+$ = 274 *m/z*.

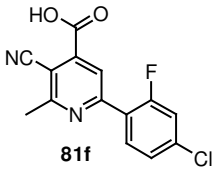

81f

81f; Prepared according to the method B; pale solid; 40% yield; $C_{14}H_8ClFN_2O_2$, M = 290.68 g/mol, HPLC-ESI-MS: $[M + H]^+$ = 291 *m/z*.

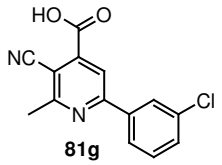

81g

81g; Prepared according to the method C; colorless solid; 67% yield; $C_{14}H_9ClN_2O_2$, M = 272.69 g/mol, HPLC-ESI-MS: $[M + H]^+$ = 273 *m/z*; m.p. 194 °C. ^{1}H NMR (400 MHz, DMSO-D_6) δ 2.80 (s, 3 H), 7.57 (m, 2 H), 8.13 (m, 1 H), 8.21 (m, 1 H), 8.30 (s, 1 H). ^{13}C NMR (100 MHz, DMSO-D_6) δ 23.9 (CH_3), 105.7 (C), 115.9 (C), 117.6 (CH), 126.0 (CH), 127.0 (CH), 130.5 (CH), 131.0 (CH), 134.0 (C), 138.4 (C), 143.2 (C), 156.9 (C), 162.9 (C), 164.5 (C). IR (neat, cm^{-1}) λ_{max}: 3011, 2819, 2635, 2524, 2214, 1713, 1624, 1572, 1513, 1425, 1381, 1373, 1322, 1263, 1233, 1144, 1093, 938, 879. FT-ICR-MS: calculated for $C_{14}H_9ClN_2O_2H^+$: 273.0425, found: 273.0425.

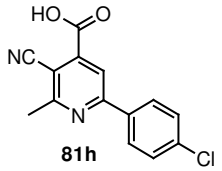

81h

81h; Prepared according to the method C; brown solid; 86% yield; $C_{14}H_9ClN_2O_2$, M = 272.69 g/mol, HPLC-ESI-MS: $[M + H]^+$ = 273 *m/z*; m.p. 295-297 °C (decomp.). ^{1}H NMR (400 MHz, DMSO-D_6) δ 2.80 (s, 3 H), 7.58 (m, 2 H), 8.20 (m, 2 H), 8.27 (s, 1 H). ^{13}C NMR (100 MHz, DMSO-D_6) δ 23.9 (CH_3), 105.3 (C), 116.0 (C), 117.3 (CH), 129.1 (CH), 129.2 (CH), 135.1 (C), 135.7 (C), 143.0 (C), 157.2 (C), 162.9 (C), 164.5 (C). IR (neat, cm^{-1}) λ_{max}: 3454, 2805, 2635, 2236, 1720, 1601, 1575, 1551, 1494, 1431, 1386, 1337, 1248, 1091, 1015, 903, 829, 746, 667. FT-ICR-MS: calculated for $C_{14}H_9ClN_2O_2H^+$: 273.0425, found: 273.0426.

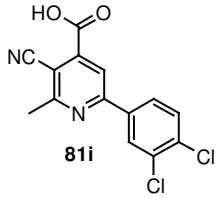

81i

81i; Prepared according to the method C; colorless solid; 54% yield; $C_{14}H_8Cl_2N_2O_2$, M = 307.14 g/mol, HPLC-ESI-MS: $[M + H]^+$ = 307 *m/z*; m.p. 165 °C. ^{1}H NMR (400 MHz, DMSO-D_6) δ 2.79 (s, 3 H), 7.75 (d, J = 8.65 Hz, 1 H), 8.14 (dd, J = 8.39, 2.03 Hz, 1 H), 8.31 (s, 1 H), 8.37 (d, J = 2.03 Hz, 1 H). ^{13}C NMR (100 MHz, DMSO-D_6) δ 23.8 (CH_3), 105.8 (C), 115.8 (C), 117.6 (CH), 127.4 (CH), 129.0 (CH), 131.2 (CH), 132.0 (C), 133.5 (C), 136.7 (C), 143.1 (C), 155.8 (C), 162.9 (C), 164.4 (C). IR (neat, cm^{-1}) λ_{max}: 3100, 2897, 2860, 2230, 1705, 1569, 1427, 1329, 1269, 1247, 1149, 1029, 887, 834, 677. FT-ICR-MS: calculated for $C_{14}H_8Cl_2N_2O_2H^+$: 307.0036, found: 307.0038.

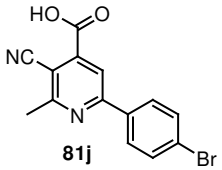

81j

81j; Prepared according to the method C; colorless solid; 72% yield - column chromatography; 35% - 20 mmol scale, 1.5 eq *t*-BuOK, crystallization from MeCN; $C_{14}H_9BrN_2O_2$, M = 317.14 g/mol, HPLC-ESI-MS: $[M + H]^+$ = 317 *m/z*. ^{1}H NMR (400 MHz, DMSO-D_6) δ 2.73 (s, 3 H), 7.70 (m, 2 H), 8.09 (m, 3 H). ^{13}C NMR (100 MHz, DMSO-D_6) δ

23.7 (CH_3), 105.6 (C), 116.7 (C), 117.3 (CH), 123.9 (C), 128.1 (CH), 131.9 (CH), 136.3 (C), 156.1 (C), 161.7 (C), 165.1 (C).

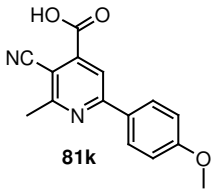

81k

81k; Prepared according to the method C; yellow solid; 81% yield - column chromatography, 55% - 20 mmol scale, 1.5 eq *t*-BuOK, crystallization from MeCN; $C_{15}H_{12}N_2O_3$, M = 268.27 g/mol, HPLC-ESI-MS: $[M + H]^+$ = 269 *m/z*; m.p. 186 °C. ^{1}H NMR (400 MHz, DMSO-D_6) δ 2.76 (s, 3 H), 3.83 (s, 3 H), 7.06 (m, *J* = 8.90 Hz, 2 H), 8.14 (m, *J* = 8.90 Hz, 2 H), 8.17 (s, 1 H). ^{13}C NMR (100 MHz, DMSO-D_6) δ 23.9 (CH_3), 55.4 (CH_3), 103.8 (C), 114.4 (CH), 116.2 (C), 116.3 (CH), 128.7 (C), 129.0 (CH), 142.5 (C), 158.2 (C), 161.6 (C), 162.7 (C), 164.7 (C). IR (neat, cm^{-1}) λ_{max}: 3011, 2974, 2871, 2842, 2237, 1742, 1602, 1565, 1513, 1454, 1388, 1322, 1292, 1263, 1226, 1174, 1144, 1026, 820, 672. FT-ICR-MS: calculated for $C_{15}H_{12}N_2O_3H^+$: 269.0921, found: 269.0921.

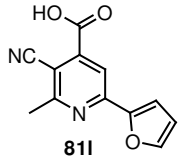

81l

81l; Prepared according to the method C; yellow solid; 63% yield; $C_{12}H_8N_2O_3$, M = 228.21 g/mol, HPLC-ESI-MS: $[M + H]^+$ = 229 *m/z*; m.p. 170 °C (decomp.). ^{1}H NMR (400 MHz, DMSO-D_6) δ 2.72 (s, 3 H), 7.22 (dd, *J* = 4.83, 3.81 Hz, 1 H), 7.83 (m, 1 H), 8.08 (m, 1 H), 8.21 (s, 1 H). ^{13}C NMR (100 MHz, DMSO-D_6) δ 23.7 (CH_3), 104.1 (C), 115.8 (CH), 116.1 (C), 129.0 (CH), 129.2 (CH), 131.8 (CH), 142.2 (C), 142.6 (C), 154.3 (C), 163.0 (C), 164.5 (C). IR (neat, cm^{-1}) λ_{max}: 3182, 3092, 2897, 2222, 1720, 1577, 1532, 1442, 1352, 1322, 1269, 1239, 1202, 1089, 1037, 917, 707, 662. FT-ICR-MS: calculated for $C_{12}H_8N_2O_3H^+$: 229.0608, found: 229.0610.

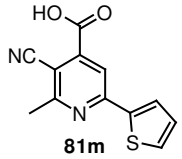

81m

81m; Prepared according to the method C; yellow solid; 61% yield; $C_{12}H_8N_2O_2S$, M = 244.27 g/mol, HPLC-ESI-MS: $[M + H]^+$ = 245 *m/z*; m.p. 207-208 °C (decomp.). ^{1}H NMR (400 MHz, DMSO-D_6) δ 2.74 (s, 3 H), 6.74 (m, 1 H), 7.39 (m, *J* = 3.31 Hz, 1 H), 7.99 (m, *J* = 8.39 Hz, 2 H). ^{13}C NMR (100 MHz, DMSO-D_6) δ 23.8 (CH_3), 104.2 (C), 113.2 (CH), 113.2 (CH), 115.3 (CH), 116.1 (C), 142.6 (C), 146.5 (CH), 150.3 (C), 151.3 (C), 163.3 (C), 164.3 (C). IR (neat, cm^{-1}) λ_{max}: 3152, 3130, 2920, 2852, 2215, 1692, 1592, 1547, 1479, 1404, 1232, 1172, 1074, 1037, 954, 887, 767, 714. FT-ICR-MS: calculated for $C_{12}H_8N_2O_2SH^+$: 245.0379, found: 245.0380.

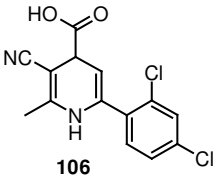

106

106; Prepared according to the method C; Brown crystals (crystallization from MeCN); $C_{14}H_{10}Cl_2N_2O_2$, M = 309.15 g/mol, HPLC-ESI-MS: $[M + H]^+$ = 309 *m/z*; m.p. 179-181 °C (decomp.). ^{1}H NMR (400 MHz, DMSO-D_6) δ 2.01 (s, 3 H), 4.02 (d, *J* = 4.83 Hz, 1 H), 4.71 (dd, *J* = 4.83, 1.53 Hz, 1 H), 7.37 (d, *J* = 8.14 Hz, 1 H), 7.46 (dd, *J* = 8.19, 2.03 Hz, 1 H), 7.69 (d, *J* = 2.03 Hz, 1 H), 8.84 (s, 1 H), 12.61 (s, 1 H). ^{13}C NMR (100 MHz, DMSO-D_6) δ 17.9 (CH_3), 41.0 (CH), 73.1 (C), 99.2 (CH), 120.9 (C), 127.5 (CH), 129.2 (CH), 132.3 (CH), 133.4 (C), 133.6 (C), 134.1 (C), 134.2 (C), 149.7 (C), 173.0 (C). IR (neat, cm^{-1}) λ_{max}: 3262, 3233, 3115, 3004, 2849, 2620, 2207, 1698, 1668, 1624, 1580, 1513, 1469, 1417, 1381, 1307, 1248, 1122, 1085, 916. FT-ICR-MS: calculated for $C_{14}H_{10}Cl_2N_2O_2H^+$: 309.0192, found: 309.0192.

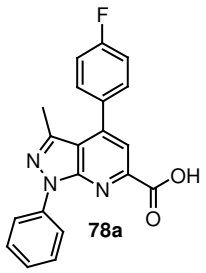

78a

78a; Prepared according to the method A (steps A1-A3, A5) using 5-methyl-2-phenyl-2*H*-pyrazol-3-ylamine as the amine in the step A3; yellow solid; 85% yield, 82% purity (HPLC-ESI-MS, 210-400 nm), $C_{20}H_{14}ClN_3O_2$, M = 363.81 g/mol, $[M + H]^+$ = 364 *m/z*.

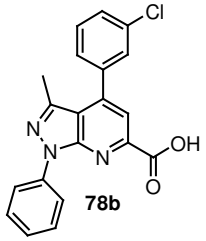

78b

78b; Prepared according to the method A (steps A1-A3, A5) using 5-methyl-2-phenyl-2*H*-pyrazol-3-ylamine as the amine in the step A3; yellow solid; 99% yield, 79% purity (HPLC-ESI-MS, 210-400 nm), $C_{20}H_{14}ClN_3O_2$, M = 363.81 g/mol, $[M + H]^+$ = 364 *m/z*.

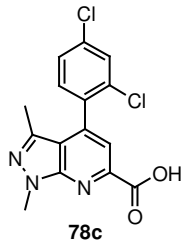

78c

78c; Prepared according to the method A (steps A1-A3, A5) using 2,5-dimethyl-2*H*-pyrazol-3-ylamine as the amine in the step A3; pale solid; 98% yield, 82% purity (HPLC-ESI-MS, 210-400 nm), $C_{15}H_{11}Cl_2N_3O_2$, M = 336.18 g/mol, $[M + H]^+$ = 336 *m/z*. ^{1}H NMR (400 MHz, DMSO-D_6) δ 2.03 (s, 3 H), 4.06 (s, 3 H), 7.54 (m, 1 H), 7.61 (m, 1 H), 7.64 (s, 1 H), 7.86 (m, 1 H). ^{13}C NMR (100 MHz, DMSO-D_6) δ 13.2 (CH_3), 33.7 (CH_3), 114.1 (C), 116.9 (CH), 127.7 (CH), 129.0 (CH), 132.3 (CH), 132.8 (C), 134.2 (C), 134.7 (C), 139.4 (C), 141.5 (C), 147.1 (C), 150.3 (C), 166.0 (C).

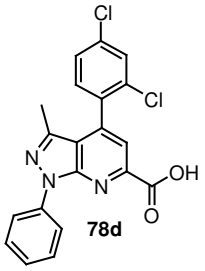

78d

78d; Prepared according to the method A (steps A1-A3, A5) using 5-methyl-2-phenyl-2*H*-pyrazol-3-ylamine as the amine in the step A3; yellow solid; 79% yield, 99% purity (HPLC-ESI-MS, 210-400 nm), $C_{20}H_{13}Cl_2N_3O_2$, M = 398.25 g/mol, HPLC-ESI-MS: $[M + H]^+$ = 398 *m/z*.

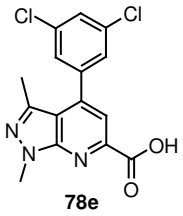

78e

78e; Prepared according to the method A (steps A1-A3, A5) using 2,5-dimethyl-2*H*-pyrazol-3-ylamine as the amine in the step A3; pale solid; 99% yield, 80% purity (HPLC-ESI-MS, 210-400 nm), $C_{15}H_{11}Cl_2N_3O_2$, M = 336.18 g/mol, HPLC-ESI-MS: $[M + H]^+$ = 336 *m/z*.

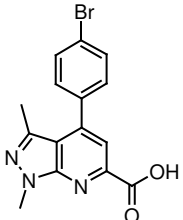

78f

78f; Prepared according to the method A (steps A1-A3, A5) using 2,5-dimethyl-2*H*-pyrazol-3-ylamine as the amine in the step A3; colorless solid; 99% yield, 88% purity (HPLC-ESI-MS, 210-400 nm), $C_{15}H_{12}BrN_3O_2$, M = 346.19 g/mol, HPLC-ESI-MS: $[M + H]^+$ = 346 *m/z*.

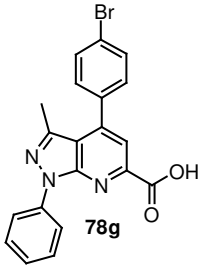

78g

78g; Prepared according to the method A (steps A1-A3, A5) using 5-methyl-2-phenyl-2*H*-pyrazol-3-ylamine as the amine in the step A3; pale solid; 84% yield, 91% purity (HPLC-ESI-MS, 210-400 nm), $C_{20}H_{14}BrN_3O_2$, M = 408.26 g/mol, HPLC-ESI-MS: $[M + H]^+$ = 408 *m/z*. ^{1}H NMR (400 MHz, DMSO-D_6) δ 2.20 (s, 3 H), 7.32 (m, 1 H), 7.55 (m, 4 H), 7.74 (m, 3 H), 8.27 (m, 2 H), 13.58 (s, 1 H). ^{13}C NMR (100 MHz, DMSO-D_6) δ 15.2 (CH_3), 115.5 (C), 118.2 (CH), 120.5 (CH), 122.9 (C), 125.9 (CH), 129.2 (CH), 131.3 (CH), 131.5 (CH), 135.3 (C), 138.8 (C), 142.1 (C), 145.1 (C), 147.4 (C), 150.2 (C), 165.9 (C).

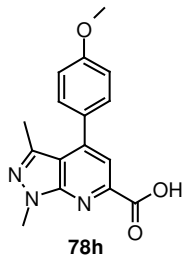

78h

78h; Prepared according to the method A (steps A1-A3, A5) using 2,5-dimethyl-2*H*-pyrazol-3-ylamine as the amine in the step A3; yellow solid; 84% yield, 75% purity (HPLC-ESI-MS, 210-400 nm), $C_{16}H_{15}N_3O_3$, M = 297.32 g/mol, HPLC-ESI-MS: $[M + H]^+$ = 298 *m/z*. ^{1}H NMR (400 MHz, DMSO-D_6) δ 2.22 (s, 3 H), 3.83 (s, 3 H), 4.03 (s, 3 H), 7.09 (m, 2 H), 7.51 (m, 2 H), 7.63 (s, 1 H). ^{13}C NMR (100 MHz, DMSO-D_6) δ 15.2 (CH_3), 33.6 (CH_3), 55.3 (CH_3), 113.6 (C), 114.0 (CH), 116.6 (CH), 128.7 (C), 130.7 (CH), 139.5 (C), 145.9 (C), 146.7 (C), 150.8 (C), 160.1 (C), 166.3 (C).

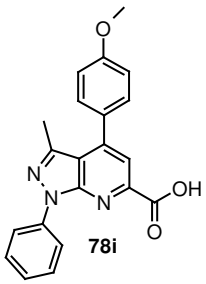

78i

78i; Prepared according to the method A (steps A1-A3, A5) using 5-methyl-2-phenyl-2*H*-pyrazol-3-ylamine as the amine in the step A3; yellow solid; 78% yield, 88% purity (HPLC-ESI-MS, 210-400 nm), $C_{21}H_{17}N_3O_3$, M = 359.39 g/mol, HPLC-ESI-MS: $[M + H]^+$ = 360 *m/z*.

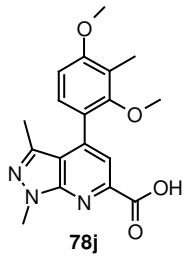

78j

78j; Prepared according to the method A (steps A1-A3, A5) using 2,5-dimethyl-2*H*-pyrazol-3-ylamine as the amine in the step A3; brown solid; 72% yield, 89% purity (HPLC-ESI-MS, 210-400 nm), $C_{18}H_{19}N_3O_4$, M = 341.37 g/mol, HPLC-ESI-MS: $[M + H]^+$ = 342 *m/z*.

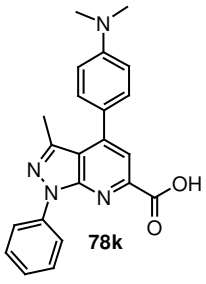

78k

78k; Prepared according to the method A (steps A1-A3, A5) using 5-methyl-2-phenyl-2*H*-pyrazol-3-ylamine as the amine in the step A3; pale yellow solid; 80% yield, 77% purity (HPLC-ESI-MS, 210-400 nm), $C_{22}H_{20}N_4O_2$, M = 372.43 g/mol, HPLC-ESI-MS: $[M + H]^+$ =

373 *m/z*. ^{1}H NMR (400 MHz, DMSO-D_6) δ 2.34 (s, 3 H), 2.98 (s, 6 H), 6.83 (m, 2 H), 7.43 (m, 5 H), 7.72 (s, 1 H), 8.31 (m, 2 H). ^{13}C NMR (100 MHz, DMSO-D_6) δ 15.8 (CH_3), 39.8 (CH_3), 111.7 (CH), 115.6 (C), 117.9 (CH), 120.5 (CH), 123.0 (C), 125.7 (CH), 129.2 (CH), 130.4 (CH), 139.0 (C), 142.5 (C), 147.2 (C), 150.7 (C), 150.9 (C), 166.3 (C).

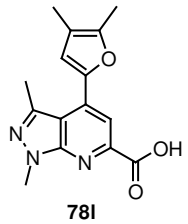

78l

78l; Prepared according to the method A (steps A1-A3, A5) using 2,5-dimethyl-2*H*-pyrazol-3-ylamine as the amine in the step A3; brown solid; 72% yield, 85% purity (HPLC-ESI-MS, 210-400 nm), $C_{15}H_{15}N_3O_3$, M = 285.31 g/mol, HPLC-ESI-MS: $[M + H]^+$ = 286 *m/z*.

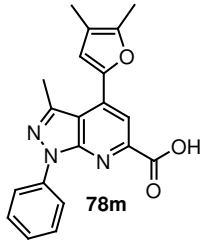

78m

78m; Prepared according to the method A (steps A1-A3, A5) using 5-methyl-2-phenyl-2*H*-pyrazol-3-ylamine as the amine in the step A3; brown solid; 99% yield, 88% purity (HPLC-ESI-MS, 210-400 nm), $C_{20}H_{17}N_3O_3$, M = 347.38 g/mol, HPLC-ESI-MS: $[M + H]^+$ = 348 *m/z*.

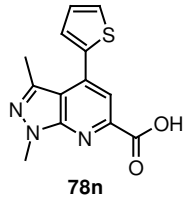

78n

78n; Prepared according to the method A (steps A1-A3, A5) using 2,5-dimethyl-2*H*-pyrazol-3-ylamine as the amine in the step A3; pale solid; 91% yield, 78% purity (HPLC-ESI-MS, 210-400 nm), $C_{13}H_{11}N_3O_2S$, M = 273.32 g/mol, HPLC-ESI-MS: $[M + H]^+$ = 274 *m/z*.

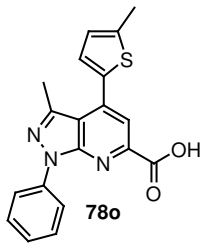

78o

78o; Prepared according to the method A (steps A1-A3, A5) using 5-methyl-2-phenyl-2*H*-pyrazol-3-ylamine as the amine in the step A3; yellow solid; 73% yield, 76% purity (HPLC-ESI-MS, 210-400 nm), $C_{19}H_{15}N_3O_2S$, M = 349.41 g/mol, HPLC-ESI-MS: $[M + H]^+$ = 350 *m/z*. ^{1}H NMR (400 MHz, DMSO-D_6) δ 2.52 (s, 3 H), 2.56 (s, 3 H), 7.00 (m, 1 H), 7.37 (m, 2 H), 7.57 (m, 2 H), 7.78 (s, 1 H), 8.27 (m, 2 H). ^{13}C NMR (100 MHz, DMSO-D_6) δ 15.1 (CH_3), 15.8 (CH_3), 114.9 (C), 118.2 (CH), 120.8 (CH), 126.0 (CH), 127.0 (CH), 129.2 (CH), 130.8 (CH), 134.2 (C), 138.8 (C), 139.2 (C), 142.3 (C), 143.3 (C), 165.9 (C).

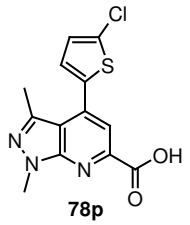

78p

78p; Prepared according to the method A using 2,5-dimethyl-2*H*-pyrazol-3-ylamine as the amine in the step A3; pale solid; 28% yield, 80% purity (HPLC-ESI-MS, 210-400 nm), $C_{13}H_{10}ClN_3O_2S$, M = 307.76 g/mol, HPLC-ESI-MS: $[M + H]^+$ = 308 *m/z*. ^{1}H NMR (400 MHz, DMSO-D_6) δ 2.41 (s, 1 H), 4.03 (s, 3 H), 7.29 (d, *J* = 3.81 Hz, 1 H) 7.41 (d, *J* = 3.81 Hz, 1 H), 7.66 (s, 1 H). ^{13}C NMR (100 MHz, DMSO-D_6) δ 15.4 (CH_3), 33.7 (CH_3), 112.7 (C), 116.8 (CH), 128.1 (CH), 130.0 (CH), 130.9 (C), 136.0 (C), 137.0 (C), 139.3 (C), 146.8 (C), 150.9 (C), 165.9 (C).

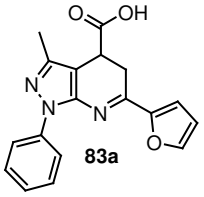

83a

83a; Prepared according to the method A (steps A1-A3, A5) using 5-methyl-2-phenyl-2*H*-pyrazol-3-ylamine as the amine in the step A3; brown solid; 56% yield, 90% purity (HPLC-ESI-MS, 210-400 nm), $C_{18}H_{15}N_3O_3$, M = 321.34 g/mol, HPLC-ESI-MS: $[M + H]^+$ = 322 *m/z*.

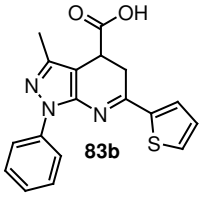

83b

83b; Prepared according to the method A (steps A1-A3, A5) using 5-methyl-2-phenyl-2*H*-pyrazol-3-ylamine as the amine in the step A3; brown solid; 88% yield, 99% purity (HPLC-ESI-MS, 210-400 nm), $C_{18}H_{15}N_3O_2S$, M = 337.40 g/mol, HPLC-ESI-MS: $[M + H]^+$ = 338 *m/z*. ^{1}H NMR (400 MHz, DMSO-D_6) δ 2.25 (s, 3 H), 2.97 (dd, *J* = 17.29, 9.41 Hz, 1 H), 3.58 (dd, *J* = 17.42, 2.42 Hz, 1 H), 3.94 (dd, *J* = 9.16, 2.54 Hz, 1 H), 7.21 (m, 1 H), 7.29 (m, 1 H), 7.48 (m, 3 H), 7.82 (m, 1 H), 7.86 (m, 1 H), 7.90 (m, 2 H). ^{13}C NMR (100 MHz, DMSO-D_6) δ 12.3 (CH_3), 28.0 (CH_2), 33.7 (CH), 102.0 (C), 121.3 (CH), 125.9 (CH), 128.6 (CH), 128.9 (CH), 131.1 (CH), 132.2 (CH), 139.0 (C), 144.1 (C), 145.3 (C), 145.6 (C), 161.9 (C), 173.7 (C).

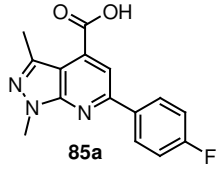

85a

85a; Prepared according to the method A using 2,5-dimethyl-2*H*-pyrazol-3-ylamine as the amine in the step A3; brown solid; 89% yield, 88% purity (HPLC-ESI-MS, 210-400 nm), $C_{15}H_{12}FN_3O_2$, M = 285.28 g/mol, HPLC-ESI-MS: $[M + H]^+$ = 286 *m/z*.

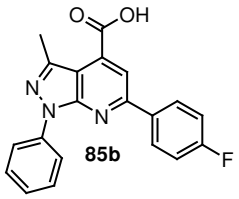

85b

85b; Prepared according to the method A using 5-methyl-2-phenyl-2*H*-pyrazol-3-ylamine as the amine in the step A3; yellow solid; 58% yield, 79% purity (HPLC-ESI-MS, 210-400 nm), $C_{13}H_{10}ClN_3O_2S$, M = 347.25 g/mol, HPLC-ESI-MS: $[M + H]^+$ = 348 *m/z*. ^{1}H NMR (400 MHz, DMSO-D_6) δ 2.65 (m, 3 H), 7.33 (m, 3 H), 7.54 (m, 2 H), 8.06 (s, 1 H), 8.21 (m, 4 H). ^{13}C NMR (100 MHz, DMSO-D_6) δ 15.6 (CH_3), 111.5 (C), 114.3 (CH), 115.9 (d, $^2J_{C\text{-}F}$ = 21.22, CH), 120.6 (CH), 125.7 (CH), 129.1 (CH), 129.4 (d, $^3J_{C\text{-}F}$ = 8.78, CH), 134.0 (d, $^4J_{C\text{-}F}$ = 2.20, C), 136.0 (C), 138.8 (C), 142.2 (C), 151.2 (C), 154.9 (C), 163.4 (d, $^1J_{C\text{-}F}$ = 248.10, C), 166.5 (C).

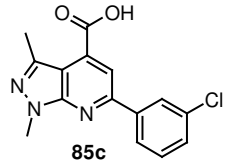

85c

85c; Prepared according to the method A using 2,5-dimethyl-2*H*-pyrazol-3-ylamine as the amine in the step A3; pale solid; 73% yield, 87% purity (HPLC-ESI-MS, 210-400 nm), $C_{15}H_{12}ClN_3O_2$, M = 301.73 g/mol, HPLC-ESI-MS: $[M + H]^+$ = 302 *m/z*.

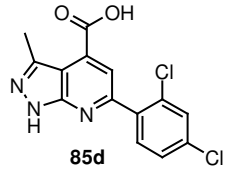

85d

85d; Prepared according to the method A using 5-methyl-2*H*-pyrazol-3-ylamine as the amine in the step A3; yellow solid; 75% yield, 79% purity (HPLC-ESI-MS, 210-400 nm), $C_{14}H_9Cl_2N_3O_2$, M = 322.15 g/mol, HPLC-ESI-MS: $[M + H]^+$ = 322 *m/z*. ^{1}H NMR (400 MHz, DMSO-D_6) δ 2.48 (s, 3 H), 6.75 (s, 1 H), 7.53 (s, 1 H), 7.59 (m, 1 H), 7.72 (m, 1 H), 7.80 (m, 1 H). ^{13}C NMR (100 MHz, DMSO-D_6) δ 14.4 (CH_3), 97.0 (CH), 108.1 (CH), 127.9 (CH), 129.6 (CH), 132.3 (C), 132.8 (CH), 135.1 (C), 135.7 (C), 136.4 (C), 149.2 (C), 154.2 (C), 155.5 (C), 161.4 (C).

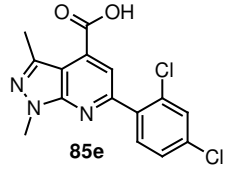

85e

85e; Prepared according to the method A using 2,5-dimethyl-2*H*-pyrazol-3-ylamine as the amine in the step A3; pale solid; 72% yield, 89% purity (HPLC-ESI-MS, 210-400 nm), $C_{15}H_{11}Cl_2N_3O_2$, M = 336.18 g/mol, HPLC-ESI-MS: $[M + H]^+$ = 336 *m/z*.

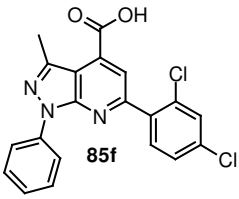

85f

85f; Prepared according to the method A using 5-methyl-2-phenyl-2*H*-pyrazol-3-ylamine as the amine in the step A3; yellow solid; 55% yield, 99% purity (HPLC-ESI-MS, 210-400 nm), $C_{20}H_{13}Cl_2N_3O_2$, M = 398.25 g/mol, HPLC-ESI-MS: $[M + H]^+$ = 398 *m/z*. ^{1}H NMR (400 MHz, DMSO-D_6) δ 2.71 (s, 3 H), 7.30 (m, 1 H), 7.54 (m, 3 H), 7.75 (m, 2 H), 7.84 (s, 1 H), 8.20 (m, 2 H). ^{13}C NMR (100 MHz, DMSO-D_6) δ 15.7 (CH_3), 111.7 (C), 118.4 (CH), 120.8 (CH), 126.0 (CH), 127.8 (CH), 129.1 (CH), 129.7 (CH), 132.4 (C), 133.2 (CH), 134.6 (C), 135.7 (C), 136.8 (C), 138.6 (C), 142.4 (C), 150.8 (C), 154.8 (C), 166.3 (C).

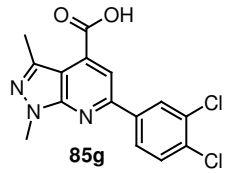

85g

85g; Prepared according to the method A using 2,5-dimethyl-2*H*-pyrazol-3-ylamine as the amine in the step A3; pale solid; 80% yield, 83% purity (HPLC-ESI-MS, 210-400 nm), $C_{15}H_{11}Cl_2N_3O_2$, M = 336.18 g/mol, HPLC-ESI-MS: $[M + H]^+$ = 336 *m/z*.

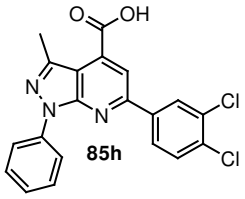

85h

85h; Prepared according to the method A using 5-methyl-2-phenyl-2*H*-pyrazol-3-ylamine as the amine in the step A3; brown solid; 56% yield, 71% purity (HPLC-ESI-MS, 210-400 nm), $C_{20}H_{13}Cl_2N_3O_2$, M = 398.25 g/mol, HPLC-ESI-MS: $[M + H]^+$ = 398 *m/z*.

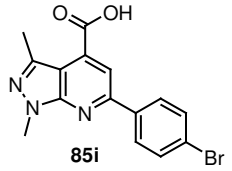

85i

85i; Prepared according to the method A using 2,5-dimethyl-2*H*-pyrazol-3-ylamine as the amine in the step A3; pale solid; 49% yield, 82% purity (HPLC-ESI-MS, 210-400 nm), $C_{15}H_{12}BrN_3O_2$, M = 346.19 g/mol, HPLC-ESI-MS: $[M + H]^+$ = 346 *m/z*. ^{1}H NMR (400 MHz, DMSO-D_6) δ 2.58 (s, 3 H), 3.99 (s, 3 H), 7.65 (m, 2 H), 7.82 (m, 1 H), 8.07 (m, 2 H).

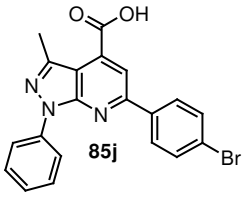

85j

85j; Prepared according to the method A using 5-methyl-2-phenyl-2*H*-pyrazol-3-ylamine as the amine in the step A3; yellow solid; 24% yield, 95% purity (HPLC-ESI-MS, 210-400 nm), $C_{20}H_{14}BrN_3O_2$, M = 408.26 g/mol, HPLC-ESI-MS: $[M + H]^+$ = 408 *m/z*.

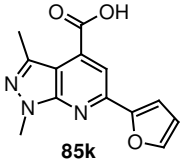

85k

85k; Prepared according to the method A using 2,5-dimethyl-2*H*-pyrazol-3-ylamine as the amine in the step A3; brown solid; 65% yield, 79% purity (HPLC-ESI-MS, 210-400 nm), $C_{14}H_{15}N_3O_3$, M = 273.29 g/mol, HPLC-ESI-MS: $[M + H]^+$ = 274 *m/z*.

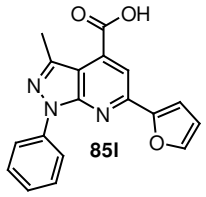

85l

85l; Prepared according to the method A using 5-methyl-2-phenyl-2*H*-pyrazol-3-ylamine as the amine in the step A3; brown solid; 57% yield, 63% purity (HPLC-ESI-MS, 210-400 nm), $C_{18}H_{13}N_3O_3$, M = 319.32 g/mol, HPLC-ESI-MS: $[M + H]^+$ = 320 *m/z*.

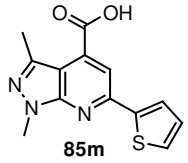

85m

85m; Prepared according to the method A using 2,5-dimethyl-2*H*-pyrazol-3-ylamine as the amine in the step A3; pale solid; 99% yield, 96% purity (HPLC-ESI-MS, 210-400 nm), $C_{13}H_{11}N_3O_2S$, M = 273.32 g/mol, HPLC-ESI-MS: $[M + H]^+$ = 274 *m/z*. ^{1}H NMR (400 MHz, DMSO-D_6) δ 2.55 (s, 3 H), 3.98 (s, 3 H), 7.20 (m, 1 H), 7.73 (m, 1 H), 7.96 (s, 1 H), 7.99 (m, 1 H), 13.95 (s, 1 H). ^{13}C NMR (100 MHz, DMSO-D_6) δ 15.3 (CH_3), 33.3 (CH_3), 109.3 (C), 112.4 (CH), 127.5 (CH), 128.7 (CH), 129.7 (CH), 135.3 (C), 139.7 (C), 143.5 (C), 150.9 (C), 151.3 (C), 166.6 (C).

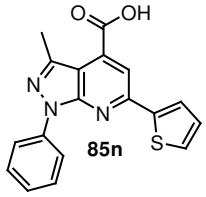

85n

85n; Prepared according to the method A using 5-methyl-2-phenyl-2*H*-pyrazol-3-ylamine as the amine in the step A3; solid; 54% yield, 86% purity (HPLC-ESI-MS, 210-400 nm), $C_{18}H_{13}N_3O_2S$, M = 335.39 g/mol, HPLC-ESI-MS: $[M + H]^+$ = 336 *m/z*. ^{1}H NMR (400 MHz, DMSO-D_6) δ 2.64 (s, 3 H), 7.19 (m, 1 H), 7.31 (m, Hz, 1 H), 7.54 (m, 2 H), 7.74 (m, 1 H), 8.00 (m, 1 H), 8.04 (s, 1 H), 8.25 (m, 2 H). ^{13}C NMR (100 MHz, DMSO-D_6) δ 15.6 (CH_3), 111.4 (C), 113.2 (CH), 120.3 (CH), 125.7 (CH), 127.8 (CH), 128.9 (C), 129.1 (CH), 130.2 (CH), 136.1 (C), 138.9 (C), 142.5 (C), 143.4 (C), 150.8 (C), 151.5 (C), 166.4 (C).

6. 1. 2. 4 Synthesis of pyrimidines.

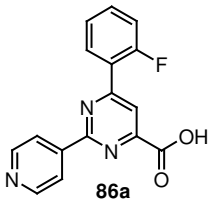

86a

86a; Prepared according to the method A (steps A1-A3, A5) using isonicotinamidine as the amine in the step A3; brown solid; 67% yield, 83% purity (HPLC-ESI-MS, 210-400 nm), $C_{16}H_{10}FN_3O_2$, M = 295.28 g/mol, HPLC-ESI-MS: $[M + H]^+$ = 396 *m/z*.

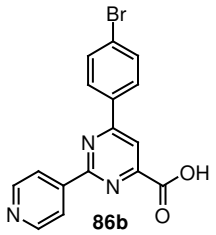

86b

86b; Prepared according to the method A (steps A1-A3, A5) using isonicotinamidine as the amine in the step A3; brown solid; 92% yield, 86% purity (HPLC-ESI-MS, 210-400 nm), $C_{16}H_{10}BrN_3O_2$, M = 356.18 g/mol, HPLC-ESI-MS: $[M + H]^+$ = 356 *m/z*.

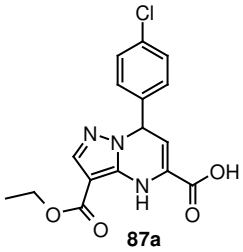

87a

87a; Prepared according to the method A (steps A1-A3, A5) using 5-amino-1*H*-pyrazole-4-carboxylic acid ethyl ester as the amine in the step A3; brown solid; 90% yield, 79% purity (HPLC-ESI-MS, 210-400 nm), $C_{16}H_{14}ClN_3O_4$, M = 347.76 g/mol, HPLC-ESI-MS: $[M + H]^+$ = 348 *m/z*.

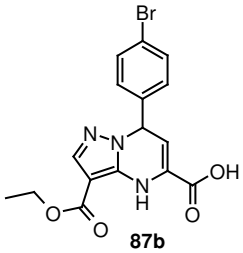

87b

87b; Prepared according to the method A (steps A1-A3, A5) using 5-amino-1*H*-pyrazole-4-carboxylic acid ethyl ester as the amine in the step A3; pale orange solid; 79% yield, 96% purity (HPLC-ESI-MS, 210-400 nm), $C_{16}H_{14}BrN_3O_4$, M = 392.21 g/mol, HPLC-ESI-MS: $[M + H]^+$ = 392 *m/z*. ^{1}H NMR (400 MHz, DMSO-D_6) δ 1.27 (t, *J* = 7.12 Hz, 3 H), 4.23 (q, *J* = 6.95 Hz, 2 H), 5.88 (m, 1 H), 6.26 (d, *J* = 4.07 Hz, 1 H), 7.17 (d, *J* = 8.39 Hz, 2 H), 7.55 (m, 2 H), 7.68 (s, 1 H), 7.91 (s, 1 H). ^{13}C NMR (100 MHz, DMSO-D_6) δ 14.3 (CH_3), 58.6 (CH), 59.7 (CH_2), 94.9 (C), 106.4 (CH), 121.5 (C), 125.5 (C), 129.1 (CH), 131.7 (CH), 140.0 (CH), 140.1 (C), 141.8 (C), 162.7 (C).

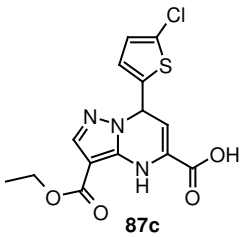

87c

87c; Prepared according to the method A (steps A1-A3, A5) using 5-amino-1*H*-pyrazole-4-carboxylic acid ethyl ester as the amine in the step A3; brown solid; 68% yield, 81% purity (HPLC-ESI-MS, 210-400 nm), $C_{14}H_{12}ClN_3O_4S$, M = 353.79 g/mol, HPLC-ESI-MS: $[M + H]^+$ = 354 *m/z*. ^{1}H NMR (400 MHz, DMSO-D_6) δ 1.27 (t, *J* = 7.12 Hz, 3 H), 4.22 (q, *J* = 7.12 Hz, 2 H), 5.97 (dd, *J* = 4.07, 1.78 Hz, 1 H), 6.50 (d, *J* = 4.32 Hz, 1 H), 7.00 (m, 2 H), 7.72 (s, 1 H), 7.97 (d, *J* = 1.53 Hz, 1 H), 14.11 (bs, 1H). ^{13}C NMR (100 MHz, DMSO-D_6) δ 14.3 (CH3), 54.3 (CH), 59.7 (CH2), 70.3 (C), 95.1 (C), 104.7 (CH), 126.4 (C), 126.5 (CH), 126.7 (CH), 129.1 (C), 140.0 (CH), 140.9 (C), 142.5 (C), 162.6 (C).

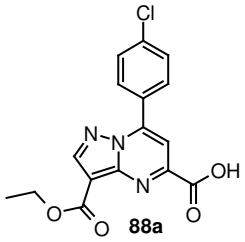

88a

88a; Prepared according to the method A using 5-amino-1*H*-pyrazole-4-carboxylic acid ethyl ester as the amine in the step A3; pale solid; 86% yield, 91% purity (HPLC-ESI-MS, 210-400 nm), $C_{16}H_{12}ClN_3O_4$, M = 345.74 g/mol, HPLC-ESI-MS: $[M + H]^+$ = 346 *m/z*.

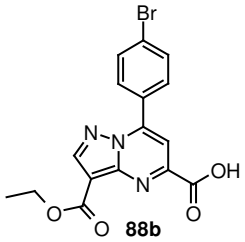

88b

88b; Prepared according to the method A using 5-amino-1*H*-pyrazole-4-carboxylic acid ethyl ester as the amine in the step A3; pale solid; 79% yield, 82% purity (HPLC-ESI-MS, 210-400 nm), $C_{16}H_{12}BrN_3O_4$, M = 39ß.20 g/mol, HPLC-ESI-MS: $[M + H]^+$ = 354 *m/z*. ^{1}H NMR (400 MHz, DMSO-D_6) δ 1.32 (t, *J* = 6.74 Hz, 3 H), 4.32 (m, 2 H), 7.83 (m, 3 H), 8.07 (m, 2 H), 8.75 (s, 1 H). ^{13}C NMR (100 MHz, DMSO-D_6) δ 14.4 (CH_3), 59.8 (CH_2), 103.6 (C), 109.0 (CH), 125.4 (C), 128.8 (C), 131.6 (CH), 131.9 (CH), 147.6 (C), 147.6 (C), 148.0 (CH), 150.6 (C), 161.3 (C), 164.8 (C).

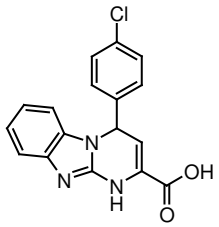

89a

89a; Prepared according to the method A (steps A1-A3, A5) using 1*H*-benzoimidazol-2-ylamine as the amine in the step A3; brown solid; 83% yield, 82% purity (HPLC-ESI-MS, 210-400 nm), $C_{17}H_{12}ClN_3O_2$, M = 325.76 g/mol, HPLC-ESI-MS: $[M + H]^+$ = 326 *m/z*.

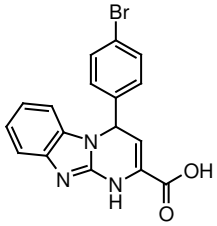

89b

89b; Prepared according to the method A (steps A1-A3, A5) using 1*H*-benzoimidazol-2-ylamine as the amine in the step A3; brown solid; 82% yield, 95% purity (HPLC-ESI-MS, 210-400 nm), $C_{17}H_{12}BrN_3O_2$, M = 370.21 g/mol, HPLC-ESI-MS: $[M + H]^+$ = 370 *m/z*. ^{1}H NMR (400 MHz, DMSO-D_6) δ 6.11 (d, *J* = 3.81 Hz, 1 H), 6.55 (d, *J* = 4.07 Hz, 1 H), 7.15 (m, 3 H), 7.45 (m, 2 H), 7.53 (m, 1 H), 7.58 (m, 2 H). ^{13}C NMR (100 MHz, DMSO-D_6) δ 56.3 (CH), 109.4 (CH), 111.2 (CH), 113.5 (CH), 122.2 (C), 123.0 (CH), 124.2 (CH), 125.2 (C), 129.4 (CH), 132.1 (CH), 138.0 (C), 144.8 (C), 162.3 (C).

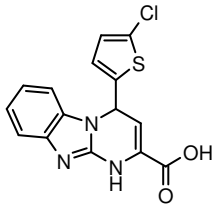

89c

89c; Prepared according to the method A (steps A1-A3, A5) using 1*H*-benzoimidazol-2-ylamine as the amine in the step A3; brown solid; 92% yield, 88% purity (HPLC-ESI-MS, 210-400 nm), $C_{15}H_{10}ClN_3O_2S$, M = 331.78 g/mol, HPLC-ESI-MS: $[M + H]^+$ = 332 *m/z*.

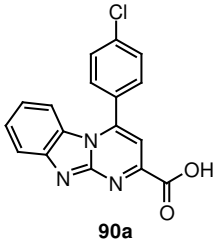

90a

90a; Prepared according to the method A using 1*H*-benzoimidazol-2-ylamine as the amine in the step A3; brown solid; 65% yield, 91% purity (HPLC-ESI-MS, 210-400 nm), $C_{17}H_{10}ClN_3O_2$, M = 323.74 g/mol, HPLC-ESI-MS: $[M + H]^+$ = 324 *m/z*. ^{1}H NMR (400 MHz, DMSO-D_6) δ 2.51 (s, 3 H), 6.75 (m, 1 H), 7.25 (m, 1 H), 7.48 (s, 1 H), 7.58 (m, 1 H), 7.88 (m, 5 H). ^{13}C NMR (100 MHz, DMSO-D_6) δ 107.7 (CH), 114.9 (CH), 119.6 (CH), 122.3 (CH), 126.7 (CH), 129.5 (CH), 130.5 (CH), 130.5 (C), 136.2 (C), 149.5 (C), 150.1 (C), 152.8 (C), 161.1 (C), 164.8 (C).

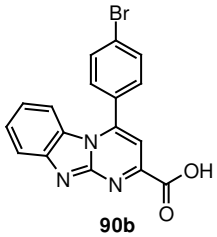

90b

90b; Prepared according to the method A using 1*H*-benzoimidazol-2-ylamine as the amine in the step A3; pale yellow solid; 96% yield, 91% purity (HPLC-ESI-MS, 210-400 nm), $C_{17}H_{10}BrN_3O_2$, M = 368.19 g/mol, HPLC-ESI-MS: $[M + H]^+$ = 368 *m/z*. ^{1}H NMR (400 MHz,

DMSO-D_6) δ 6.75 (m, 1 H) 7.26 (m, 1 H) 7.49 (m, 1 H) 7.58 (m, 1 H) 7.75 (m, 2 H) 7.95 (m, 3 H).

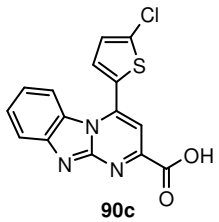

90c

90c; Prepared according to the method A using 1*H*-benzoimidazol-2-ylamine as the amine in the step A3; brown solid; 86% yield, 90% purity (HPLC-ESI-MS, 210-400 nm), $C_{15}H_8ClN_3O_2S$, M = 329.77 g/mol, HPLC-ESI-MS: $[M + H]^+$ = 330 *m/z*.

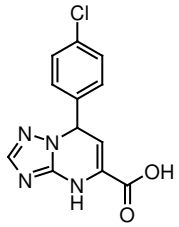

91a

91a; Prepared according to the method A (steps A1-A3, A5) using [1,2,4]triazol-3-ylamine as the amine in the step A3; brown solid; 87% yield, 86% purity (HPLC-ESI-MS, 210-400 nm), $C_{12}H_9ClN_4O_2$, M = 276.68 g/mol, HPLC-ESI-MS: $[M + H]^+$ = 277 *m/z*.

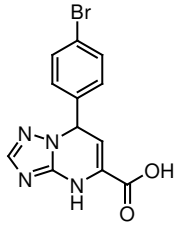

91b

91b; Prepared according to the method A (steps A1-A3, A5) using [1,2,4]triazol-3-ylamine as the amine in the step A3; brown solid; 81% yield, 93% purity (HPLC-ESI-MS, 210-400 nm), $C_{12}H_9BrN_4O_2$, M = 321.14 g/mol, HPLC-ESI-MS: $[M + H]^+$ = 321 m/z. ^{1}H NMR (400 MHz, DMSO-D_6) δ 5.76 (d, *J* = 3.05 Hz, 1 H), 6.27 (d, *J* = 3.56 Hz, 1 H), 7.16 (m, 2 H), 7.56 (m, 2 H), 7.64 (s, 1 H), 9.97 (s, 1 H). ^{13}C NMR (100 MHz, DMSO-D_6) δ 58.7 (CH), 105.6 (CH), 121.5 (C), 127.8 (C), 129.0 (CH), 131.7 (CH), 140.2 (C), 150.0 (CH), 162.8 (C).

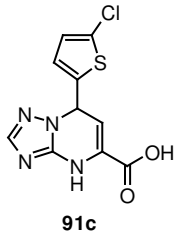

91c

91c; Prepared according to the method A (steps A1-A3, A5) using [1,2,4]triazol-3-ylamine as the amine in the step A3; brown solid; 70% yield, 80% purity (HPLC-ESI-MS, 210-400 nm), $C_{10}H_7ClN_4O_2S$, M = 282.71 g/mol, HPLC-ESI-MS: $[M + H]^+$ = 283 *m/z*.

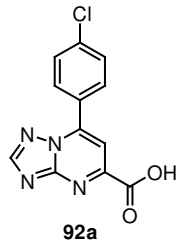

92a

92a; Prepared according to the method A using [1,2,4]triazol-3-ylamine as the amine in the step A3; brown solid; 82% yield, 89% purity (HPLC-ESI-MS, 210-400 nm), $C_{12}H_7ClN_4O_2$, M = 274.67 g/mol, HPLC-ESI-MS: $[M + H]^+$ = 275 *m/z*.

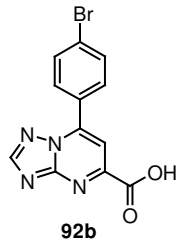

92b

92b; Prepared according to the method A using [1,2,4]triazol-3-ylamine as the amine in the step A3; pale solid; 63% yield, 82% purity (HPLC-ESI-MS, 210-400 nm), $C_{12}H_7BrN_4O_2$, M = 319.12 g/mol, HPLC-ESI-MS: $[M + H]^+$ = 319 *m/z*. ^{1}H NMR (400 MHz, DMSO-D_6) δ 7.85 (m, 2 H), 8.01 (s, 1 H), 8.18 (m, 2 H), 8.88 (s, 1 H). ^{13}C NMR (100 MHz, DMSO-D_6) δ 109.0 (CH), 125.8 (C), 128.6 (C), 131.7 (CH), 131.8 (CH), 147.2 (C), 152.6 (C), 155.3 (C), 157.2 (CH), 164.7 (C).

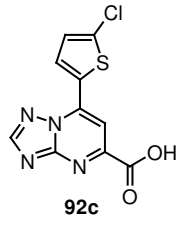

92c

92c; Prepared according to the method A using [1,2,4]triazol-3-ylamine as the amine in the step A3; brown solid; 74% yield, 98% purity (HPLC-ESI-MS, 210-400 nm), $C_{10}H_5ClN_4O_2S$, M = 280.69 g/mol, HPLC-ESI-MS: $[M + H]^+$ = 281 *m/z*. ^{1}H NMR (400 MHz, DMSO-D_6) δ 7.45 (d, *J* = 4.07 Hz, 1 H), 8.41 (s, 1 H), 8.59 (d, *J* = 4.32 Hz, 1 H), 8.94 (s, 1 H), 14.15 (s, 1 H). ^{13}C NMR (100 MHz, DMSO-D_6) δ 105.0 (CH), 128.0 (C), 128.3 (CH), 133. 5 (CH), 138.7 (C), 140.8 (C), 152.1 (C), 154.8 (C), 156.8 (CH), 164.8 (C).

6. 1. 2. 5 Synthesis of pyridine *N*-oxides.

6. 1. 2. 5. 1 General procedure for the synthesis of pyridine *N*-oxides 93.

5-Cyano-6-methyl-4-aryl-pyridine-2-carboxylic acid **74** (1 eq, 0.25 mmol) was dissolved in acetic acid (2 mL) and 30% hydrogen peroxide was added (2 mL). The mixture was stirred for 2 h at 80 ºC and then kept at room temperature for 16 h. The resulting crystals were filtered, washed with acetic acid and water, and air dried to give the product **93**.

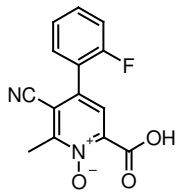

93a

93a; colorless crystals; 62% yield, $C_{14}H_9FN_2O_3$, M = 272.24 g/mol, HPLC-ESI-MS: $[M + H]^+$ = 273 *m/z*. ^{1}H NMR (400 MHz, $CDCl_3$) δ 2.76 (s, 3 H), 7.46 (m, 2 H), 7.65 (m, 2 H), 8.25 (s, 1 H). ^{13}C NMR (100 MHz, $CDCl_3$) δ 16.9 (CH_3), 113.9 (C), 114.4 (C), 116.3 (d, $^2J_{C\text{-}F}$ = 21.23 Hz, CH), 121.9 (d, $^2J_{C\text{-}F}$ = 13.9 Hz, C), 125.3 (d, $^3J_{C\text{-}F}$ = 3.66 Hz, CH), 126.6 (CH), 131.2 (d, $^4J_{C\text{-}F}$ = 1.46 Hz, CH), 133.1 (d, $^3J_{C\text{-}F}$ = 8.05 Hz, CH), 139.1 (C), 139.5 (C), 153.3 (C), 158.6 (d, $^1J_{C\text{-}F}$ =248.10, C), 160.3 (C).

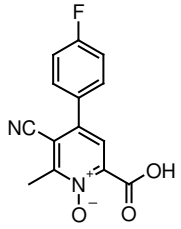

93b

93b; yellow crystals; 60% yield, $C_{14}H_9FN_2O_3$, M = 272.24 g/mol, HPLC-ESI-MS: $[M + H]^+$ = 273 *m/z*. m.p. 160-162 °C. ^{1}H NMR (400 MHz, $CDCl_3$) δ 2.95 (s, 3 H), 7.29 (m, 2 H), 7.66 (m, 2 H), 8.45 (s, 1 H). ^{13}C NMR (100 MHz, $CDCl_3$) δ 17.2 (CH_3), 113.6 (C), 113.6 (C), 116.9 (d, $^2J_{C\text{-}F}$ = 21.95 Hz, CH), 127.3 (CH), 129.6 (d, $^4J_{C\text{-}F}$ = 3.66 Hz, C), 130.7 (d, $^3J_{C\text{-}F}$ = 8.78, CH), 138.6 (C), 144.7 (C), 153.8 (C), 160.1 (C), 164.5 (d, $^1J_{C\text{-}F}$ = 253.95, C). IR (neat, cm^{-1}) λ_{max}: 3347, 3071, 2991, 2926, 2867, 2809, 2221, 1735, 1655, 1510, 1401, 1365, 1292, 1241, 1161, 1060, 1002, 907, 828, 777. FT-ICR-MS: calculated for $C_{14}H_9FN_2O_3Na^+$: 295.0489, found: 295.0490.

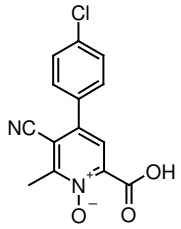

93c

93c; colorless crystals; 50% yield, $C_{14}H_9ClN_2O_3$, M = 288.69, HPLC-ESI-MS: $[M + H]^+$ = 289 *m/z*. ^{1}H NMR (400 MHz, $CDCl_3$) δ 2.76 (s, 3 H), 7.72 (m, 4 H), 8.23 (s, 1 H). ^{13}C NMR (100 MHz, $CDCl_3$) δ 16.9 (CH_3), 113.1 (C), 114.4 (C), 125.5 (CH), 129.2 (CH), 130.6 (CH), 132.8 (C), 135.7 (C), 139.2 (C), 143.5 (C), 153.3 (C), 160.3 (C).

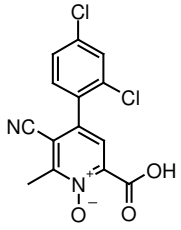

93d

93d; pale crystals; 56% yield, $C_{14}H_2Cl_2N_2O_3$, M = 323.14, HPLC-ESI-MS: $[M + H]^+$ = 323 *m/z*.

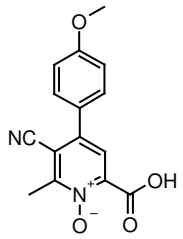

93e

93e; yellow crystals; 88% yield, $C_{15}H_{12}N_2O_4$, M = 284.27, HPLC-ESI-MS: $[M + H]^+$ = 284 *m/z*.

6. 1. 2. 5. 2 General procedure for the synthesis of pyridine *N*-oxides 98.

3-Cyano-2-methyl-6-aryl-isonicotinic acid **81** (1 eq, 0.25 mmol) was dissolved in acetic acid (2 mL), then 30% hydrogen peroxide was added (2 mL). After stirring for 5 h at 100 ºC the mixture was poured on ice/water and extracted with chloroform (3 x 10 mL). The aqueous phase was then concentrated in vacuo and dried by lyophilization to afford the product **98**.

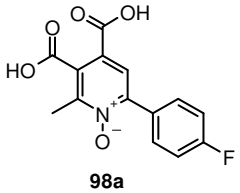

98a

98a; pale solid; 90% yield, $C_{14}H_{10}FN_2O_5$, M = 291.24, HPLC-ESI-MS: $[M + H]^+$ = 292 *m/z*.

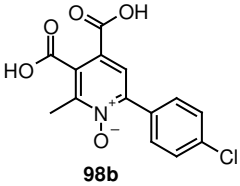

98b

98b; colorless solid; 75% yield, $C_{14}H_{10}ClNO_5$, M = 307.69, HPLC-ESI-MS: $[M + H]^+$ = 307 *m/z*. ^{1}H NMR (400 MHz, D_2O) δ 2.47 (s, 3 H), 7.45 (m, *J* = 8.65 Hz, 2 H), 7.52 (m, *J* = 8.39 Hz, 2 H), 7.80 (s, 1 H).

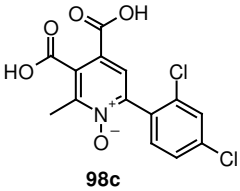

98c

98c; colorless crystals; 88% yield, $C_{14}H_9Cl_2NO_5$, M = 342.14, HPLC-ESI-MS: $[M + H]^+$ = 342 *m/z*. M.p. 172-173°C (dec.). ^{1}H NMR (400 MHz, D_2O) δ 2.49 (s, 3 H), 7.36 (d, *J* = 8.39 Hz, 1 H), 7.47 (d, *J* = 8.14 Hz, 1 H), 7.64 (s, 1 H), 7.85 (s, 1 H). ^{13}C NMR (100 MHz, D_2O/ DMSO-D_6) δ 16.7 (CH_3), 128.0 (CH), 129.2 (C), 129.4 (CH), 131.0 (CH), 131.7 (C), 133.3 (CH), 135.7 (C), 137.8 (C), 140.2 (C), 147.8 (C), 148.4 (C), 168.7 (C), 173.8 (C). IR (neat, cm^{-1}) λ_{max}: 3520, 3415, 3175, 3032, 2882, 2785, 1705, 1577, 1412, 1374, 1322, 1262, 1202, 1142, 1092, 1052, 977, 902, 857, 812, 774, 677. FT-ICR-MS: calculated for $C_{14}H_9Cl_2NO_5H^+$: 341.9931, found: 341.9929.

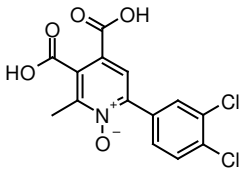

98d

98d; pale solid; 65% yield, $C_{14}H_9Cl_2NO_5$, M = 342.14, HPLC-ESI-MS: $[M + H]^+$ = 342 *m/z*.

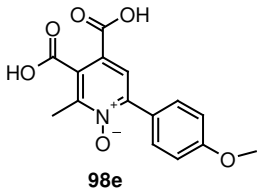

98e

98e; pale solid; 85% yield, $C_{14}H_9Cl_2NO_5$, M = 303.27, HPLC-ESI-MS: $[M + H]^+$ = 304 *m/z*.

6. 1. 2. 6 General procedure for the amidation - synthesis of 94 and 99.

5-Cyano-6-methyl-4-aryl-pyridine-2-carboxylic acid **74** or 3-cyano-2-methyl-6-aryl-isonicotinic acid **81** (1 eq, 0.15 mmol) was dissolved in 5 mL DCM. Benzotriazol-1-yl-oxytripyrrolidinophosphonium hexafluorophosphate (1.1 eq, 0.17 mmol 0.864 g) and triethylamine (2 eq, 0.30 mmol, 41 µl) were successively added followed by addition of amine or 1-hydroxybenzotriazol ammonium salt (1.5 eq, 0.23 mmol, 0.035 g). After 3 h stirring at room temperature (the reaction monitored by TLC), the solvent was removed and the product as a solid was isolated by filtration on silica gel.

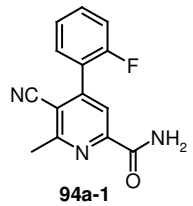

94a-1

94a-1; pale solid; 90% yield, $C_{14}H_{10}FN_3O$, M = 255.25 g/mol, HPLC-ESI-MS: $[M + H]^+$ = 256 *m/z*. ^{1}H NMR (400 MHz, $CDCl_3$) δ 2.82 (s, 3 H), 6.08 (s, 1 H), 7.22 (m, 2 H), 7.37 (m, 1 H), 7.45 (m, 1 H), 7.81 (s, 1 H), 8.11 (s, 1 H).

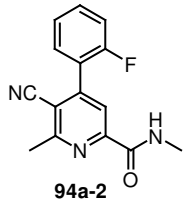

94a-2

94a-2; colorless solid; 89% yield, $C_{15}H_{12}FN_3O$, M = 269.28 g/mol, HPLC-ESI-MS: $[M + H]^+$ = 270 *m/z*. ^{1}H NMR (400 MHz, $CDCl_3$) δ 2.86 (s, 3 H), 3.06 (d, J = 5.34 Hz, 3 H), 7.27 (m, 2 H), 7.43 (m, 1 H), 7.51 (m, 1 H), 8.04 (s, 1 H), 8.16 (s, 1 H). ^{13}C NMR (100 MHz, $CDCl_3$) δ 23.9 (CH_3), 26.3 (CH_3), 111.4 (C), 115.8 (C), 116.5 (d, $^2J_{C\text{-}F}$ = 21.95 Hz, CH), 120.7 (CH), 123.6 (d, $^2J_{C\text{-}F}$ = 14.64 Hz, C), 124.8 (d, $^3J_{C\text{-}F}$ = 3.66 Hz, CH), 130.6 (d, $^4J_{C\text{-}F}$ = 1.64 Hz, CH), 132.3 (d, $^3J_{C\text{-}F}$ = 8.78 Hz, CH), 149.8 (C), 151.1 (C), 159.1 (d, $^1J_{C\text{-}F}$ =251.03, C), 161.2 (C), 163.3 (C).

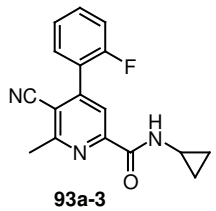

93a-3

94a-3; pale solid; 99% yield, $C_{17}H_{14}FN_3O$, M = 295.32 g/mol, HPLC-ESI-MS: $[M + H]^+$ = 296 *m/z*. ^{1}H NMR (400 MHz, $CDCl_3$) δ 0.70 (m, 2 H), 0.91 (m, 2 H), 2.85 (s, 3 H), 2.95 (m, 1 H), 7.28 (m, 2 H), 7.41 (m, 1 H), 7.51 (m, 1 H), 8.04 (s, 1 H), 8.15 (s, 1 H). ^{13}C NMR (100 MHz, $CDCl_3$) δ 6.6 (CH_2), 22.7 (CH), 23.9 (CH_3), 111.5 (C), 115.8 (C), 116.5 (d, $^2J_{C\text{-}F}$ = 21.95 Hz, CH), 120.6 (CH), 123.6 (d, $^2J_{C\text{-}F}$ = 14.64 Hz, C), 124.8 (d, $^3J_{C\text{-}F}$ = 3.66 Hz, CH), 130.6 (d, $^4J_{C\text{-}F}$ = 2.19 Hz, CH), 132.3 (d, $^3J_{C\text{-}F}$ = 8.78 Hz, CH), 149.8 (C), 150.9 (C), 159.1 (d, $^1J_{C\text{-}F}$ =251.03, C), 161.2 (C), 164.03 (C).

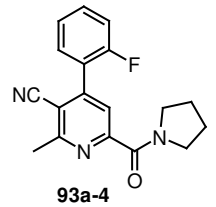

93a-4

94a-4; colorless solid; 95% yield, $C_{18}H_{16}FN_3O$, M = 209.35 g/mol, HPLC-ESI-MS: $[M + H]^+$ = 310 *m/z*. ^{1}H NMR (400 MHz, $CDCl_3$) δ 1.95 (m, 4 H), 2.86 (s, 3 H), 3.68 (m, 2 H), 3.76 (m, 2 H), 7.23 (m, 1 H), 7.29 (m, 1 H), 7.42 (m, 1 H), 7.49 (m, 1 H), 7.78 (s, 1 H). ^{13}C NMR (100 MHz, $CDCl_3$) δ 23.9 (CH_3), 24.0 (CH_2), 26.6 (CH_2), 47.1 (CH_2), 49.1 (CH_2), 109.9 (C), 115.9 (C), 116.4 (d, $^2J_{C\text{-}F}$ = 21.22 Hz, CH), 122.3 (CH), 123.7 (d, $^2J_{C\text{-}F}$ = 14.64 Hz, C), 124.7 (d, $^3J_{C\text{-}F}$ = 3.66 Hz, CH), 130.6 (d, $^4J_{C\text{-}F}$ = 2.19 Hz, CH), 132.1 (d, $^3J_{C\text{-}F}$ = 8.78 Hz, CH), 148.9 (C), 155.9 (C), 159.1 (d, $^1J_{C\text{-}F}$ =251.02, C), 161.2 (C), 164.7 (C).

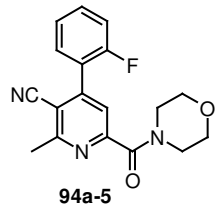

94a-5

94a-5; colorless solid; 89% yield, $C_{18}H_{16}FN_3O_2$, M = 325.35 g/mol, HPLC-ESI-MS: $[M + H]^+$ = 326 *m/z*.

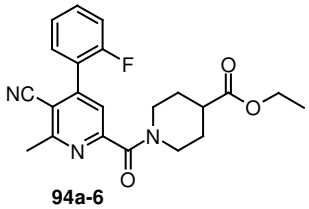

94a-6

94a-6; colorless solid; 90% yield, $C_{22}H_{22}FN_3O_3$, M = 395.44 g/mol, HPLC-ESI-MS: $[M + H]^+$ = 396 *m/z*.

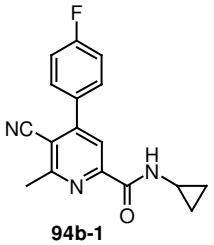

94b-1

94b-1; colorless solid; 94% yield, $C_{17}H_{14}FN_3O$, M = 295,32 g/mol, HPLC-ESI-MS: $[M + H]^+$ = 296 *m/z*. ^{1}H NMR (400 MHz, $CDCl_3$) δ 0.68 (m, 2 H), 0.90 (m, 2 H), 2.83 (s, 3 H), 2.94 (m, 1 H), 7.21 (t, *J* = 8.65 Hz, 2 H), 7.61 (m, 2 H), 8.03 (s, 1 H), 8.13 (s, 1 H). ^{13}C NMR (100 MHz, $CDCl_3$) δ 6.6 (CH_2), 22.7 (CH), 23.9 (CH_3), 109.6 (C), 116.3 (d, $^2J_{C\text{-}F}$ = 21.96, CH), 116.3 (C), 119.3 (CH), 130.6 (d, $^3J_{C\text{-}F}$ = 8.78, CH), 131.6 (d, $^4J_{C\text{-}F}$ = 3.66, C), 150.9 (C), 153.8 (C), 161.7 (C), 163.5 (d, $^1J_{C\text{-}F}$ = 251.76, C), 165.2 (C).

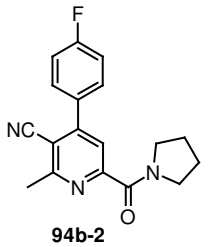

94b-2

94b-2; colorless solid; 99% yield, $C_{18}H_{16}FN_3O$, M = 309.35 g/mol, HPLC-ESI-MS: $[M + H]^+$ = 310 *m/z*. ^{1}H NMR (400 MHz, $CDCl_3$) δ 1.95 (m, 4 H) 2.85 (s, 3 H) 3.72 (m, 4 H) 7.21 (m, 2 H) 7.60 (m, *J* = 8.77, 5.21 Hz, 2 H) 7.78 (s, 1 H). ^{13}C NMR (100 MHz, $CDCl_3$) δ 23.8 (CH_2), 24.1 (CH_3), 26.6 (CH_2), 47.1 (CH_2), 49.1 (CH_2), 108.2 (C), 116.3 (d, $^2J_{C\text{-}F}$ = 21.96, CH), 116.4 (C), 121.3 (CH), 130.5 (d, $^3J_{C\text{-}F}$ = 8.78, CH), 131.8 (d, $^4J_{C\text{-}F}$ = 2.93, C), 153.1 (C), 156.0 (C), 161.7 (C), 163.9 (d, $^1J_{C\text{-}F}$ = 251.03, C), 165.1 (C).

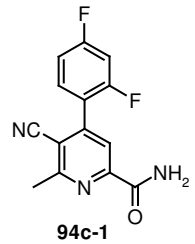

94c-1

94c-1; pale solid; 86% yield, $C_{14}H_9F_2N_3O$, M = 273.24 g/mol, HPLC-ESI-MS: $[M + H]^+$ = 274 *m/z*. ^{1}H NMR (400 MHz, $CDCl_3$) δ 2.88 (s, 3 H), 6.11 (s, 1 H), 7.04 (m, 2 H), 7.44 (m, 1 H), 7.87 (s, 1 H), 8.14 (s, 1 H).

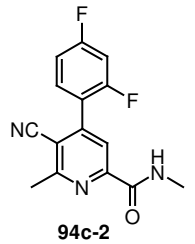

94c-2

94c-2; colorless solid; 75% yield, $C_{15}H_{11}F_2N_3O$, M = 287.27 g/mol, HPLC-ESI-MS: $[M + H]^+$ = 288 *m/z*. ^{1}H NMR (400 MHz, $CDCl_3$) δ 2.86 (s, 3 H), 3.06 (d, *J* = 5.09 Hz, 3 H), 7.03 (m, 2 H), 7.42 (m, 1 H), 8.02 (s, 1 H), 8.13 (s, 1 H). ^{13}C NMR (100 MHz, $CDCl_3$) δ 24.0 (CH_3), 26.3 (CH_3), 105.1 (t, $^2J_{C\text{-}F}$ = 25.25, CH), 111.4 (C), 112.4 (dd, $^{2,4}J_{C\text{-}F}$ = 21.79, 3.66 Hz, CH), 115.6 (C), 119.8 (dd, $^{2,4}J_{C\text{-}F}$ = 14.65, 4.36 Hz, C), 120.4 (CH), 131.7 (dd, $^3J_{C\text{-}F}$ = 10.06, 3.66

Hz, CH), 148.8 (C), 151.2 (C), 159.6 (dd, $^{1,3}J_{C\text{-}F}$ = 254.23, 12.45 Hz, C), 161.3 (C), 163.2 (C), 164.2 (dd, $^{1,3}J_{C\text{-}F}$ = 254.07, 11.72 Hz, C).

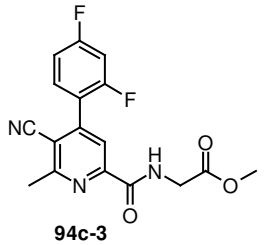

94c-3

94c-3; yellow solid; 82% yield, $C_{17}H_{13}F_2N_3O_3$, M = 345.31 g/mol, HPLC-ESI-MS: $[M + H]^+$ = 346 *m/z*.

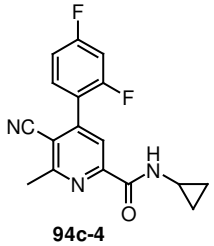

94c-4

94c-4; colorless solid; 81% yield, $C_{17}H_{13}F_2N_3O$, M = 313,31 g/mol, HPLC-ESI-MS: $[M + H]^+$ = 314 *m/z*. ^{1}H NMR (400 MHz, $CDCl_3$) δ 0.68 (m, 2 H), 0.89 (m, 2 H), 2.83 (s, 3 H), 2.93 (m, 1 H), 7.02 (m, 2 H), 7.41 (m, 1 H), 8.03 (s, 1 H), 8.11 (s, 1 H). ^{13}C NMR (100 MHz, $CDCl_3$) δ 6.6 (CH_2), 22.7 (CH), 23.8 (CH_3), 105.1 (t, $^2J_{C\text{-}F}$ = 25.25, CH), 111.4 (C), 112.3 (dd, $^{2,4}J_{C\text{-}F}$ = 21.79, 3.66 Hz, CH), 115.6 (C), 119.8 (dd, $^{2,4}J_{C\text{-}F}$ = 14.65, 4.36 Hz, C), 120.4 (CH), 131.7 (dd, $^3J_{C\text{-}F}$ = 9.50, 4.16 Hz, CH), 148.7 (C), 150.0 (C), 159.5 (dd, $^{1,3}J_{C\text{-}F}$ = 253.19, 12.45 Hz, C), 161.3 (C), 163.9 (C), 164.2 (dd, $^{1,3}J_{C\text{-}F}$ = 253.66, 12.59 Hz, C).

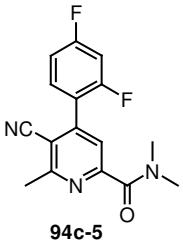

94c-5

94c-5; colorless solid; 94% yield, $C_{16}H_{13}F_2N_3O$, M = 301.30 g/mol, HPLC-ESI-MS: $[M + H]^+$ = 302 *m/z*.

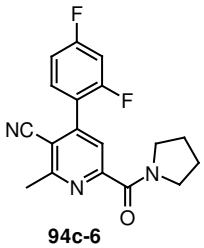

94c-6

94c-6; pale solid; 76% yield, $C_{18}H_{15}F_2N_3O$, M = 327.34 g/mol, HPLC-ESI-MS: $[M + H]^+$ = 302 *m/z*.

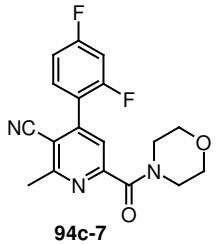

94c-7

94c-7; colorless solid; 87% yield, $C_{18}H_{15}F_2N_3O_2$, M = 343.34 g/mol, HPLC-ESI-MS: $[M + H]^+$ = 344 *m/z*.

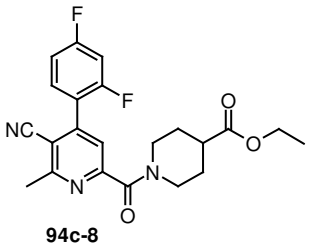

94c-8

94c-8; yellow solid; 76% yield, $C_{22}H_{21}F_2N_3O_3$, M = 413.43 g/mol, HPLC-ESI-MS: $[M + H]^+$ = 414 *m/z*.

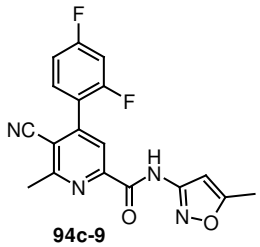

94c-9

94c-9; colorless solid; 71% yield, $C_{18}H_{12}F_2N_4O_2$, M = 354.32 g/mol, HPLC-ESI-MS: $[M + H]^+$ = 355 *m/z*. ^{1}H NMR (400 MHz, $CDCl_3$) δ 2.46 (s, 3 H), 2.92 (s, 3 H), 6.85 (s, 1 H), 7.06 (m, 2 H), 7.46 (m, 1 H), 8.18 (s, 1 H), 10.40 (s, 1 H). ^{13}C NMR (100 MHz, $CDCl_3$) δ 12.7 (CH_3), 23.9 (CH_3), 96.1 (CH), 105.2 (t, $^2J_{C\text{-}F}$ = 25.62, CH), 112.5 (dd, $^{2,4}J_{C\text{-}F}$ = 21.56, 3.66 Hz, CH), 115.5 (C), 119.6 (dd, $^{2,4}J_{C\text{-}F}$ = 14.37, 3.66 Hz, C), 121.1 (CH), 131.7 (dd, $^3J_{C\text{-}F}$ = 9.80, 3.30 Hz, CH), 149.2 (C), 149.7 (C), 159.6 (dd, $^{1,3}J_{C\text{-}F}$ = 253.50, 12.45 Hz, C), 160.5 (C), 161.9 (C), 164.4 (dd, $^{1,3}J_{C\text{-}F}$ = 255.97, 12.44 Hz, C), 170.5 (C).

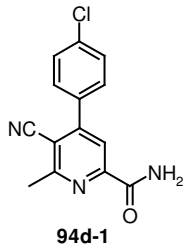

94d-1

94d-1; colorless solid; 73% yield, $C_{14}H_{10}ClN_3O$, M = 271.71 g/mol, HPLC-ESI-MS: $[M + H]^+$ = 272 *m/z*; m.p. 214-216 °C (dec.). ^{1}H NMR (400 MHz, DMSO-D_6) δ 2.81 (s, 3 H), 7.69 (m, 4 H), 7.96 (s, 2 H), 8.28 (s, 1 H). ^{13}C NMR (100 MHz, DMSO-D_6) δ 23.7 (CH_3), 109.2 (C), 116.5 (C), 119.2 (CH), 129.1 (CH), 130.5 (CH), 134.4 (C), 135.2 (C), 151.8 (C), 152.6 (C), 161.6 (C), 164.6 (C). IR (neat, cm^{-1}) λ_{max}: 3449, 3360, 3277, 3155, 3041, 2218, 1707, 1643, 1580, 1535, 1490, 1420, 1382, 1356, 1318, 1241, 1152, 1095, 1018, 910, 852, 827, 699. FT-ICR-MS: calculated for $C_{14}H_{10}ClN_3ONa^+$: 294.0405, found: 294.0404.

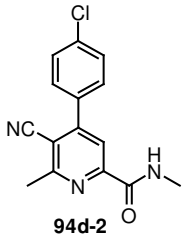

94d-2

94d-2; colorless solid; 79% yield, $C_{15}H_{12}ClN_3O$, M = 285.74 g/mol, HPLC-ESI-MS: $[M + H]^+$ = 286 *m/z*.

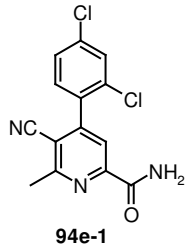

94e-1

94e-1; colorless solid; 80% yield, $C_{14}H_9Cl_2N_3O$, M = 306.15 g/mol, HPLC-ESI-MS: $[M + H]^+$ = 306 *m/z*. ^{1}H NMR (400 MHz, $CDCl_3$) δ 2.88 (s, 3 H), 6.14 (s, 1 H), 7.26 (d, *J* = 8.14 Hz, 1 H), 7.40 (dd, *J* = 8.14, 2.03 Hz, 1 H), 7.57 (d, *J* = 2.03 Hz, 1 H), 7.84 (s, 1 H), 8.10 (s, 1 H). ^{13}C NMR (100 MHz, $CDCl_3$) δ 23.9 (CH_3), 112,0 (C), 115.3 (C), 120.9 (CH), 127.7 (CH), 130.3 (CH), 131.1 (CH), 133.1 (C), 133.2 (C), 136.8 (C), 150.7 (C), 151.9 (C), 161.5 (C), 164.9 (C).

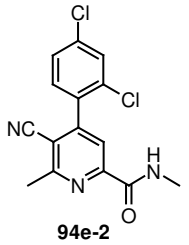

94e-2

94e-2; colorless solid; 83% yield, $C_{15}H_{11}Cl_2N_3O$, M = 320.18 g/mol, HPLC-ESI-MS: $[M + H]^+$ = 320 *m/z*. ^{1}H NMR (400 MHz, $CDCl_3$) δ 2.85 (s, 3 H), 3.06 (d, *J* = 5.09 Hz, 3 H), 7.25 (d, *J* = 8.14 Hz, 1 H), 7.39 (dd, *J* = 8.27, 1.91 Hz, 1 H), 7.56 (d, *J* = 2.03 Hz, 1 H), 8.03 (m, 1 H), 8.09 (s, 1 H). ^{13}C NMR (100 MHz, $CDCl_3$) δ 23.9 (CH_3) 26.3 (CH_3) 111.6 (C) 115.4 (C) 120.6 (CH) 127.7 (CH) 130.2 (CH) 131.1 (CH) 133.2 (C) 133.2 (C) 136.7 (C) 151.1 (C) 151.9 (C) 161.1 (C) 163.2 (C).

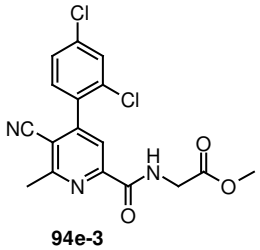

94e-3

94e-3; colorless solid; 99% yield, $C_{17}H_{13}Cl_2N_3O_3$, M = 378.22 g/mol, HPLC-ESI-MS: $[M + H]^+$ = 378 *m/z*. ^{1}H NMR (400 MHz, $CDCl_3$) δ 2.87 (s, 3 H), 3.79 (s, 3 H), 4.27 (d, *J* = 5.85 Hz, 2 H), 7.25 (d, *J* = 8.14 Hz, 1 H), 7.39 (dd, *J* = 8.27, 1.91 Hz, 1 H), 7.56 (d, *J* = 2.03 Hz, 1 H), 8.07 (s, 1 H), 8.45 (t, *J* = 5.34 Hz, 1 H). ^{13}C NMR (100 MHz, $CDCl_3$) δ 23.9 (CH_3), 41.3

(CH_2), 53.5 (CH_3), 112.0 (C), 115.2 (C), 120.8 (CH), 127.7 (CH), 130.2 (CH), 131.1 (CH), 133.1 (C), 133.1 (C), 136.8 (C), 150.4 (C), 151.9 (C), 161.4 (C), 161.8 (C), 169.8 (C).

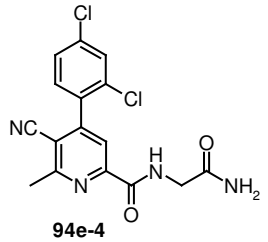

94e-4

94e-4; colorless solid; 99% yield, $C_{16}H_{12}Cl_2N_4O_2$, M = 363.21 g/mol, HPLC-ESI-MS: $[M + H]^+$ = 363 *m/z*.

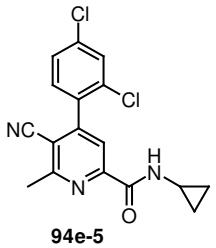

94e-5

94e-5; colorless solid; 88% yield, $C_{17}H_{13}Cl_2N_3O$, M = 346.22 g/mol, HPLC-ESI-MS: $[M + H]^+$ = 346 *m/z*. ^{1}H NMR (400 MHz, $CDCl_3$) δ 0.69 (m, 2 H), 0.91 (m, 2 H), 2.84 (s, 3 H), 2.94 (m, 1 H), 7.24 (d, *J* = 8.14 Hz, 1 H), 7.39 (dd, *J* = 8.14, 2.03 Hz, 1 H), 7.56 (d, *J* = 2.03 Hz, 1 H), 8.03 (s, 1 H), 8.08 (s, 1 H). ^{13}C NMR (100 MHz, $CDCl_3$) δ 6.6 (CH_2), 22.7 (CH), 23.8 (CH_3), 111.7 (C), 115.4 (C), 120.4 (CH), 127.7 (CH), 130.2 (CH), 131.1 (CH), 133.2 (C), 133.1 (C), 136.8 (C), 151.0 (C), 151.9 (C), 161.1 (C), 163.9 (C).

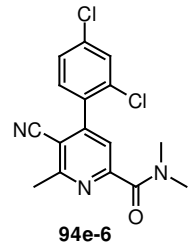

94e-6

94e-6; colorless solid; 99% yield, $C_{16}H_{13}Cl_2N_3O$, M = 334.21 g/mol, HPLC-ESI-MS: $[M + H]^+$ = 334 *m/z*.

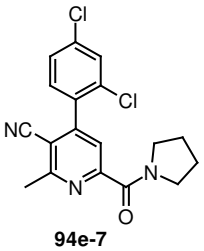

94e-7

94e-7; colorless solid; 78% yield, $C_{18}H_{15}Cl_2N_3O$, M = 360.25 g/mol, HPLC-ESI-MS: $[M + H]^+$ = 360 *m/z*. ^{1}H NMR (400 MHz, $CDCl_3$) δ 1.95 (m, 4 H), 2.85 (s, 3 H), 3.68 (t, *J* = 6.49 Hz, 2 H), 3.78 (m, 2 H), 7.26 (d, *J* = 8.39 Hz, 1 H), 7.39 (dd, *J* = 8.27, 1.91 Hz, 1 H), 7.56 (d, *J* = 2.03 Hz, 1 H), 7.72 (s, 1 H). ^{13}C NMR (100 MHz, $CDCl_3$) δ 23.9 (CH_2), 23.9 (CH_3), 26.6 (CH_2), 47.2 (CH_2), 49.1 (CH_2), 110.0 (C), 115.5 (C), 122.2 (CH), 127.7 (CH), 130.2 CH), 131.2 (CH), 133.1 (C), 133.3 (C), 136.6 (C), 151.0 (C), 155.8 (C), 161.1 (C), 164.4 (C).

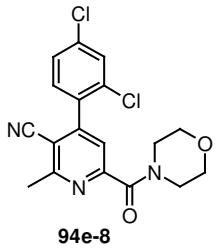

94e-8

94e-8; colorless solid; 81% yield, $C_{18}H_{15}Cl_2N_3O_2$, M = 376.25 g/mol, HPLC-ESI-MS: $[M + H]^+$ = 376 *m/z*.

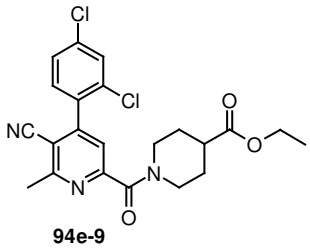

94e-9

94e-9; yellow solid; 87% yield, $C_{22}H_{21}Cl_2N_3O_3$, M = 446.34 g/mol, HPLC-ESI-MS: $[M + H]^+$ = 446 *m/z*.

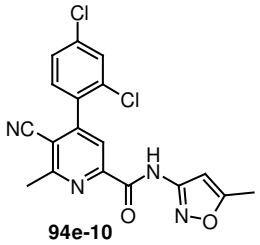

94e-10

94e-10; colorless solid; 85% yield, $C_{18}H_{12}Cl_2N_4O_2$, M = 387.23 g/mol, HPLC-ESI-MS: $[M + H]^+$ = 387 *m/z*.

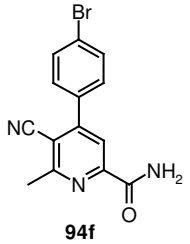

94f

94f; colorless solid; 63% yield, $C_{14}H_{10}BrN_3O$, M = 316.16 g/mol, HPLC-ESI-MS: $[M + H]^+$ = 316 *m/z*.

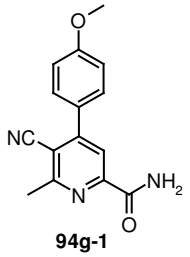

94g-1

94g-1; colorless solid; 67% yield, $C_{15}H_{13}N_3O_2$, M = 267.29 g/mol, HPLC-ESI-MS: $[M + H]^+$ = 268 *m/z*.

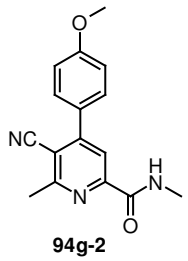

94g-2

94g-2; colorless solid; 60% yield, $C_{16}H_{15}N_3O_2$, M = 281.32 g/mol, HPLC-ESI-MS: $[M + H]^+$ = 282 *m/z*.

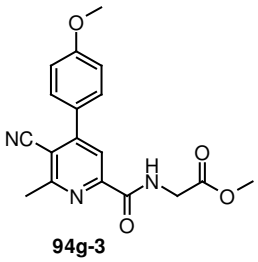

94g-3

94g-3; colorless solid; 93% yield, $C_{18}H_{17}N_3O_4$, M = 339.35 g/mol, HPLC-ESI-MS: $[M + H]^+$ = 340 *m/z*.

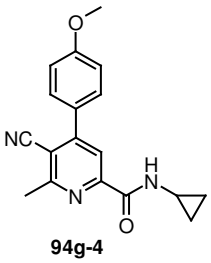

94g-4

94g-4; colorless solid; 79% yield, $C_{18}H_{17}N_3O_2$, M = 307.36 g/mol, HPLC-ESI-MS: $[M + H]^+$ = 308 *m/z*; m.p. 157 °C. ^{1}H NMR (400 MHz, $CDCl_3$) δ 0.63 (m, 2 H), 0.84 (m, 2 H), 2.76 (s, 3 H), 2.89 (m, 1 H), 3.81 (s, 3 H), 6.98 (m, 2 H), 7.55 (m, 2 H), 8.00 (s, 1 H), 8.08 (s, 1 H). ^{13}C NMR (100 MHz, $CDCl_3$) δ 6.6 (CH_2), 22.7 (CH), 24.0 (CH_3), 55.4 (CH_3), 109.2 (C), 114.5 (CH), 116.8 (C), 119.2 (CH), 127.8 (C), 130.1 (CH), 150.6 (C), 154.5 (C), 161.4 (C), 161.7 (C), 164.3 (C). IR (neat, cm^{-1}) λ_{max}: 3332, 3077, 2920, 2852, 2222, 1660, 1629, 1607, 1577, 1547, 1509, 1427, 1359, 1277, 1239, 1157, 984, 917, 842, 774, 699. FT-ICR-MS: calculated for $C_{18}H_{17}N_3O_2H^+$: 308.1394, found: 308.1393.

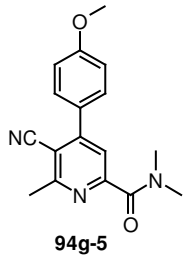

94g-5

94g-5; colorless solid; 99% yield, $C_{17}H_{17}N_3O_2$, M = 295.34 g/mol, HPLC-ESI-MS: $[M + H]^+$ = 296 *m/z*.

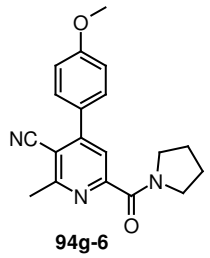

94g-6

94g-6; colorless solid; 99% yield, $C_{19}H_{19}N_3O_2$, M = 321.38 g/mol, HPLC-ESI-MS: $[M + H]^+$ = 322 *m/z*.

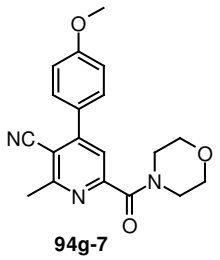

94g-7

94g-7; colorless solid; 99% yield, $C_{19}H_{19}N_3O_3$, M = 337.38 g/mol, HPLC-ESI-MS: $[M + H]^+$ = 338 *m/z*.

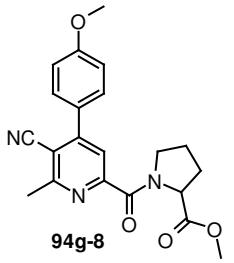

94g-8

94g-8; colorless solid; 80% yield, $C_{21}H_{21}N_3O_4$, M = 379.42 g/mol, HPLC-ESI-MS: $[M + H]^+$ = 380 *m/z*.

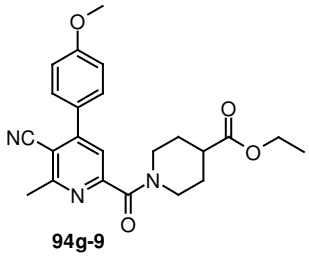

94g-9

94g-9; colorless solid; 99% yield, $C_{23}H_{25}N_3O_4$, M = 407.47 g/mol, HPLC-ESI-MS: $[M + H]^+$ = 408 *m/z*.

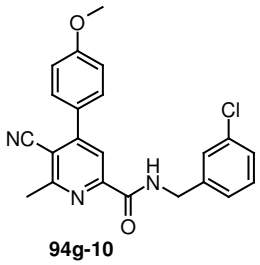

94g-10

94g-10; colorless solid; 99% yield, $C_{22}H_{18}ClN_3O_2$, M = 391.86 g/mol, HPLC-ESI-MS: $[M + H]^+$ = 392 *m/z*.

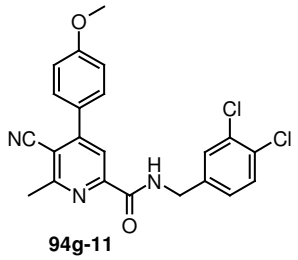

94g-11

94g-11; colorless solid; 99% yield, $C_{22}H_{17}Cl_2N_3O_2$, M = 426.31 g/mol, HPLC-ESI-MS: $[M + H]^+$ = 426 *m/z*; m.p. 152 °C. ^{1}H NMR (400 MHz, $CDCl_3$) δ 2.83 (s, 3 H), 3.87 (s, 3 H), 4.63 (d, *J* = 6.36 Hz, 2 H), 7.04 (m, 2 H), 7.20 (m, 1 H), 7.40 (d, *J* = 8.39 Hz, 1 H), 7.44 (d, *J* = 2.03 Hz, 1 H), 7.62 (m, 2 H), 8.17 (s, 1 H), 8.44 (m, 1 H). ^{13}C NMR (100 MHz, $CDCl_3$) δ 24.0 (CH_3), 42.5 (CH_2), 55.4 (CH_3), 109.5 (C), 114.6 (CH), 116.8 (C), 119.6 (CH), 127.1 (CH), 127.6 (C), 129.7 (CH), 130.1 (CH), 130.7 (CH), 131.7 (C), 132.8 (C), 138.2 (C), 150.3 (C), 154.6 (C), 161.5 (C), 161.9 (C), 163.2 (C). IR (neat, cm^{-1}) λ_{max}: 3415, 3385, 2927, 2357, 2222, 1735, 1682, 1517, 1457, 1352, 1269, 1232, 1179, 1142, 1059, 999, 887, 797. FT-ICR-MS: calculated for $C_{22}H_{17}Cl_2N_3O_2Na^+$: 448.0590, found: 448.0591.

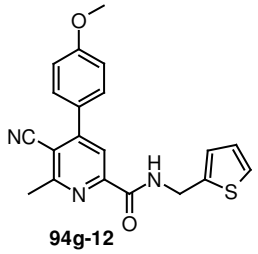

94g-12

94g-12; colorless solid; 81% yield, $C_{20}H_{17}N_3O_2S$, M = 363.44 g/mol, HPLC-ESI-MS: $[M + H]^+$ = 364 *m/z*; m.p. 178 °C. ^{1}H NMR (400 MHz, $CDCl_3$) δ 2.82 (s, 3 H), 3.87 (s, 3 H), 4.84 (d, *J* = 6.10 Hz, 2 H), 6.97 (m, 1 H), 7.05 (m, 3 H), 7.24 (m, 1 H), 7.62 (m, 2 H), 8.18 (s, 1 H), 8.40 (t, *J* = 5.47 Hz, 1 H). ^{13}C NMR (100 MHz, $CDCl_3$) δ 24.0 (CH_3), 38.3 (CH_2), 55. (CH_3), 109.3 (C), 114.5 (CH), 116.8 (C), 119.6(CH), 125.4 (CH), 126.3 (CH), 127.0 (CH), 127.7 (C), 130.1 (CH), 140.3 (C), 150.5 (C), 154.5 (C), 161.4 (C), 161.8 (C), 162.8 (C). IR (neat, cm^{-1}) λ_{max}: 3325, 3077, 2935, 2882, 2222, 1652, 1629, 1599, 1577, 1539, 1517, 1427, 1359, 1284, 1232, 1142, 1074, 924, 834, 684. FT-ICR-MS: calculated for $C_{20}H_{17}N_3O_2SNa^+$: 386.0934, found: 386.0936.

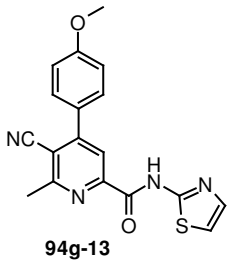

94g-13

94g-13; colorless solid; 79% yield, $C_{18}H_{14}N_4O_2S$, M = 350.40 g/mol, HPLC-ESI-MS: $[M + H]^+$ = 351 *m/z*.

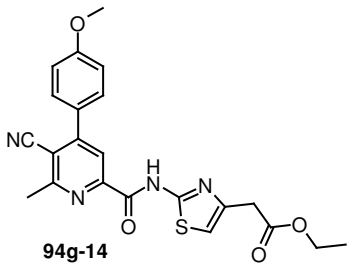

94g-14

94g-14; colorless solid; 69% yield, $C_{22}H_{20}N_4O_4S$, M = 436.49 g/mol, HPLC-ESI-MS: $[M + H]^+$ = 437 *m/z*.

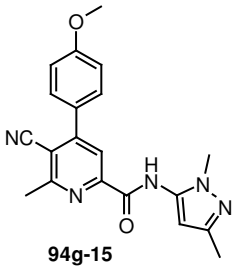

94g-15

94g-15; yellow solid; 99% yield, $C_{20}H_{19}N_5O_2$, M = 361.41 g/mol, HPLC-ESI-MS: $[M + H]^+$ = 362 *m/z*; m.p. 196 °C. ^{1}H NMR (400 MHz, $CDCl_3$) δ 2.26 (s, 3 H), 2.90 (s, 3 H), 3.78 (s, 3 H), 3.87 (s, 3 H), 6.28 (s, 1 H), 7.05 (m, 2 H), 7.64 (m, 2 H), 8.22 (s, 1 H), 9.80 (s, 1 H). ^{13}C NMR (100 MHz, $CDCl_3$) δ 13.9 (CH_3), 24.1 (CH_3), 35.2 (CH_3), 55.4 (CH_3), 98.6 (CH), 110.0 (C), 114.7 (CH), 116.6 (C), 119.8 (CH), 127.3 (C), 130.1 (CH), 135.2 (C), 147.7 (C), 149.5 (C), 155.0 (C), 160.4 (C), 161.6 (C), 162.0 (C). IR (neat, cm^{-1}) λ_{max}: 3210, 2901, 2856, 1735, 1661, 1550, 1462, 1417, 1358, 1285, 1211, 1181, 1100, 1041, 982, 717. FT-ICR-MS: calculated for $C_{20}H_{19}N_5O_2H^+$: 362.1612, found: 362.1613.

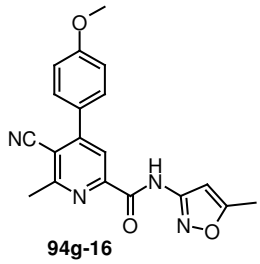

94g-16

94g-16; yellow solid; 26% yield, $C_{19}H_{16}N_4O_3$, M = 348.36 g/mol, HPLC-ESI-MS: $[M + H]^+$ = 349 *m/z*.

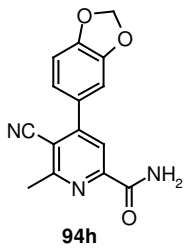

94h

94h; pale solid; 99% yield, $C_{15}H_{11}N_3O_3$, M = 281.27 g/mol, HPLC-ESI-MS: $[M + H]^+$ = 282 *m/z*.

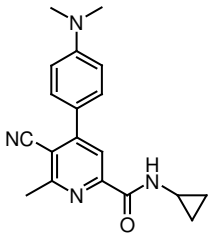

94i-1

94i-1; yellow solid; 86% yield, $C_{19}H_{20}N_4O$, M = 320.40 g/mol, HPLC-ESI-MS: $[M + H]^+$ = 321 *m/z*.

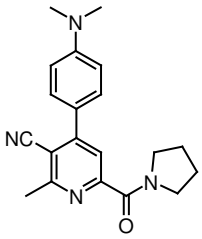

94i-2

94i-2; yellow solid; 66% yield, $C_{20}H_{22}N_4O$, M = 334.42 g/mol, HPLC-ESI-MS: $[M + H]^+$ = 335 *m/z*.

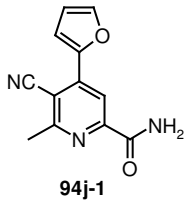

94j-1

94j-1; pale solid; 99% yield, $C_{12}H_9N_3O_2$, M = 227.22 g/mol, HPLC-ESI-MS: $[M + H]^+$ = 228 *m/z*.

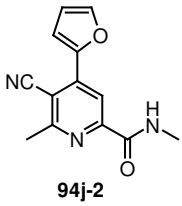

94j-2

94j-2; colorless solid; 99% yield, $C_{13}H_{11}N_3O_2$, M = 241.25 g/mol, HPLC-ESI-MS: $[M + H]^+$ = 242 *m/z*. ^{1}H NMR (400 MHz, $CDCl_3$) δ 2.83 (s, 3 H), 3.07 (d, *J* = 5.09 Hz, 3 H), 6.64 (m, 1 H), 7.61 (m, 1 H), 7.69 (m, 1 H), 8.03 (s, 1 H), 8.48 (s, 1 H). ^{13}C NMR (100 MHz, $CDCl_3$) δ 24.0 (CH_3), 26.3 (CH_3), 103.8 (C), 113.0 (CH), 114.83 (CH), 114.84 (CH), 117.0 (C), 141.6 (C), 145.6 (CH), 147.9 (C), 151.2 (C), 162.0 (C), 163.6 (C).

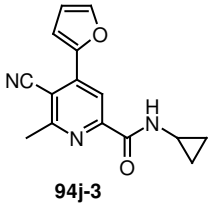

94j-3

94j-3; colorless solid; 87% yield, $C_{15}H_{13}N_3O_2$, M = 267.29 g/mol, HPLC-ESI-MS: $[M + H]^+$ = 268 *m/z*.

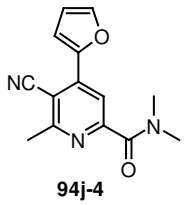

94j-4

94j-4; colorless solid; 99% yield, $C_{14}H_{13}N_3O_2$, M = 255.28 g/mol, HPLC-ESI-MS: $[M + H]^+$ = 256 *m/z*.

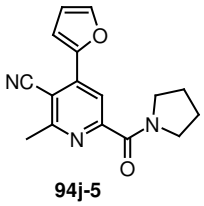

94j-5

94j-5; colorless solid; 93% yield, $C_{16}H_{15}N_3O_2$, M = 281.32 g/mol, HPLC-ESI-MS: $[M + H]^+$ = 282 *m/z*.

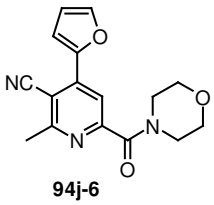

94j-6

94j-6; colorless solid; 99% yield, $C_{16}H_{15}N_3O_3$, M = 297.32 g/mol, HPLC-ESI-MS: $[M + H]^+$ = 298 *m/z*.

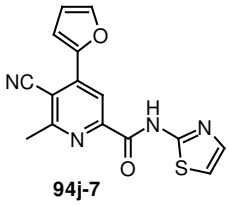

94j-7

94j-7; pale solid; 99% yield, $C_{15}H_{10}N_4O_2S$, M = 310.34 g/mol, HPLC-ESI-MS: $[M + H]^+$ = 311 *m/z*.

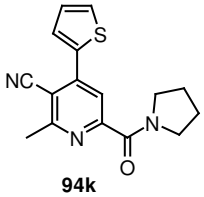

94k

94k; pale solid; 81% yield, $C_{16}H_{15}N_3OS$, M = 297.38 g/mol, HPLC-ESI-MS: $[M + H]^+$ = 298 *m/z*.

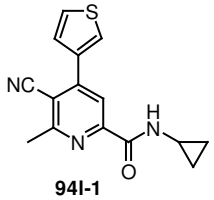

94l-1

94l-1; colorless solid; 86% yield, $C_{15}H_{13}N_3OS$, M = 283.35 g/mol, HPLC-ESI-MS: $[M + H]^+$ = 284 *m/z*.

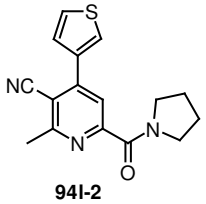

94l-2

94l-2; colorless solid; 80% yield, $C_{16}H_{15}N_3OS$, M = 297.38 g/mol, HPLC-ESI-MS: $[M + H]^+$ = 298 *m/z*. ^{1}H NMR (400 MHz, $CDCl_3$) δ 1.96 (m, 4 H), 2.85 (s, 3 H), 3.73 (m, 4 H), 7.49 (dd, *J* = 5.09, 3.05 Hz, 1 H), 7.53 (m, 1 H), 7.87 (s, 1 H), 7.96 (dd, *J* = 2.92, 1.40 Hz, 1 H). ^{13}C NMR (100 MHz, $CDCl_3$) δ 24.0 (CH_2), 24.2 (CH_2), 26.6 (CH_3), 47.2 (CH_2), 49.1 (CH_2), 107.0 (C), 117.1 (C), 120.5 (CH), 127.1 (CH), 127.2 (CH), 127.2 (CH), 136.2 (C), 147.9 (C), 156.1 (C), 162.0 (C), 165.0 (C).

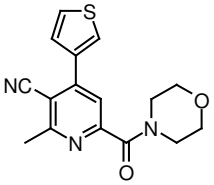

94l-3

94l-3; colorless solid; 99% yield, $C_{16}H_{15}N_3O_2S$, M = 313.38 g/mol, HPLC-ESI-MS: $[M + H]^+$ = 314 *m/z*.

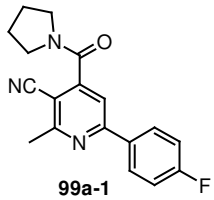

99a-1

99a-1; colorless solid; 68% yield, $C_{18}H_{16}FN_3O$, M = 309.35 g/mol, HPLC-ESI-MS: $[M + H]^+$ = 310 *m/z*; m.p. 208 °C. ^{1}H NMR (400 MHz, $CDCl_3$) δ 1.98 (m, 4 H) 2.84 (s, 3 H) 3.33 (t, *J* = 6.89 Hz, 2 H) 3.70 (t, *J* = 6.87 Hz, 2 H) 7.16 (m, 2 H) 7.58 (s, 1 H) 8.04 (m, 2 H). ^{13}C NMR (100 MHz, $CDCl_3$) δ 24.1 (CH_3), 24.3 (CH_2), 26.0 (CH_2), 46.1 (CH_2), 48.3 (CH_2), 103.4 (C), 114.3 (CH), 115.6 (C), 116.1 (d, $^2J_{C\text{-}F}$ = 21.95 Hz, CH), 129.5 (d, $^3J_{C\text{-}F}$ = 8.79 Hz, CH), 133.3 (d, $^4J_{C\text{-}F}$ = 2.93 Hz, C), 149.81 (C), 158.9 (C), 162.5 (C), 164.3 (C), 164.5 (d, $^1J_{C\text{-}F}$ = 251.76 Hz, C). FT-ICR-MS: calculated for $C_{18}H_{16}FN_3ONa^+$: 332.1170, found: 332.1169.

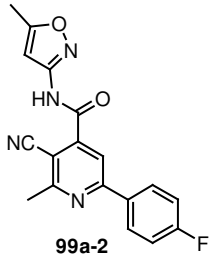

99a-2

99a-2; colorless solid; 99% yield, $C_{18}H_{13}FN_4O_2$, M = 336,33 g/mol, HPLC-ESI-MS: $[M + H]^+$ = 336 *m/z*.

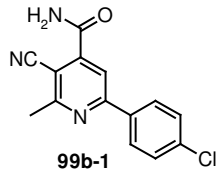

99b-1

99b-1; colorless solid; 99% yield, $C_{14}H_{10}ClN_3O$, M = 271.71 g/mol, HPLC-ESI-MS: [M + H]$^+$ = 272 *m/z*; m.p. 203-205 °C (dec.). ^{1}H NMR (400 MHz, DMSO-D$_6$) δ 2.77 (s, 3 H), 7.60 (m, 2 H), 8.04 (s, 1 H), 8.17 (s, 1 H), 8.21 (m, 2 H), 8.41 (s, 1 H). ^{13}C NMR (100 MHz, DMSO-D$_6$) δ 23.8 (CH_3), 104.6 (C), 115.7 (CH), 116.1 (C), 129.1 (CH), 129.2 (CH), 135.4 (C), 135.7 (C), 147.5 (C), 156.9 (C), 162.4 (C), 165.5 (C). IR (neat, cm^{-1}) λ_{max}: 3467, 3348, 3178, 2948, 2859, 2222, 1666, 1570, 1540, 1414, 1311, 1244, 1199, 1073, 1007, 836, 733, 651. FT-ICR-MS: calculated for $C_{14}H_{10}ClN_3ONa^+$: 294.0405, found: 294.0404.

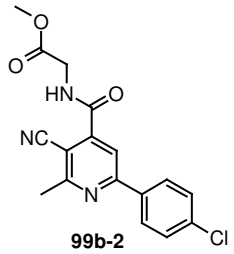

99b-2

99b-2; colorless solid; 80% yield, $C_{17}H_{14}ClN_3O_3$, M = 343.77 g/mol, HPLC-ESI-MS: [M + H]$^+$ = 344 *m/z*; m.p. 185 °C. FT-ICR-MS: calculated for $C_{17}H_{14}ClN_3O_3Na^+$: 366.0616, found: 366.0617.

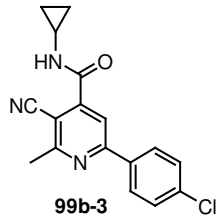

99b-3

99b-3; colorless solid; 95% yield, $C_{17}H_{14}ClN_3O$, M = 311.27 g/mol, HPLC-ESI-MS: [M + H]$^+$ = 312 *m/z*; m.p. 260-261 °C (decomp.). FT-ICR-MS: calculated for $C_{17}H_{14}ClN_3ONa^+$: 334.0718, found: 334.0719.

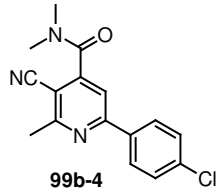

99b-4

99b-4; colorless solid; 80% yield, $C_{16}H_{14}ClN_3O$, M = 299.76 g/mol, HPLC-ESI-MS: [M + H]$^+$ = 300 *m/z*. ^{1}H NMR (400 MHz, ACETONE-D6) δ 2.80 (s, 3 H), 2.99 (s, 3 H), 3.11 (s, 3 H), 7.55 (m, 2 H), 7.93 (s, 1 H), 8.22 (m, 2 H). ^{13}C NMR (100 MHz, ACETONE-D6) δ 24.1 (CH_3), 34.7 (CH_3), 38.5 (CH_3), 105.0 (C), 115.5 (CH), 116.1 (C), 129.8 (CH), 129.8 (CH), 136.8 (C), 137.1 (C), 150.9 (C), 158.6 (C), 162.9 (C), 166.3 (C).

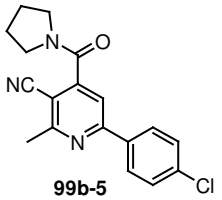

99b-5

99b-5; colorless solid; 99% yield, $C_{18}H_{16}ClN_3O$, M = 325.80 g/mol, HPLC-ESI-MS: $[M + H]^+$ = 326 *m/z*; m.p. 201 °C. ^{1}H NMR (400 MHz, $CDCl_3$) δ 1.98 (m, 4 H) 2.84 (s, 3 H) 3.32 (m, 2 H) 3.70 (m, 2 H) 7.44 (d, *J* = 8.65 Hz, 2 H) 7.60 (s, 1 H) 7.98 (d, *J* = 8.65 Hz, 2 H). ^{13}C NMR (100 MHz, $CDCl_3$) δ 24.1 (CH_3), 24.2 (CH_2), 26.0 (CH_2), 46.1 (CH_2), 48.3 (CH_2), 103.7 (C), 114.5 (CH), 115.5 (C), 128.7 (CH), 129.2 (CH), 135.4 (C), 137.0 (C), 149.8 (C), 158.7 (C), 162.5 (C), 164.2 (C). FT-ICR-MS: calculated for $C_{18}H_{16}ClN_3ONa^+$: 348.0874, found: 348.0873.

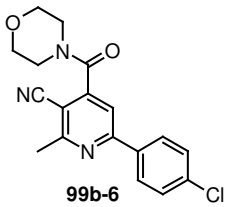

99b-6

99b-6; yellow solid; 92% yield, $C_{18}H_{16}ClN_3O_2$, M = 341.80 g/mol, HPLC-ESI-MS: $[M + H]^+$ = 342 *m/z*; ^{1}H NMR (400 MHz, $CDCl_3$) δ 2.85 (s, 3 H), 3.34 (m, 2 H), 3.71 (dd, *J* = 5.09, 3.56 Hz, 2 H), 3.83 (m, 4 H), 7.46 (m, 2 H), 7.58 (s, 1 H), 7.99 (m, 2 H). FT-ICR-MS: calculated for $C_{18}H_{16}ClN_3O_2Na^+$: 364.0823, found: 364.0820.

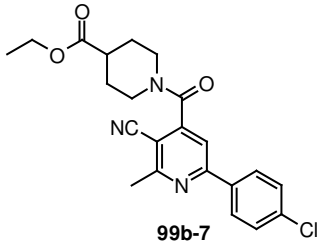

99b-7

99b-7; colorless solid; 99% yield, $C_{22}H_{22}ClN_3O_3$, M = 411.89 g/mol, HPLC-ESI-MS: $[M + H]^+$ = 412 *m/z*; m.p. 170 °C. ^{1}H NMR (400 MHz, $CDCl_3$) δ 1.25 (t, *J* = 7.12 Hz, 3 H) 1.88 (m, 3 H) 2.09 (m, 1 H) 2.60 (m, 1 H) 2.84 (s, 3 H) 3.20 (m, 2 H) 3.47 (m, 1 H) 4.15 (q, *J* = 7.12 Hz, 2 H) 4.47 (m, 1 H) 7.46 (m, 2 H) 7.55 (s, 1 H) 7.99 (m, 2 H). ^{13}C NMR (100 MHz, $CDCl_3$) δ 14.1 (CH_3), 24.1 (CH_3), 27.5 (CH_2), 28.3 (CH_2), 40.5 (CH), 41.2 (CH_2), 46.3 (CH_2), 60.8 (CH_2), 103.7 (C), 114.4 (CH), 115.3 (C), 128.7 (CH), 129.3 (CH), 135.4 (C), 137.1 (C), 148.9 (C), 158.8 (C), 162.5 (C), 164.5 (C), 173.6 (C). FT-ICR-MS: calculated for $C_{22}H_{22}ClN_3O_3Na^+$: 434.1242, found: 434.1240.

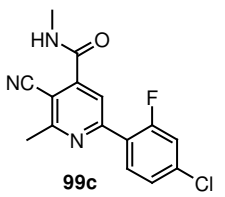

99c

99c; colorless solid; 85% yield, $C_{15}H_{11}ClFN_3O$, M = 303.73 g/mol, HPLC-ESI-MS: $[M + H]^+$ = 304 *m/z*. ^{1}H NMR (400 MHz, $CDCl_3$) δ 2.85 (s, 3 H), 3.06 (d, *J* = 5.09 Hz, 3 H), 7.30 (m, 2 H), 7.37 (m, 1 H), 8.03 (s, 1 H), 8.12 (s, 1 H). ^{13}C NMR (100 MHz, $CDCl_3$) δ 23.9 (CH_3), 26.3 (CH_3), 111.2 (C), 115.6 (C), 117.4 (d, $^2J_{C\text{-}F}$ = 24.88 Hz, CH), 120.5 (CH), 122.2 (d, $^2J_{C\text{-}F}$

= 14.63 Hz, C), 125.4 (d, $^{3}J_{C\text{-}F}$ = 3.66 Hz, CH), 131.3 (d, $^{4}J_{C\text{-}F}$ = 2.93 Hz, CH), 137.6 (d, $^{3}J_{C\text{-}F}$ = 10.25 Hz, CH), 148.6 (C), 151.2 (C), 159.0 (d, $^{1}J_{C\text{-}F}$ =253.96, C), 161.4 (C), 163.2 (C).

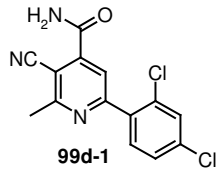

99d-1

99d-1; colorless solid; 89% yield, $C_{14}H_9Cl_2N_3O$, M = 306.15 g/mol, HPLC-ESI-MS: $[M + H]^+$ = 306 *m/z*.

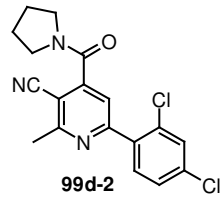

99d-2

99d-2; colorless solid; 90% yield, $C_{18}H_{15}Cl_2N_3O$, M = 360.25 g/mol, HPLC-ESI-MS: $[M + H]^+$ = 360 *m/z*; m.p. 129-132 °C. ^{1}H NMR (400 MHz, $CDCl_3$) δ 1.99 (m, 4 H) 2.85 (s, 3 H) 3.34 (m, 2 H) 3.69 (m, 2 H) 7.37 (dd, *J* = 8.39, 2.03 Hz, 1 H) 7.50 (d, *J* = 2.03 Hz, 1 H) 7.58 (m, 2 H). ^{13}C NMR (100 MHz, $CDCl_3$) δ 24.0 (CH_3), 24.2 (CH_2), 26.1 (CH_2), 46.1 (CH_2), 48.4 (CH_2), 104.6 (C), 115.2 (C), 119.3 (CH), 127.8 (CH), 130.2 (CH), 132.5 (CH), 132.7 (C), 135.7 (C), 136.3 (C), 148.9 (C), 158.4 (C), 162.6 (C), 163.8 (C). FT-ICR-MS: calculated for $C_{18}H_{15}Cl_2N_3ONa^+$: 382.0484, found: 382.0483.

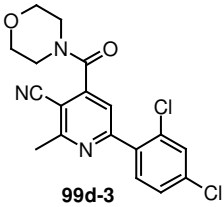

99d-3

99d-3; colorless solid; 83% yield, $C_{18}H_{15}Cl_2N_3O_2$, M = 376.25 g/mol, HPLC-ESI-MS: $[M + H]^+$ = 376 *m/z*; m.p. 131-132 °C. ^{1}H NMR (400 MHz, $CDCl_3$) δ 2.86 (s, 3 H) 3.36 (m, 2 H) 3.71 (m, 2 H) 3.82 (m, 4 H) 7.38 (dd, *J* = 8.39, 2.03 Hz, 1 H) 7.51 (d, *J* = 2.03 Hz, 1 H) 7.56 (s, 1 H) 7.59 (d, *J* = 8.39 Hz, 1 H). ^{13}C NMR (100 MHz, $CDCl_3$) δ 24.0 (CH_3), 42.4 (CH_2), 47.5 (CH_2), 66.5 (CH_2), 66.6 (CH_2), 104.7 (C), 115.0 (C), 119.5 (CH), 127.8 (CH), 130.2 (CH), 132.5 (CH), 132.7 (C), 135.4 (C), 136.5 (C), 147.3 (C), 158.5 (C), 162.7 (C), 164.3 (C). FT-ICR-MS: calculated for $C_{18}H_{15}Cl_2N_3O_2Na^+$: 398.0434, found: 398.0436.

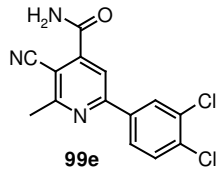

99e

99e; colorless solid; 99% yield, $C_{14}H_9Cl_2N_3O$, M = 306.15 g/mol, HPLC-ESI-MS: $[M + H]^+$ = 306 *m/z*.

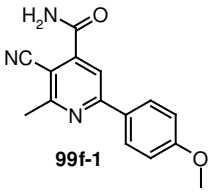

99f-1

99f-1; colorless solid; 99% yield, $C_{15}H_{13}N_3O_2$, M = 267.29 g/mol, HPLC-ESI-MS: $[M + H]^+$ = 268 *m/z*. ^{1}H NMR (400 MHz, DMSO-D_6) δ 2.75 (s, 3 H), 3.83 (s, 3 H), 7.09 (m, 2 H), 7.99 (s, 1 H), 8.07 (s, 1 H), 8.18 (m, 2 H), 8.38 (s, 1 H). ^{13}C NMR (100 MHz, DMSO-D_6) δ 23.8 (CH_3), 55.4 (CH_3), 103.1 (C), 114.4 (CH), 114.6 (CH), 116.4 (C),129.0 (C), 129.1 (CH), 147.3 (C), 158.0 (C), 161.5 (C), 162.2 (C), 165.8 (C).

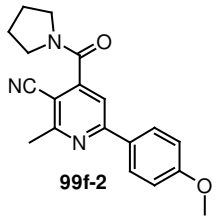

99f-2

99f-2; colorless solid; 89% yield, $C_{19}H_{19}N_3O_2$, M = 321.38 g/mol, HPLC-ESI-MS: $[M + H]^+$ = 322 *m/z*; m.p. 140 °C. ^{1}H NMR (400 MHz, $CDCl_3$) δ 1.97 (m, 4 H), 2.82 (s, 3 H), 3.32 (t, *J* = 6.49 Hz, 2 H), 3.69 (t, *J* = 6.87 Hz, 2 H), 3.85 (s, 3 H), 6.98 (m, 2 H), 7.55 (s, 1 H), 8.00 (m, 2 H). ^{13}C NMR (100 MHz, $CDCl_3$) δ 24.1 (CH_3), 24.3 (CH_2), 26.0 (CH_2), 46.0 (CH_2), 48.3 (CH_2), 55.4 (CH_3), 102.4 (C), 113.7 (CH), 114.4 (CH), 115.8 (C), 129.0 (CH), 129.5 (C), 149.5 (C), 159.6 (C), 161.9 (C), 162.3 (C), 164.6 (C). IR (neat, cm^{-1}) λ_{max}: 3070, 2974, 2878, 2222, 1624, 1580, 1543, 1440, 1358, 1322, 1285, 1255, 1226, 1189, 1159, 1078, 975, 849, 776, 702. FT-ICR-MS: calculated for $C_{19}H_{19}N_3O_2Na^+$: 344.1370, found: 344.1367.

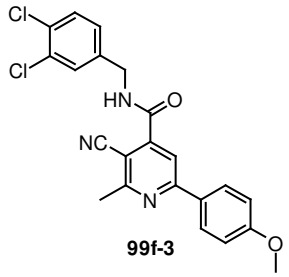

99f-3

99f-3; colorless solid; 99% yield, $C_{22}H_{17}Cl_2N_3O_2$, M = 426.31 g/mol, HPLC-ESI-MS: $[M + H]^+$ = 426 *m/z*; m.p. 242 °C. ^{1}H NMR (400 MHz, DMSO-D_6) δ 2.76 (s, 3 H), 3.83 (s, 3 H), 4.52 (d, *J* = 5.85 Hz, 2 H), 7.10 (m, 2 H), 7.39 (dd, *J* = 8.39, 2.03 Hz, 1 H), 7.62 (d, *J* = 8.39 Hz, 1 H), 7.66 (d, *J* = 2.03 Hz, 1 H), 8.11 (s, 1 H), 8.20 (m, 2 H), 9.50 (t, *J* = 5.85 Hz, 1 H). ^{13}C NMR (100 MHz, DMSO-D_6) δ 23.9 (CH_3), 41.8 (CH_2), 55.4 (CH_3), 103.5 (C), 114.4 (CH), 114.7 (CH), 116.8 (C), 127.8 (CH), 129.0 (C), 129.1 (CH), 129.5 (CH), 129.6 (C), 130.6 (CH), 131.0 (C), 139.8 (C), 146.8 (C), 158.1 (C), 161.6 (C), 162.2 (C), 164.2 (C). IR (neat, cm^{-1}) λ_{max}: 3454, 3100, 2893, 2834, 2347, 1764, 1698, 1595, 1513, 1425, 1381, 1336, 1248, 1167, 1130, 1093, 1019.019.8, 835, 753. FT-ICR-MS: calculated for $C_{22}H_{17}Cl_2N_3O_2H^+$: 426.0771, found: 426.0772.

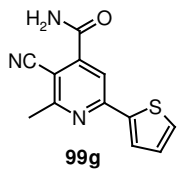

99g

99g; colorless solid; 86% yield, $C_{12}H_9N_3OS$, M = 243.29 g/mol, HPLC-ESI-MS: $[M + H]^+$ = 244 *m/z*.

6. 1. 2. 7 General procedure for the synthesis of pyridine hydrazides 100.

A suspension of **81** (0.3 mmol) in 50% hydrazine/water (2mL) in a sealed tube was heated at 150 °C for 24 h. The precipitate was filtered, washed with water and air-dried to afford the product **100**.

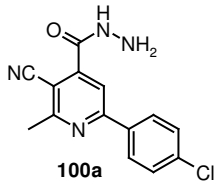

100a

100a; yellow solid; 94% yield, $C_{14}H_{11}ClN_4O$, M = 286.72 g/mol, HPLC-ESI-MS: $[M + H]^+$ = 289 *m/z*; m.p. 336-339 °C (dec.). ^{1}H NMR (400 MHz, DMSO-D_6) δ 3.08 (s, 3 H), 5.56 (s, 2 H), 7.57 (d, *J* = 8.39 Hz, 2 H), 8.22 (d, *J* = 8.65 Hz, 2 H), 8.37 (s, 1 H), 12.00 (s, 1 H). ^{13}C NMR (100 MHz, DMSO-D_6) δ 26.7 (CH_3), 112.4 (CH), 118.6 (C), 128.7 (CH), 129.1 (CH), 134.9 (C), 136.0 (C), 136.5 (C), 146.1 (C), 154.0 (C), 157.3 (C), 157.7 (C). IR (neat, cm^{-1}) λ_{max}: 3295, 3202, 2992, 2906, 2826, 1659, 1609, 1541, 1474, 1412, 1381, 1350, 1165, 1103, 1035, 998, 825, 782, 733. FT-ICR-MS: calculated for $C_{14}H_{11}ClN_4OH^+$: 287.0694, found: 287.0694.

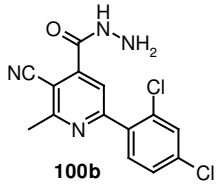

100b

100b; yellow solid; 75% yield, $C_{14}H_{10}Cl_2N_4O$, M = 321.17 g/mol, HPLC-ESI-MS: $[M + H]^+$ = 321 *m/z*.

6. 1. 2. 8 General procedure for the synthesis of dicyanopyridines 95 and 101.

5-Cyano-6-methyl-4-aryl-pyridine-2-carboxylic acid amide **94** or 5-cyano-6-methyl-2-aryl-pyridine-4-carboxylic acid amide **99** (0.2 mmol) was dissolved in $POCl_3$ (2 mL), and the mixture was heated at 100 ºC for 1 h. The exess of the reagent was removed in vacuo and the product was isolated by column chromatography (PE/EA, 10:1).

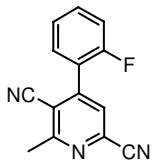

95a

95a; colorless solid; 79% yield, $C_{14}H_8FN_3$, M = 237.24 g/mol, HPLC-ESI-MS: $[M + H]^+$ = 238 *m/z*.

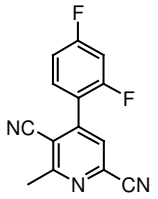

95b

95b; pale solid; 70% yield, $C_{14}H_7F_2N_3$, M = 255.23 g/mol, HPLC-ESI-MS: $[M + H]^+$ = 256 *m/z*. ^{1}H NMR (400 MHz, $CDCl_3$) δ 2.90 (s, 3 H), 7.07 (m, 2 H), 7.45 (m, 1 H), 7.65 (s, 1 H). ^{13}C NMR (100 MHz, $CDCl_3$) δ 24.2 (CH_3), 105.4 (t, $^2J_{C\text{-}F}$ = 25.62, CH), 112.4 (C), 112.8 (dd, $^{2,4}J_{C\text{-}F}$ = 22.08, 3.66 Hz, CH), 114.7 (C), 115.9 (C), 118.4 (dd, $^{2,4}J_{C\text{-}F}$ = 15.13, 4.18 Hz, C), 126.6 (CH), 131.6 (dd,$^{1,3}J_{C\text{-}F}$ = 10.12, 2.93 Hz, CH), 135.3 (C), 148.4 (C), 159.6 (dd, $^{1,3}J_{C\text{-}F}$ = 254.39, 14.44 Hz, C), 164.3 (C), 156.5 (dd, $^{1,3}J_{C\text{-}F}$ = 255.57, 12.45 Hz, C).

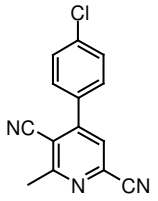

95c

95c; colorless solid; 86% yield, $C_{14}H_8ClN_3$, M = 253.69 g/mol, HPLC-ESI-MS: $[M + H]^+$ = 254 *m/z*; m.p. 174-176 °C. ^{1}H NMR (400 MHz, $CDCl_3$) δ 2.91 (s, 3 H, Me), 7.55 (m, 4 H), 7.66 (s, 1 H). ^{13}C NMR (100 MHz, $CDCl_3$) δ 24.2 (CH_3), 110.8 (C), 115.2 (C), 116.0 (C), 125.5 (CH), 129.7 (CH), 129.8 (CH), 132.5 (C), 135.4 (C), 137.6 (C), 153.4 (C), 164.6 (C). IR (neat, cm^{-1}) λ_{max}: 3449, 3363, 3267, 3155, 3089, 2948, 2229, 1807, 1703, 1637, 1585, 1533, 1481, 1422, 1362, 1318, 1229, 1088, 1007, 822. FT-ICR-MS: calculated for $C_{14}H_8ClN_3H^+$: 254.0480, found: 254.0478.

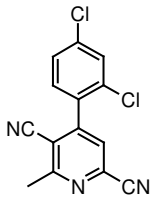

95d

95d; colorless solid; 99% yield, $C_{14}H_7Cl_2N_3$, M = 288.14 g/mol, HPLC-ESI-MS: $[M + H]^+$ = 288 *m/z*; ^{1}H NMR (400 MHz, $CDCl_3$) δ 2.91 (s, 3 H), 7.30 (m, 1 H), 7.46 (m, 1 H), 7.62 (m, 2 H). ^{13}C NMR (100 MHz, $CDCl_3$) δ 24.0 (CH_3), 112.8 (C), 114.3 (C), 115.8 (C), 126.6 (CH), 128.0 (CH), 130.4 (CH), 131.0 (CH), 131.6 (CH), 133.0 (C), 135.0 (C), 137.5 (C), 151.5 (C), 164.0 (C).

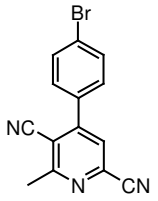

95e

95e; colorless solid; 94% yield, $C_{14}H_8BrN_3$, M = 298.14 g/mol, HPLC-ESI-MS: $[M + H]^+$ = 298 *m/z*; ^{1}H NMR (400 MHz, $CDCl_3$) δ 2.90 (s, 3 H), 7.46 (m, 2 H), 7.64 (s, 1 H), 7.71 (m, 2

H). ^{13}C NMR (100 MHz, $CDCl_3$) δ 24.2 (CH_3), 110.8 (C), 115.2 (C), 116.0 (C), 125.4 (CH), 126.0 (C), 129.9 (CH), 132.8 (CH), 132.9 (C), 135.4 (C), 153.5 (C), 164.6 (C).

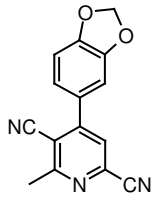

95f

95f; pale solid; 99% yield, $C_{15}H_9N_3O_2$, M = 263.26 g/mol, HPLC-ESI-MS: $[M + H]^+$ = 264 *m/z*.

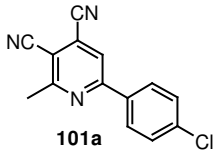

101a

101a; colorless solid; 84% yield, $C_{14}H_8ClN_3$, M = 253.69 g/mol, HPLC-ESI-MS: $[M + H]^+$ = 254 *m/z*; m.p. 193 °C. ^{1}H NMR (400 MHz, $CDCl_3$) δ 2.90 (s, 3 H), 7.50 (m, 2 H), 7.89 (s, 1 H), 8.01 (m, 2 H). ^{13}C NMR (100 MHz, DMSO-D_6) δ 24.3 (CH_3), 108.0 (C), 114.0 (C), 114.1 (C), 119.5 (CH), 124.8 (C), 128.8 (CH), 129.6 (CH), 134.1 (C), 138.2 (C), 159.2 (C), 163.4 (C). IR (neat, cm^{-1}) λ_{max}: 3378, 3252, 3155, 3096, 2963, 2926, 2229, 1644, 1577, 1540, 1451, 1407, 1370, 1325, 1236, 1088, 999, 881, 844, 747, 644. FT-ICR-MS: calculated for $C_{14}H_8ClN_3Na^+$: 276.0299, found: 276.0299.

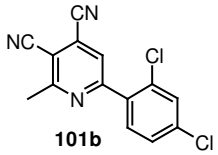

101b

101b; colorless solid; 80% yield, $C_{14}H_7Cl_2N_3$, M = 288.14 g/mol, HPLC-ESI-MS: $[M + H]^+$ = 288 *m/z*. ^{1}H NMR (400 MHz, $CDCl_3$) δ 2.93 (s, 3 H), 7.43 (dd, *J* = 8.39, 1.78 Hz, 1 H), 7.55 (d, *J* = 1.78 Hz, 1 H), 7.64 (d, *J* = 8.39 Hz, 1 H), 7.96 (s, 1 H). ^{13}C NMR (100 MHz, $CDCl_3$) δ 24.2 (CH_3), 108.8 (C), 113.7 (C), 113.8 (C), 123.9 (C), 124.3 (CH), 128.0 (CH), 130.4 (CH), 132.6 (CH), 132.8 (C), 134.3 (C), 137.2 (C), 158.9 (C), 163.4 (C).

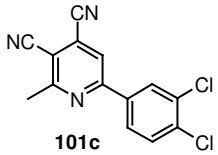

101c

101c; colorless solid; 75% yield, $C_{14}H_7Cl_2N_3$, M = 288.14 g/mol, HPLC-ESI-MS: $[M + H]^+$ = 288 *m/z*; ^{1}H NMR (400 MHz, $CDCl_3$) δ 2.92 (s, 3 H), 7.62 (m, 1 H), 7.88 (m, 2 H), 8.22 (m, 1 H). ^{13}C NMR (100 MHz, $CDCl_3$) δ 24.3 (CH_3), 108.7 (C), 113.8 (C), 113.9 (C), 119.6 (CH), 125.1 (C), 126.4 (CH), 129.5 (CH), 131.3 (CH), 134.0 (C), 135.5 (C), 136.3 (C), 157.9 (C), 163.6 (C).

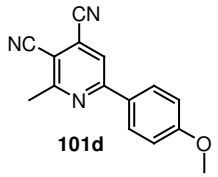

101d

101d; colorless solid; 99% yield, $C_{15}H_{11}N_3O$, M = 249.27 g/mol, HPLC-ESI-MS: $[M + H]^+$ = 250 *m/z*; ^{1}H NMR (400 MHz, $CDCl_3$) δ 2.86 (s, 3 H), 3.89 (s, 3 H), 7.02 (m, 2 H), 7.82 (s, 1 H) 8.03 (m, 2 H). ^{13}C NMR (100 MHz, $CDCl_3$) δ 24.3 (CH_3), 55.5 (CH_3), 106.4 (C), 114.3 (C), 114.5 (C), 114.7 (CH), 118.9 (CH), 124.3 (C), 128.2 (C), 129.3 (CH), 159.9 (C), 162.6 (C), 163.2 (C).

6. 1. 2. 9 General procedure for the synthesis of nicotinic amides 96.

t-BuOK (3 eq, 3.0 mmol, 0.336 g) was added to a suspension of 5-cyano-2-pyridine carboxylic acid **74** (1 eq, 1 mmol) in water (15 mL). The mixture was heated at 100 ˚C for 3 h. After cooling to room temperature the mixture was concentrated in vacuo, acidified with 1M HCl and extracted with DCM. The combined organic phases were dried over anhydrous Na_2SO_4, concentrated and the residue was used without further purification.

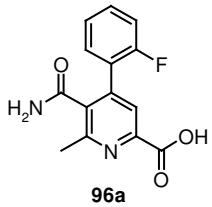

96a

96a; pale solid; 80% yield, $C_{14}H_{11}FN_2O_3$, M = 274.25 g/mol, HPLC-ESI-MS: $[M + H]^+$ = 275 *m/z*. ^{1}H NMR (400 MHz, DMSO-D_6) δ 2.59 (s, 3 H), 7.29 (m, 2 H), 7.47 (m, 2 H), 7.64 (s, 1 H), 7.79 (s, 1 H), 7.97 (s, 1 H). ^{13}C NMR (100 MHz, DMSO-D_6) δ 22.3 (CH_3), 115.8 (d, $^2J_{C\text{-}F}$ = 21.22 Hz, CH), 123.4 (CH), 124.3 (d, $^3J_{C\text{-}F}$ = 3.66 Hz, CH), 124.7 (d, $^2J_{C\text{-}F}$ = 14.64 Hz, C), 130.8 (d, $^4J_{C\text{-}F}$ = 2.20 Hz, CH), 131.0 (d, $^3J_{C\text{-}F}$ = 8.05 Hz, CH), 135.8 (C), 141.1 (C), 146.8 (C), 154.9 (C), 158.8 (d, $^1J_{C\text{-}F}$ =246.64 Hz, C), 165.7 (C), 168.3 (C).

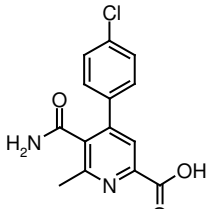

96b

96b; colorless solid; 65% yield, $C_{14}H_{11}ClN_2O_3$, M = 290.71 g/mol, HPLC-ESI-MS: $[M + H]^+$ = 291 *m/z*. ^{1}H NMR (400 MHz, DMSO-D_6) δ 2.57 (s, 3 H), 7.54 (m, 4 H), 7.69 (s, 1 H), 7.81 (s, 1 H), 7.97 (s, 1 H). ^{13}C NMR (100 MHz, DMSO-D_6) δ 22.2 (CH_3), 122.5 (CH), 128.6 (CH), 130.1 (CH), 133.8 (C), 134.8 (C), 136.3 (C), 145.5 (C), 147.4 (C), 154.8 (C), 165.8 (C), 168.9 (C).

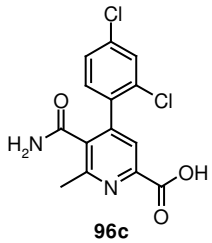

96c

96c; colorless solid; 99% yield, $C_{14}H_{11}Cl_2N_2O_3$, M = 325.15 g/mol, HPLC-ESI-MS: $[M + H]^+$ = 325 *m/z*. ^{1}H NMR (400 MHz, DMSO-D_6) δ 2.59 (s, 3 H), 7.42 (m, 1 H), 7.52 (m, 1 H), 7.64 (s, 1 H), 7.74 (m, 2 H), 7.93 (s, 1 H). ^{13}C NMR (100 MHz, DMSO-D_6) δ 22.3

(CH_3), 123.1 (CH), 127.0 (CH), 128.9 (CH), 132.0 (CH), 132.1 (C), 134.2 (C), 134.7 (C), 135.6 (C), 143.6 (C), 146.8 (C), 154.7 (C), 165.7 (C), 167.8 (C).

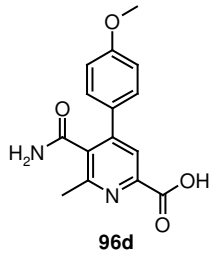

96d

96d; colorless solid; 91% yield, $C_{15}H_{14}N_2O_4$, M = 286.29 g/mol, HPLC-ESI-MS: $[M + H]^+$ = 287 *m/z*. ^{1}H NMR (400 MHz, DMSO-D_6) δ 2.55 (s, 3 H), 3.79 (s, 3 H), 7.02 (m, 2 H), 7.51 (d, 2 H), 7.65 (s, 1 H), 7.79 (s, 1 H), 7.93 (s, 1 H). ^{13}C NMR (100 MHz, DMSO-D_6) δ 22.2 (CH_3), 55.3 (CH_3), 114.1 (CH), 122.5 (CH), 129.6 (CH), 134.7 (C), 146.2 (C), 147.1 (C), 154.6 (C), 159.8 (C), 165.9 (C), 169.3 (C).

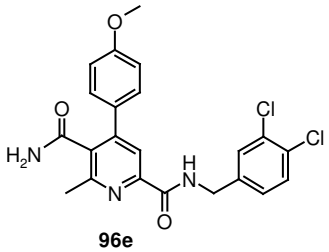

96e

96e; colorless solid; 88% yield, $C_{22}H_{19}Cl_2N_3O_3$, M = 444.32 g/mol, HPLC-ESI-MS: $[M + H]^+$ = 444 *m/z*; m.p. 151 °C. ^{1}H NMR (400 MHz, $CDCl_3$) δ 2.62 (s, 3 H), 3.82 (s, 3 H), 4.58 (d, *J* = 6.36 Hz, 1 H), 5.74 (s, 1 H), 5.81 (s, 1 H), 6.92 (m, 2 H), 7.18 (dd, *J* = 8.39, 2.03 Hz, 1 H), 7.39 (d, *J* = 8.39 Hz, 2 H), 7.45 (m, 3 H), 7.97 (s, 1 H), 8.48 (t, *J* = 6.36 Hz, 1 H). ^{13}C NMR (100 MHz, $CDCl_3$) δ 22.5 (CH_3), 42.3 (CH_2), 55.3 (CH_3), 114.3 (CH), 120.3 (CH), 127.1 (CH), 129.2 (C), 129.6 (CH), 129.7 (CH), 130.6 (CH), 131.5 (C), 132.7 (C), 132.7 (C), 138.5 (C), 147.8 (C), 148.4 (C), 154.9 (C), 160.5 (C), 164.0 (C), 170.3 (C). IR (neat, cm^{-1}) λ_{max}: 3705, 3668, 3351, 3107, 2974, 2864, 1735, 1661, 1506, 1358, 1285, 1240, 1137, 1056, 1026, 820, 650. FT-ICR-MS: calculated for $C_{22}H_{19}Cl_2N_3O_3Na^+$: 466.0696, found: 466.0696.

6. 1. 2. 10 Synthesis of pyridine *N*-hydroxyamidine 102.

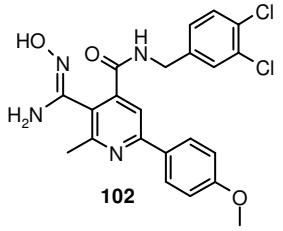

102

Hydroxylamine hydrochloride (3 eq, 3 mmol, 0.209 g) and *t*-BuOK (3 eq, 3 mmol, 0.337 g) were successively added to the suspension of **99f-3** (1 eq, 1 mmol, 0.425 g) in DMSO (6 mL). The mixture was stirred for 2 h at 100 ºC, cooled to room temperature and diluted with water. The yellow precipitate was filtered, washed with water and air dried to give the product **102** as a yellow solid (0.430 g, 94%). $C_{22}H_{20}Cl_2N_4O_3$, M = 459.34 g/mol, HPLC-ESI-MS: $[M + H]^+$ = 459 *m/z*; m.p. 270 °C (dec.). ^{1}H NMR (400 MHz, DMSO-D_6) δ 2.57 (s, 3 H), 3.81 (s, 3 H), 4.44 (d, *J* = 5.85 Hz, 2 H), 5.88 (s, 2 H), 7.05 (m, 1 H), 7.40 (m, 1 H), 7.61 (m, 1 H), 7.73

(s, 1 H), 8.08 (m, 2 H), 8.75 (t, J = 5.85 Hz, 1 H), 9.45 (s, 1 H). ^{13}C NMR (100 MHz, DMSO-D_6) δ 22.6 (CH_3), 41.5 (CH_2), 55.3 (CH_3), 114.2 (CH), 114.5 (CH), 124.2 (C), 127.5 (CH), 128.1 (CH), 129.0 (CH), 129.2 (C), 130.3 (C), 130.6 (CH), 130.7 (C), 140.2 (C), 145.5 (C), 149.8 (C), 155.1 (C), 157.7 (C), 160.5 (C), 166.9 (C). IR (neat, cm^{-1}) λ_{max}: 3484, 3329, 3210, 2886, 2834, 2783, 1735, 1639, 1558, 1513, 1462, 1417, 1358, 1285, 1255, 1181, 1122, 1026, 938, 827, 606. FT-ICR-MS: calculated for $C_{22}H_{20}Cl_2N_4O_3H^+$: 459.0985, found: 459.0986.

6. 1. 2. 11 Synthesis of pyridine tetrazoles.

General procedure for the synthesis of 97: NH_4Cl (5 eq, 0.80 mmol, 0.043 g) and NaN_3 (5eq, 0.80 mmol, 0.052 g) were added to a solution of the amide **94** (1 eq, 0.16 mmol) in DMF (2 mL). The mixture was heated in a sealed tube at 120 °C for 24 h. After cooling, the solvent was removed in vacuo, the crude residue was taken up in water and treated with 1M HCl until a suspension was formed. The solid was filtered, washed with water and Et_2O. The product was isolated by filtration on silica gel using DCM/MeOH (10:1) as eluent.

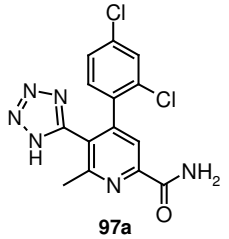

97a

97a; yellow solid; 80% yield, $C_{14}H_{10}Cl_2N_6O$, M = 349.18 g/mol, HPLC-ESI-MS: $[M + H]^+$ = 349 *m/z*. ^{1}H NMR (400 MHz, DMSO-D_6) δ 1.47 (s, 3 H), 6.24 (m, 1 H), 6.41 (m, 1 H), 6.62 (m, 1 H), 6.89 (s, 2 H), 7.28 (s, 1 H). ^{13}C NMR (100 MHz, DMSO-D_6) δ 23.1 (CH_3), 120.7 (CH), 127.3 (CH), 128.9 (CH), 132.1 (CH), 132.2 (C), 134.2 (C), 134.7 (C), 148.2 (C), 150.9 (C), 157.1 (C), 165.1 (C).

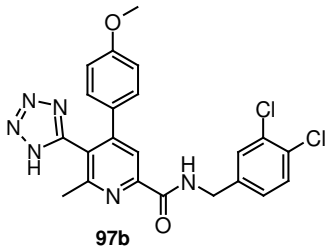

97b

97b; yellow oil; 89% yield, $C_{22}H_{18}Cl_2N_6O_2$, M = 469.33 g/mol, HPLC-ESI-MS: $[M + H]^+$ = 469 *m/z*. ^{1}H NMR (400 MHz, DMSO-D_6) δ 2.24 (s, 3 H, Me), 3.70 (s, 3 H), 4.51 (d, J = 6.36 Hz), 6.76 (m, 2 H), 7.07 (m, 2 H), 7.34 (m, 1 H), 7.59 (m, 2 H), 7.84 (s, 1 H), 9.40 (t, J = 6.36 Hz, 1 H). ^{13}C NMR (100 MHz, DMSO-D_6) δ 23.2 (CH_3), 41.5 (CH_2), 55.0 (CH_3), 113.5 (CH), 119.7 (CH), 127.9 (CH), 129.3 (C), 129.5 (CH), 130.0 (CH), 130.5 (CH), 130.6 (C), 130.8 (C), 141.0 (C), 146.9 (C), 148.3 (C), 149.6 (C), 156.6 (C), 157.7 (C), 159.0 (C), 164.2 (C). IR (neat, cm^{-1}) λ_{max}: 3289, 3037, 2918, 1837, 1666, 1614, 1511, 1459, 1392, 1340, 1288, 1259, 1185, 1051, 1022, 829, 755. FT-ICR-MS: calculated for $C_{22}H_{18}Cl_2N_6O_2Na^+$: 491.0761 , found: 491.0765.

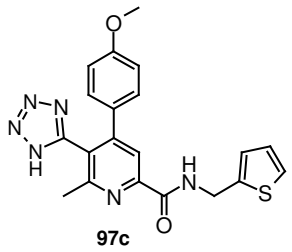

97c

97c; Pale solid; 99% yield, $C_{20}H_{18}N_6O_2S$, M = 406.47 g/mol, HPLC-ESI-MS: $[M + H]^+$ = 407 *m/z*.

Synthesis of pyridine tetrazole 108:

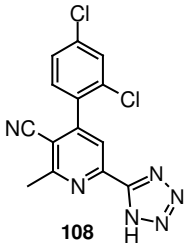

108

NH_4Cl (5 eq, 1.50 mmol, 0.080 g) and NaN_3 (5 eq, 1.50 mmol, 0.098 g)were added to a solution of **95d** (1 eq, 0.30 mmol, 0.086 g) in DMF (2 mL). The mixture was heated in a sealed tube at 70 ^oC for 2 h. After cooling, the solvent was removed in vacuo, the crude residue was filtrated on silica gel with DCM/MeOH (10:1) as eluent. The resulting solid was washed with water and air dried to afford product (0.092 g, 93%) as a yellow solid. $C_{14}H_8Cl_2N_6$, M = 331.17 g/mol, HPLC-ESI-MS: $[M + H]^+$ = 331 *m/z*; ^1H NMR (400 MHz, DMSO-D_6) δ 2.86 (s, 3 H), 7.68 (m, 2 H), 7.93 (m, 1 H), 8.13 (s, 1 H). ^{13}C NMR (100 MHz, DMSO-D_6) δ 23.7 (CH_3), 109.2 (C), 115.7 (C), 120.3 (CH), 128.0 (CH), 129.5 (CH), 132.2 (CH), 132.4 (C), 133.5 (C), 135.5 (C), 147.8 (C), 147.8 (C), 150.7 (C), 162.3 (C).

Synthesis of pyridine tetrazole 109:

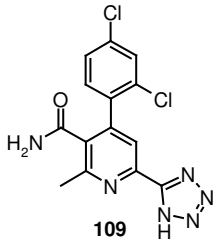

109

t-BuOK (3 eq, 0.9 mmol, 0.101 g) was added to a solution of **108** (1 eq, 0.3 mmol, 0.099 g) in water (5 mL). The mixture was heated at 100 ^oC for 3 h. After cooling, the mixture was acidified with 1M HCl. The precipitate was filtered, washed with water and air dried to afford the product (104 mg, 99%) as a yellow solid. $C_{14}H_{10}Cl_2N_6O$, M = 349.18 g/mol, HPLC-ESI-MS: $[M + H]^+$ = 349 *m/z*; ^1H NMR (400 MHz, DMSO-D_6) δ 2.69 (s, 3 H), 7.49 (m, 1 H), 7.56 (m, 1 H), 7.70 (s, 1 H), 7.80 (m, 1 H), 7.95 (s, 1 H), 7.99 (s, 1 H). ^{13}C NMR (100 MHz, DMSO-D_6) δ 22.5 (CH_3), 120.9 (CH), 127.1 (CH), 129.0 (CH), 132.1 (CH), 132.9 (C), 134.3 (C), 134.6 (C), 134.7 (C), 142.8 (C), 144.3 (C), 155.0 (C), 155.6 (C), 167.8 (C).

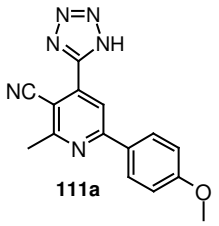

111a

111a; Prepared according to the procedure for **108**, using compound **101d** as a starting material. Pale solid; 85% yield, $C_{15}H_{12}N_6O$, M = 292.30 g/mol, HPLC-ESI-MS: $[M + H]^+$ = 293 *m/z*. ^{1}H NMR (400 MHz, DMSO-D_6) δ 2.78 (s, 3 H), 3.83 (s, 3 H), 7.08 (m, 2 H), 8.14 (m, 2 H), 8.34 (s, 1 H). ^{13}C NMR (100 MHz, DMSO-D_6) δ 24.3 (CH_3), 55.4 (CH_3), 102.6 (C), 114.4 (CH), 115.1 (CH), 116.6 (C), 128.9 (CH), 129.0 (C), 138.4 (C), 157.9 (C), 161.4 (C), 162.8 (C).

6. 1. 2. 12 Synthesis of pyrrolopyridines.

Method A

51% aqueous solution of hydrazine (20 eq, 3 mmol) was added dropwise to a suspension of the tertiary amide (1 eq, 0.15 mmol) and Raney Nickel (1 mL, 50% slurry in water) dissolved in MeOH (50 mL). After stirring for 3-16 h at rt (reaction monitored by TLC), the catalyst was filtered off and the solvent was removed under reduced pressure. The residue was taken up in water and extracted with DCM/EA. The combined organic phases were dried over anhydrous Na_2SO_4 and concentrated. The product was isolated by column chromatography with DCM/MeOH (40:1) as eluent.

Method B

B-1a. The cyanopyridine **81** (1 eq, 0.2 mmol) and nickel (II) chloride hexahydrat (1 eq, 0.2 mmol, 0.048 g) were dissolved in MeOH (5 ml). $NaBH_4$ (7 eq, 1.4 mmol, 0.053 g) was added very cautiously while stirring the solution vigorously. The progress of the reaction was monitored by LC/MS. After 24 h the reaction mixture was filtered through a celite pad and the solvent was removed under vacuum. The residue was taken up in water and extracted with DCM. The aqueous layer was lyophilized to give a solid product that was used in the next step without further purification.

B-1b. 5-Cyano-4-aryl-6-methyl-pyridine-2-carboxylic acid **81** (1 eq, 0.25 mmol) was dissolved in acetic acid (0.25 mL) and 10% Pd/C (10% m/m) was added. The mixture was degassed and hydrogenated under 1.0 atm pressure of H_2 for 24 h at 60 ˚C. The catalyst was filtered off and the solvent was removed on vacuum. The residue was taken up in water and extracted with DCM. Aqueous layer was lyophilized to give a solid product that was used in the next step without further purification.

B-2. Boc_2O (1.5 eq, 0.225 mmol, 0.049 g) was added to a solution of **116** (1 eq, 0.15 mmol) in dioxane/4M NaOH (10:1, 5.5 mL) and the mixture was stirred for 16 h at 60 ˚C. The solvent was removed in vacuo and the product was isolated by filtration on silica gel using DCM/MeOH (40:1) as eluent.

B-3. The Boc-protected pyrrolopyridine **117** (1 eq, 0.10 mmol) was treated with 25% TFA/DCM (5 mL) at rt. After 1 h the solvent was removed under reduced pressure, the residue was taken up in water and extracted with DCM/EA. The combined organic phases were dried over anhydrous Na_2SO_4 and concentrated. The product was isolated by column chromatography with DCM/MeOH (40:1) as eluent.

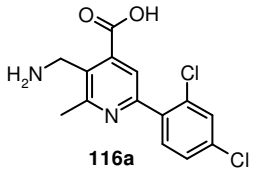

116a

116a; Prepared according to the procedure B-1a using **81c** as a starting material; colorless solid; 64% yield, $C_{14}H_{12}Cl_2N_2O_2$, M = 311.17 g/mol, HPLC-ESI-MS: $[M + H]^+$ = 311 *m/z*.

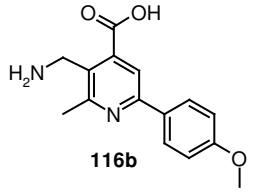

116b

116b; Prepared according to the procedure B-1b using **81k** as a starting material; pale solid; 76% yield, $C_{15}H_{16}N_2O_3$, M = 272.31 g/mol, HPLC-ESI-MS: $[M + H]^+$ = 273 *m/z*.

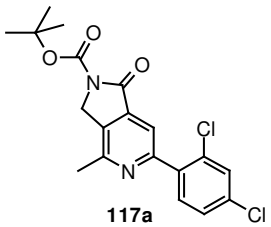

117a

117a; Prepared according to the procedure B-1a, B-2 using **116a** as a starting material; colorless solid; 85% yield, $C_{19}H_{18}Cl_2N_2O_3$, M = 393.27 g/mol, HPLC-ESI-MS: $[M + H]^+$ = 392 *m/z*. ^{1}H NMR (400 MHz, $CDCl_3$) δ 1.60 (s, 9 H), 2.66 (s, 3 H), 4.78 (s, 2 H), 7.32 (m, 1 H), 7.47 (m, 1 H), 7.51 (m, 1 H), 7.88 (s, 1 H). ^{13}C NMR (100 MHz, $CDCl_3$) δ 21.1 (CH_3), 28.0 (CH_3), 47.9 (CH_2), 84.0 (C), 116.9 (CH), 127.4 (CH), 129.9 (CH), 132.3 (C), 132.4 (CH), 133.0 (C), 135.2 (C), 136.8 (C), 139.3 (C), 150.0 (C), 154.4 (C), 155.7 (C), 165.1 (C).

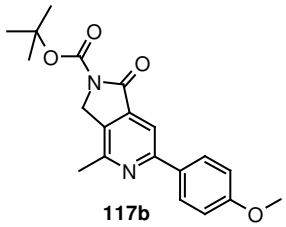

117b

117b; Prepared according to the procedure B-1b, B-2 using **116b** as a starting material; colorless solid; 74% yield, $C_{20}H_{22}N_2O_4$, M = 354.41 g/mol, HPLC-ESI-MS: $[M + H]^+$ = 355 *m/z*. ^{1}H NMR (400 MHz, $CDCl_3$) δ 1.61 (s, 9 H), 2.64 (s, 3 H), 3.86 (s, 3 H), 4.75 (s, 2 H), 6.99 (m, 2 H), 7.93 (s, 1 H), 8.00 (m, 2 H). ^{13}C NMR (100 MHz, $CDCl_3$) δ 21.3 (CH_3), 28.1 (CH_3), 48.0 (CH_2), 55.4 (CH_3), 83.8 (C), 111.4 (CH), 114.2 (CH), 128.4 (CH), 130.7 (C), 131.1 (C), 139.9 (C), 150.1 (C), 153.9 (C), 157.4 (C), 160.8 (C), 165.9 (C).

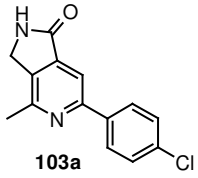

103a

103a; Prepared according to the Method A using **99b-5** as a starting material; colorless solid; 80% yield, $C_{14}H_{11}ClN_2O$, M = 258.71 g/mol, HPLC-ESI-MS: $[M + H]^+$ = 259 *m/z*. ^{1}H NMR (400 MHz, DMSO-D_6) δ 2.56 (s, 3 H), 4.44 (s, 2 H), 7.51 (m, 2 H), 7.97 (s, 1 H), 8.16 (m 2 H), 8.95 (s, 1 H). ^{13}C NMR (100 MHz, DMSO-D_6) δ 20.9 (CH_3), 43.8 (CH_2), 110.9 (CH), 128.5 (CH), 128.7 (CH), 133.9 (C), 136.4 (C), 137.2 (C), 141.5 (C), 153.9 (C), 154.0 (C), 168.7 (C).

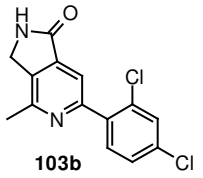

103b

103b; Prepared according to the Method A using **99d-2** as a starting material (66% yield) and according to the Method B (step B-3) using **117a** as a starting material (99% yield); colorless solid; $C_{14}H_{10}Cl_2N_2O$, M = 293.15 g/mol, HPLC-ESI-MS: $[M + H]^+$ = 293 m/z. ^{1}H NMR (400 MHz, DMSO-D_6) δ 2.57 (s, 3 H), 4.49 (s, 2 H), 7.54 (m, 1 H), 7.62 (m, 1 H), 7.69 (s, 1 H), 7.74 (m, 1 H), 9.02 (s, 1 H). ^{13}C NMR (100 MHz, DMSO-D_6) δ 20.7 (CH_3), 43.9 (CH_2), 115.4 (CH), 127.6 (CH), 129.4 (CH), 132.2 (C), 133.1 (CH), 133.9 (C), 136.8 (C), 137.5 (C), 140.6 (C), 153.8 (C), 154.2 (C), 168.4 (C).

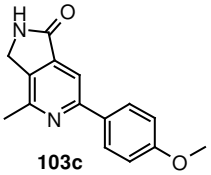

103c

103c; Prepared according to the Method A using **99f-2** as a starting material (69% yield) and according to the Method B (step B-3) using **117b** as a starting material (95% yield); colorless solid; $C_{15}H_{14}N_2O_2$, M = 254.29 g/mol, HPLC-ESI-MS: $[M + H]^+$ = 255 *m/z*. ^{1}H NMR (400 MHz, DMSO-D_6) δ 2.56 (s, 3 H), 3.81 (s, 3 H), 4.44 (s, 2 H), 7.03 (m, 2 H), 7.88 (s, 1 H), 8.10 (m, 2 H), 8.91 (s, 1 H). ^{13}C NMR (100 MHz, DMSO-D_6) δ 21.0 (CH_3), 43.8 (CH_2), 55.2 (CH_3), 109.9 (CH), 114.1 (CH), 128.1 (CH), 130.9 (C), 135.2 (C), 141.4 (C), 153.5 (C), 160.2 (C), 168.9 (C).

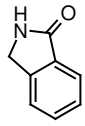

115

115; Prepared according to the Method A; colorless solid; 90% yield, C_8H_7NO, M = 133.15 g/mol, HPLC-ESI-MS: $[M + H]^+$ = 134 *m/z*. ^{1}H NMR (400 MHz, $CDCl_3$) δ 4.46 (s, 2 H), 7.47 (m, 2 H), 7.56 (m, 1 H), 7.68 (s, 1 H), 7.87 (m, 1 H). ^{13}C NMR (100 MHz, DMSO-D_6) δ 45.7 (CH_2), 123.2 (CH), 123.7 (CH), 128.0 (CH), 131.7 (CH), 132.1 (C), 143.6 (C), 172.1 (C).

Synthesis of 118:

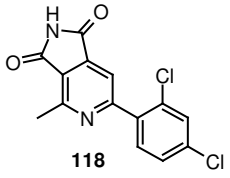

118

Iodine (1 eq, 1 mmol, 0.254 g), TFA (3 eq, 3 mmol, 0.222 mL), and *t*-BuI (0.4 eq, 0.4 mmol, 0.053 mL) were added to a solution of pyrrolopyridine **103b** (1 eq, 1 mmol, 0.293 g) in

DMSO (2 mL). The mixture was heated at 120 ˚C for 3 h. After cooling to room temperature an aqueous solution of $Na_2S_2O_3$ (0.1 M, 10 mL). The precipitate was filtered, washed with water, MeOH and DCM and air dried to give the product as a pale solid (0.211 g, 69%). $C_{14}H_8Cl_2N_2O_2$, M = 307.14 g/mol, HPLC-ESI-MS: $[M + H]^+$ = 307 *m/z*. ^{1}H NMR (400 MHz, DMSO-D_6) δ 2.80 (s, 3 H), 7.56 (m, 1 H), 7.65 (m, 1 H), 7.76 (m, 1 H), 7.86 (s, 1 H), 11.66 (s, 1 H). ^{13}C NMR (100 MHz, DMSO-D_6) δ 20.6 (CH_3), 115.4 (CH), 122.8 (C), 127.8 (CH), 129.6 (CH), 132.3 (C), 133.1 (CH), 134.8 (C), 136.6 (C), 141.4 (C), 155.8 (C), 159.8 (C), 167.7 (C), 169.2 (C).

6. 1. 2. 13 Synthesis of 5-aminomethyl-pyridines 120.

6. 1. 2. 13. 1. Route A.

General procedure for the synthesis of 123: These compounds were prepared according to the procedure for **116** (Method B-1b), using compounds **74** as a starting material.

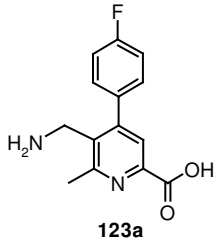

123a

123a; orange solid; 52% yield, $C_{14}H_{13}FN_2O_2$, M = 260.27 g/mol, HPLC-ESI-MS: $[M + H]^+$ = 261 *m/z*.

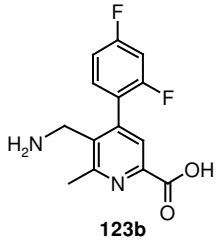

123b

123b; pale solid; 69% yield, $C_{14}H_{12}F_2N_2O_2$, M = 278.26 g/mol, HPLC-ESI-MS: $[M + H]^+$ = 279 *m/z*.

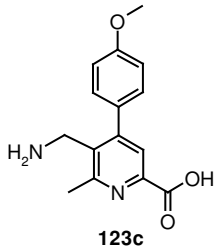

123c

123c; pale solid; 72% yield, $C_{15}H_{16}N_2O_3$, M = 272.31 g/mol, HPLC-ESI-MS: $[M + H]^+$ = 273 *m/z*.

General procedure for the synthesis of 124 - Boc-protection: Boc_2O (1.5 eq, 0.225 mmol, 0.049 g) was added to a solution of **123** (1 eq, 0.15 mmol, 0.041 g) in dioxane/water (10:1, 5.5 mL) and the mixture was stirred for 16 h. The solvent was removed under reduced pressure and the product was isolated by column chromatography with DCM/MeOH (40:1) as eluent.

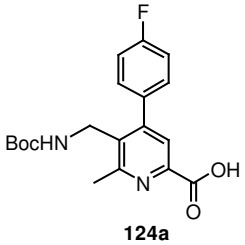

124a

124a; colorless solid; 68% yield, $C_{19}H_{21}FN_2O_4$, M = 360.39 g/mol, HPLC-ESI-MS: $[M + H]^+$ = 361 *m/z*.

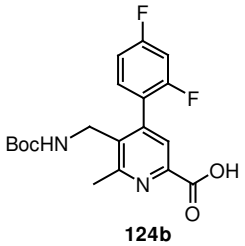

124b

124b; colorless solid; 62% yield, $C_{19}H_{20}F_2N_2O_4$, M = 378.38 g/mol, HPLC-ESI-MS: $[M + H]^+$ = 379 *m/z*.

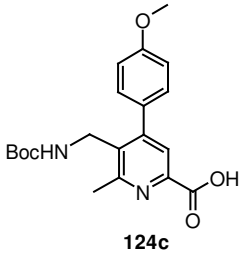

124c

124c; colorless solid; 79% yield, $C_{20}H_{24}N_2O_5$, M = 372.43 g/mol, HPLC-ESI-MS: $[M + H]^+$ = 373 *m/z*.

General procedure for the synthesis of 125: These compounds were prepared according to the procedure for **94** and **99**, using compounds **124** as a starting material.

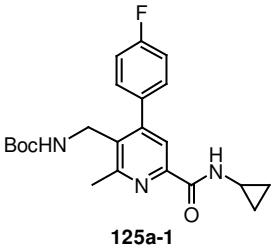

125a-1

125a-1; colorless solid; 57% yield, $C_{22}H_{26}FN_3O_3$, M = 399.47 g/mol, HPLC-ESI-MS: $[M + H]^+$ = 400 *m/z*. ^{1}H NMR (400 MHz, $CDCl_3$) δ 0.66 (m, 2 H), 0.86 (m, 2 H), 1.39 (s, 9 H), 2.64 (s, 3 H), 2.91 (m, 1 H), 4.27 (d, J = 4.6 Hz, 2 H), 4.62 (s, 1 H), 7.11 (m, 2 H), 7.23 (m, 2 H), 7.81 (s, 1 H), 8.07 (s, 1 H). ^{13}C NMR (100 MHz, $CDCl_3$) δ 6.5 (CH_2), 22.7 (CH_3), 23.9 (CH), 28.3 (CH_3), 39.0 (CH_2), 79.8 (C), 115.7 (d, $^2J_{C\text{-}F}$ = 22.0 Hz, CH), 121.1 (CH), 130.2 (d, $^3J_{C\text{-}F}$ = 8.05 Hz, CH), 131.7 (C), 134.2 (d, $^4J_{C\text{-}F}$ = 3.7 Hz, C), 147.5 (C), 151.0 (C), 155.2 (C), 157.8 (C), 162.8 (d, $^1J_{C\text{-}F}$ =248.8, C), 165.5 (C).

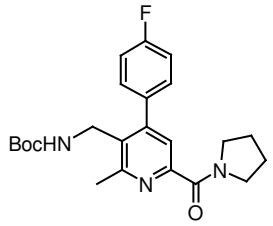

125a-2

125a-2; colorless solid; 92% yield, $C_{23}H_{28}FN_3O_3$, M = 413.50 g/mol, HPLC-ESI-MS: $[M + H]^+ = 414$ *m/z*.

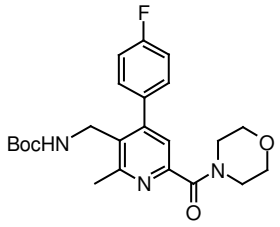

125a-3

125a-3; colorless solid; 84% yield, $C_{23}H_{28}FN_3O_4$, M = 429.50 g/mol, HPLC-ESI-MS: $[M + H]^+ = 430$ *m/z*.

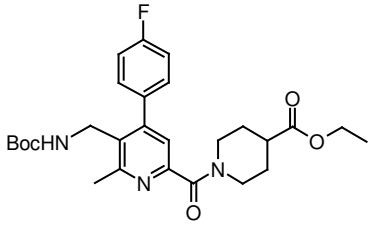

125a-4

125a-4; colorless solid; 92% yield, $C_{30}H_{34}FN_3O_5$, M = 499.59 g/mol, HPLC-ESI-MS: $[M + H]^+ = 501$ *m/z*.

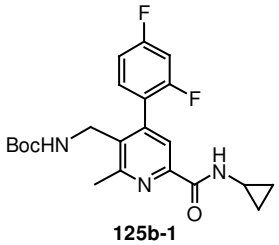

125b-1

125b-1; colorless solid; 46% yield, $C_{22}H_{25}F_2N_3O_3$, M = 417.46 g/mol, HPLC-ESI-MS: $[M + H]^+ = 418$ *m/z*.

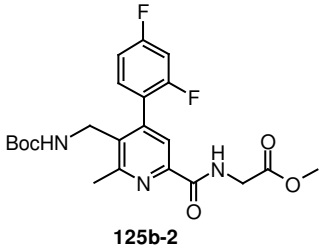

125b-2

125b-2; colorless solid; 67% yield, $C_{22}H_{25}F_2N_3O_5$, M = 449.46 g/mol, HPLC-ESI-MS: $[M + H]^+ = 450$ *m/z*.

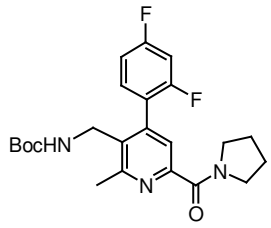

125b-3

125b-3; colorless solid; 92% yield, $C_{23}H_{27}F_2N_3O_3$, M = 431.49 g/mol, HPLC-ESI-MS: $[M + H]^+$ = 432 *m/z*.

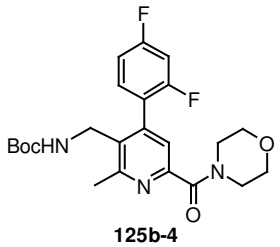

125b-4

125b-4; colorless solid; 91% yield, $C_{23}H_{27}F_2N_3O_4$, M = 447.49 g/mol, HPLC-ESI-MS: $[M + H]^+$ = 448 *m/z*.

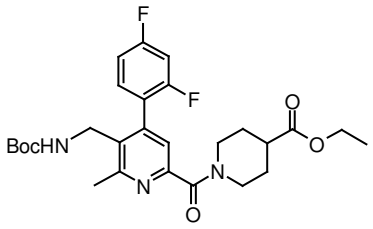

125b-5

125b-5; colorless solid; 76% yield, $C_{27}H_{33}F_2N_3O_5$, M = 517.58 g/mol, HPLC-ESI-MS: $[M + H]^+$ = 519 *m/z*.

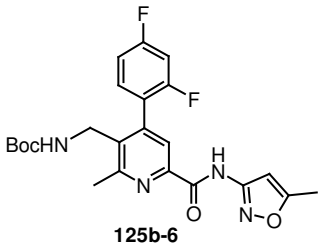

125b-6

125b-6; colorless solid; 58% yield, $C_{23}H_{24}F_2N_4O_4$, M = 458.47 g/mol, HPLC-ESI-MS: $[M + H]^+$ = 459 *m/z*.

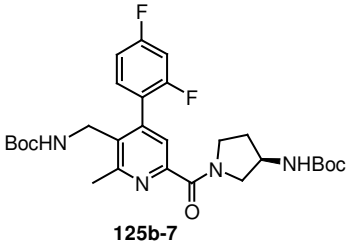

125b-7

125b-7; colorless solid; 92% yield, $C_{29}H_{37}F_2N_3O_5$, M = 545.64 g/mol, HPLC-ESI-MS: $[M + H]^+$ = 547 *m/z*.

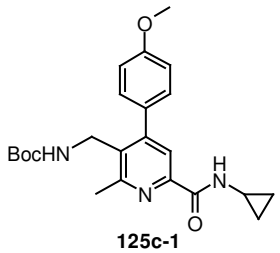

125c-1

125c-1; colorless solid; 74% yield, $C_{23}H_{29}N_3O_4$, M = 411.51 g/mol, HPLC-ESI-MS: $[M + H]^+$ = 412 *m/z*.

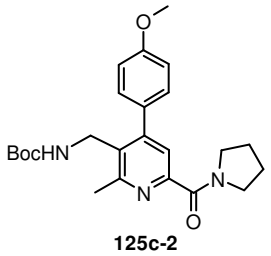

125c-2

125c-2; colorless solid; 72% yield, $C_{24}H_{31}N_3O_4$, M = 425.53 g/mol, HPLC-ESI-MS: $[M + H]^+$ = 426 *m/z*.

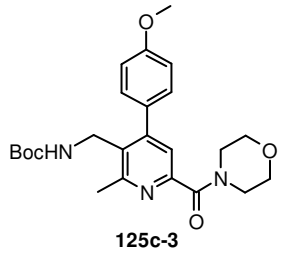

125c-3

125c-3; colorless solid; 92% yield, $C_{24}H_{31}N_4O_5$, M = 441.43 g/mol, HPLC-ESI-MS: $[M + H]^+$ = 442 *m/z*.

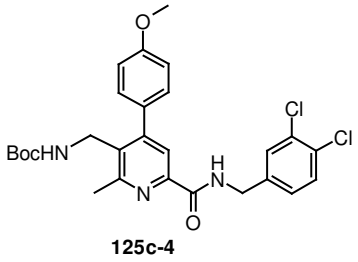

125c-4

125c-4; colorless solid; 88% yield, $C_{27}H_{29}Cl_2N_3O_4$, M = 530.46 g/mol, HPLC-ESI-MS: $[M + H]^+$ = 531 *m/z*.

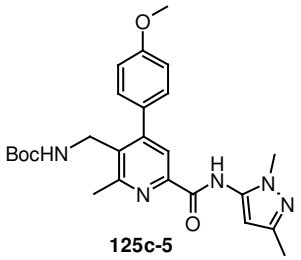

125c-5

125c-5; colorless solid; 62% yield, $C_{25}H_{31}N_5O_4$, M = 465.56 g/mol, HPLC-ESI-MS: $[M + H]^+$ = 467 *m/z*.

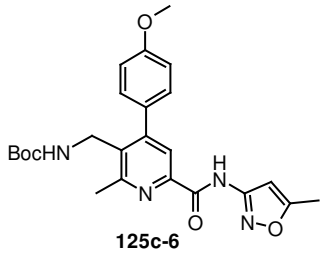

125c-6

125c-6; colorless solid; 57% yield, $C_{24}H_{28}N_4O_5$, M = 452.52 g/mol, HPLC-ESI-MS: $[M + H]^+$ = 454 *m/z*. ^{1}H NMR (400 MHz, $CDCl_3$) δ 1.41 (s, 9 H), 2.42 (s, 3 H), 2.66 (s, 3 H), 3.84 (s, 3 H), 4.33 (d, J = 4.3 Hz, 2 H), 4.61 (s, 1 H), 6.85 (s, 1 H), 6.95 (m, 2 H), 7.20 (m, 2 H), 7.88 (s, 1 H), 10.50 (s, 1 H). ^{13}C NMR (100 MHz, $CDCl_3$) δ 12.7 (CH_3), 22.5 (CH_3), 28.3 (CH_3), 39.1 (CH_2), 55.3 (CH_3), 79.7 (C), 96.0 (CH), 114.2 (CH), 121.8 (CH), 129.7 (CH), 130.1 (C), 132.8 (C), 146.0 (C), 152.0 (C), 155.0 (C), 157.6 (C), 158.3 (C), 159.8 (C), 162.1 (C), 170.0 (C).

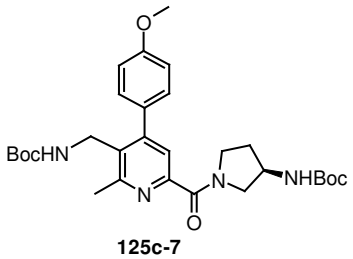

125c-7

125c-7; colorless solid; 89% yield, $C_{30}H_{41}N_3O_6$, M = 539.68 g/mol, HPLC-ESI-MS: $[M + H]^+$ = 541 *m/z*.

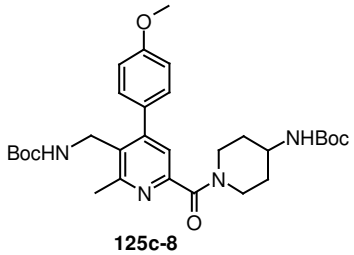

125c-8

125c-8; colorless solid; 53% yield, $C_{30}H_{42}N_4O_4$, M = 554.70 g/mol, HPLC-ESI-MS: $[M + H]^+$ = 556 *m/z*.

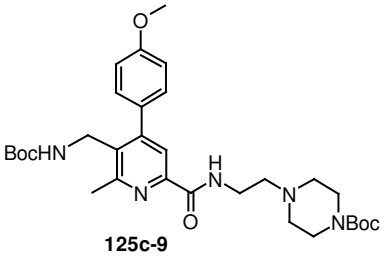

125c-9

125c-9; colorless solid; 92% yield, $C_{32}H_{46}N_4O_6$, M = 539.68 g/mol, HPLC-ESI-MS: $[M + H]^+$ = 541 *m/z*.

General procedure for the synthesis of 120 - deprotection: The Boc - protected aminomethyl-pyridine **125** (0.10 mmol) was treated with 25% TFA/DCM (5 mL) at rt. After 1 h the solvent was removed under reduced pressure, the residue was taken up in water and extracted with DCM/EA. The combined organic phases were dried over anhydrous Na_2SO_4 and concentrated. The product was isolated by column chromatography with DCM/MeOH (40:1) as eluent.

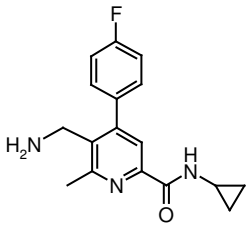

120a-1

120a-1; colorless solid; 99% yield, $C_{17}H_{18}FN_3O$, M = 299.35 g/mol, HPLC-ESI-MS: $[M + H]^+$ = 300 *m/z*. ^{1}H NMR (400 MHz, Methanol-D_4) δ 0.55 (m, 2 H), 0.70 (m, 2 H), 2.62 (s, 3 H), 2.74 (m, 1 H), 3.98 (s, 2 H), 7.13 (m, 2 H), 7.28 (m, 2 H), 7.65 (s, 1 H). ^{13}C NMR (100 MHz, Methanol-D_4) δ 6.7 (CH_2), 22.8 (CH_3), 23.6 (CH), 38.2 (CH_2), 117.0 (d, $^2J_{C\text{-}F}$ = 22.7 Hz, CH), 122.2 (CH), 131.2 (C), 131.9 (d, $^3J_{C\text{-}F}$ = 8.1 Hz, CH), 135.3 (d, $^4J_{C\text{-}F}$ = 2.9 Hz, C), 149.8 (C), 153.1 (C), 159.8 (C), 164.5 (d, $^1J_{C\text{-}F}$ =247.4 Hz, C), 167.7 (C). FT-ICR-MS: calculated for $C_{17}H_{18}FN_3OH^+$: 300.1507, found: 300.1505.

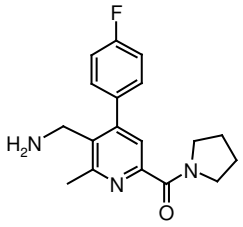

120a-2

120a-2; colorless solid; 95% yield, $C_{18}H_{20}FN_3O$, M = 313.38 g/mol, HPLC-ESI-MS: $[M + H]^+$ = 314 *m/z*. ^{1}H NMR (400 MHz, Methanol-D_4) δ 1.96 (m, 4 H), 2.74 (s, 3 H), 3.61 (m, 2 H), 3.69 (m, 2 H), 3.95 (s, 2 H), 7.25 (m, 2 H), 7.44 (m, 3 H). ^{13}C NMR (100 MHz, Methanol-D_4) δ 22.5 (CH_3), 25.0 (CH_2), 27.3 (CH_2), 39.1 (CH_2), 47.9 (CH_2), 50.3 (CH_2), 116.8 (d, $^2J_{C\text{-}F}$ = 22.0 Hz, CH), 123.5 (CH), 131.9 (d, $^3J_{C\text{-}F}$ = 8.8 Hz, CH), 132.9 (C), 135.6 (d, $^4J_{C\text{-}F}$ = 2.9 Hz, C), 152.3 (C), 153.6 (C), 159.2 (C), 164.4 (d, $^1J_{C\text{-}F}$ = 247.4 Hz, C), 168.2 (C). FT-ICR-MS: calculated for $C_{18}H_{20}FN_3OH^+$: 314.1663, found: 314.1662.

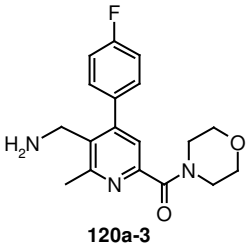

120a-3

120a-3; colorless solid; 89% yield, $C_{18}H_{20}FN_3O_2$, M = 329.38 g/mol, HPLC-ESI-MS: $[M + H]^+$ = 330 *m/z*. ^{1}H NMR (400 MHz, $CDCl_3$) δ 2.70 (s, 3 H), 3.68 (s, 2 H), 3.79 (m, 6 H), 7.12 (m, 2 H), 7.35 (m, 3 H). ^{13}C NMR (100 MHz, $CDCl_3$) δ 22.5 (CH_3), 39.8 (CH_2), 42.7 (CH_2), 47.8 (CH_2), 66.8 (CH_2), 67.0 (CH_2), 115.5 (d, $^2J_{C\text{-}F}$ = 21.2 Hz, CH), 123.0 (CH), 130.3 (d, $^3J_{C\text{-}F}$ = 8.1 Hz, CH), 134.2 (C), 134.5 (d, $^4J_{C\text{-}F}$ = 3.7 Hz, C), 150.0 (C), 151. 0 (C), 157.1 (C), 162.7 (d, $^1J_{C\text{-}F}$ = 248.1 Hz, C), 167.4 (C). FT-ICR-MS: calculated for $C_{18}H_{20}FN_3O_2H^+$: 330.1612, found: 330.1611.

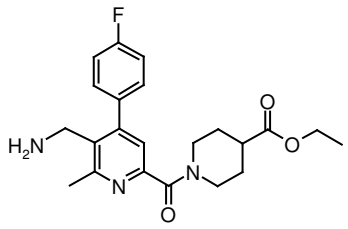

120a-4

120a-4; colorless solid; 99% yield, $C_{22}H_{26}FN_3O_3$, M = 399.47 g/mol, HPLC-ESI-MS: $[M + H]^+$ = 400 *m/z*. ^{1}H NMR (400 MHz, $CDCl_3$) δ 1.29 (m, 3 H), 1.82 (m, 3 H), 2.07 (m, 3 H), 2.59 (m, 1 H), 2.72 (s, 3 H), 3.05 (m, 1 H), 3.21 (m, 1 H), 3.83 (s, 2 H), 3.98 (m, 1 H), 4.16 (q, J = 7.1 Hz, 2 H), 4.53 (m, 1 H), 7.14 (m, 2 H), 7.28 (s, 1 H), 7.37 (m, 2 H). ^{13}C NMR (100 MHz, $CDCl_3$) δ 14.1 (CH_3), 22.4 (CH_3), 27.7 (CH_2), 28.4 (CH_2), 39.6 (CH_2), 41.0 (CH), 41.6 (CH_2), 46.5 (CH_2), 60.6 (CH_2), 115.5 (d, $^2J_{C\text{-}F}$ = 21.2 Hz, CH), 122.2 (CH), 130.3 (d, $^3J_{C\text{-}F}$ = 8.1 Hz, CH), 133.5 (C), 134.5 (d, $^4J_{C\text{-}F}$ = 3.7 Hz, C), 149.9 (C), 151.7 (C), 157.3 (C), 162.6 (d, $^1J_{C\text{-}F}$ = 248.1 Hz, C), 167.5 (C), 174.1 (C). FT-ICR-MS: calculated for $C_{22}H_{26}FN_3O_3H^+$: 400.2031, found: 400.2032.

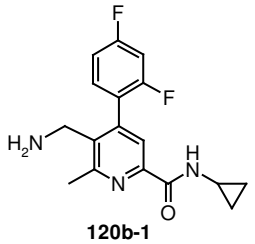

120b-1

120b-1; colorless solid; 86% yield, $C_{17}H_{17}F_2N_3O$, M = 317.34 g/mol, HPLC-ESI-MS: $[M + H]^+$ = 318 *m/z*. ^{1}H NMR (400 MHz, Methanol-D_4) δ 0.70 (m, 2 H), 0.86 (m, 2 H), 2.78 (s, 3 H), 2.89 (m, 1 H), 4.15 (s, 2 H), 7.20 (m, 2 H), 7.45 (m, 1 H), 7.84 (s, 1 H). FT-ICR-MS: calculated for $C_{17}H_{17}F_2N_3OH^+$: 318.1413, found: 318.1412.

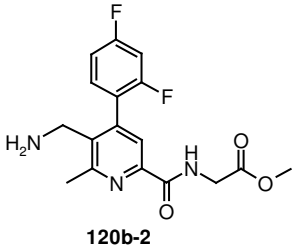

120b-2

120b-2; colorless solid; 99% yield, $C_{17}H_{17}F_2N_3O_3$, M = 349.34 g/mol, HPLC-ESI-MS: $[M + H]^+$ = 350 *m/z*. ^{1}H NMR (400 MHz, $CDCl_3$) δ 2.73 (s, 3 H), 3.74 (s, 2 H), 3.78 (s, 3 H), 4.26 (d, J = 5.59 Hz, 1 H), 6.95 (m, 2 H), 7.23 (m, 1 H), 7.85 (s, 1 H), 8.52 (t, J = 5.47 Hz, 1 H). FT-ICR-MS: calculated for $C_{17}H_{17}F_2N_3O_3H^+$: 350.1311, found: 350.1309.

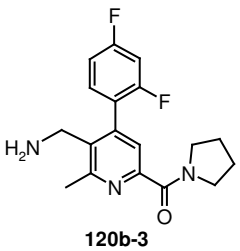

120b-3

120b-3; colorless solid; 95% yield, $C_{18}H_{19}F_2N_3O$, M = 331.37 g/mol, HPLC-ESI-MS: $[M + H]^+$ = 332 *m/z*.

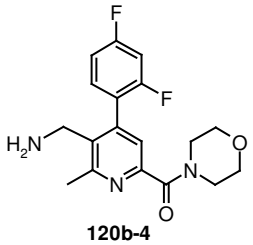

120b-4

120b-4; colorless solid; 91% yield, $C_{18}H_{19}F_2N_3O_2$, M = 347.37 g/mol, HPLC-ESI-MS: $[M + H]^+$ = 348 *m/z*. ^{1}H NMR (400 MHz, $CDCl_3$) δ 2.66 (s, 3 H), 3.69 (m, 10 H), 6.90 (m, 2 H), 7.22 (m, 2 H).

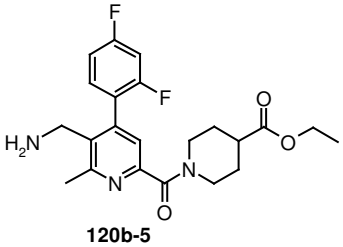

120b-5

120b-5; yellow solid; 89% yield, $C_{22}H_{25}F_2N_3O_3$, M = 417.46 g/mol, HPLC-ESI-MS: $[M + H]^+$ = 418 *m/z*.

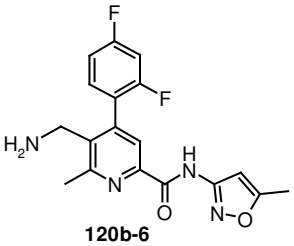

120b-6

120b-6; colorless solid; 98% yield, $C_{18}H_{16}F_2N_4O_2$, M = 358.35 g/mol, HPLC-ESI-MS: $[M + H]^+$ = 359 *m/z*. ^{1}H NMR (400 MHz, Methanol-D_4) δ 2.44 (s, 3 H), 2.85 (s, 3 H), 4.19 (s, 2 H), 6.77 (s, 1 H), 7.23 (m, 2 H), 7.48 (m, 1 H), 7.98 (s, 1 H). FT-ICR-MS: calculated for $C_{18}H_{16}F_2N_4O_2H^+$: 359.1314, found: 359.1311.

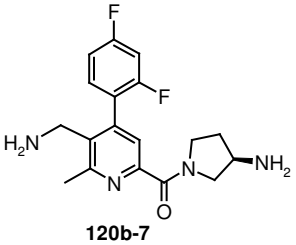

120b-7

120b-7; pale solid; 92% yield, $C_{18}H_{20}F_2N_4O$, M = 346.38 g/mol, HPLC-ESI-MS: $[M + H]^+$ = 346 *m/z*.

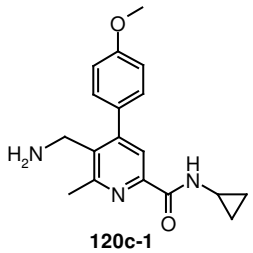

120c-1

120c-1; colorless solid; 87% yield, $C_{18}H_{21}N_3O_2$, M = 311.39 g/mol, HPLC-ESI-MS: $[M + H]^+$ = 312 *m/z*. FT-ICR-MS: calculated for $C_{18}H_{21}N_3O_2H^+$: 312.1707, found: 312.1708.

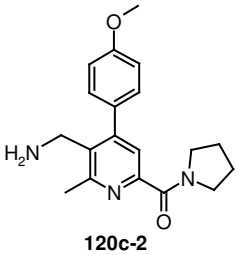

120c-2

120c-2; colorless solid; 78% yield, $C_{19}H_{23}N_3O_2$, M = 325.41 g/mol, HPLC-ESI-MS: $[M + H]^+$ = 326 *m/z*. FT-ICR-MS: calculated for $C_{19}H_{23}N_3O_2H^+$: 326.1863, found: 326.1864.

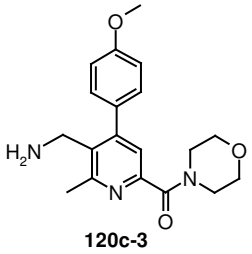

120c-3

120c-3; colorless solid; 99% yield, $C_{19}H_{23}N_3O_3$, M = 341.41 g/mol, HPLC-ESI-MS: $[M + H]^+$ = 342 *m/z*. ^{1}H NMR (400 MHz, $CDCl_3$) δ 2.63 (s, 3 H), 3.73 (m, 13 H), 6.91 (m, 2 H), 7.23 (m, 3 H). FT-ICR-MS: calculated for $C_{19}H_{23}N_3O_3H^+$: 342.1812, found: 342.1811.

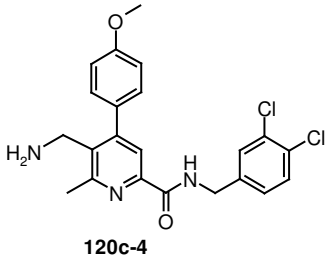

120c-4

120c-4; colorless solid; 99% yield, $C_{22}H_{21}Cl_2N_3O_2$, M = 430.34 g/mol, HPLC-ESI-MS: $[M + H]^+$ = 431 *m/z*. ^{1}H NMR (400 MHz, $CDCl_3$) δ 2.70 (s, 3 H), 3.86 (s, 3 H), 4.62 (d, *J* = 6.4 Hz, 2 H), 6.98 (m, 2 H), 7.21 (m, 1 H), 7.29 (m, 2 H), 7.42 (m, 2 H), 7.94 (s, 1 H), 8.54 (t, *J* = 6.2 Hz, 1 H). ^{13}C NMR (100 MHz, $CDCl_3$) δ 22.5 (CH_3), 39.8 (CH_2), 42.2 (CH_2), 55.3 (CH_3), 114.0 (CH), 121.8 (CH), 127.1 (CH), 129.6 (CH), 129.7 (CH), 130.5 (CH), 130.8 (C), 131.3 (C), 132.6 (C), 138.8 (C), 146.7 (C), 151.1 (C), 157.0 (C), 159.7 (C), 164.6 (C). FT-ICR-MS: calculated for $C_{22}H_{21}Cl_2N_3O_2H^+$: 430.1084, found: 430.1084.

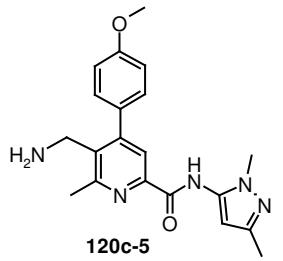

120c-5

120c-5; colorless solid; 68% yield, $C_{20}H_{23}N_5O_2$, M = 365.44 g/mol, HPLC-ESI-MS: $[M + H]^+$ = 366 *m/z*.

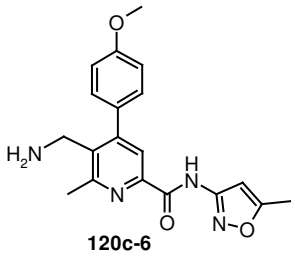

120c-6

120c-6; colorless solid; 87% yield, $C_{19}H_{20}N_4O_3$, M = 352.40 g/mol, HPLC-ESI-MS: $[M + H]^+$ = 353 *m/z*. ^{1}H NMR (400 MHz, Methanol-D_4) δ 2.43 (s, 3 H), 2.95 (s, 3 H), 3.88 (s, 3 H), 4.41 (s, 2 H), 6.73 (s, 1 H), 7.14 (m, 2 H), 7.47 (m, 2 H), 8.16 (s, 1 H). ^{13}C NMR (100 MHz, Methanol-D_4) δ 12.4 (CH_3), 21.5 (CH_3), 37.7 (CH_2), 56.1 (CH_3), 97.4 (CH), 115.9 (CH), 124.7 (CH), 129.6 (C), 131.5 (CH), 146.3 (C), 158.1 (C), 158.9 (C), 159.7 (C), 161.5 (C), 162.5 (C), 171.9 (C). FT-ICR-MS: calculated for $C_{19}H_{20}N_4O_3H^+$: 353.1608, found: 353.1608.

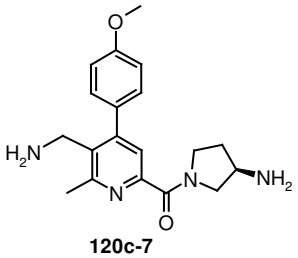

120c-7

120c-7; colorless solid; 82% yield, $C_{19}H_{24}N_4O_2$, M = 340.43 g/mol, HPLC-ESI-MS: $[M + H]^+$ = 340 *m/z*.

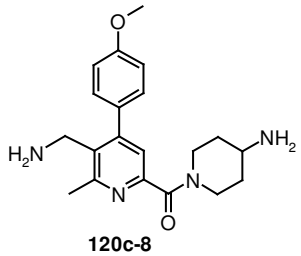

120c-8

120c-8; colorless solid; 79% yield, $C_{20}H_{26}N_4O_2$, M = 354.46 g/mol, HPLC-ESI-MS: $[M + H]^+$ = 355 *m/z*. FT-ICR-MS: calculated for $C_{20}H_{26}N_4O_2H^+$: 355.2129, found: 355.2128.

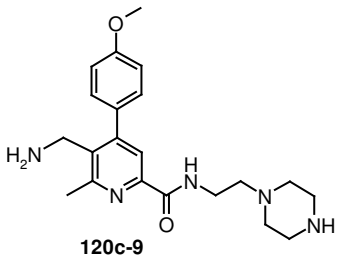

120c-9

120c-9; colorless solid; 88% yield, $C_{21}H_{29}N_5O_2$, M = 383.50 g/mol, HPLC-ESI-MS: $[M + H]^+$ = 383 *m/z*.

6. 1. 2. 13. 2 Route B.

Raney Nickel (6 mL, 50% slurry in water) was added to a solution of **94** (1 eq, 0.15 mmol, 0.048 g) in AcOH (5 mL). Upon disappearance of the starting material (3-24 h), the catalyst was filtered off through celite and the solvent was removed under reduced pressure. The residue was taken up in water, using 4M NaOH the solution was adjusted to pH = 8 and extracted with DCM/EA. The product, a colorless solid was purified by column chromatography with DCM/MeOH (10:1) as eluent.

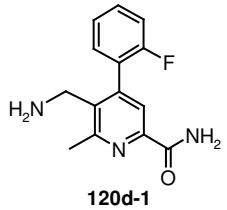

120d-1

120d-1; colorless solid; 64% yield, $C_{14}H_{14}FN_3O$, M = 259.29 g/mol, HPLC-ESI-MS: $[M + H]^+$ = 260 *m/z*. ^{1}H NMR (400 MHz, $CDCl_3$) δ 1.35 (s, 2 H), 2.75 (s, 3 H), 3.76 (s, 2 H), 5.98 (s, 1 H), 7.21 (m, 3 H), 7.41 (m, 1 H), 7.93 (m, 2 H). ^{13}C NMR (100 MHz, $CDCl_3$) δ 22.5 (CH_3), 40.7 (CH_2), 115.7 (d, $^2J_{C\text{-}F}$ = 22.0 Hz, CH), 122.0 (CH), 124.5 (d, $^3J_{C\text{-}F}$ = 3.7 Hz, CH), 126.1 (d, $^2J_{C\text{-}F}$ = 16.8 Hz, C), 130.4 (d, $^3J_{C\text{-}F}$ = 8.8 Hz, CH), 130.8 (d, $^4J_{C\text{-}F}$ = 2.9 Hz, CH), 137.6 (C), 144.7 (C), 146.9 (C), 157.1 (C), 158.9 (d, $^1J_{C\text{-}F}$ = 245.2 Hz, C), 166.8 (C).

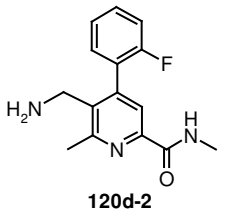

120d-2

120d-2; pale solid; 70% yield, $C_{15}H_{16}FN_3O$, M = 273.31 g/mol, HPLC-ESI-MS: $[M + H]^+$ = 274 *m/z*.

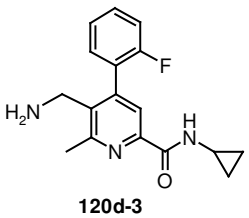

120d-3

120d-3; colorless solid; 53% yield, $C_{17}H_{18}FN_3O$, M = 299.35 g/mol, HPLC-ESI-MS: $[M + H]^+$ = 300 *m/z*. ^{1}H NMR (400 MHz, $CDCl_3$) δ 0.64 (m, 2 H), 0.83 (m, 2 H), 1.50 (s, 2 H), 2.67 (s, 3 H), 2.88 (m, 1 H), 3.69 (s, 2 H), 7.12 (m, 1 H), 7.19 (m, 2 H), 7.37 (m, 1 H), 7.86 (s, 1 H), 8.10 (s, 1 H).^{13}C NMR (100 MHz, $CDCl_3$) δ 6.5 (CH_2), 22.3 (CH_3), 22.4 (CH), 40.6 (CH_2), 116.2 (d, $^2J_{C\text{-}F}$ = 22.0 Hz, CH), 121.4 (CH), 124.4 (d, $^3J_{C\text{-}F}$ = 3.7 Hz, CH), 126.1 (d, $^2J_{C\text{-}F}$ = 16.8 Hz, C), 130.3 (d, $^3J_{C\text{-}F}$ = 8.1 Hz, CH), 130.8 (d, $^4J_{C\text{-}F}$ = 2.9 Hz, CH), 137.1 (C), 144.7 (C), 147.1 (C), 156.7 (C), 158.9 (d, $^1J_{C\text{-}F}$ = 245.9 Hz, C), 165.5 (C).

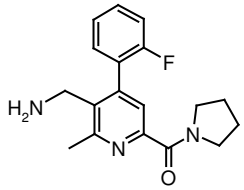

120d-4

120d-4; colorless solid; 48% yield, $C_{18}H_{20}FN_3O$, M = 313.38 g/mol, HPLC-ESI-MS: $[M + H]^+$ = 314 *m/z*. ^{1}H NMR (400 MHz, $CDCl_3$) δ 1.90 (m, 6 H), 2.70 (s, 3 H), 3.63 (m, 2 H), 3.74 (m, 4 H), 7.13 (m, 1 H), 7.22 (m, 2 H), 7.38 (m, 1 H), 7.47 (s, 1 H). ^{13}C NMR (100 MHz, $CDCl_3$) δ 22.4 (CH_3), 24.0 (CH_2), 26.5 (CH_2), 40.5 (CH_2), 46.8 (CH_2), 49.1 (CH_2), 115.7 (d, $^2J_{C\text{-}F}$ = 21.96 Hz, CH), 123.0 (CH), 124.4 (d, $^3J_{C\text{-}F}$ = 3.7 Hz, CH), 126.2 (d, $^2J_{C\text{-}F}$ = 16.8 Hz, C), 130.3 (d, $^3J_{C\text{-}F}$ = 8.8 Hz, CH), 130.9 (d, $^4J_{C\text{-}F}$ = 3.7 Hz, CH), 135.1 (C), 144.3 (C), 152.0 (C), 156.6 (C), 158.9 (d, $^1J_{C\text{-}F}$ = 245.9 Hz, C), 166.3 (C).

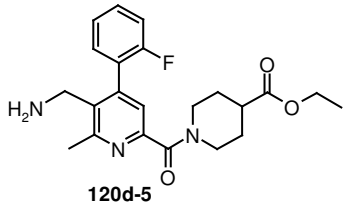

120d-5

120d-5; colorless solid; 25% yield, $C_{22}H_{26}FN_3O_3$, M = 399.47 g/mol, HPLC-ESI-MS: $[M + H]^+$ = 400 *m/z*. FT-ICR-MS: calculated for $C_{22}H_{26}FN_3O_3H^+$: 400.2031, found: 400.2030.

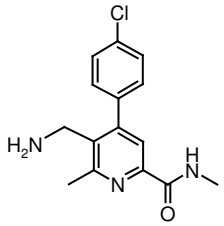

120e

120e; colorless solid; 38% yield, $C_{15}H_{16}ClN_3O$, M = 289.77 g/mol, HPLC-ESI-MS: $[M + H]^+$ = 290 *m/z*. FT-ICR-MS: calculated for $C_{15}H_{16}ClN_3OH^+$: 290.1055, found: 290.1054.

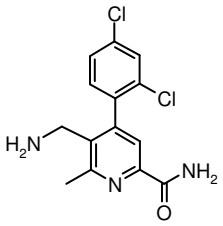

120f-1

120f-1; colorless solid; 45% yield, $C_{14}H_{13}Cl_2N_3O$, M = 310.19 g/mol, HPLC-ESI-MS: [M + H]$^+$ = 310 *m/z*. ^{1}H NMR (400 MHz, DMSO-D_6) δ 2.72 (s, 3 H), 3.38 (d, *J* = 13.2 Hz, 1 H), 3.63 (d, *J* = 13.2 Hz, 1 H), 7.49 (d, *J* = 8.1 Hz, 1 H), 7.54 (m, 1 H), 7.57 (s, 1 H), 7.67 (s, 1 H), 7.78 (d, *J* = 1.5 Hz, 1 H), 8.06 (s, 1 H). ^{13}C NMR (100 MHz, DMSO-D_6) δ 22.3 (CH_3), 39.8 (CH_2), 120.5 (CH), 127.5 (CH), 128.9 (CH), 132.1 (CH), 132.6 (C), 133.9 (C), 136.1 (C), 136.8 (C), 146.3 (C), 147.4 (C), 157.7 (C), 165.8 (C). FT-ICR-MS: calculated for $C_{14}H_{13}Cl_2N_3OH^+$: 310.0508, found: 310.0508.

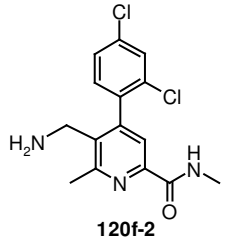

120f-2

120f-2; colorless solid; 51% yield, $C_{15}H_{15}Cl_2N_3O$, M = 324.21 g/mol, HPLC-ESI-MS: [M + H]$^+$ = 324 *m/z*. ^{1}H NMR (400 MHz, $CDCl_3$) δ 2.71 (s, 3 H), 3.02 (d, *J* = 5.1 Hz, 3 H), 3.60 (d, *J* = 13.5 Hz, 1 H), 3.71 (d, *J* = 13.5 Hz, 1 H), 7.14 (d, *J* = 8.4 Hz, 1 H), 7.32 (dd, *J* = 8.1, 2.03 Hz, 1 H), 7.50 (d, *J* = 2.0 Hz, 1 H), 7.79 (s, 1 H), 8.07 (s, 1 H). ^{13}C NMR (100 MHz, $CDCl_3$) δ 22.4 (CH_3), 26.1 (CH_3), 40.4 (CH_2), 121.0 (CH), 127.3 (CH), 129.6 (CH), 131.1 (CH), 133.3 (C), 135.0 (C), 136.1 (C), 136.6 (C), 147.1 (C), 147.4 (C), 157.0 (C), 164.8 (C). FT-ICR-MS: calculated for $C_{15}H_{15}Cl_2N_3OH^+$: 324.0665, found: 324.0666.

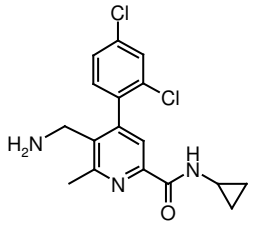

120f-3

120f-3; colorless solid; 34% yield, $C_{17}H_{17}Cl_2N_3O$, M = 350.25 g/mol, HPLC-ESI-MS: [M + H]$^+$ = 350 *m/z*. ^{1}H NMR (400 MHz, Methanol-D_4) δ 0.69 (m, 2 H), 0.84 (m, 2 H), 2.75 (s, 3 H), 2.88 (m, 1 H), 3.61 (d, *J* = 13.7 Hz, 1 H), 3.82 (d, *J* = 14.0 Hz, 1 H), 7.37 (d, *J* = 8.1 Hz, 1 H), 7.49 (m, 1 H), 7.66 (d, *J* = 2.0 Hz, 1 H), 7.68 (s, 1 H). ^{13}C NMR (100 MHz, Methanol-D_4) δ 6.6 (CH_2), 22.6 (CH_3), 23.6 (CH), 40.0 (CH_2), 121.9 (CH), 128.9 (CH), 130.6 (CH), 132.9 (CH), 134.4 (C), 136.5 (C), 137.2 (C), 148.9 (C), 149.1 (C), 159.4 (C), 167.8 (C). FT-ICR-MS: calculated for $C_{17}H_{17}Cl_2N_3OH^+$: 350.0821, found: 350.0821.

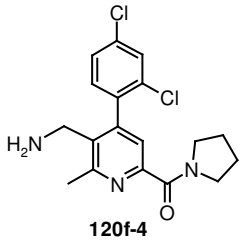

120f-4

120f-4; colorless solid; 48% yield, $C_{18}H_{19}Cl_2N_3O$, M = 364.28 g/mol, HPLC-ESI-MS: [M + H]$^+$ = 364 *m/z*. ^{1}H NMR (400 MHz, Methanol-D_4) δ 1.96 (m, 4 H), 2.75 (s, 3 H), 3.62 (t, *J* = 6.4 Hz, 2 H), 3.72 (m, 3 H), 3.98 (d, *J* = 14.2 Hz, 1 H), 7.40 (m, 2 H), 7.51 (dd, *J* = 8.4, 2.0 Hz, 1 H), 7.68 (d, *J* = 2.0 Hz, 1 H). ^{13}C NMR (100 MHz, Methanol-D_4) δ 22.5 (CH_3), 25.0 (CH_2), 27.4 (CH_2), 39.1 (CH_2), 48.0 (CH_2), 50.4 (CH_2), 123.4 (CH), 129.0 (CH), 130.7 (CH),

132.4 (C), 133.0 (CH), 134.4 (C), 136.6 (C), 136.8 (C), 149.5 (C), 154.2 (C), 159.4 (C), 167.8 (C). FT-ICR-MS: calculated for $C_{18}H_{19}Cl_2N_3OH^+$: 364.0978, found: 364.0980.

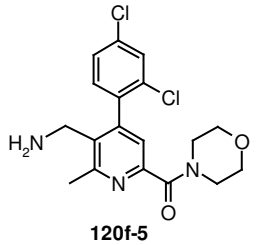

120f-5

120f-5; colorless solid; 44% yield, $C_{18}H_{19}Cl_2N_3O_2$, M = 380.28 g/mol, HPLC-ESI-MS: $[M + H]^+$ = 380.28 *m/z*. ^{1}H NMR (400 MHz, $CDCl_3$) δ 2.73 (s, 3 H), 3.70 (m, 8 H), 3.79 (s, 2 H), 7.22 (m, 2 H), 7.35 (dd, *J* = 8.1, 1.5 Hz, 1 H), 7.51 (d, *J* = 1.8 Hz, 1 H). ^{13}C NMR (100 MHz, $CDCl_3$) δ 22.5 (CH_3), 40.2 (CH_2), 42.7 (CH_2), 47.8 (CH_2), 66.7 (CH_2), 66.9 (CH_2), 122.6 (CH), 127.3 (CH), 129.6 (CH), 131.1 (CH), 133.2 (C), 135.1 (C), 135.8 (C), 146.8 (C), 151.1 (C), 157.3 (C), 167.1 (C). FT-ICR-MS: calculated for $C_{18}H_{19}Cl_2N_3O_2H^+$: 380.0927, found: 380.0928.

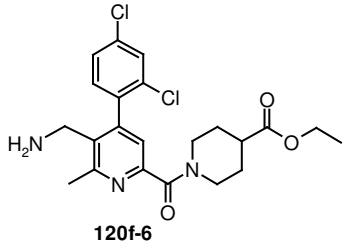

120f-6

120f-6; yellow solid; 15% yield, $C_{22}H_{25}Cl_2N_3O_3$, M = 450.37 g/mol, HPLC-ESI-MS: $[M + H]^+$ = 450 *m/z*. FT-ICR-MS: calculated for $C_{22}H_{25}Cl_2N_3O_3H^+$: 450.1346, found: 450.1349.

6. 1. 2. 13. 3 Synthesis of 120h.

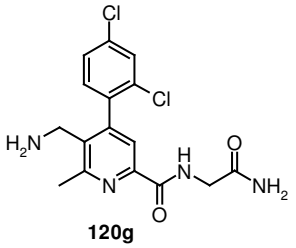

120g

120g: To the degassed solution of **94e-4** (1 eq, 0.25 mmol, 0.091 g) in acetic acid (0.25 mL) Raney Nickel (6 mL, 50% slurry in water) was added and the mixture was stirred 48 h at 50 ^{o}C under argon. The catalyst was filtered off through celite and the solvent was removed under reduced pressure. The residue was taken up in water, using 4M NaOH the solution was adjusted to pH = 8 and extracted with DCM/EA. The product, a colorless solid (0.055 g, 60%), was purified by column chromatography with DCM/MeOH (10:1) as eluent. $C_{16}H_{16}Cl_2N_4O_2$, M = 367.24 g/mol, HPLC-ESI-MS: $[M + H]^+$ = 367 *m/z*. ^{1}H NMR (400 MHz, DMSO-D_6) δ 1.09 (s, 2 H), 2.75 (s, 3 H), 3.51 (m, 2 H), 3.91 (d, *J* = 5.1 Hz, 2 H), 7.13 (s, 1 H), 7.53 (m, 4 H), 7.78 (s, 1 H), 8.77 (t, *J* = 5.1 Hz, 1 H). ^{13}C NMR (100 MHz, $CDCl_3$) δ 22.2 (CH_3), 31.3 (CH_2), 42.0 (CH_2), 120.3 (CH), 127.5 (CH), 128.9 (CH), 132.1 (CH), 133.9 (C), 136.0 (C), 146.4 (C), 146.8 (C), 157.7 (C), 163.5 (C), 170.5 (C).

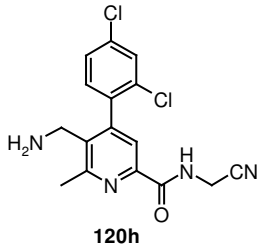

120h

120h: 120g (0.054 g, 0.15 mmol) was dissolved in $POCl_3$ (2 mL), and the mixture was heated at 70 ºC for 2 h. The excess of the reagent was removed in vacuo. The product as a yellow solid (0.037 g, 70%) was isolated by column chromatography (MeOH/DCM, 40:1). $C_{16}H_{14}Cl_2N_4O$, M = 349.22 g/mol, HPLC-ESI-MS: $[M + H]^+$ = 349 *m/z*. ^{1}H NMR (400 MHz, DMSO-D_6) δ 2.75 (s, 3 H), 3.40 (m, 1 H), 3.66 (d, J = 12.0 Hz, 1 H), 4.31 (d, J = 5.6 Hz, 2 H), 7.54 (m, 2 H), 7.60 (s, 1 H), 7.80 (m, 1 H), 9.36 (t, J = 5.7 Hz, 1 H). ^{13}C NMR (100 MHz, DMSO-D_6) δ 22.3 (CH_3), 27.7 (CH_2), 39.6 (CH_2), 117.5 (C), 120.8 (CH), 127.6 (CH), 129.0 (CH), 132.1 (CH), 132.6 (C), 134.0 (C), 135.8 (C), 137.2 (C), 146.1 (C), 146.6 (C), 158.2 (C), 164.3 (C). FT-ICR-MS: calculated for $C_{16}H_{14}Cl_2N_4OH^+$: 349.0617, found: 349.0620.

6. 1. 2. 14 Synthesis of 6-aminomethyl-pyridines 121.

General procedure for the synthesis of 126: Triethylamine (1.2 eq, 1.2 mmol, 0.167 mL) and ethyl chloroformate (1.2 eq, 1.2 mmol, 0.114 mL) were added successively to the solution of **96** eq, 1 mmol) in THF (15 mL) and the mixture was stirred at rt for 30 minutes. After decreasing the temperature to 0 ˚C, the solution of sodium borohydride (10 eq, 10 mmol, 0.378 g) in water (5 mL) was added dropwise and the mixture was stirred at 0 ˚C for additional 30 minutes. The residue was acidified with 1M HCl, concentrated in vacuo and extracted with DCM/EA. The combined organic phases were dried over anhydrous Na_2SO_4 and concentrated. The product **126** was isolated by column chromatography with DCM/MeOH (10:1) as eluent.

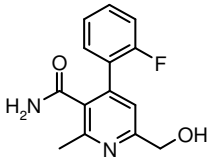

126a

126a; colorless solid; 61% yield, $C_{14}H_{13}FN_2O_2$, M = 260.27 g/mol, HPLC-ESI-MS: $[M + H]^+$ = 261 *m/z*. ^{1}H NMR (400 MHz, DMSO-D_6) δ 2.50 (s, 3 H), 4.56 (d, J = 5.6 Hz, 2 H), 5.46 (t, J = 5.9 Hz, 1 H), 7.26 (m, 3 H), 7.44 (m, 3 H), 7.79 (s, 1 H). ^{13}C NMR (100 MHz, DMSO-D_6) δ 22.3 (CH_3), 63.9 (CH_2), 115.7 (d, $^2J_{C\text{-}F}$ = 22.0 Hz, CH), 118.5 (CH), 124.1 (d, $^3J_{C\text{-}F}$ = 3.7 Hz, CH), 125.9 (d, $^2J_{C\text{-}F}$ = 15.4 Hz, C), 130.5 (d, $^3J_{C\text{-}F}$ = 8.1 Hz, CH), 130.9 (d, $^4J_{C\text{-}F}$ = 2.9 Hz, CH), 131.3 (C), 140.7 (C), 153.3 (C), 158.8 (d, $^1J_{C\text{-}F}$ =246.6, C), 160.6 (C), 169.0 (C).

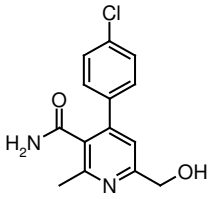

126b

126b; colorless solid; 71% yield, $C_{14}H_{13}ClN_2O_2$, M = 276.72 g/mol, HPLC-ESI-MS: $[M + H]^+$ = 277 *m/z*. ^{1}H NMR (400 MHz, DMSO-D_6) δ 2.49 (s, 3 H), 4.57 (d, J = 5.6 Hz, 2 H), 5.49 (t, J = 5.3 Hz, 1 H), 7.25 (s, 1 H), 7.53 (m, 5 H), 7.83 (s, 1 H). ^{13}C NMR (100 MHz, DMSO-D_6) δ 22.2 (CH_3), 63.95 (CH_2), 117.6 (CH), 128.5 (CH), 1230.0 (CH), 130.4 (C), 133.3 (C), 137.4 (C), 144.9 (C), 153.3 (C), 161.1 (C), 169.7 (C).

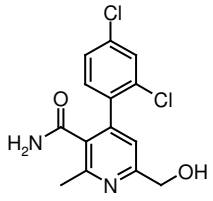

126c

126c; colorless solid; 77% yield, $C_{14}H_{12}Cl_2N_2O_2$, M = 311.17 g/mol, HPLC-ESI-MS: $[M + H]^+$ = 311 m/z. ^{1}H NMR (400 MHz, DMSO-D_6) δ 2.55 (s, 3 H), 4.63 (s, 2 H), 7.23 (s, 1 H), 7.27 (m, 1 H), 7.31 (m, 1 H), 7.50 (m, 1 H). ^{13}C NMR (100 MHz, DMSO-D_6) δ 22.2 (CH_3), 65.2 (CH_2), 120.3 (CH), 128.0 (CH), 130.4 (CH), 132.3 (C), 133.1 (CH), 134.6 (C), 136.3 (C), 136.8 (C), 146.4 (C), 155.3 (C), 162.1 (C), 172.2 (C).

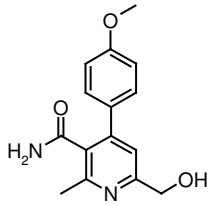

126d

126d; colorless solid; 99% yield, $C_{15}H_{16}N_2O_3$, M = 272.31 g/mol, HPLC-ESI-MS: $[M + H]^+$ = 273 *m/z*. ^{1}H NMR (400 MHz, DMSO-D_6) δ 2.47 (s, 3 H), 3.79 (s, 3 H), 4.55 (d, J = 5.9 Hz, 2 H), 5.43 (m, 1 H), 7.01 (m, 2 H), 7.23 (s, 1 H), 7.46 (m, 3 H), 7.77 (s, 1 H). ^{13}C NMR (100 MHz, DMSO-D_6) δ 22.1 (CH_3), 55.2 (CH_3), 64.0 (CH_2), 113.9 (CH), 117.6 (CH), 129.4 (CH), 130.4 (C), 130.8 (C), 145.7 (C), 153.1 (C), 159.4 (C), 160.7 (C), 170.1 (C).

General procedure for the synthesis of 127: Thionyl chloride (4 eq, 2 mmol, 0.145 mL) was added to a suspension of **126** (1 eq, 0.5 mmol) in toluene (10 mL) and the mixture was stirred at 60 ˚C for 16 h. The solvent was removed under reduced pressure and the product **127** was isolated by column chromatography with DCM/MeOH gradient (40:1 to 10:1) as eluent.

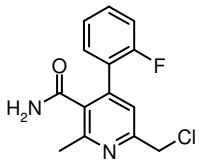

127a

127a; colorless solid; 85% yield, $C_{14}H_{12}Cl_2FN_2O$, M = 278.72 g/mol, HPLC-ESI-MS: $[M + H]^+$ = 279 *m/z*. ^{1}H NMR (400 MHz, $CDCl_3$) δ 2.65 (s, 3 H), 4.64 (s, 2 H), 5.61 (s, 1 H), 5.88 (s, 1 H), 7.18 (m, 2 H), 7.38 (m, 3 H). ^{13}C NMR (100 MHz, $CDCl_3$) δ 22.6 (CH_3), 46.2 (CH_2), 115.9 (d, $^2J_{C\text{-}F}$ = 22.0 Hz, CH), 121.56 (CH), 124.5 (d, $^3J_{C\text{-}F}$ = 3.7 Hz, CH), 124.8 (d, $^2J_{C\text{-}F}$ = 15.4 Hz, C), 130.8 (d, $^4J_{C\text{-}F}$ = 2.9 Hz, CH), 130.9 (d, $^3J_{C\text{-}F}$ = 8.1 Hz, CH), 142.3 (C), 155.6 (C), 156.2 (C), 159.1 (d, $^1J_{C\text{-}F}$ =246.6, C), 160.3 (C), 169.5 (C).

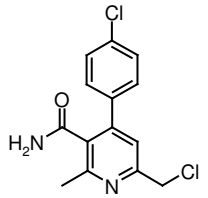

127b

127b; colorless solid; 76% yield, $C_{14}H_{12}Cl_2N_2O$, M = 295.17 g/mol, HPLC-ESI-MS: $[M + H]^+$ = 295 *m/z*. ^{1}H NMR (400 MHz, DMSO-D_6) δ 2.51 (s, 3 H), 4.77 (s, 2 H), 7.39 (s, 1 H), 7.53 (m, 4 H), 7.59 (s, 1 H), 7.91 (s, 1 H). ^{13}C NMR (100 MHz, DMSO-D_6) δ 22.1 (CH_3), 46.5 (CH_2), 121.0 (CH), 128.5 (CH), 130.0 (CH), 131.7 (C), 133.6 (C), 136.6 (C), 145.5 (C), 154.4 (C), 155.4 (C), 169.2 (C).

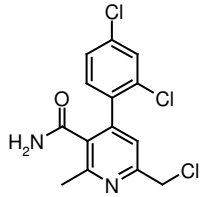

127c

127c; colorless solid; 75% yield, $C_{14}H_{11}Cl_3N_2O$, M = 329.62 g/mol, HPLC-ESI-MS: $[M + H]^+$ = 330 *m/z*. ^{1}H NMR (400 MHz, DMSO-D_6) δ 2.53 (s, 3 H), 4.78 (s, 2 H), 7.31 (s, 1 H), 7.40 (d, J = 8.1 Hz, 1 H), 7.50 (dd, J = 7.5, 2.0 Hz, 1 H), 7.54 (s, 1 H), 7.73 (d, J = 2.0 Hz, 1 H), 7.86 (s, 1 H). ^{13}C NMR (100 MHz, DMSO-D_6) δ 22.3 (CH_3), 46.3 (CH_2), 121.5 (CH), 127.0 (CH), 128.9 (CH), 132.0 (CH), 132.5 (C), 132.8 (C), 134.0 (C), 135.2 (C), 143.7 (C), 154.3 (C), 154.9 (C), 168.1 (C).

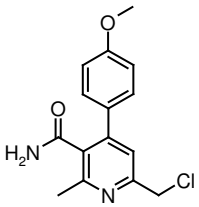

127d

127d; colorless solid; 79% yield, $C_{15}H_{15}ClN_2O_2$, M = 290.75 g/mol, HPLC-ESI-MS: $[M + H]^+$ = 291 *m/z*. ^{1}H NMR (400 MHz, DMSO-D_6) δ 2.50 (s, 3 H), 3.79 (s, 3 H), 4.76 (s, 2 H), 7.01 (m, 2 H), 7.36 (s, 1 H), 7.47 (m, 2 H), 7.55 (s, 1 H), 7.86 (s, 1 H). ^{13}C NMR (100 MHz, DMSO-D_6) δ 22.3 (CH_3), 46.3 (CH_2), 55.2 (CH_3), 114.0 (CH), 121.0 (CH), 129.5 (CH), 130.1 (C), 131.6 (C), 146.3 (C), 154.2 (C), 155.1 (C), 159.6 (C), 169.7 (C).

General procedure for the synthesis of 128: 127 (1 eq, 0.5 mmol) was dissolved in dry DMF (2 mL) and a suspension of phthalimide (1.5 eq, 0.75 mmol, 0.110 g) and *t*-BuOK (1.5 eq, 0.75 mmol, 0.084 g) in DMF (2 mL) was added. The mixture was stirred at 60 ˚C for 4 h, then the solvent was removed under reduced pressure and the product **128** was isolated by column chromatography (DCM/MeOH, 40:1).

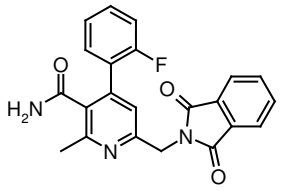

128a

128a; colorless solid; 65% yield, $C_{22}H_{16}FN_3O_3$, M = 389.39 g/mol, HPLC-ESI-MS: $[M + H]^+$ = 390 *m/z*. ^{1}H NMR (400 MHz, DMSO-D_6) δ 2.42 (s, 3 H), 4.90 (s, 2 H), 7.23 (m, 3 H), 7.41 (m, 3 H), 7.87 (m, 4 H), 7.94 (s, 1 H).

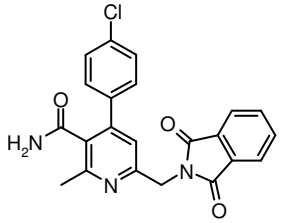

128b

128b; colorless solid; 82% yield, $C_{22}H_{16}ClN_3O_3$, M = 405.84 g/mol, HPLC-ESI-MS: $[M + H]^+$ = 406 *m/z*. ^{1}H NMR (400 MHz, DMSO-D_6) δ 2.40 (s, 3 H), 4.90 (s, 2 H), 7.23 (s, 1 H), 7.48 (m, 4 H), 7.53 (s, 1 H), 7.88 (m, 5 H). ^{13}C NMR (100 MHz, DMSO-D_6) δ 22.7 (CH_3), 42.6 (CH_2), 119.1 (CH), 123.6 (CH), 128.7 (CH), 130.4 (CH), 131.4 (C), 132.1 (C), 133.8 (C), 134.9 (CH), 137.2 (C), 145.6 (C), 154.2 (C), 154.8 (C), 168.2 (C), 169.7 (C).

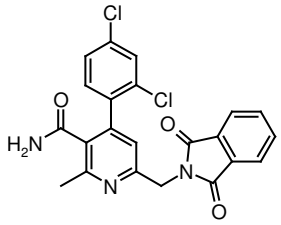

128c

128c; colorless solid; 80% yield, $C_{22}H_{15}Cl_2N_3O_3$, M = 440.29 g/mol, HPLC-ESI-MS: $[M + H]^+$ = 440 *m/z*. ^{1}H NMR (400 MHz, DMSO-D_6) δ 2.42 (s, 3 H), 4.90 (s, 2 H), 7.16 (s, 1 H), 7.35 (d, J = 8.4 Hz, 1 H), 7.46 (dd, J = 8.1, 1.8 Hz, 2 H), 7.67 (d, J = 1.8 Hz, 1 H), 7.79 (s, 1 H), 7.88 (m, 4 H). ^{13}C NMR (100 MHz, DMSO-D_6) δ 22.5 (CH_3), 46.2 (CH_2), 119.2 (CH), 123.3 (CH), 126.9 (CH), 128.8 (CH), 131.8 (C), 132.1 (CH), 132.8 (C), 133.8 (C), 134.6 (CH), 135.5 (C), 143.5 (C), 153.8 (C), 154.0 (C), 167.8 (C), 168.3 (C).

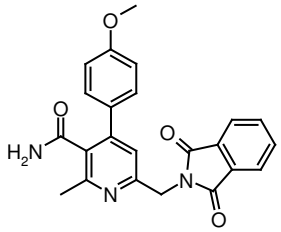

128d

128d; colorless solid; 90% yield, $C_{23}H_{19}Cl_2N_3O_4$, M = 401.43 g/mol, HPLC-ESI-MS: $[M + H]^+$ = 402 *m/z*. ^{1}H NMR (400 MHz, DMSO-D_6) δ 2.38 (s, 3 H), 3.76 (s, 3 H), 4.89 (s, 2 H), 6.98 (m, 2 H), 7.17 (s, 1 H), 7.42 (m, 2 H), 7.48 (s, 1 H), 7.80 (s, 1 H), 7.88 (m, 4 H). ^{13}C NMR (100 MHz, DMSO-D_6) δ 22.3 (CH_3), 42.2 (CH_2), 55.2 (CH_3), 113.9 (CH), 118.8 (CH), 123.3 (CH), 129.5 (CH), 130.2 (C), 131.0 (C), 131.8 (C), 134.6 (CH), 146.1 (C), 153.7 (C), 154.1 (C), 159.5 (C), 167.8 (C), 169.8 (C).

General procedure for the synthesis of 121: 128 (1 eq, 0.5 mmol) was suspended in 30% KOH (5 mL) and the mixture was stirred at 110 ˚C for 4 h. After cooling to room temperature the product was extracted with DCM. The combined organic phases were dried over anhydrous Na_2SO_4 and concentrated. The product was purified by column chromatography with DCM/MeOH (10:1) as eluent.

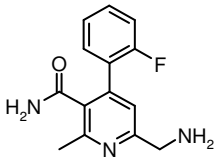

121a

121a; yellow solid; 91% yield, $C_{14}H_{14}FN_3O$, M = 259.29 g/mol, HPLC-ESI-MS: $[M + H]^+$ = 260 *m/z*. ^{1}H NMR (400 MHz, DMSO-D_6) δ 2.50 (s, 3 H), 3.79 (s, 2 H), 7.27 (m, 3 H), 7.42 (m, 3 H), 7.76 (s, 1 H). ^{13}C NMR (100 MHz, DMSO-D_6) δ 22.4 (CH_3), 47.1 (CH_2), 115.6 (d, $^2J_{C\text{-}F}$ = 22.0 Hz, CH), 119.4 (CH), 124.1 (d, $^3J_{C\text{-}F}$ = 3.7 Hz, CH), 126.0 (d, $^2J_{C\text{-}F}$ = 15.4 Hz, C), 130.4 (d, $^3J_{C\text{-}F}$ = 8.1 Hz, CH), 131.0 (d, $^4J_{C\text{-}F}$ = 2.9 Hz, CH), 131.1 (C), 140.7 (C), 153.2 (C), 158.8 (d, $^1J_{C\text{-}F}$ =248.1, C), 161.8 (C), 169.1 (C).

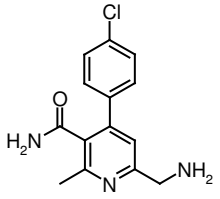

121b

121b; yellow solid; 89% yield, $C_{14}H_{14}ClN_3O$, M = 275.74 g/mol, HPLC-ESI-MS: $[M + H]^+$ = 276 *m/z*. ^{1}H NMR (400 MHz, DMSO-D_6) δ 2.48 (s, 3 H), 7.27 (s, 1 H), 7.51 (m, 5 H), 7.81 (s, 1 H). ^{13}C NMR (100 MHz, DMSO-D_6) δ 22.2 (CH_3), 47.2 (CH_2), 118.4 (CH), 128.4 (CH), 130.0 (CH), 130.1 (C), 133.3 (C), 137.5 (C), 144.8 (C), 153.2 (C), 162.3 (C), 169.8 (C).

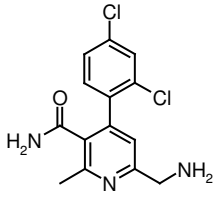

121c

121c; colorless solid; 84% yield, $C_{14}H_{13}Cl_2N_3O$, M = 310.19 g/mol, HPLC-ESI-MS: $[M + H]^+$ = 310 *m/z*. ^{1}H NMR (400 MHz, DMSO-D_6) δ 2.50 (s, 3 H), 3.80 (s, 2 H), 7.18 (s, 1 H), 7.44 (m, 3 H), 7.72 (m, 2 H). ^{13}C NMR (100 MHz, DMSO-D_6) δ 22.4 (CH_3), 47.0 (CH_2), 118.9 (CH), 126.8 (CH), 128.8 (CH), 130.8 (C), 132.1 (CH), 132.8 (C), 133.6 (C), 136.0 (C), 143.1 (C), 153.1 (C), 161.7 (C), 168.7 (C).

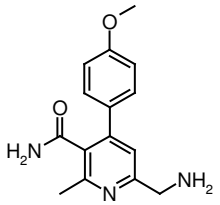

121d

121d; yellow solid; 79% yield, $C_{15}H_{17}N_3O_2$, M = 271.32 g/mol, HPLC-ESI-MS: $[M + H]^+$ = 272 *m/z*. ^{1}H NMR (400 MHz, DMSO-D_6) δ 2.46 (s, 3 H), 3.77 (s, 2 H), 3.78 (s, 3 H), 6.99 (d, *J* = 8.7 Hz, 2 H), 7.24 (s, 1 H), 7.46 (m, 3 H), 7.74 (s, 1 H). ^{13}C NMR (100 MHz, DMSO-D_6) δ 22.2 (CH_3), 47.2 (CH_2), 55.2 (CH_3), 113.8 (CH), 118.4 (CH), 129.5 (CH), 130.1 (C), 130.9 (C), 145.6 (C), 153.1 (C), 159.4 (C), 161.9 (C), 170.3 (C).

6. 1. 2. 15 Synthesis of 3-aminomethyl-pyridines 122.

6. 1. 2. 15. 1 Route A.

General procedure for the synthesis of 129 - Boc-protection: Boc_2O (1.5 eq, 0.225 mmol, 0.049 g) was added to a solution of **116** (1 eq, 0.15 mmol) in dioxane (5 mL) and the mixture was stirred for 16 h at 60 ºC. The solvent was removed under reduced pressure and the product was isolated by column chromatography with DCM/MeOH (40:1) as eluent.

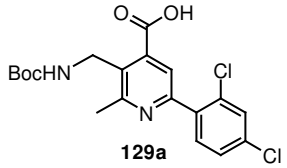

129a

129a; pale solid; 43% yield, $C_{19}H_{20}Cl_2N_2O_4$, M = 411.29 g/mol, HPLC-ESI-MS: $[M + H]^+$ = 411 *m/z*.

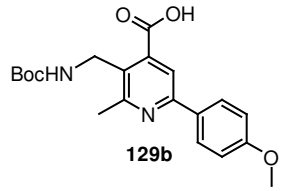

129b

129b; colorless solid; 38% yield, $C_{20}H_{24}N_2O_5$, M = 372.43 g/mol, HPLC-ESI-MS: $[M + H]^+$ = 373 *m/z*.

General procedure for the synthesis of 130: These compounds were prepared according to the procedure for **94** and **99**, using compound **129** as a starting material.

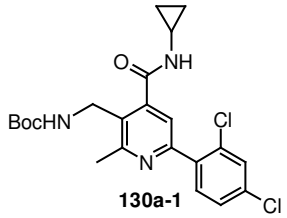

130a-1

130a-1; colorless solid; 63% yield, $C_{22}H_{25}Cl_2N_3O_3$, M = 450.37 g/mol, HPLC-ESI-MS: $[M + H]^+$ = 450 *m/z*.

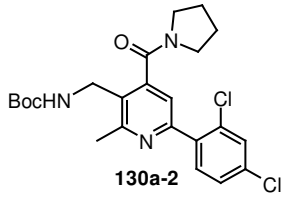

130a-2

130a-2; colorless solid; 54% yield, $C_{23}H_{27}Cl_2N_3O_3$, M = 464.40 g/mol, HPLC-ESI-MS: $[M + H]^+$ = 464 *m/z*.

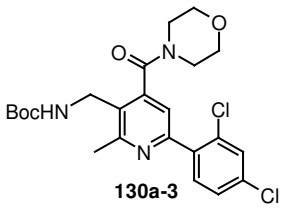

130a-3

130a-3; colorless solid; 80% yield, $C_{23}H_{27}Cl_2N_3O_5$, M = 480.40 g/mol, HPLC-ESI-MS: $[M + H]^+$ = 480 *m/z*.

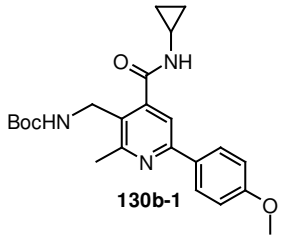

130b-1

130b-1; colorless solid; 76% yield, $C_{23}H_{29}N_3O_4$, M = 411.51 g/mol, HPLC-ESI-MS: $[M + H]^+$ = 412 *m/z*.

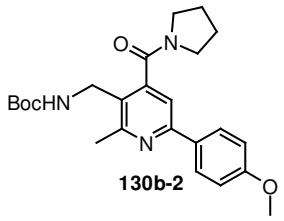

130b-2

130b-2; colorless solid; 86% yield, $C_{24}H_{31}N_3O_4$, M = 425.53 g/mol, HPLC-ESI-MS: $[M + H]^+$ = 426 *m/z*.

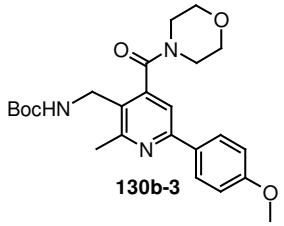

130b-3

130b-3; colorless solid; 92% yield, $C_{24}H_{31}N_3O_5$, M = 441.53 g/mol, HPLC-ESI-MS: $[M + H]^+$ = 442 *m/z*.

General procedure for the synthesis of 122 - deprotection: These compounds were prepared according to the procedure for **120a-c**, using compound **130** as a starting material.

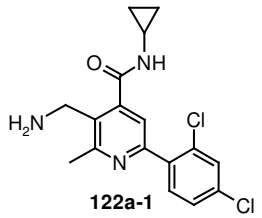

122a-1

122a-1; colorless solid; 65% yield, $C_{17}H_{17}Cl_2N_3O$, M = 350.25 g/mol, HPLC-ESI-MS: $[M + H]^+$ = 350 *m/z*.

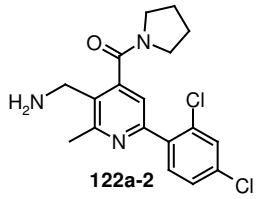

122a-2

122a-2; yellow solid; 57% yield, $C_{18}H_{19}Cl_2N_3O$, M = 364.28 g/mol, HPLC-ESI-MS: $[M + H]^+$ = 364 *m/z*.

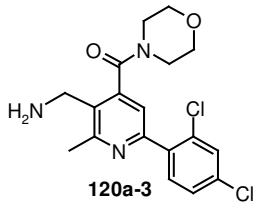

120a-3

122a-3; colorless solid; 63% yield, $C_{18}H_{19}Cl_2N_3O_2$, M = 380.28 g/mol, HPLC-ESI-MS: $[M + H]^+$ = 380 *m/z*.

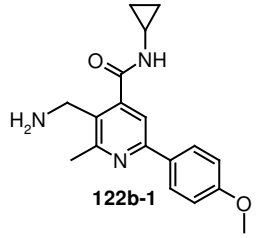

122b-1

122b-1; colorless solid; 75% yield, $C_{18}H_{21}N_3O_2$, M = 311.39 g/mol, HPLC-ESI-MS: $[M + H]^+$ = 312 *m/z*.

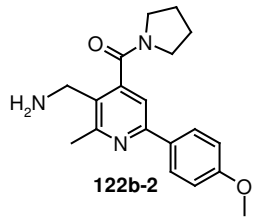

122b-2

122b-2; yellow solid; 83% yield, $C_{19}H_{23}N_3O_2$, M = 325.41 g/mol, HPLC-ESI-MS: $[M + H]^+$ = 326 *m/z*.

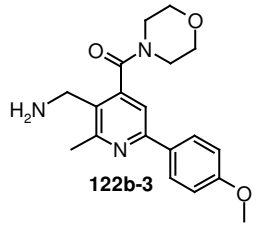

122b-3

122b-3; yellow solid; 70% yield, $C_{19}H_{23}N_3O_3$, M = 341.41 g/mol, HPLC-ESI-MS: $[M + H]^+$ = 442 *m/z*.

6. 1. 2. 15. 2 Route B.

51% aqueous solution of hydrazine (20 eq, 3 mmol, 0.20 mL) was added dropwise with in 20 min to a suspension of **99** (1 eq, 0.15 mmol) and Raney Nickel (1 mL, 50% slurry in water) dissolved in THF (60 mL). The catalyst was then filtered off and the solution was acidified with TFA (5 mL). The solvent was removed under reduced pressure and the product was purified by column chromatography with DCM/MeOH (10:1) as eluent.

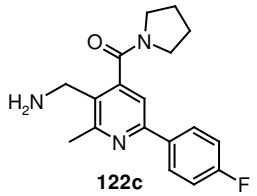

122c

122c; colorless solid; 46% yield, $C_{18}H_{20}FN_3O$, M = 313.38 g/mol, HPLC-ESI-MS: $[M + H]^+$ = 314 *m/z*.

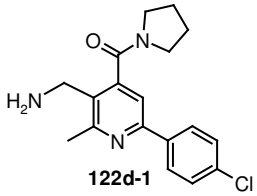

122d-1

122d-1; colorless solid; 53% yield, $C_{18}H_{20}ClN_3O$, M = 329.83 g/mol, HPLC-ESI-MS: $[M + H]^+$ = 330 *m/z*. ^{1}H NMR (400 MHz, $CDCl_3$) δ 1.99 (m, 4 H), 2.78 (s, 3 H), 3.43 (t, J = 6.6 Hz, 2 H), 3.67 (t, J = 7.0 Hz, 2 H), 4.18 (s, 2 H), 7.49 (m, 2 H), 7.87 (s, 1 H), 8.08 (m, 2 H). ^{13}C NMR (100 MHz, $CDCl_3$) δ 22.8 (CH_3), 25.2 (CH_2), 27.1 (CH_2), 39.2 (CH_2), 47.4 (CH_2), 30.5 (CH_2), 117.0 (CH), 123.7 (C), 129.7 (CH), 130.0 (CH), 137.1 (C), 137.8 (C), 148.4 (C), 157.7 (C), 161.9 (C), 168.7 (C).

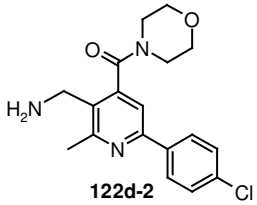

122d-2

122d-2; colorless solid; 48% yield, $C_{18}H_{20}ClN_3O_2$, M = 345.83 g/mol, HPLC-ESI-MS: $[M + H]^+$ = 346 *m/z*.

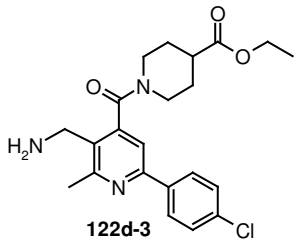

122d-3

122d-3; colorless solid; 52% yield, $C_{22}H_{26}ClN_3O_3$, M = 415.92 g/mol, HPLC-ESI-MS: $[M + H]^+$ = 416 *m/z*.

6. 2 Biological screening.

Antimycotic assay: 10 000 HeLa cells (Human cervix carcinoma [ATCC, Cat. No. CCL-2]) per well or CHO cells were seeded in a 96 well plate in the presence or absence of 10 µM compound, infected with *Candida albicans* (SC5314) [CFU 5-500 (optimum 50, 50 µL 1000 CFU/mL)] and incubated at 37°C 5% CO_2 in a total volume of 200 µL media (RPMI 1640, 10% FCS, 1% glutamine) for 5 days .

a) Experiment description.

Dye:	Fluorescein diacetat	**Cells:**	HeLa	**Cell control:**	A1:H1
Filter:	Ex.485 Em.538	**m.o.i.:**	0.005	**Microbe control:**	A2:D2
Experiment no.:	can train 1	**Microbe:**	Candida albicans SC 5314	**Drug control:**	E2:H2
Name:	Doris	**Incubation:**	5 Days	**Compound position:**	A3-H12
Date:	16-21.10.2008	**Incubation time:**	10-15 min	**Concentration:**	10 µM

b) Fluorescence measurement.

Crude Date (fluorescence)

1	**2**	**3**	**4**	**5**	**6**	**7**	**8**	**9**	**10**	**11**	**12**	
16578	2669	819	997	1716	1151	1784	1175	529	1616	2031	2250	**A**
14928	2620	425	1006	1996	1067	1743	802	1156	1361	672	273	**B**
16272	2156	1320	2215	739	1334	908	1719	1807	2053	1033	310	**C**
16576	2722	1119	930	1247	497	9393	2243	2069	1556	1864	2146	**D**
15268	15759	1233	1690	1232	3887	580	1033	2556	1433	1740	3046	**E**
14819	15032	1886	1611	2348	1867	3130	2323	1558	578	3909	650	**F**
16596	15846	1455	2080	2793	1700	1856	2818	1517	2156	522	3000	**G**
17218	15705	1409	2362	2049	1483	2444	2207	1006	2310	2894	2096	**H**

c) Antimicrobial activity.

Antimicrobial activity (percent of cell control)												
1	**2**	**3**	**4**	**5**	**6**	**7**	**8**	**9**	**10**	**11**	**12**	
104%	1%	-13%	-11%	-6%	-10%	-6%	-10%	-15%	-7%	-4%	-2%	**A**
92%	1%	-16%	-11%	-4%	-11%	-6%	-13%	-10%	-9%	-14%	-17%	**B**
102%	-3%	-9%	-2%	-13%	-9%	-12%	-6%	-5%	-4%	-11%	-17%	**C**
104%	1%	-11%	-12%	-10%	-15%	**51%**	-2%	-4%	-7%	-5%	-3%	**D**
94%	98%	-10%	-6%	-10%	10%	-15%	-11%	0%	-8%	-6%	4%	**E**
91%	93%	-5%	-7%	-1%	-5%	4%	-2%	-7%	-15%	10%	-14%	**F**
104%	99%	-8%	-3%	2%	-6%	-5%	2%	-8%	-3%	-15%	3%	**G**
109%	98%	-8%	-1%	-4%	-8%	-1%	-2%	-11%	-2%	3%	-3%	**H**

Figure 14. Plot of absorbance at 405 nm *versus* time.

To monitor the immediate effect of *C. albicans* on the host cells the individual wells were microscopically analysed after 18 h of incubation for growth of *C. albican*s and the state of the host cells. After 5 days the activities of the compounds were determined by analysing the relative number and vitality of surviving human cell lines as measured by hydrolysis of fluorescein diacetate. The wells of the plate were washed with phosphate-buffered saline (PBS, 200 µL) and then filled with 200 µL PBS containing 10 µg/mL fluorescein diacetate. After a 45-min incubation at room temperature, fluorescence [RFU (relative fluorescence units)] was measured at 485 nm excitation and 538 nm emission wavelength (Figure 14). The activity was calculated using the equation:

$$Activity(\%) = \frac{RFU_{test-well}}{(RFU_{cell-control} - RFU_{microbe-control})} .$$

A cut off of 40% of total fluorescence intensity per well in comparison to the control wells containing only host cells was chosen to select compounds preventing growth of *C. albicans* to a significant extend without strongly impairing the vitality of the host cells.

Absorbance based antimicotic assay: Immune cells (BMDMs, bone marrow-derived macrophages - $2.5x10^3$ cells/mL) in YPD media were dispensed in a 96 well plate. The cells were infected with *Candida glabrata* and incubated at 30 °C in a total volume of 200 µL media in the presence of the appropriate compound at eight different concentrations. After 2 days the plate was shaken on a MixMate and the absorbance (OD_{600}) was measured with Vicor plate reader.

In vitro DPP-4 inhibition assay: The screening of the compounds for DPP-4 inhibitory activity was performed by using a DPP-4 drug discovery kit (AK499-0001, Enzo Life Sciences). The inhibition of the human recombinant DPP-4 activity was measured by following the increase of absorbance upon cleavage of the chromogenic substrate Gly-Pro-pNA (pNA is *p*-nitroaniline) according to the protocol of the manufacturer (Scheme 59).

Scheme 73. DPP-4 catalyzed hydrolysis of chromogenic substrate - Gly-Pro-*p*-nitroanilin.

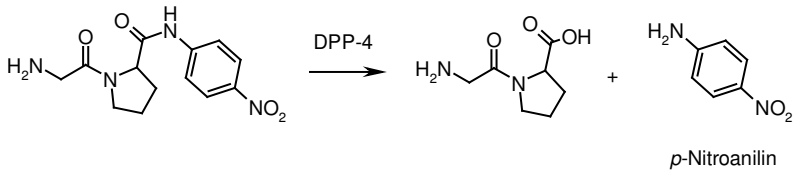

In order to determine the range over which the reaction was linear, the absorbance at 405 nm was continuously measured for 60 min (Figure 15). As an optimal time for the experiment 16 min were chosen.

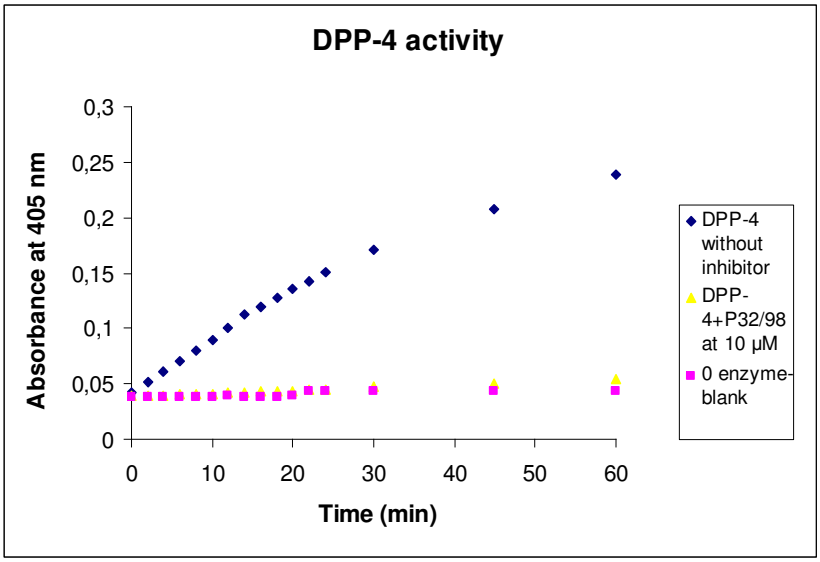

Figure 15. Plot of absorbance at 405 nm *versus* time.

Reactions were carried out at 37 ˚C in Tris buffer (50 mM, pH 7.5) containing 0.18 mU/well of enzyme, 50 µM of substrate (the final substrate concentration was chosen around K_m value obtained under the assay conditions) and variable concentration of the inhibitor. For the compound dilutions DMSO was used and its final solvent concentration did not exceed 1%. Enzyme DPP-4 was first preincubated with the compounds for 10 min prior the substrate addition. After preincubation period the substrate was added and the reaction was followed by continuous absorbance measurement at 405 nm for 16 min using a MRX Revelation plate reader (Dynex Technologies). The experiment was repeated 3 times for each test compound and the values were averaged.

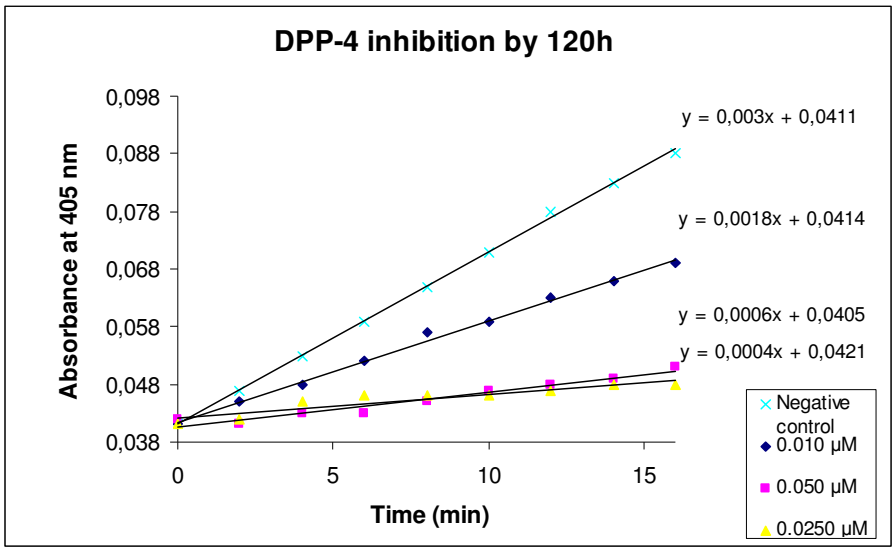

Figure 16. DPP-4 assay: inhibition of DPP-4 by **120h.**

To obtain the IC_{50} values the active compounds were titrated up to eight concentrations (Figure 16). The IC_{50} values were calculated from the trend line of the curve generated after plotting the percentage of activity versus inhibitor concentration. Percent remaining activity in presence of the inhibitor was calculated using the equation: $\%Activity = \frac{V_i}{V} \cdot 100$,

where V_i is the initial velocity in presence of the inhibitor at concentration i, V is the initial velocity of the negative control (enzyme without inhibitor).

The type of inhibition was determined by measuring the rate of hydrolysis of Gly-Pro-pNA at four different concentrations of substrate and inhibitor. To calculate the initial rate of pNA formation the absorption at 405 nm was converted to nanomoles of pNA using a standard calibration curve (Figure 17).

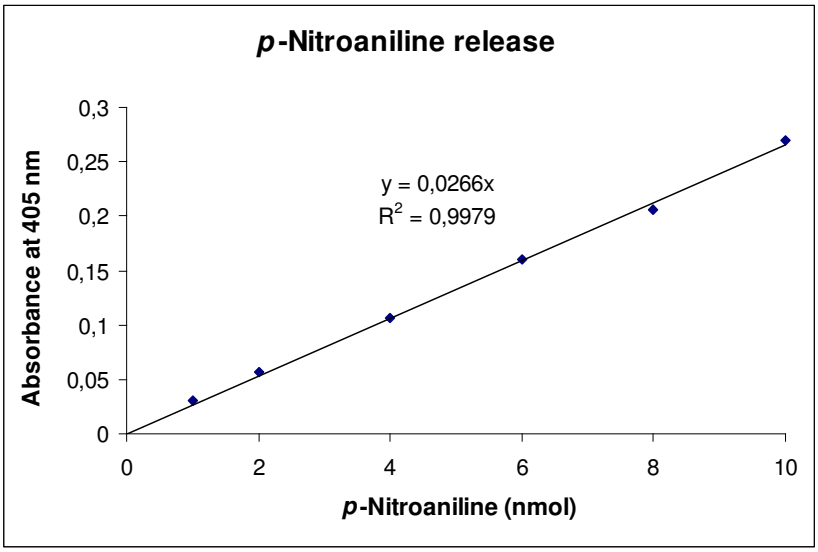

Figure 17. UV-absorption measurement of *p*-nitroaniline release: calibration curve.

For each concentration of inhibitor the initial rates were used for Lineweaver-Burk plots (Figure 18). The inhibition constant K_i was obtained from the expression:

$$K_i = \frac{i}{\left[\left(\frac{K_p}{K_m}\right) - 1\right]}$$

where K_m is concentration of substrate that leads to half-maximal velocity, and K_p is the effective Michaelis constant in presence of the inhibitor at concentration i.

a) Release of pNA at the different substrate concentration (10, 50, 100 and 150 µM) without inhibitor.

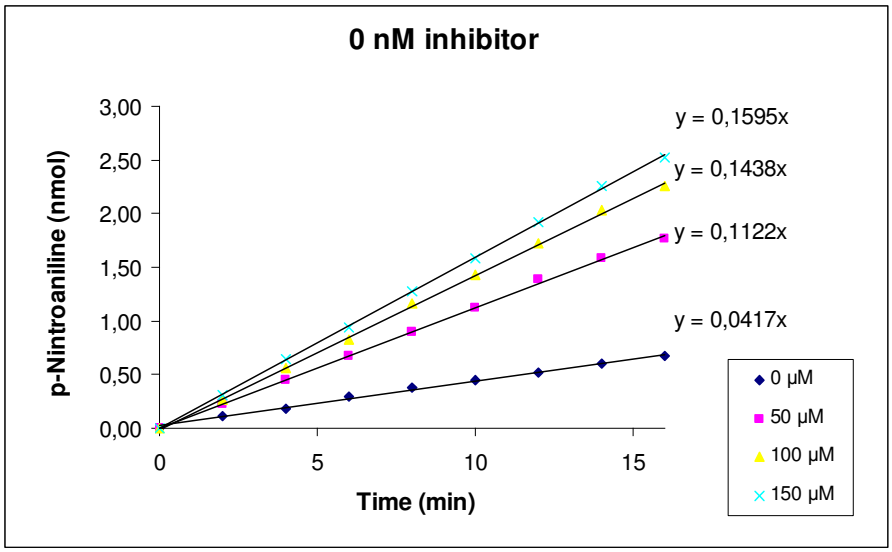

b) Release of pNA at the different substrate concentration with the inhibitor at 10 nM concentration.

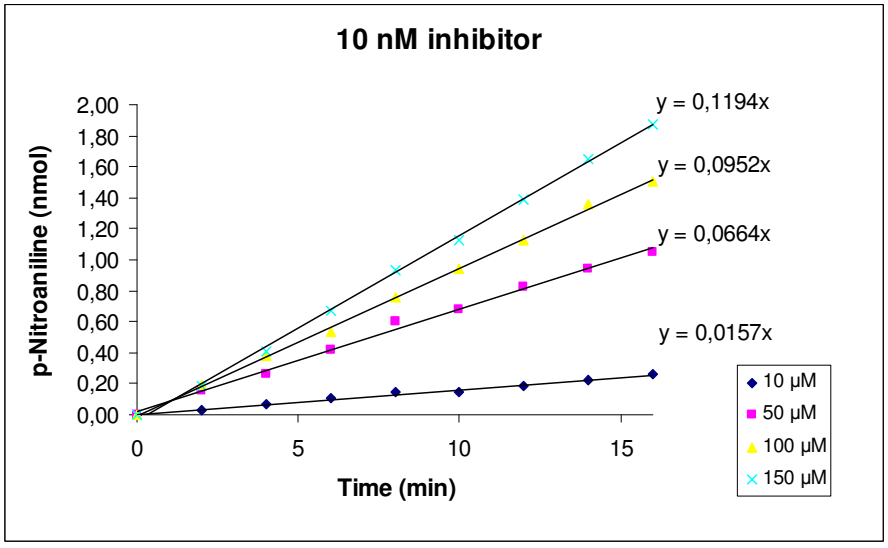

c) Release of pNA at the different substrate concentration with the inhibitor at 50 nM concentration.

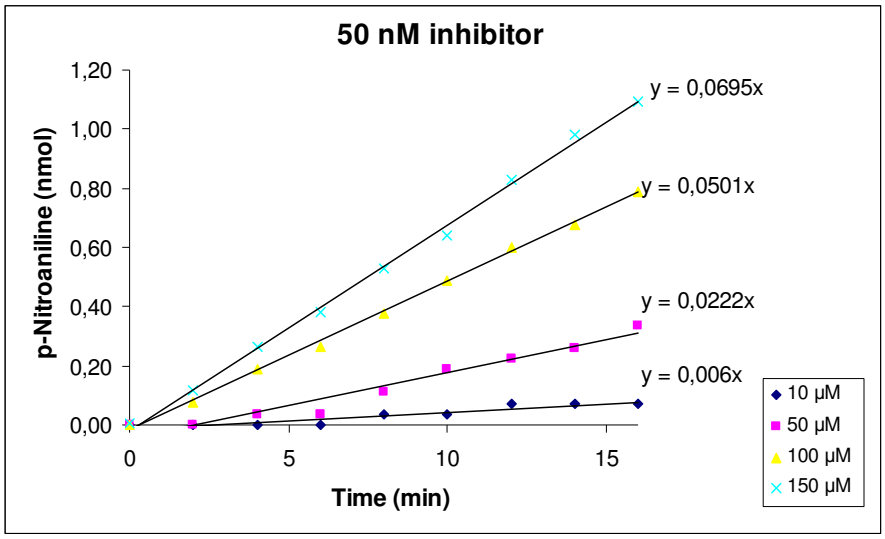

d) Lineweaver-Burk plot - competitive inhibition.

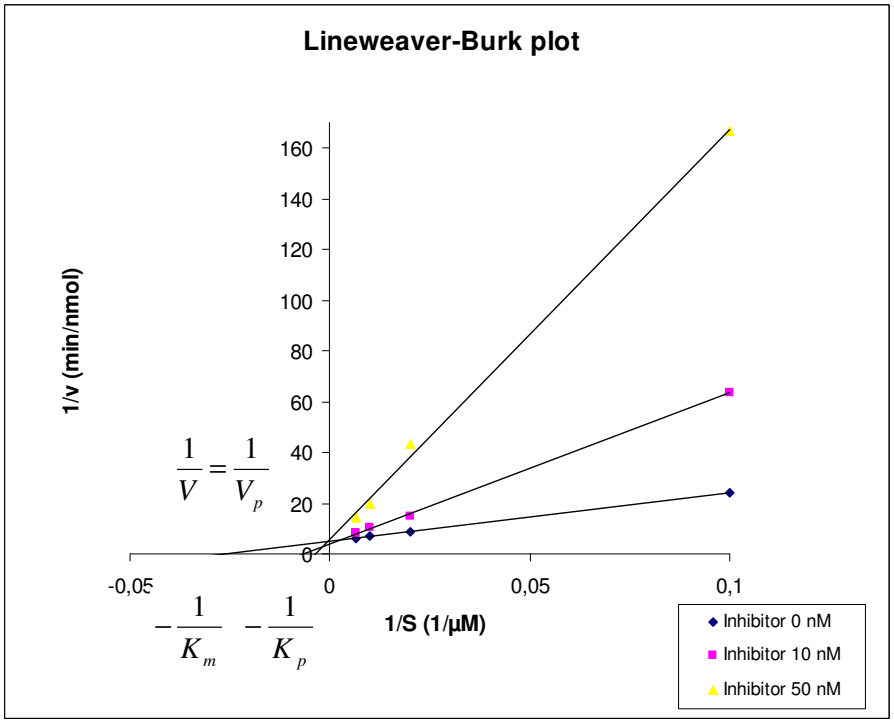

Figure 18. Data analysis for the inhibition type and K_i calculation.

$$V_m = 3.3\frac{pmol}{s}$$

$$-\frac{1}{K_m} = -0.0267$$

$$K_m = 37.5\mu M$$

$$-\frac{1}{K_p} = \frac{1}{K_m\left(1+\frac{i}{K_i}\right)}$$

$$K_i = 5.5 \pm 2nM$$

Calculated K_i

$$K_i = \frac{IC_{50}}{\left(1+\frac{S}{K_m}\right)}$$

$$IC_{50} = 11.44\ nM$$

$$K_i = 4.9 \pm 0.5nM$$

Type of inhibition: competitive

In vitro DPP-8 inhibition assay: The screening of the compounds for DPP-8 inhibitory activity was performed using human recombinant DPP-8, supplied by Enzo Life Sciences. The substrate used for the screening was Gly-Pro-pNA. As DPP-8 catalytic efficiency for this substrate is 2-fold lower in comparison to DPP-4 the assay condition had to be modified. The substrate concentration, 300 µM, was chosen around K_m value (221 µM) obtained under assay conditions. The release of the pNA was investigated at different substrate concentrations (Figure 19). The K_m value was then generated from Lineweaver-Burk plot (Figure 20). Other parameters and conditions of the assay were identical as previously described. Under this assay condition the enzyme activity as well as its inhibition by P32/98 (positive control) could be clearly observed (Figure 21).

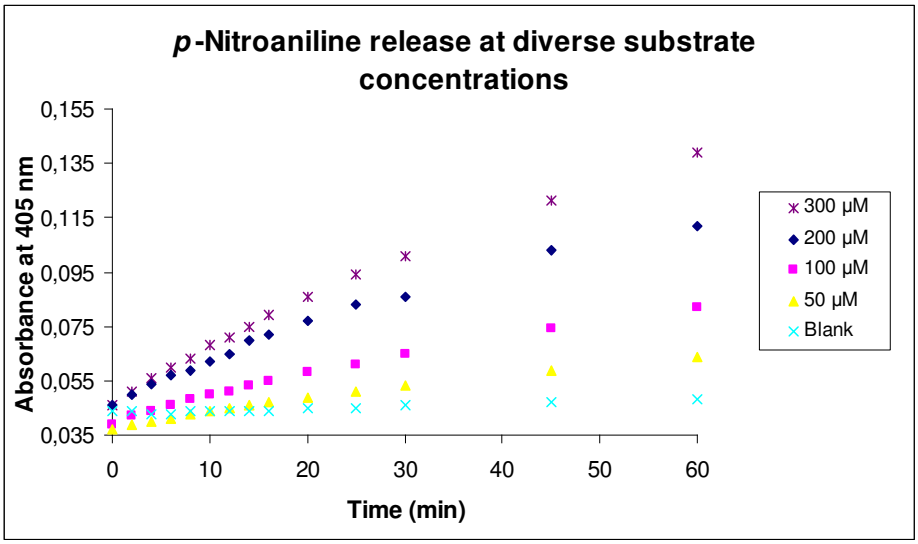

Figure 19. Evaluation of the assay conditions for DPP-8 inhibitory screening.

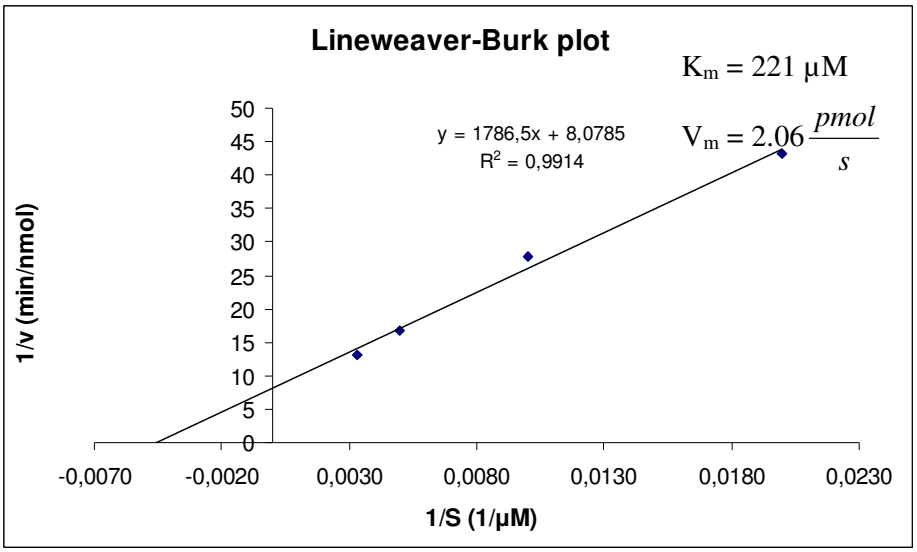

Figure 20. Lineweaver-Burk plot of the substrate cleavage by DPP-8.

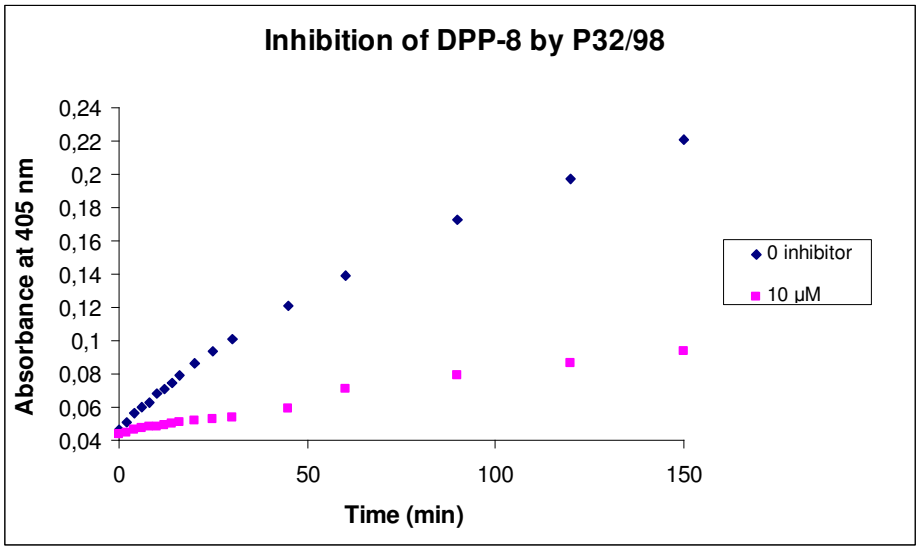

Figure 21. DPP-8 inhibition by P32/98.

The aminomethyl-pyridines **120** were investigated for its DPP-8 inhibitory activity. IC_{50} values were calculated after plotting the data for up to eight inhibitor concentrations. The assay was repeated 3 times for each test compound and the values were averaged.

Toxicity of the compounds: The toxicity of the compounds at 10 µM was investigated with HeLa cells (Human cervix carcinoma [ATCC Cat.No. CCL-2]) at the Fraunhofer Institute in Stuttgart.

7. Literature.

1. Mitscher, L. A.; Dutta, A. *Combinatorial Chemistry and Multiple Parallel Synthesis*, 6th ed., Vol. 2; JWA: New York, 2003.
2. Bannwarth, W.; Felder, E. *Combinatorial Chemistry a Practical Approach*, Vol. 9; VCH: Weinheim, 2000.
3. Koppitz, M; Knut, E. *Drug Discov. Today* **2006**, 11, 561-568.
4. Lipinski, C. A.; Lombardo, F.; Dominy, B. W.; Feeney, P. J. *Adv. Drug Del. Rev.* **1997**, *23*, 3-25.
5. Chaiken, I. M.; Janda, K. D. *Molecular Diversity and Combinatorial Chemistry; Libraries and Drug Discovery*; ACS: Washington, 1996.
6. Leach, A. R.; Hann, M. M. *Drug Discov. Today* **2000**, *5,* 326-336.
7. Waszkowycz, B.; Perkins, T. D. J.; Sykes, R. A.; Li, J. *IBM Systems Journal* **2001**, *40*, 360-376.
8. Subha, K.; Kumar, G. R.; Rajalakshmi, R.; Aravindhan, G. *Biomarkers in Cancer* **2010**, *2*, 35-42.
9. Henry, G. D. *Tetrahedron* **2004**, *60*, 6043-6061.
10. www.drugbank.ca
11. Tomlin, C. *The Pesticide Manual*, 10th ed.; British Crop Protection Council/Royal Society of Medicine: Farnhan/Cambridge, 1994.
12. Kidwai, M.; Venkataramanan, R.; Rastogi, S.; Sapra, P. *Curr. Med. Chem. - Anti-Infective Agents* **2003**, *2*, 27-71.
13. Leem, S. H.; Park, J. E.; Kim, I. S.; Chae, J. Y.; Sugino, A.; Sunwoo, Y. *Mol. Cells* **2003**, *15*, 55-61.
14. FRAC Code List: Fungicides sorted by mode of action, 2009.
15. Masner, P.; Kerkenaar, A. *Pestic. Sci.* **1988**, *22*, 61-69.
16. Kato, T.; Shoami, M.; Kawase, Y. *J. Pesticide Sci.* **1980**, *5*, 69-79.
17. Tillman, R. W.; Ferguson, M. W. *Phytopathology* **1980**, *70*, 441-444.
18. Wedig, J. H.; Maibach, H. I. *J. Am. Acad. Dermatol.* **1981**, *5*, 433-438.
19. a) Luo, Q.-L.; Li, J.-Y.; Liu, Z.-Y.; Chen, L.-L.; Li, J.; Qian, Z.; Shen, Q.; Li, Y.; Lushington, G. H.; Ye, Q.-Z.; Nan, F.-J. *J. Med. Chem.* **2003**, *46*, 2631-2640. b) Chen, L.-L.; Li, J.; Li, J.-Y.; Luo, Q.-L.; Mao, W.-F.; Shen, Q.; Nan, F.-J.; Ye, Q.-Z. *Acta Pharmacol. Sin.* **2004**, *25*, 907-914. c) Luo, Q.-L.; Li, J.-Y.; Liu, Z.-Y.; Chen, L.-L.; Li, J.; Ye, Q.-Z.; Nan, F.-J. *Bioorg. Med. Chem. Lett.* **2005**, *15*, 635-638.

20. Yar, M. S.; Ali, M., A.; Sriram, D.; Yogeeswari, P. *Acta Pol. Pharm. Drug Res.* **2006**, *63*, 491-496.
21. Prasad,Y. R.; Kumar, P. P.; Kumar, P. R. *E-J. Chem.* **2008**, *5*, 144-148.
22. a) Alptuzun, V.; Parlar, S.; Tasli, H.; Erciyas, E. *Molecules* **2009**, *14*, 5203-5215. b) Matsukura, M. WO 2009/084621.
23. a) Obando, D.; Pantarat, N.; Handke, R.; Koda, Y.; Widmer, F.; Djordjevic, J. T.; Ellis, D. H.; Sorrell, T. C.; Jolliffe, K. A. *Bioorg. Med. Chem. Lett.* **2009**, *17*, 6329-6339. b) Ng, C. K. L.; Singhal, V.; Widmer, F.; Wright, L. C.; Sorrell, T. C.; Jolliffe, K. A. *Bioorg. Med. Chem.* **2007**, *15*, 3422-3429.
24. Stephens, C. E.; Tanious, F.; Kim, S.; Wilson, W. D.; Schell, W. A.; Perfect, J. R.; Franzblau, S. G.; Boykin, D. W. *J. Med. Chem.* **2001**, *44*, 1741-1748.
25. a) El-Galil, A.; Amr, E.; Mohamed, A. M.; Ibrahim, A. A. *Z. Naturforsch.* **2003**, *58b*, 861-868. b) Casnati, A.; Fabbi, M; Pelizzi, N.; Pochini, A.; Sansone, F; Ungaro, R. *Bioorg. Med. Chem. Lett.* **1996**, *6*, 2699-2704. c) Rudkevich, D. M.; Verboom, W.; Reinhoudt, D. N. *J. Org. Chem.* **1994**, *59*, 3683-3686. d) Pinkhossik, E.; Stibor, I.; Cosnati, A.; Ungaro, R. *J. Org. Chem.* **1997**, *62*, 8654-8659.
26. a) Buciński, A.; Socha, A; Wnuk, M.; Bączek, T.; Nowaczyk, A.; Krysiński, J.; Goryński, K.; Koba, M. *J. Microbiol. Methods* **2009**, *76*, 25-29. b) Ingale, K.; Choudhari, P.; Bhatia, M.; Bhatia, N.; Mulani, A. *Drug Invention Today* **2009**, *1*, 108-111.
27. Grammenos, W.; Glättlim, A.; Lohmnann, J. K.; Puhl, M.; Müller, B.; Vrettou-Schultes, M. WO 2009/141274.
28. http://who.int/diabetes/en/
29. Ducker, D. *J. Diabetes Care*, **2007**, *30*, 1335-1343.
30. Mohler, M. L.; He, Y.; Wu, Z.; Hwang, D. J.; Miller, D. D. *Med. Res. Rev.* **2009**, *29*, 125-195.
31. a) Humphries, P- S.; Almaden, J. V.; Barnum, S. J.; Carlson, T. J.; Do, Q.-Q. T.; Fraser, J. D.; Hess, M.; Kim, Y. H.; Ogilviec, K. M.; Sunb, S. *Bioorg. Med. Chem. Lett.* **2006**, *16*, 6116-6119. b) Shearer, B. G.; Wiethe, R. W.; Ashe, A.; Billin, A. N.; Way, J. M.; Stanley, T. B.; Wagner, C. D.; Xu, R. X.; Leesnitzer, L. M.; Merrihew, R. V.; Shearer, T. W.; Jeune, M. R.; Ulrich, J. C.; Willson, T. M. *J. Med. Chem.* **2010**, *53*, 1857-1861.
32. Siu, M.; Johnson, T. O.; Wang, Y.; Nair, S. K.; Taylor, W. D.; Cripps, S. J.; Matthews, J. J.; Edwards, M. P.; Pauly, T. A.; Ermolieff, J.; Castro, A.; Hosea, N. A.; LaPaglia, A.; Fanjul, A. N.; Vogel, J. E. *Bioorg. Med. Chem. Lett.* **2009**, *19*, 3493-3497.

33. Johnson, D.; Shepherd, R. M.; Gill, D.; Gorman, T.; Smith, D. M.; Dunne, M. J. *Diabetes* **2007**, *56*, 1694-1702.
34. Johnson, D.; Shepherd, R. M.; Gill, D.; Gorman, T.; Smith, D. M.; Dunne, M. J. *Biochem. Soc. Trans.* **2007**, *35*, 1208-1210.
35. a) Takahashi, K.; Hashimoto, N.; Nakama, C.; Kamata, K.; Sasaki, K.; Yoshimoto, R.; Ohyama, S.; Hosaka, H.; Maruki, H.; Nagata, Y.; Eiki, J.-I.; Nishimura, T. *Bioorg. Med. Chem.* **2009**, *17*, 7042-7051. b) Ishikawa, M.; Nonoshita, K.; Ogino, Y.; Nagae, Y.; Tsukahara, D.; Hosaka, H.; Maruki, H.; Ohyama, S.; Yoshimoto, R.; Sasaki, K.; Nagata, Y.; Eiki, Y.-I.; Nishimura, T. *Bioorg. Med. Chem. Lett.* **2009**, *19*, 4450-4454. c) Nishimura, T.; Iino, T.; Mitsuya, M.; Bamba, M.; Watanabe, H.; Tsukahara, D.; Kamata, K.; Sasaki, K.; Ohyama, S.; Hosaka, H.; Futamura, M.; Nagata, Y.; Eiki, J. *Bioorg. Med. Chem. Lett.* **2009**, *19*, 1357-1360. d) Mitsuya, M.; Kamata, K.; Bamba, M.; Watanabe, H.; Sasaki, Y.; Sasaki, K.; Ohyama, S.; Hosaka, H.; Nagata, Y.; Eiki, J.; Nishimura, T. *Bioorg. Med. Chem. Lett.* **2009**, *19*, 2718-2721. e) Kamata, K.; Mitsuya, M.; Nishimura, T.; Eiki, J. I.; Nagata, Y. *Structure* **2004**, *12*, 429-438.
36. Burgdorf, L. T.; Beier, N.; Gleitz, J.; Charon, C.; Cravo, D. WO 2009/046784.
37. Mitsuya, M.; Bamba, M.; Sakai, F.; Watanabe, H.; Sasaki, Y.; Nishimura, T.; Eiki, J.-I.; US 2010/0041660.
38. Pauly, R. P.; Demuth, H. U.; Rosche, F.; Schmidt, J.; White, H. A.; Lynn, F.; McIntosh, C. H.; Pederson, R. A. *Reg. Pept.* **1996**, *64*, 148-148.
39. Hopsu-Havu, V. K.; Glenner, G. G, *Histochem.* **1966**, *7*, 197-201.
40. Lorey, S.; Faust, J.; Mrestani-Klaus, C.; Kähne, T.; Ansorge, S.; Neubert, K.; Bühling, F. *J. Biol. Chem.* **2002**, 277, 33170-33177.
41. Barnett, A. H. *Clin. Endocrin.* **2009**, *70*, 343-353.
42. Green, B. D; Flatt, P. R.; Bailey, C. J. *Diab. Vasc. Dis. Res.* **2006**, *3*, 159-165.
43. Havale, S. H.; Pal, M. *Bioorg. Med. Chem.* **2009**, *17*, 1783-1802.
44. Quesada, I.; Tuduri, E.; Ripoll, C.; Nadal, A. *J. Endocrin.* **2008**, *199*, 5-19.
45. a) Kuhn, B.; Hennig, M.; Mattei, P. *Curr. Top. Med. Chem.* **2007**, *7*, 609-619. b) Sebokova, E.; Christ, A. D.; Boehringer, M.; Mizrahi, J. *Curr. Top. Med. Chem.* **2007**, *7*, 547-555. c) Thornberry, N. A.; Weber, A. E. *Curr. Top. Med. Chem.* **2007**, *7*, 557-568.
46. a) Edmondson, S. D.; Fisher, M. H.; Kim, D.; Maccoss, M.; Parmee, E. R.; Weber, A. E.; Xu, J. WO 2003/004498. b) Villhauer, E. B. WO 2000/034241. c) Robl, J. A.; Sulsky, R. B.; Augeri, D. J.; Magnin, D. R.; Hamann, L. G.; Betebenner, D. A. WO 2001/068603.

47. a) Fukushima, H.; Hiratate, A.; Takahashi, M.; Mikami, A.; Saito-Hori, M.; Munetomo, E.; Kitano, K.; Chonan, S.; Saito, H.; Suzuki, A.; Takaoka, Y.; Yamamoto, K. *Bioorg. Med. Chem.* **2008**, *16*, 4093-4106. b) Fukushima, H.; Hiratate, A.; Takahashi, M.; Saito-Hori, M.; Munetomo, E.; Kitano, K.; Saito, H.; Takaoka, Y.; Yamamoto, K. *Chem. Pharm. Bull*. **2008**, *56*, 1110-1117.

48. Lübbers, T.; Böhringer, M.; Gobbi, L.; Hennig, M.; Hunziker, D.; Kuhn, B.; Löffler, B.; Mattei, P.; Narquizian, R.; Peters, J.-U.; Ruff, Y.; Wessel, H. P.; Wyss, P. *Bioorg. Med. Chem. Lett.* **2007**, *17*, 2966-2970.

49. Schade, J.; Stephan, M.; Schmiedl, A.; Wagner, *L.*; Niestroj, A. J.; Demuth, H. U.; Frerker, N.; Klemann, C.; Raber, K. A.; Pabst, R.; von Hörsten, S. *J. Histochem. Cytochem.* **2008**, *56*, 147-155.

50. a) Van der Veken, P.; Haemers, A.; Augustyns, K. *Curr. Top. Med. Chem.* **2007**, *7*, 621-635. b) Van der Veken, P.; De Meester, I.; Dubois, V.; Soroka, A.; Van Goethem, S.; Maes, M.-B.; Brandt, I.; Lambeir, A.-M.; Chen, X.; Haemers, A.; Scharpé, S.; Augustyns, K. *Bioorg. Med. Chem. Lett.* **2008**, *18*, 4154-4158.

51. a) Hughes, T. E.; Mone, M. D.; Russell, M. E.; Weldon, S. C.; Villhauer, E. B. *Biochemistry* **1999,** *38,* 11597-11603. b) Villhauer, E. B.; Brinkman, J. A.; Naderi, G. B.; Dunning, B. E.; Mangold, B. L.; Mone, M. D.; Russell, M. E.; Weldon, S. C.; Hughes, T. E. *J. Med. Chem.* **2002,** *45,* 2362-2365. c) Mulakayala, N.; Reddy, Ch. U.; Pal, M. *Tetrahedron* **2010**, *66*, 4919-4938.

52. Madar, D. J.; Kopecka, H.; Pireh, D.; Yong, H.; Pei, Z.; Li, X.; Wiedeman, P. E.; Djuric, S. W.; Von Geldern, T. W.; Fickes, M. G.; Bhagavatula, L.; McDermott, T.; Wittenberger, S.; Richards, S: J.; Longenecker, K. L.; Stewart, K. D.; Lubben, T. H.; Ballaron, S. J.; Stashko, M. A.; Long, M. A.; Wells, H.; Zinker, B. A.; Mika, A. K.; Beno, D. W. A.; Kempf-Grote, A. J.; Polakowski, J.; Segreti, J.; Reinhart, G. A.; Fryer, R. M.; Sham, H. L.; Trevillyan, J. M. *J. Med. Chem.* **2006,** *49,* 6416-6420.

53. a) Boehringer, M.; Loeffler, B. M.; Peters, J.-U.; Steger, M.; Weiss, P. WO 2003/068757. b) Peters, J. U.; Weber, S.; Kritter, S.; Weiss, P.; Wallier, A.; Zimmerli, D.; Boehringer, M.; Steger, M.; Loeffler, B. M. *Bioorg. Med. Chem. Lett.* **2004**, *14*, 3579-3580.

54. a) Oi, S.; Maezaki, H.; Suzuki, N.; WO 2005/042488. b) Szczepankiewicz, B. G.; Kurukulasuriya, R. *Curr. Top. Med. Chem.* **2007**, *7*, 569-578. c) Maezaki, H.; Suzuki, N. WO 2006/090915.

55. Blaszczak, L. C.; Nathes, B. M.; Pulley, S. R.; Robertson, M. A.; Sheehan, S. M.; Shi, Q.; Watson, B. M.; Wiley, M. R. WO 2007/015767.

56. a) Devastale, P.; Wang, W.; Hamann, L. G.; O'Connor, S. P. Fevig, J. M. WO 2006/127287. b) Fevig, J. M.; Feng, J. WO 2008/064107.
57. Birch, A. M.; Kemmitt, P. D.; Martin, N. G.; Ward, R. A. US 2008/0009512.
58. Wu, Y.-C.; Liu, L.; Li, H.-J.; Wang, D.; Chen, Y.-J. *J. Org. Chem.* **2006**, *71*, 6592-6595.
59. Messer, R.; Schmitz, A.; Moesch, L.; Häner, R. *J. Org. Chem.* **2004**, *69*, 8558-8560.
60. a) Henry, G. D. *Tetrahedron* **2004**, *60*, 6043-6061; b) Powers, D. G.; Casebier, D. S.; Fokas, D.; Ryan, W. J.; Troth, J. R.; Coffen, D. L. *Tetrahedron* **1998**, *54*, 4085-4096; c) Marzinzik, A. L.; Felder, E. R. *J. Org. Chem.* **1998**, *63*, 723-727; d) Bowman, M. D.; Jacobson, M. M.; Blackwell, H. E. *Org. Lett.* **2006**, *8*, 1645-1648.
61. a) Hermkens, P. H. H.; Ottenheijm, H. C. J.; Rees, D. *Tetrahedron* **1997**, *53*, 5643-5678; b) Hermkens, P. H. H.; Ottenheijm, H. C. J.; Rees, D. *Tetrahedron*, **1996**, *52*, 4527-4554.
62. Lu, G. S.; Mojsov, S.; Tam, J. P.; Merrifield, R. B. *J. Org. Chem.* **1981**, *46*, 3433-3436.
63. a) Chebanov, V. A.; Sakhno, Y. I.; Desenko, S. M.; Shishkina, S. V.; Musatov, V. I.; Shishkin, O. V.; Knyazeva, I. V. *Synthesis* **2005**, *15*, 2597-2601; b) Chebanov, V. A.; Sakhno, Y. I.; Desenko, S. M.; Chernenko, V. N.; Musatov, V. I.; Shishkina, S. V.; Shishkin, O. V.; Kappe, C. O. *Tetrahedron* **2007**, *63*, 1229-1242; c) Quiroga, J.; Trilleras, J.; Insuasty, B.; Abonía, R.; Nogueras, M.; Cobo, J. *Tetrahedron Lett.* **2008**, *49*, 2689-2691; c) Chaumontet, M.; Piccardi, R.; Baudoin, O. *Angew. Chem. Int. Ed.* **2009**, *179*, 179-182.
64. a) Yamamoto, J.; Iyagawa, M.; Yamauchi, S.; Nakazawa, O.; Umezu, M. *Tetrahedron* **1981**, *37*, 1871-1873; b) Ochiai, J. *J. Org. Chem.* **1953**, *18*, 534-551.
65. Youssif, S. *ARKIVOC* **2001**, 242-268.
66. Dydio, P.; Zielinski, T.; Jurczak, J. *J. Org. Chem.* **2009**, *74*, 1525-1530.
67. Piwinski, J. J.; Wong, J. K.; Chan, T.-M.; Green, M. J.; Ganguly, A. K. *J. Org. Chem.* **1990**, *55*, 3341-3350.
68. Ji, J.; Schrimpf, M. R.; Sippy, K. B.; Bunnelle, W. H.; Li, T.; Anderson, D. J.; Faltynek, C.; Surowy, C. S.; Dyhring, T.; Ahring, P. K.; Meyer, M. D. *J. Med. Chem.* **2007**, *50*, 5493-5508.
69. Denton, T. T.; Zhang, X.; Cashman, J. R. *J. Med. Chem.* **2005,** *48,* 224-239.
70. a) Peglion, J.-L. ; Poitevin, C.; Mannoury La Cour, C.; Dupuis, D.; Millan, M. J. *Bioorg. Med. Chem. Lett.* **2009**, *19*, 2133-2138. b) Khurana, J. M.; Kukreja, G. *Synth. Commun.* **2002**, *32,* 1265-1269.
71. Hadvary, P.; Labler, L.; Muller, K.; Schmid, G.; Tschopp, T. B.; Van de Waterbeemd, H. *J. Med. Chem.*, **1994**, *37*, 3889-3901.

72. Kramer, R. A.; Bröhmer, M. C.; Forkel, N. V.; Bannwarth, W. *Eur. J. Org. Chem.* **2009**, *25,* 4273-4283.

73. a) Kleymann, G.; Werling, H. O. *J. Biomol. Screen.* **2004**, *9*, 578-587; b) Gillum, A. M.; Tsay, E. Y.; Kirsch, D. R. *Mol. Gen. Genet.* **1984**, *198***,** 179-182.

74. a) Rasmussen, H. B.*;* Branner, S.*;* Wiberg, F. C.*;* Wagtmann, N. *Nat. Struct. Biol.* **2003**, *10,* 19-25. b) Lorey, S.; Stöckel-Maschek, A.; Faust, J.; Brandt, W.; Stiebitz, B.; Gorrell, M. D.; Kähne, T.; Mrestani-Klaus, C.; Wrenger, S.; Reinhold, D.; Ansorge, S.; Neubert, K. *Eur. J. Biochem.* **2003***, 270,* 2147-2156. c) Sebakova, E.; Christ, A. D.; Boehringer, M.; Mizrahi, J. *Curr. Top. Med. Chem.* **2007**, *7*, 547-555. d) Shrikanth, H. H.; Pal, M. *Bioorg. Med. Chem. Lett.* **2009**, *17*, 1783-1802.

75. Schaffner, A.-P.; Kaczanowska, K.; Baechle, D. EP 09012781.2.

76. a) Bieg, T.; Szeja, W. *Synthesis*, **1985**, 76-77. b) Bemis, J. E.; Vu, C. B.; Xie, R.; Nunes, J. J.; Yee Ng, P.; Disch, J. S.; Milne, J. C.; Carney, D. P.; Lynch, A. V.; Jin, L.; Smith, J. J.; Lavu, S.; Iffland, A.; Jirousek, M. R.; Perni, R. B. *Bioorg. Med. Chem. Lett.* **2009**, 19, 2350-2353.

77. Dixon, M.; Webb, E. C. *Enzymes*, 2nd ed.; Longman: London, 1971.